UNIVERSITÄT FÜR BODENKULTUR WIEN
University of Natural Resources
and Life Sciences, Vienna

Doctoral Dissertation

The untold story of the underdog: Bacterial auxiliary activities 3 enzyme, its activities and subcellular location

submitted by

Ludovika Jessica Virginia, M.Si

in partial fulfilment of the requirements for the academic degree

Doctor of Philosophy (PhD)

Vienna, March 2023

Supervisor:

Assoc. Prof. Dr. Clemens K. Peterbauer
Institute for Food Technology
Department of Food Science and Technology

Co-Supervisor:

Professor Emma R. Master
Department of Chemical Engineering & Applied Chemistry
University of Toronto

Affidavit

I hereby declare that I have authored this dissertation independently, and that I have not used any assistance other than that which is permitted. The work contained herein is my own except where explicitly stated otherwise. All ideas taken in wording or in basic content from unpublished sources or from published literature are duly identified and cited, and the precise references included. Any contribution from colleagues is explicitly stated in the authorship statement of the published papers.

I further declare that this dissertation has not been submitted, in whole or in part, in the same or a similar form, to any other educational institution as part of the requirements for an academic degree.

I hereby confirm that I am familiar with the standards of Scientific Integrity and with the guidelines of Good Scientific Practice, and that this work fully complies with these standards and guidelines.

Vienna, 20.03.2023

Ludovika Jessica VIRGINIA *(manu propria)*

Preface

This research was conducted with the generous support of the Austrian Agency for International Cooperation in Education and Research (OeAD-GmbH), Ernst Mach Grant, ASEA-UNINET (ICM-2018-10323). Over the period November 2018 to November 2021.

The research abroad presented in this doctoral dissertation was supported by Marietta Blau-Stipendium (MPC-2021-00137) and conducted in University of Toronto, Canada. Over the period November 2021 to June 2022.

The conferences attended and part of research abroad study conducted in this research was supported by Doctroal Porgram BioToP -Biomolecular Technology of Proteins. Supported by the Austrian Science Fund FWF grant W1224.

The Journey of a thousand miles begins with one step – Lao Tzu

This thesis is dedicated to those who dare to step out their comfort zone.

Acknowledgement

I still remember vividly like it just happened yesterday. March 15th 2018, an email from the one with the most prominent contribution in this thesis, Clemens Peterbauer, reached me. From then on, my life has never been the same again. The word Thank You is not enough to express my sincere gratitude for having you, Clemens, as my supervisor. But I cannot think of any other word, so; Vielen Dank for giving me opportunity to work in this project, for your kind help on my writing (may it be grant proposal, manuscripts, and this thesis), and suggestion whenever I had problems in the experiment. Not only helping me a lot on getting through OeAD scholarship, which I am really grateful for supporting me financially the first 3 years of my study, but also allowing me to apply for BioToP, which make my PhD life more colourful. So, in this opportunity I also want to give my gratitude to all people involve in BioToP, all the pI, program coordinator, and students, you all are so awesome. Thank you for all the fun, retreats, conferences, ski-trip, and also seminars which shape me into a better scientist. Undoubtedly, the whole story of knowing Clemens, OeAD, and BioToP cannot be separated from the role of the one and only Dietmar Haltrich. Thank you so much for all your support and input, not only restricted in science, but also in other casual aspects. You are like the kinase who make protein (me) into phosphorylated protein (upgraded me) by attaching the phosphate from ATP (Clemens, BioToP, OeAD). The last 1642 days of my life would not be the same without your role.

Still in the same supervision-science related category, I also want to give my genuine gratitude to the admirable Emma Master. I am so lucky to learn literally a lot from you, thank you for the amazing supervision, guidance, and not just limited in scientific stuff but also you show me how to be a better person. My research abroad at University of Toronto had been very rewarding, and it was also thanks to Owen, Olan, Thu, Xue Bin, Anuphama, and all the BioZone member in UofT. All of you make it so easy for me to blend in, and so hard to say goodbye. Thank you for all the friendship. I also want to thank the resident at 975 Dufferin St. and all my Indonesian friends residing in Toronto, you are like edible gold sprinkle on the cake who made my days there unforgettable.

I also want to thank the whole research group, the most diverse and supportive group I have ever been. A special thanks to Leo, for the fruitful discussion and lots of guidance especially during my first year, you have no idea how helpful it was for me. I also want to thank my interns Yvonne, Johanna, and Luis as without your help, my thesis could not be written as it is today. As an international student without family in foreign land, I want to give my gratefulness to special persons Dita, Nisit, Pang, Hu Cheng, Neus, Lidiia, Silja, Pui, Esther, Bas, Kwan, Angela, Lorenz, Flo, thank you for becoming my other family here. This institute is so dynamic that people come and go, but for me, all of you always stay in my heart. So, for those who I might forget to mention, believe me, you have a spot in my heart.

Speaking of friends, I also want to thank my best friends Rena, Bie, Ella, Gandhi, Adi, Pucca, Gris thank you for always being there for me despite ocean apart. And also, CIGT group, Arild, Rey, Meika, Ucul, Sabar, Adhi, it is always hilarious whenever we do video call considering we are in 6 different time zones. My highest special thanks go to my partner, Yuzer, who always be there in my ups and downs, and stands as a constant reminder to put aside things beyond our control and enjoy every moment. Thank you for your support and confidence that I can do it, whenever I doubted myself. I cannot wait for our next journey, thank you for doing life with me.

Last but not least, I want to thank my family, especially my mom Inge, my dad Erik, and my little sister Jesslyn. Thank you for all your support and prayers. I will not be here as I am today if it is not because all of what you have given to me. Thank you for always believe in me.

Abstract

Plants and biomass degrading microbes have evolved together in mutual dependence that resembles an arms race. Plants use the recalcitrant lignocellulose for structural purposes and protection against invasive microbes. In parallel, microbes evolved enzymes allowing them to overcome these barriers to varying degrees. Laccase and peroxidases are the main tools, yet the deconstruction of plant cell wall is not that simple. Radical compounds from degraded lignin can repolymerize, and H_2O_2 is an obligatory co-substrate to fuel peroxidases. These issues are solved by the presence of Auxiliary Activity (family 3) enzymes, such as contained in lignin-degrading fungi. Other than fungi, a number of bacteria were observed to metabolize lignin components and derivatives. Many genes annotated as peroxidases were identified, suggesting such bacteria should contain auxiliary enzymes. Pyranose oxidase is the only AA3 enzyme found to have significantly similar counterparts in bacteria. A biological role of providing H_2O_2 and reduction of radical products suggests an extracellular localization of bacterial POx. Using a recombinantly expressed bacterial POx, *Ka*POx, we verified its secretion facilitated by an upstream in-frame sequence constituting a putative signal peptide. To strengthen this finding, another study on putative bacterial Glucose-Methanol-Choline oxidoreductase from *Streptomyces* was conducted. The study concluded that the putative GMC oxidoreductase from *Streptomyces alboniger* was also a secretory enzyme and active towards glucose, thus named *Sa*POx. Among the AA3 family to date, POx is the only representative in bacteria. Therefore, it was intriguing to explore other bacterial AA3 enzymes. We succeeded in expressing two putative bacterial AA3 enzymes and verified the subcellular location on two bacterial POx, strengthening the predicted biological role of bacterial POx in lignin degradation.

Kurzfassung

Pflanzen und Biomasse-abbauende Mikroben haben sich in gegenseitiger Abhängigkeit entwickelt, die einem Wettrüsten gleicht. Pflanzen nutzen die Lignozellulose für ihre Struktur und zum Schutz vor invasiven Mikroben. Parallel dazu haben Mikroben Enzyme entwickelt, um diese Barriere zu überwinden. Laccase und Peroxidasen sind dabei die wichtigsten Werkzeuge, allerdings sind weitere Hilfsenzyme (AA3) für den Ligninabbau notwendig. Diese kommen in Lignin abbauenden Pilzen vor, doch wurden auch eine Reihe von Bakterien beobachtet, die Ligninkomponenten und -derivate metabolisieren. Viele als Peroxidasen annotierte Gene wurden identifiziert, was darauf hindeutet, dass solche Bakterien Hilfsenzyme enthalten sollten. Pyranose Oxidase ist das einzige fungale AA3-Enzym, das signifikante Ähnlichkeiten in Bakterien aufweist. Die biologische Rolle von H_2O_2 Produktion und der Reduktion von Radikalprodukten legt eine extrazelluläre Lokalisation von bakteriellen POx nahe. Unter Verwendung einer bereits bekannten bakteriellen POx, *Ka*POx, verifizierten wir die Sekretion von POx, die durch ein potenzielles Signalpeptid ermöglicht wird. Um diese Hypothese zu untermauern, wurde eine weitere Studie mit einer bakteriellen Glucose-Methanol-Cholin Oxidoreduktase durchgeführt. Die Studie kam zu dem Schluss, dass die GMC-Oxidoreduktase aus *Streptomyces alboniger* auch ein sekretorisches Enzym und aktiv gegenüber Glukose ist. Von allen bekannten AA3-Enzymen kommen in Bakterien lediglich Vertreter mit Ähnlichkeit zu POx vor. Daher war es von Interesse, anderen bakteriellen AA3-Enzymen zu charakterisieren. Es gelang uns, zwei bakterielle AA3-Enzyme zu exprimieren und die subzelluläre Lokalisierung bei zwei bakteriellen POx zu verifizieren, wodurch die Hypothese der biologischen Rolle von bakterieller POx beim Ligninabbau gestärkt wurde.

Table of contents

Introduction

Contents

1. Introduction

Look deep into nature, and then you will understand everything better. – Albert Einstein

Human civilization has accomplished so many things, we even set foot on the moon more than half a century ago. Yet, to date, more than two decades after the millennium hype in 2000, we are still unable to cultivate most of the existing bacteria on planet earth (Stewart, 2012). There are reasons why we cannot cultivate 'unculturable' bacteria, and one of them is in nature, bacteria depend on each other for growth (Wade, 2002). The interaction can occur not only within the same species but also in different species, genera, and even in other domains (Weiland-Bräuer, 2021), and the interaction appears not only in mutualistic or synergistic mode but also can be competitive or parasitic (Bodor *et al*., 2020; Weiland-Bräuer, 2021). For instance, fighting for the essential life factors such as space and resources (Hibbing et al., 2010). This competition is similar to what we can observe in more easily visible creatures like lions or even humans. The difference is that the fights and the aftermath are clearly visible and / or audible for these multicellular organisms since they can run and roar. However, the fights are hardly seen in microscopic organisms, although we might see the aftermath and speculate that war had happened (Thambugala *et al*., 2020). In fact, the typical outcome of the microbe's warfare is often lethal (Granato *et al*., 2019). Therefore, just because the dynamic movement is not visible does not mean everything is at peace.

Microbes are not the only living organisms with limited motion. Multicellular organisms like plants and molds, including filamentous fungi, which form fruiting bodies, are also sessile. Consequently, they require other strategies to win or survive when battling with others. Not to mention, they also need another way to communicate since they are mute. Some renowned strategies are plants producing metabolites for growth, communication, defence or even offence mechanisms. As for bacteria, to compensate for their limitation in mobility, they have secretion systems for numerous purposes (Pessione, 2021), for instance, to launch their weapon in the form of enzymes for nutrition hunting. Thus, although the life of these (micro)organisms seems boring and stagnant, beneath their quiet life lies such a complex mode to generate molecules and secretion pathways to keep existing on earth. More importantly, although these survival modes are for the sake of themselves, however animals and also mankind can grasp advantages from them. Therefore, exploration of this subject is important.

1.1 The silent war

The battle between plants and microbes has developed over time, and the strategy used by microbes is to attack the first obstacle, plant cell walls (Lagaert *et al*., 2009). Composed of mostly polysaccharides (cellulose and hemicellulose), plant cell wall act as a fortress. Another component in plant cell walls is lignin, where its deposition is recognized as a plant defence response (Ithal *et al*., 2007). The presence of lignin in the cell wall composition provides a more rigid structure, which prevents the degradation of polysaccharides from attack from the microbes (Yuan et al., 2021). Together all these components are called lignocellulose, the most abundant biopolymer available on earth as waste biomass (Chandra & Madakka, 2019).

The chemical complexity of lignin has increased during the course of evolution from gymnosperms to the most evolved grasses. This process goes alongside the evolution of enzymatic systems in microorganisms capable of degrading lignin and lignocellulosic composite structures (Janusz *et al*., 2017). Studies on these degradation capabilities of lignin have focused primarily on white-

rot and brown-rot fungi rather than bacteria counterparts (Bugg *et al*., 2011). Considering the efficiency of degrading lignin, it is reasonable that research on lignin-degrading fungi is more prominent than that of bacterial systems.

1.1.1. The plant fortresses

The percentage of building block-generating plant cell walls can vary depending on the type of plants, either softwood, hardwood, or herbaceous. But in general, it is a complex lignocellulosic material consisting of cellulose (33-51%), hemicellulose (19-34%), pectin (2-20%), and lignin (20-40%) in the shape of a honeycomb-like structure (Gibson, 2012). Due to its multi-functionality, which provides a structural framework to support growth and acts as the first line of defence against pathogen encounters (Houston *et al*., 2016), the plant cell wall consists of primary and secondary walls. The primary cell wall is highly elastic and composed mainly of randomly distributed cellulose fibres in a matrix with hemicelluloses and pectin. Laid down by dividing and growing cells, it is the first layer to be formed (Plomion *et al*., 2001). When the cell is fully developed, the primary cell wall may deposit an additional rigidifying layer of different composition, the secondary cell wall (Gacias-Amengual *et al*., 2022), providing strength and imperviousness in plant against pathogens (Miedes *et al*., 2014).

Based on the thickness and orientation of cellulose microfibril, the secondary cell wall is divided into three layers, namely S1, S2, and S3. The thickest amongst them is S2, which influences the most mechanical properties of the cell wall and has the most lignin content (Gacias-Amengual *et al*., 2022). Lignin is a heteropolymer which is challenging to break down due to the strong bonds between its building blocks, mainly *p*-coumaryl alcohol, coniferyl alcohol, and sinapyl alcohol (Becker & Wittmann, 2019). Each building block gives rise to different unit in lignin polymer, mostly *p*-hydroxyphenyl (H) from *p*-coumaryl alcohol, guaiacyl (G) from coniferyl alcohol, and syringyl (S) from sinapyl alcohol. Lignification is the final stage of cell differentiation in lignifying tissues. During lignification, lignin is deposited through free radical reactions within the carbohydrate matrix of the cell wall (Zeng *et al*., 2017).

Regardless of the composition can be varied among species and plant tissue. Still, as a complex phenolic polymer (Liu *et al*., 2018), lignin presents a chemically and structurally complex molecule providing a unique resistance towards chemical and enzymatic degradation.

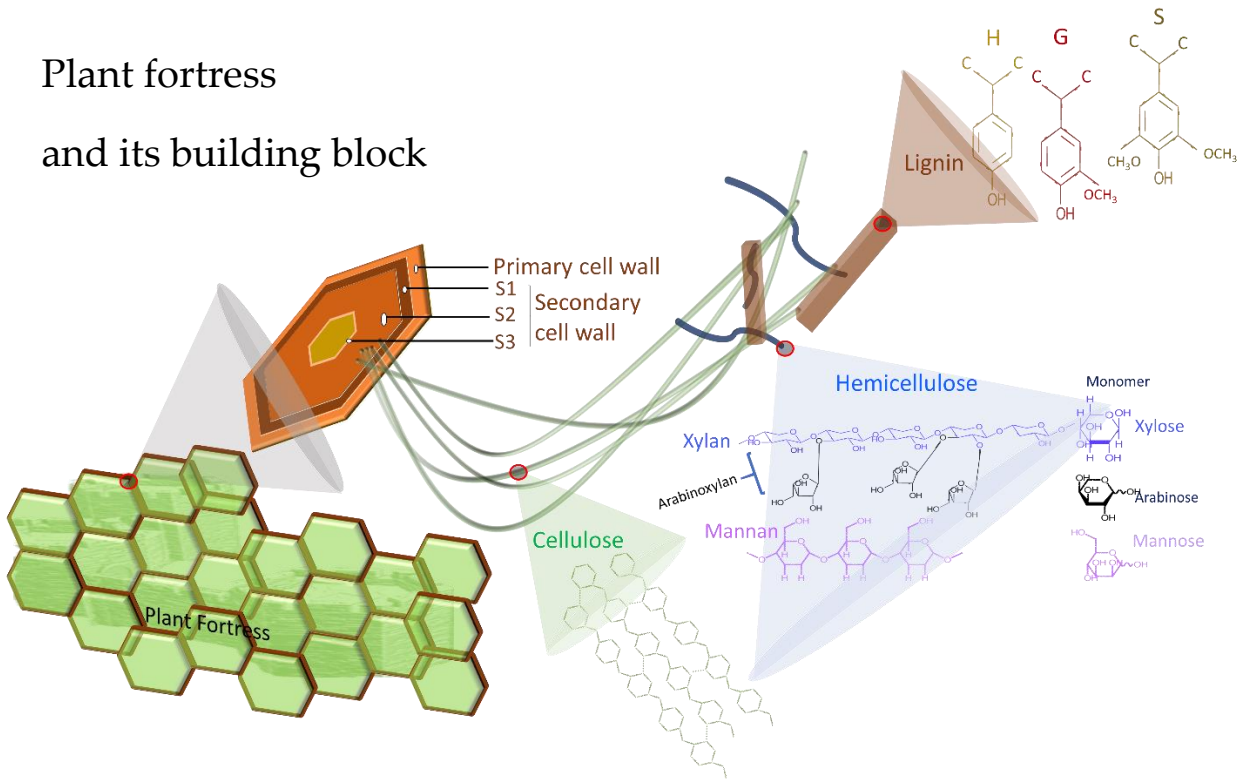

Figure 1-1 Plant cell wall and its component

1.1.2 The fungi arms

Thanks to those efforts exploring attacks on lignin by fungi, we now have the list of biological equipment in the form of enzymes that play a role in this process (Figure 1-2). In general, enzymes involved in lignin degradation are divided into two groups: lignin-modifying enzymes (LME) and lignin-degrading auxiliary enzymes (LDA) (Janusz *et al*., 2017). The prominent families of LMEs are phenol oxidase (laccases) and heme-containing peroxidases (POD), namely lignin (LiP), manganese (MnP), and versatile peroxidases (VP) (Dashtban *et al*., 2010). White-rot fungi, in particular excel in producing these secretory enzymes, where the mode of action of these enzymes, as suggested by its name, require molecular oxygen (O_2) for phenol oxidase / laccase, whereas POD use hydrogen peroxide (H_2O_2) as co-substrate for lignin degradation (Sigoillot *et al*., 2012).

The other group, LDA, cannot degrade lignin single-handedly, yet they are necessary to complete the degradation process (Silva Coelho-Moreira *et al*., 2013). Enzymes known as LDA are glyoxal oxidase (GLOx) which generates extracellular H_2O_2 by the oxidation of simple dicarbonyl and hydroxycarbonyl compounds (Kersten & Cullen, 1993; Yamada *et al*., 2014), and based on the unusual free radical-coupled copper active site, GLOx is classified among other copper radical oxidases in Carbohydrate Active enZymes database as Auxiliary Activity (AA) family 5 (Daou *et al*., 2016; Whittaker *et al*., 1999). Apart from GLOx, other LDA included glucose dehydrogenase (GDH), cellobiose dehydrogenase (CDH), aryl alcohol oxidase (AAO), and pyranose 2-oxidase (POx) (Janusz *et al*., 2017), where these enzymes are classified as AA3, glucose-methanol-choline (GMC) oxidoreductase family with Flavin-Adenine-Dinucleotide (FAD) as a cofactor, in the Carbohydrate Active Enzyme (CAZy) database (Lombard *et al*., 2014).

Supported by complete secretory enzymes LME and LDA found in their secretomes (Levasseur *et al*., 2008), in nature, only aerobic white-rot fungi show complete lignin degradation (Dashtban *et al*.,

2010; Janusz *et al*., 2017). However, in conditions where O_2 is limited, these fungi lack a piece of enzymatic machinery to mineralize lignin (Wilhelm *et al*., 2019). Cleavage of aromatic ring requires O_2 or its partially reduced species; Thus, an aerobic environment is the prerequisite of lignin degradation by white-rot fungi (Berg & McClaugherty, 2014). Then what about lignin degradation when O_2 is limited, such as deep down the ground, is it possible?

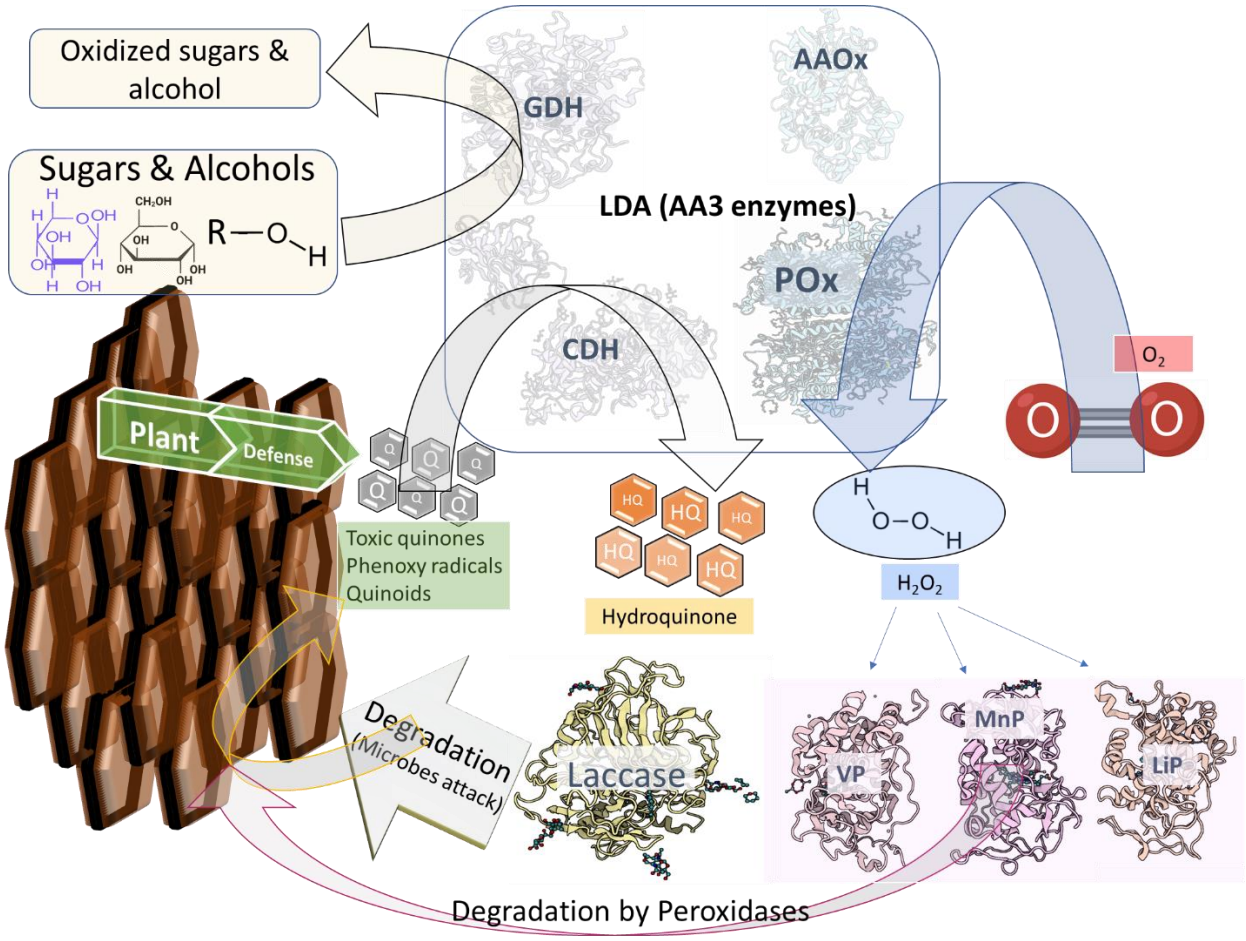

Figure 1-2 Fungi enzymes vs plant cell wall. Crystal structure obtained from Protein Data Bank (GDH: 4YNT, CDH: 4QI7, AAO: 3FIM, laccase: 1KYA, VP: 3FKG, LiP: 6A6Q, and MnP: 1MNP). This figure was modified from (Sützl *et al*., 2018).

1.1.3 The underdog

Unlike white-rot fungi, which are mostly absent in deeper mineral soil, many bacteria can grow in the condition with limited O_2. With such an advantage, bacteria represent the most likely lignin-degraders when O_2 is limited (DeAngelis *et al*., 2011; Hall *et al*., 2015). Moreover, in the presence of O_2, a number of bacteria are also known to be able to degrade lignin (Odier E, *et al*., 1981). In contrast with white-rot fungi, where its growth on lignin is visible, more effort is needed to investigate bacterial lignin degradation. The most frequent method used was lignocellulose enrichment culture followed by a screening process, mainly utilizing model substrate and isolation of potential candidates. (Crawford, 1978; Rashid *et al*., 2015; Taylor *et al*., 2012). Approached using pure culture to observe bacterial lignin degradation showed promising results, it revealed several soil bacteria could degrade model lignin compound. This suggests a bacterial role in catabolizing low-molecular weight phenolic compounds, a

partially degraded form of lignin (Brown *et al*., 2012; Crawford, 1978; Masai *et al*., 2007; Rashid *et al*., 2015; Taylor *et al*., 2012; Wilhelm *et al*., 2019). The solid evidence on bacterial lignin degradation emphasizes the need to explore this research area further.

Nonetheless, as mentioned previously, most bacteria on earth are hard to be cultured for various reasons. Thus, relying on the cultivation enrichment method means we might miss numerous other potential candidates. However, although the numbers of bacteria are still unculturable, as technology improves, we can conduct metagenomic approaches, which enables us to overcome the obstacle of bacterial cultivation with culture-independent method. Towards genome sequencing projects, our information on potential lignin degradation capabilities in bacterial genomes increased rapidly. It revealed the presence of a multitude of enzymes hypothetically annotated as lignin-modifying enzymes across a wide range of mostly α- and γ-Proteobacteria and Actinobacteria (Cragg *et al*., 2015; Janusz *et al*., 2017).

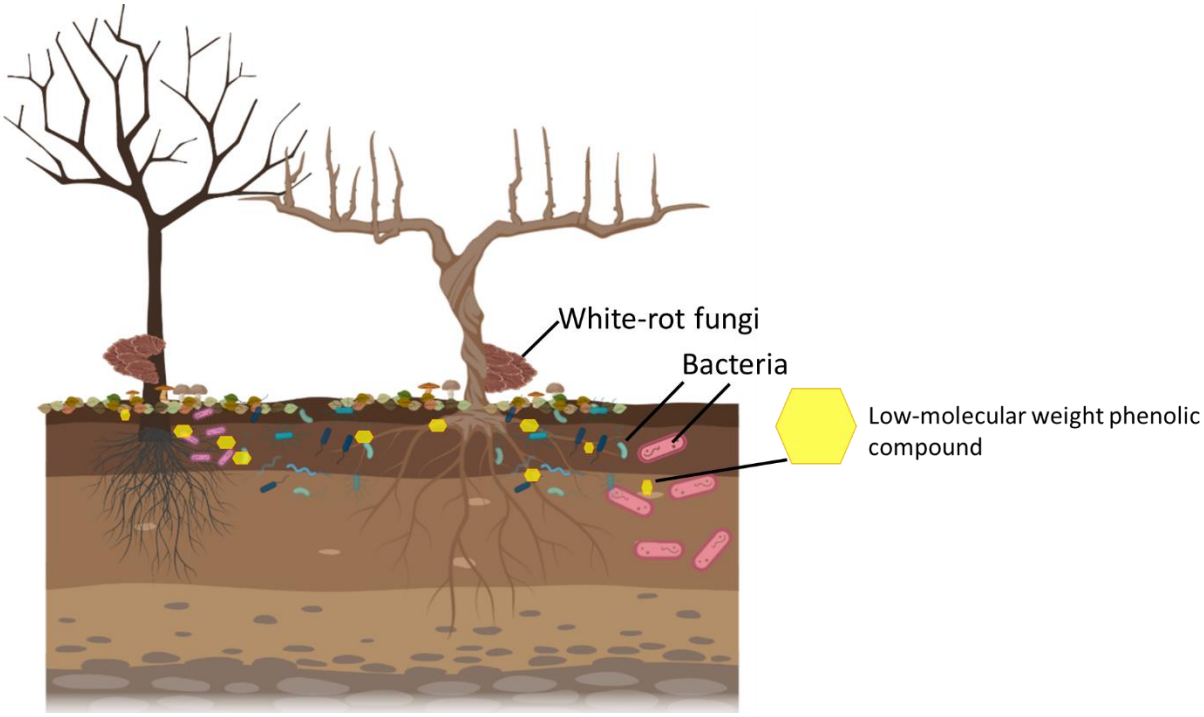

Figure 1-3 Scheme of lignin degrading bacteria. Illustration was made with Biorender (https://app.biorender.com/)

1.1.4. The bacterial enzymes

Regardless of the occurrence of predicted lignin modifying enzymes in bacteria genome, it still needs to be well understood if bacterial lignin depolymerization follows pathways comparable to those known from white-rot fungi. The availability of advanced "-omics" technology accelerates the investigation of bacterial lignin degradation. Secreted enzyme systems are believed to play a significant role in bacterial lignin degradation (Salvachúa *et al*., 2020; Xu *et al*., 2022). One of a known secreted enzymes that occurred in both lignin-degrading fungi and bacteria is laccase (de Gonzalo *et al*., 2016), a multi-copper oxidase which catalyses the oxidation of 1 electron of a wide range phenolic compounds (Mayolo-Deloisa *et al*., 2020). The most studied bacterial laccases in lignin degradation are from actinomycetes, particularly *Streptomyces* species (Fernandes *et al*., 2014). Studies on purified laccase from *Streptomyces coelicolor* conducted *in vitro* revealed that laccase oxidation of lignocellulosic substrates produces aryl cation radicals. This molecule promotes repolymerization and competes with

enzymatic depolymerization of the starting material. But within *in vivo* conditions, the degradation of lignin by depolymerization can be explained by the presence of cooperative enzymes that prevent the formation of radical species, thereby acting as quenchers (de Gonzalo *et al*., 2016). **This emphasizes the requirement of synergistic efforts rather than one-man show for bacterial lignin depolymerization.**

In lignin-degrading fungi, heme-containing peroxidases (POD) are acknowledged as the other required enzymes to trigger lignin decomposition (Chapter 1.1.2, The fungi arms). Interestingly, genomic and proteomic data, together with biochemical studies on lignin-degrading bacteria, showed no homologs found of such most common fungal POD, LiPs and MnPs (Brown *et al*., 2011; Davis *et al*., 2013). Instead, bacteria are relatively abundant in another type of peroxidase, namely dye-decolorizing peroxidases (DyPs) (van Bloois *et al*., 2010). Other than DyPs, genes annotated as catalase peroxidases and versatile peroxidases were identified in Actinobacteria genomes (Brown *et al*., 2012; Brown & Chang, 2014). In fungal counterparts, various fungal oxidases are secreted to produce the required H_2O_2 to fuel POD, obtaining effective peroxidase-based lignin degradation. **Therefore, since bacteria also contain peroxidases, such bacteria should also contain lignin-degrading auxiliary enzymes (LDA) such as GLOx (AA5), and AA3 enzymes (Chapter 1.1.2, The fungi arms).**

1.2. Let's talk about the assistant (The assistant part 1)

As implicated, Auxiliary Activity enzymes (AA) gained their name due to their function, which works in concert with other enzymes to accelerate lignocellulose conversion. A large and varying group of AA is represented by family AA3 (Sützl *et al*., 2018). Known to contain FAD as a cofactor for its catalytic activity, AA3 are structurally related to the GMC oxidoreductases family (Cavener, 1992). In CAZy database, AA3 was divided into four subfamilies based on their sequences, substrates, and co-substrates: cellobiose dehydrogenase (subfamily 1), aryl alcohol oxidase / dehydrogenase, glucose oxidase / dehydrogenase, and pyranose dehydrogenase (subfamily 2), alcohol oxidase (subfamily 3), and pyranose oxidase (subfamily 4). A snoop of each member from AA3 will be given below.

1.2.1. AA3_1

Entitled as the only known extracellular hemoflavoenzyme, cellobiose dehydrogenase (EC 1.1.99.18) is the first member of AA3 family (Csarman *et al*., 2020). The flavin-dependent dehydrogenase (DH) domain acts as the catalytic domain, which oxidizes substrate at its highest catalytic efficiency towards cellobiose, cello-oligosaccharides, and lactose (Scheiblbrandner & Ludwig, 2020). Connected via a flexible linker to the heme-binding cytochrome (CYT) domain, making the architecture of this enzyme harbouring CYT at its N-terminal and DH at its C-terminal. The CYT domain is also classified as iron reductase, AA8, in CAZy database (Levasseur *et al*., 2013). It is suggested CYT domain play a role in interdomain electron transfer and interprotein electron transfer (Felice *et al*., 2021).

In brief, the mechanism of cellobiose dehydrogenase (CDH) is oxidizing the reducing end of cellobiose and cellooligosaccharides to 1,5-lactones. In order to re-oxidize the reduced enzyme, electron acceptors such as cyctochrome c, 2,6-dichloroindophenol (DCPIP), 1,4-benzoquinone and its derivatives, also metal ion such as Fe (III) are required. Yet, the natural electron acceptor of the enzyme remains unknown (Baminger *et al*., 2001; Felice *et al*., 2021).

1.2.2. AA3_2

The second subfamily contains the most members, from aryl alcohol oxidoreductase, both oxidase and dehydrogenase (AAO / AADH); Glucose oxidoreductase, both oxidase and dehydrogenase

(GOx / GDH); and pyranose dehydrogenase (PDH). According to sequence-based classification, aryl alcohol oxidoreductases are strongly related with glucose oxidase (Levasseur *et al*., 2013), and high-sequence similarities of GDH and PDH to GOx and AADH regard them to one family of AA3_2 (Mori *et al*., 2011; Sützl *et al*., 2018).

Aryl-alcohol oxidases (EC 1.1.3.7) catalyse the oxidation of a primary alcohol group of a range of different aromatic and aliphatic unsaturated alcohols. These substrates could be generated in the process of lignocellulose decomposition by fungi. This enzymatic reaction generates corresponding aldehydes formation and reduced O_2 to H_2O_2. The known substrate which gives high catalytic efficiency is *p*-anisyl alcohol, where veratryl and cinnamyl alcohol are also notable as good electron donors. Structure-wise, AAOs are monomeric, with two domain enzymes harbouring non-covalently attached FAD (Ferreira et al., 2015).

Glucose oxidase (EC 1.1.3.4) and dehydrogenase (EC 1.1.5.9) are two different FAD-dependent enzymes which specifically oxidize β-D-glucose at the anomeric carbon to δ-gluconolactone (D-glucono-1,5-lactone). The difference between these two enzymes lies in their preferences toward electron acceptor. Molecular O_2 can be reduced into H_2O_2 by GOx, while GDH prefers an alternative electron acceptor. The first solved crystal structure from the AA3 enzyme back in 1993 is GOx derived from *Aspergillus niger* (*An*GOx, 2.3 Å, PDB 1GAL) by (Hecht *et al*., 1993). It is a homo-dimeric glycoprotein with a non-covalently but tightly bound FAD cofactor. The first crystal structure of GDH derived from *A. flavus* was resolved in 2015 (Yoshida *et al*., 2015), GDHs are found either as monomeric or homodimeric proteins. Unlike GOx, which exhibits very high selectivity towards β-D-glucose over D-xylose, some GDH in the other hand, show significant activity with D-xylose. Still, GDH and GOx are very closely related phylogenetically and structure-wise.

Pyranose dehydrogenase (EC 1.1.99.29) is an extracellular enzyme found in a relatively restricted group of litter-degrading basidiomycetes, but not in white-rot fungi (Volc *et al*., 2001). As the name itself imply, the reactivity of PDH towards oxygen is insignificant. Instead, it reduces number of metal ions including ferrocenium, various quinones, [1]ABTS cation radical where the natural electron acceptor still unknown (Kujawa *et al*., 2007). Crystal structure of PDH derived from *Leucoagaricus (Agaricus) meleagris*, *Lm*PDH (1.6 Å, PDB 4H7U, Tan *et al*., 2013) shows two domains, substrate and flavin binding domain. Here, FAD is covalently bound to His residue in the active site. Studies on catalytic efficiencies of *Lm*PDH (Sygmund *et al*., 2008) showed L-arabinose, D-glucose, and D-galactose are the preferred substrate.

1.2.3. AA3_3

Alcohol oxidase (EC 1.1.3.13) or sometimes referred as methanol oxidase is generally known as a key enzyme in methylotrophic yeast (e.g. *Pichia pastoris*, as known as *Komagataella phaffii*). It catalyses the oxidation of primary alcohols (saturated and unsaturated) to the corresponding aldehydes. The structure of alcohol oxidase (AOx) derived from *P. pastoris* 2.35 Å, PDB 5HSA, (Koch *et al*., 2016) revealed a homo-octameric with each subunit harbouring non-covalently bound FAD. The FAD syntheses by *P. pastoris* have a modification in which it contains an arabityl rather than canonical ribityl chain attached to the isoalloxazine moiety. Unlike the yeast fellow, AOx originated from basidiomycete and phytopathogenic fungi are not getting much attention and are considered to play different roles. In yeast, AOx plays a major role in methanol metabolism and assimilation, whereas the role as H_2O_2 provider for fungal attack on lignocellulose is suggested for brown-rot fungi. As for the

[1] 2,2′-azino-bis(3-ethylbenzothiazoline-6-sulfonic acid)

phytopathogenic basidiomycete, *Moniliophthora perniciosa*, the causative agent of witches' broom disease in cocoa tree, AOx is also secreted but rather for different intention. Instead for attacking the plant, it was proposed that *M. perniciosa* secret AOx to utilize methanol derived from the demethylation of pectin (de Oliveira *et al*., 2012).

1.2.4. AA3_4

Pyranose oxidase (EC 1.1.3.10) is the most distantly related member of the AA3 family and does not show high conservation of typical family motifs in AA3 family. Crystal structures of fungal pyranose oxidases (POx) derived from *Trametes ochracea* a.k.a *T. multicolor* (*To*POx / *Tm*POx, 1.8 Å, PDB 1TT0, Hallberg *et al*., 2004), *Peniphora* sp. (PsPOx, 2.35 Å, PDB 1TZL, Bannwarth *et al*., 2004), and *P. chrysosporium* (*Pc*POx 1.8 Å, PDB 4MIF, Hassan *et al*., 2013) reveal the diverse structural features, confirming its diversity both sequentially and structurally. Therefore, although POx was already described in 1968 (Janssen & Ruelius, 1968), it was only later that POx was identified as a member of the GMC family (Albrecht & Lengauer, 2003). Based on the solved structure, fungal POx has an FAD covalently linked to a His residue in the active site. It is a homotetrameric protein where each of the four two-domain subunits contains one active site. A small extension from each subunit, named head domain, was speculated to be involved in oligomerization or interaction with other proteins or cell wall polysaccharides (Hallberg *et al*., 2004).

Numbers of monosaccharides including D-galactose, D-xylose, D-gluconol 1,5-lactone, or D-glucose can be utilized by POx as its electron donor at relevant rates (Leitner *et al*., 2001; Pisanelli *et al*., 2009). In terms of D-glucose as substrate, unlike GOx (AA3_2), which activity is limited to α -D-glucose, POx is able to utilize both α- and β-D-glucose. The activity of fungal POx is rather limited to monosaccharide substrates is caused by a highly mobile active-site loop, which restricts access to the active site. Moreover, the active site is only accessible through tunnels from the polypeptide surface to a large internal cavity, formed by the four subunits.

As suggested by the name, POx can utilize molecular O_2 as an electron acceptor to transfer two electrons from the reduced FAD, and generate H_2O_2. The oxidative reaction of POx involves the formation of a C4a-hydroperoxyflavin intermediate, a typical intermediate for monooxygenases, which had previously not been detected in other flavin-dependent oxidases (Wongnate & Chaiyen, 2013). Interestingly, other than O_2, better catalytic efficiency was observed when alternative electron acceptors such as (substituted) quinones and (complexed) metal ions were used for POx.

Regarding subcellular location, fungal POx is associated with membrane-bound vesicles, and other membrane structures in the periplasmic space of fungal hyphae, and is extracellularly associated with polysaccharides (Daniel *et al*., 1992).

1.2.5. Flavin Adenin Dinucelotide (FAD), essence of AA3 enzyme

All mentioned AA3 members above hold FAD, a molecule formed of a riboflavin moiety (vitamin B_2) coupled to a phosphate group of an ADP molecule. Thus, FAD availability relies on vitamin B2, its precursor (Schnekenburger & Diederich, 2015). In humans, the presence of FAD is crucial in metabolism. The same goes for AA3 enzymes. Located at the active site, FAD anchored there for a good reason. The role of FAD in AA3 enzymes is to receive a direct hydride transfer from the oxidized substrate. The FAD has isoalloxazine ring in which the atom N5 plays a role in this hydride transfer (Piano *et al*., 2017; Walker *et al*., 1967). As a result, FAD is reduced to $FADH_2$. This process is known as reductive half-reaction. The other half-reaction is the process of re-oxidizing the $FADH_2$; Thus, it goes back to the oxidized state, FAD, known as oxidative half-reaction. The latter process involves a co-

substrate, termed electron acceptor. Molecules such as O_2 or alternative electron acceptors (different quinones, metal ions) were reduced, generating H_2O_2, hydroquinone, or reduced metal ions, respectively. Holding such a crucial part in the enzymatic reaction, FAD is renowned as a cofactor of AA3 enzymes.

From the flavin point of view, regardless it is a versatile molecule that can perform several different reactions and interact with diverse substrates; However, its catalytic potential can be handy only when the cofactor is embedded in a protein matrix with an appropriate architecture and chemical environment. Therefore, the catalytic process resulted by each flavoenzyme is indeed dictated by the protein (Piano *et al*., 2017). The complex of functional AA3 enzymes harbouring FAD is known as holoenzyme, and an enzyme without the presence of the co-factor is known as apoenzyme. The dependency of FAD makes a highly conserved flavin binding domain in all AA3 members with βαβ mononucleotide-binding motif, known as Rossmann fold.

Embedded FAD in protein can exist in five forms: fully oxidized (FAD), anionic radical form ($FAD^{\bullet -}$), neutral radical form ($FADH^{\bullet}$), anionic reduced form ($FADH^{-}$) and a neutral reduced form ($FADH_2$) (Schwinn *et al*., 2020). The UV-visible absorption spectrum can be utilized to detect the different redox states of complex FAD in protein. The most state of FAD used to observe enzyme activity is the fully oxidized and neutral reduced form. When embedded in protein milieu, UV-vis spectra of oxidized FAD will show peaks around 370 nm and 450 nm, while in neutral reduced form, these two peaks are flattened. While in its free state, flavin is a highly fluorescent substance (Sato *et al*., 2013).

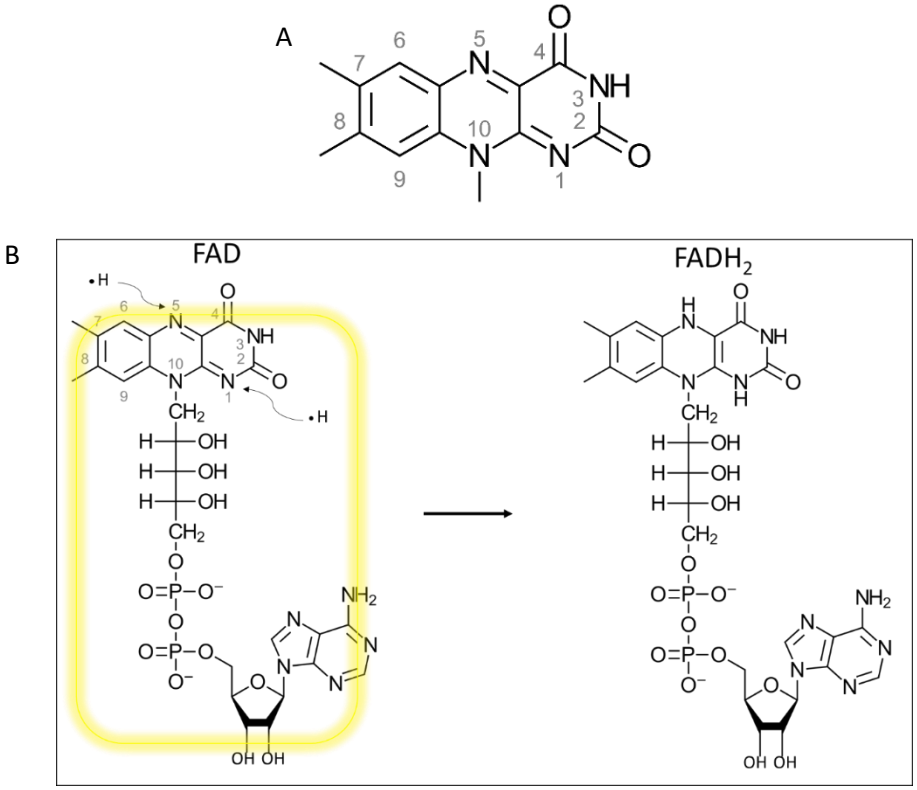

Figure 1-4 Structure of Flavin Adenine Dinucleotide (FAD). Isoalloxazine ring of FAD (A) and reduced FAD to $FADH_2$ (B)

1.2.6. Mechanism of the assistant

Apart from having various electron donors (substrates), AA3 enzymes have a common mechanism, in which the FAD-enzyme complex will get reduced due to oxidizing substrate, where the

presence of an electron acceptor (co-substrate) will bring back the oxidized state of FAD. Depending on the electron acceptor, the enzyme can be considered to have oxidase activity when it can use O_2 as an electron acceptor, or dehydrogenase activity when it prefers to use other molecules.

Understanding the enzyme mechanism of action will enable us to design an assay for detecting its activity. Enzyme activity is determined in unit (U). It defined the amount of enzyme that catalyzes the conversion of one micromole of substrate per minute under the specified conditions of the assay method. In the case of oxidoreductase enzymes, the modified substrate can be either an electron donor or an electron acceptor. Therefore, the enzyme activity assay can be conducted by following either depletion of the electron donor (the various substrate ranging from sugar to alcohol), or reduction of the electron acceptor (O_2 or the other molecules).

1.2.7. Spectrophotometer measurement

A spectrophotometer is an instrument which enables us to detect changes in the (enzymatic) reaction by following the signal produced within a specific wavelength. The most popular and frequent detection mode used is absorbance, fluorescence intensity, and luminescence. In general, the spectrophotometer detects light signals produced, converted, or transmitted by a sample. The signal is measured by a detector which then converts photons into numbers. Depending on the nature of the optical signal, measured samples may need to be excited by light at a specific wavelength. For example, the fluorescence detection derived from mono-Red Fluorescent Protein (mRFP) used in Chapter 4.2. Excitation at 584 nm was conducted for mRFP, where the emission was analyzed at 603 nm.

Detection mode using the absorbance comes in handy for following enzyme activity of the oxidoreductase, because it can follow the reduction of electron acceptor. The measured wavelength should be adjusted depending on the electron acceptor used. It is also important to note that the absorbance of the electron acceptor may influence with pH. For instance, [2]DCPIP has different coefficient extinction and character in acidic and neutral pH. When the assay condition is conducted in acidic pH, reduction of DCPIP is measured at 520 nm, whereas at pH higher than 6, absorbance at 600 nm is utilized. Another parameter that needs to be considered is the type of cuvette / plate used. Some electron acceptor requires measurement in UV-wavelength; Thus, UV cuvette / plate will be highly recommended for this purpose. For instance, 1,4-Benzoquinone which reduced into hydroquinone and measured at UV wavelength 290 nm. Other than that, reduced ferrocenium hexafluorophosphate (Fc) is also measured at the border between UV and visible wavelength, 300 nm. In this case, UV cuvette / plate will be suggested to conduct the assay.

For dehydrogenase reaction, measurement of reduced electron acceptor can be observed directly. However, in the case of oxidase activity, where O_2 is reduced into H_2O_2, following this molecule was not that easy using photo spectrometer principle. Basically, the direct measurement of H_2O_2 can be conducted at 240 nm, yet at this wavelength lots of things also give signal. Therefore, indirect measurement of H_2O_2 is preferred. One technique to measure the formation of H_2O_2 is towards ABTS assay (Miller & Rice-Evans, 1997). The measurement is based on colour reaction generated from oxidized ABTS to ABTS radical (green). The ABTS is oxidized by peroxidase which is fuelled by the presence of H_2O_2. Thus, changing colour can be associated with generated H_2O_2 derived from reduced O_2.

[2] 2,6-Dichlorophenolindophenol

1.2.8. High Performance Liquid Chromatography (HPLC)

The separation technique using a high-performance pump to deliver solvent at stable flow is the general description of HPLC. Besides a precise pump, this instrument also consists of a column where the separation takes place, and a detector which converts the amount of each component into an electrical signal. In the case of detecting enzymatic activity, HPLC can be used to detect either substrate depletion or product formation. Therefore, depending on the observed molecule(s), all three components need to be adapted (solvent, column, and detector). For some molecules, one condition can be used to detect both substrate and product. However, it mostly requires different conditions to detect the substrate and the respective product.

Methods to separate and detect sugars (mono-, di-, and oligo-) in HPLC are easily accessible. Detection of aromatic compounds and alcohol can also be conducted in HPLC. Therefore, in this study, an approach using HPLC for enzyme activity was useful to observe substrate (electron donor) depletion or respective product formation. Moreover, depending on the detector and overall condition, the detection of electron acceptor can also be observed using this instrument. Nonetheless, unlike plate reader which can easily measure the rate of enzyme activity, for HPLC, rate of enzyme activity required time-course experiment, which is not practical compared to plate reader. All in all, detection via HPLC can confirm respective product(s) formation from oxidized substrate(s) allowing a valid proof of enzyme activity performance during reaction.

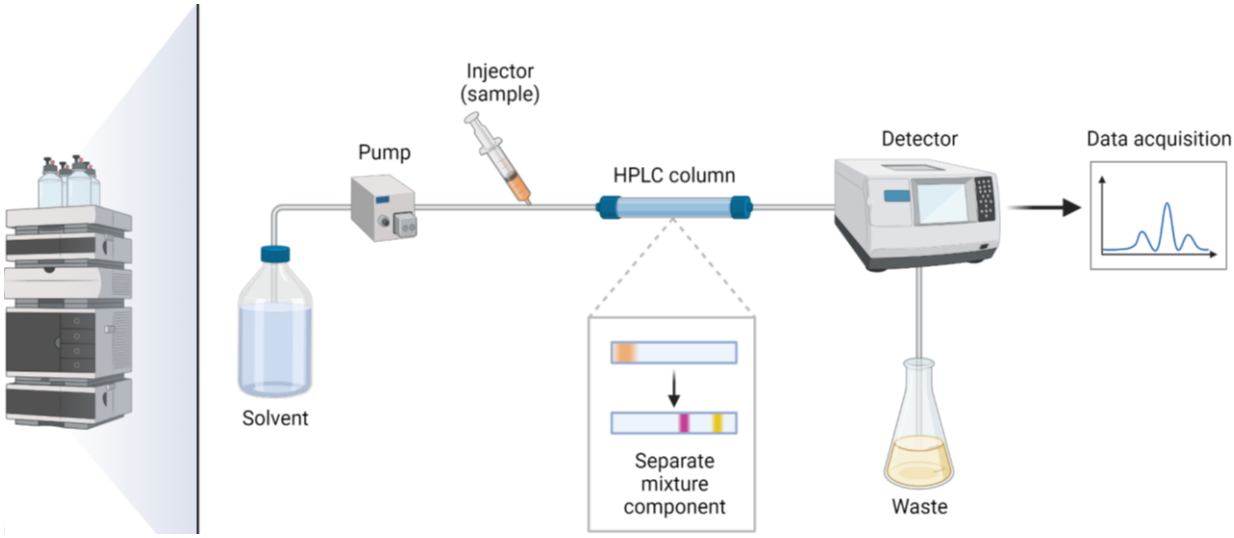

Figure 1-5 Scheme of High-Performance Liquid Chromatography (HPLC). Illustration was made with Biorender (https://app.biorender.com/)

1.3. Rise of the bacterial's assistant (The assistant part 2)

Some AA3 members have been well characterized and even crystallized, yet as a group, AA3's function is relatively undisclosed with an open possibility for lignocellulose degradation derived from some of its members (Kracher *et al*., 2016; Sützl *et al*., 2018). For instance, cellobiose dehydrogenases are more specific for disaccharides such as cellobiose and additionally contain a heme domain (Zámocký *et al*., 2004). They were recently shown to play a major role in oxidative cellulose degradation by transferring electrons to Lytic Polysaccharide Monoxygenases (LPMO; Kracher *et al*., 2016). Pyranose dehydrogenase is capable of oxidizing disaccharides and gluco-oligosaccharides at the C-1, C-2, C-3 and also at the C-1,2, C-2,3, C-3,4 atom, and uses alternative electron acceptors like (substituted) quinones or complexed metal ions (Peterbauer, 2020; Peterbauer & Volc, 2010). Pyranose

oxidoreductases (POx) catalyse the oxidation of aldopyranoses to 2-ketoaldoses and hydrogen peroxide. Most pyranose oxidases also use benzoquinone as electron acceptors, often with higher efficiency than oxygen (Leitner *et al*., 2001; Pisanelli *et al*., 2009; Salaheddin *et al*., 2010). Therefore, other than providing H_2O_2 for activation of POD, these enzymes are also implicated in reduction during the redox cycling of quinone (Martinez *et al*., 2005).

Most characterized AA3 are derived from fungi, and **POx is the only enzyme found to have significant similarities in bacterial genomes in a recent study**. The first report of bacterial pyranose 2-oxidase is derived from *Pseudoarthrobacter siccitolerans* (*As*POx) (Mendes *et al*., 2016). The recombinant enzyme produced in *E. coli* is a 64-kDa monomer with a FAD cofactor that oxidizes D-glucose. Both oxygen and 1,4-benzoquinone act as electron acceptors. The enzyme showed low thermal stability and the kinetic values were lower than in enzymes from fungal origin. The second report on bacterial POx originated from *Kitasatospora aureofaciens* (*Ka*POx). It was recombinantly expressed in *E. coli* and characterized (Herzog *et al*., 2019). Substrate specificity for *Ka*POx is mostly monosaccharide and it also harbours dual activity of oxidase and dehydrogenase, as fungal POx. Phylogenetic analysis showed a close relation between *Ka*POx and its fungal counterpart (Figure 1-6), strengthening the possible horizontal gene transfer hypothesis. The most recent report on bacterial POx was conducted by Kostelac *et al*., 2022, where heterologous expression in *E. coli* was also utilized to produce POx derived from *Streptomyces canus* (*Sc*POx). Kinetic study showed low catalytic efficiency when monosaccharides were used as substrates for *Sc*POx. Nonetheless, various C-glycosides can be oxidized by *Sc*POx. Compared to the monosaccharides, *Sc*POx shows higher specific activity towards the bulky substrate of C-glycosides, namely puerarin and mangiferin.

Of the few characterized bacterial POx, all represented distinct substrate preferences. It is also reflected by the phylogenetic analysis, where characterized bacterial and fungal POx has been compared altogether with putative pyranose oxidase sequences (Figure 1-7). All three characterized bacterial POx are distant from each other, yet the position of *Ka*POx remains close to fungal POx, as shown in Figure 1-6. In general, the phylogenetic tree constructed by Kostelac *et al*., 2022 portrayed the diversity of bacterial POx, supporting what is also shown in fungal POx (Sützl *et al*., 2018), which does not show highly conserved family motifs of AA3 family. **All this makes POx the most diverse AA3 member, in which AA3 role itself is still poorly understood.**

1.4 The connecting line

Bacterial lignin degradation is still poorly understood. However, we can narrow down the investigation area with the available discovery to date. Studies revealing bacterial pyranose oxidase open possibilities of other novel AA3 enzymes derived from bacteria yet to be found. Exploring this field can fill in the gap in the role and significance of these enzymes. Therefore, one of the conducted projects in this study was expressing and characterizing bacterial AA3 enzymes (Chapter 3.1). Since the cultivation method has its limitation, for instance, target enzymes could only be expressed in the presence of a certain molecule, or when the carbon source was limited, not to mention that both conditions are required; Thus, heterologous recombinant expression was preferred in this study.

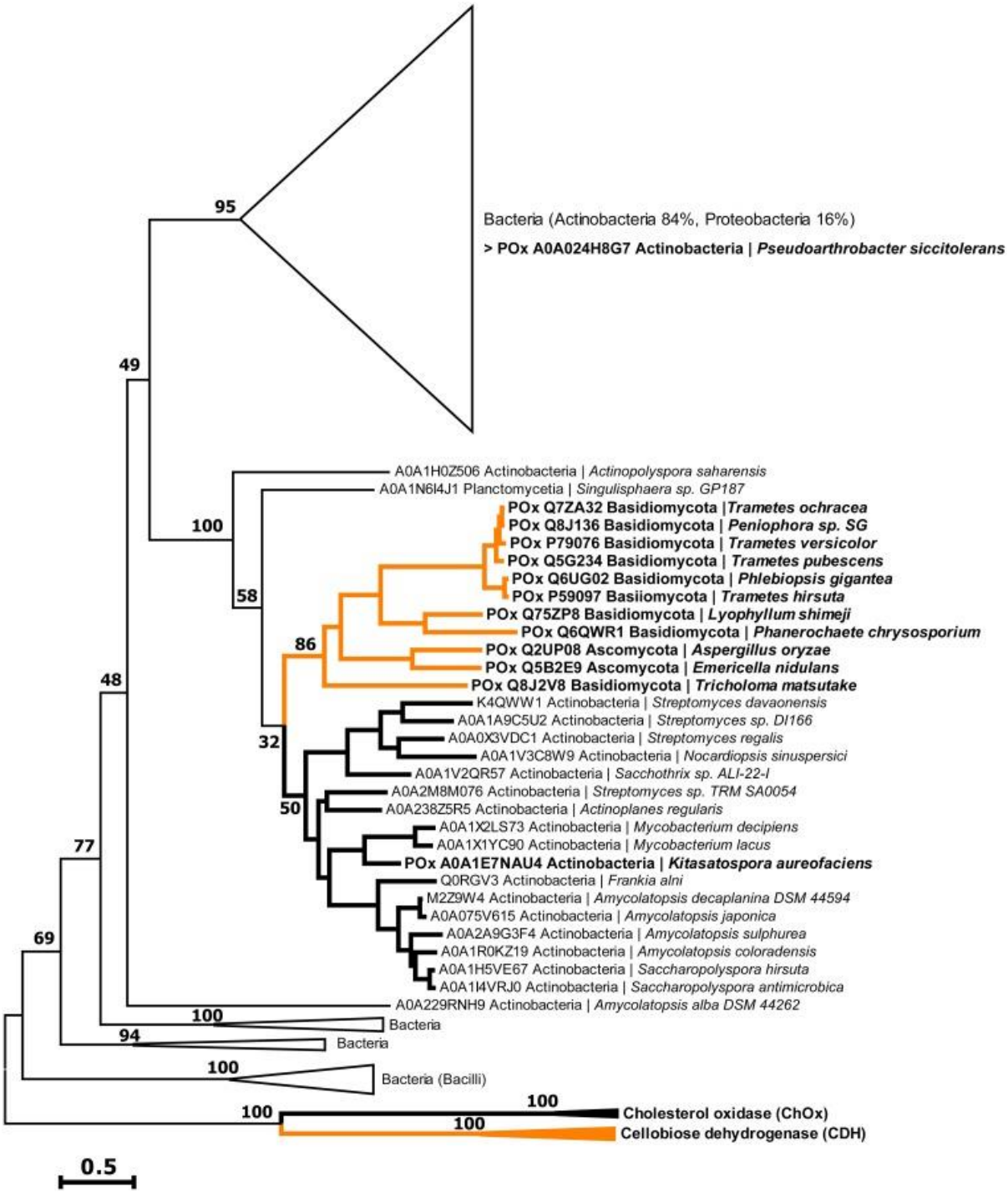

Figure 1-6 Phylogenetic tree revealing *Ka*POx position close to fungal ones (Herzog *et al.,* 2019).

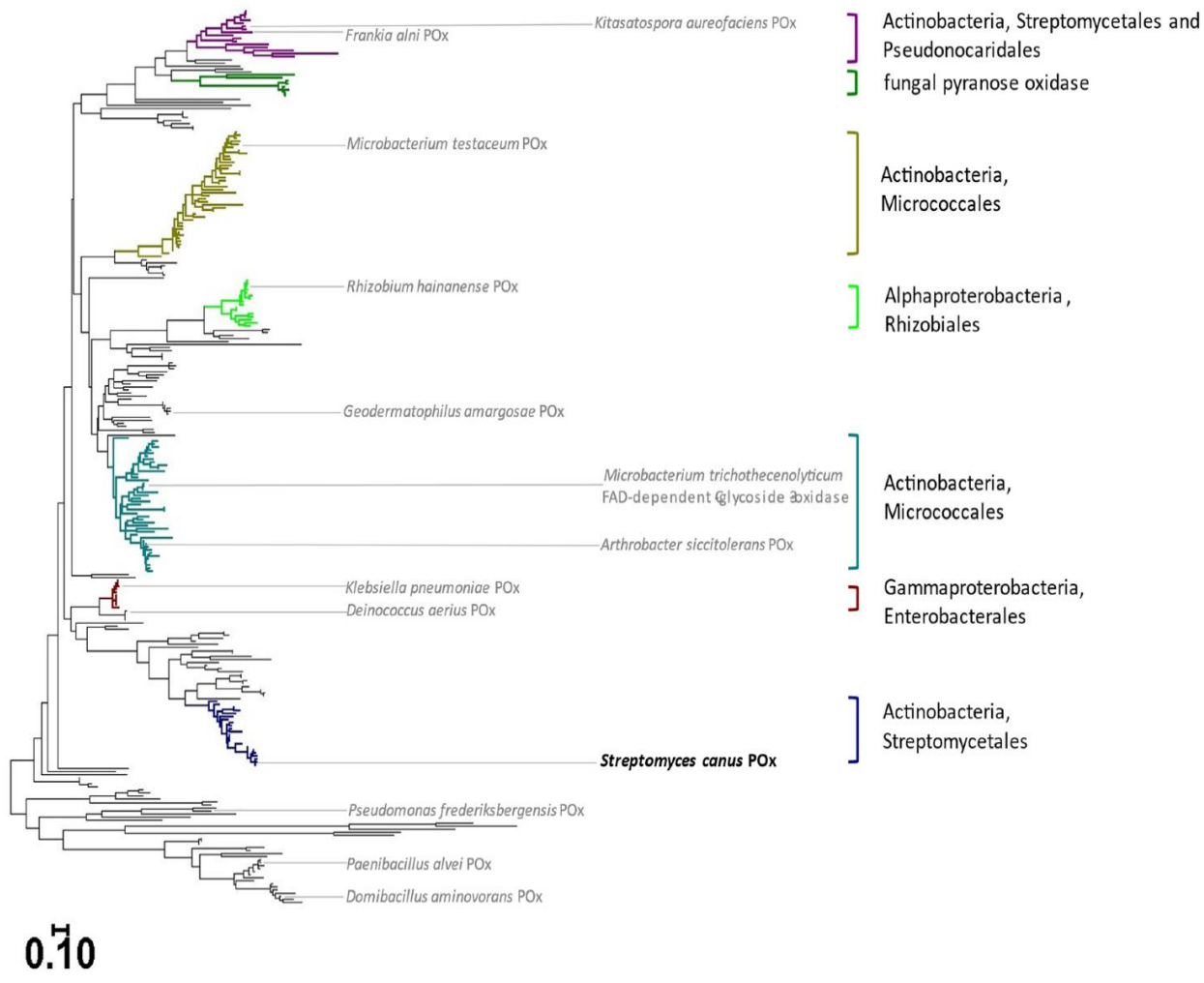

Figure 1-7 Phylogenetic tree of bacterial POx revealing position of each characterized bacterial POx (Kostelac *et al*., 2022)

Apart from investigating other bacterial AA3 enzymes, further examination of the already characterized bacterial AA3 enyzmes, POx, is also needed, particularly to elucidate its subcellular location. Among characterized bacterial POx, the one derived from *K. aureofaciens* is the most suitable model for this purpose. It is represented as the closest one to the fungal counterpart, where the mechanism of how fungal degrade lignin is much better informed, and more importantly due its dual properties (oxidase and dehydrogenase activity). It was proposed that the oxidase activity of *Ka*POx provides H_2O_2 for peroxidase activation in lignin depolymerization, whereas repolymerization generated from lignin-derived radicals can be prevented with its dehydrogenase activity, which also protects the cells against that radical damage (Herzog *et al*., 2019). Both putative biological roles are only plausible if POx is located extracellularly. Otherwise, the produced H_2O_2 would have to be transported out of the cells for activation of peroxidases, and free radicals derived from lignin depolymerization would have to be imported into the cell. Should *Ka*POx not be secreted, both hypothetical scenarios remain inefficient and unlikely, yet, confirming the subcellular location of *Ka*POx is still required to establish a valid confirmation. Recombinant expression in other bacterial systems was again used to overcome the mentioned limitation regarding the cultivation method.

Inspection of subcellular location towards other bacterial POx is also suggested in order to support the hypothesis of secreted POx mentioned above. Heterologous recombinant expression was

selected as the method to conduct the study. Since recombinant protein expression is the main technique used in these studies, it is important to understand its advantage and challenge.

1.5 Heterologous recombinant expression

The introduction of genetic material encoding protein, in the form of either DNA, cDNA, or RNA, to other systems which originally did not harbour that particular gene, is called heterologous expression. The heterologous expression can be conducted in various systems, from bacteria, yeast, fungi, insect cell, and even mammalian cell. The introduction of the target gene can be accomplished towards the expression vector (plasmid) and gene insertion into the host genome. In these studies, our focus is leaning towards enzymes originating from bacteria. Therefore, the following parts will only briefly mention the bacteria expression system.

1.5.1. Escherichia coli expression system

Undoubtedly, *E. coli* is still the most commonly used system for recombinant protein expression in research and industrial application. *Escherichia coli* is a Gram-negative bacterium with publicly available genetic information. It requires only a simple process set up, shows fast growth, and a large number of molecular tools for genetic modifications are available (Lozano Terol *et al*., 2021; Miklos *et al*., 2011). These advantages make *E. coli* eminent as an applied biotechnological tool. Nonetheless, as we know, "nobody's perfect" and neither is *E. coli*. Studies showed that the formation of inclusion bodies is common in *E. coli* expression system, also the inability to perform post-translational modifications, limited ability to build disulfide bonds, high metabolic burden, and the lack of an efficient secretion system (Baig *et al*., 2014; Mairhofer *et al*., 2013; Marschall *et al*., 2017). These all contributed to the flaw, which must be considered before selecting *E. coli* as expression system.

As the most common drawback in *E. coli* expression system, the inclusion body (IB) often appeared due to unbalance speed rate between expressed polypeptides and their folding. The inclusion body is aggregated protein molecules. The occurrence of inclusion body can also be influenced by high temperature in the protein expression process, high concentration of inducer, reduced environment of bacterial cytosol, lack of chaperones and post-translational machinery (Singh *et al*., 2015). In humans, protein aggregation is associated with misfolding protein diseases, such as Huntington, Alzheimer, and Parkinson's disease (Bhatwa *et al*., 2021; de Strooper & Karran, 2016; Gregersen *et al*., 2006; Stirling *et al*., 2003). As for *E. coli*, the inclusion body resulted in insoluble and inactive protein. Nonetheless, there is a silver lining in this inclusion body issue. In *E. coli*, protein IBs provide a unique source of an almost pure target protein and the potential for biotechnological applications.

The unique characteristic of IB includes: (1) mechanical and chemically stable (de Marco *et al*., 2019; Rinas *et al*., 2017), (2) it aggregates homogenously (Ramón *et al*., 2014), (3) and certain proteins might contain bio-functional preparations despite the former reports on inactive protein complexes (Singh *et al*., 2020; Singhvi *et al*., 2020). Numbers of studies to resurrect inclusion bodies' activity have also been conducted, such as unfolding protein and re-folding it. Still, it is worth to note that the general protocol for obtaining active protein derived from IB still depends on the character of the protein itself. Therefore, depending on the application and the character of the protein itself, some might prefer to avoid IB formation.

Prevention of IB formation can be conducted by (1) lowering the temperature used in the fermentation process, (2) using a mild inducer such as lactose instead of IPTG (isopropylthio-β-galactoside), (3) co-expression with chaperone, and (4) making the target protein more soluble by fusing it to other known soluble protein. The latter two approaches can also be useful for proteins which hard

to be expressed. Chaperones are proteins that have the ability to prevent non-specific aggregation and guide another protein along the proper pathways for folding. It has a barrel-like shape surrounding the target protein, and many are termed heat shock proteins because chaperone is generated in large amounts when a cell is exposed to heat. Whereas in general, most proteins are destabilized and tend to misfold in this condition. Plasmid harbouring chaperone for *E. coli* is commercially available, for instance pGro7 which contains chaperone *gro*ES-*gro*EL, or pG-KJE8 which harbours *dna*K.*dna*J-*grp*E *gro*ES-*gro*EL. To apply the chaperone approach, these mention plasmids should be co-expressed together with plasmid containing our target gene(s).

As for increasing solubility during the expression process, one strategy is to fuse the target gene with a known soluble gene encoding protein. Maltose binding protein (MBP) is one of the most popular fusion partners for this approach, which can also be used for affinity purification. It can be found in many bacterial species, including *E. coli*, as a periplasmic portion of the ATP-binding cassette (ABC) maltose / maltodextrin transporter. MBP has a large protein-protein interaction surface on the same side of the maltose ligand-binding pocket (Jin *et al*., 2017). The mechanism of how MBP enhance solubility to passenger protein remains unclear. Some studies suggest its role as molecular chaperone (Bach *et al*., 2001; Kapust & Waugh, 1999) while others indicate chaperone seem to play role after passenger protein has been rendered soluble by MBP (Raran-Kurussi & Waugh, 2012). In general, the MBP is placed in the N-terminal of the target protein and separated with short linker sequence, containing a protease cleavage site for further separation. Despite many successful studies on enhanced the solubility of passenger protein, aggregation or precipitation towards certain passenger proteins once cleaved were reported (Duong-Ly & Gabelli, 2015; Malhotra, 2009).

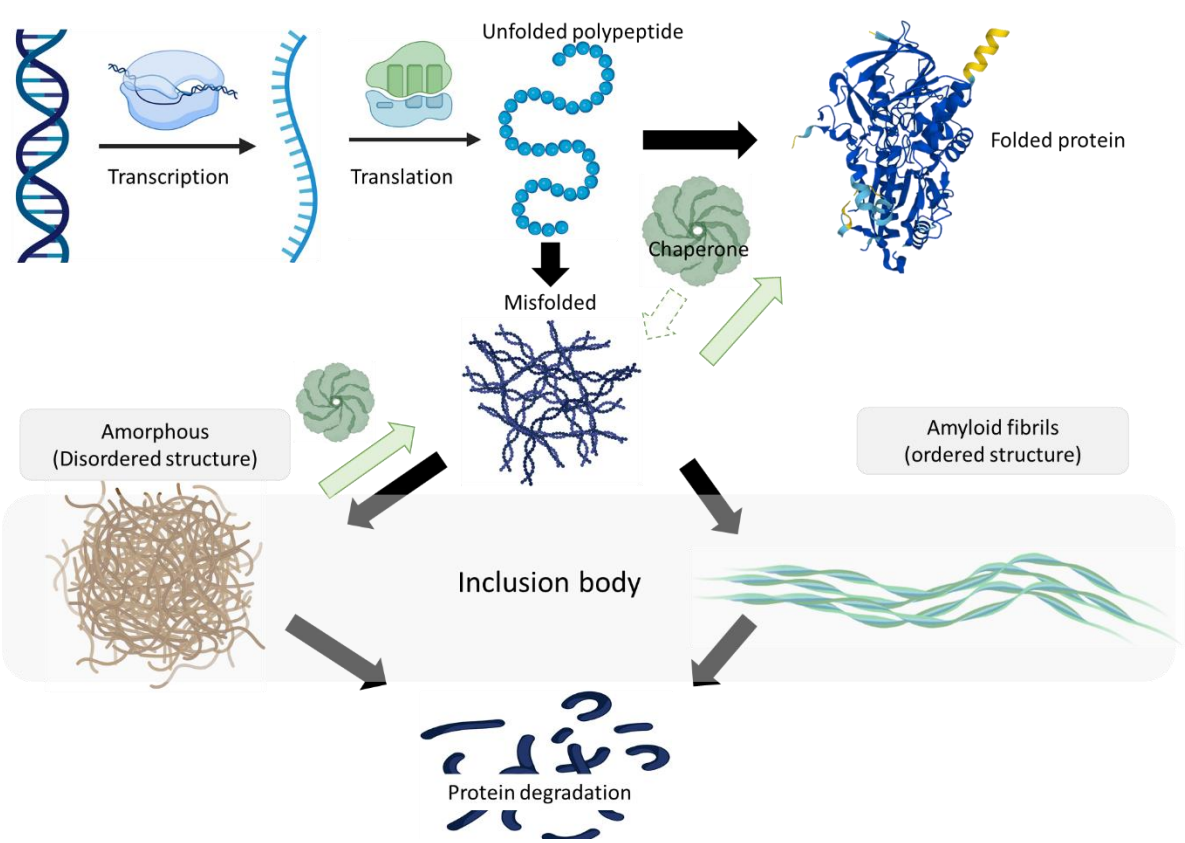

Figure 1-8 Heterologous protein expression in *Escherichia coli* and inclusion body formation. Illustration was made with Biorender (https://app.biorender.com/).

1.5.1.1. Escherichia coli secretion system

In general, recombinant protein can be located in the cytoplasm, membrane, extracellularly in medium, and special for *E. coli*, it can also be in the periplasm. As Gram-negative bacteria, the cell envelopes of *E. coli* contain outer membrane (OM), where in between OM and cytoplasmic / inner membrane (IM) lies periplasmic space. The periplasm of Gram-negative provides a unique and challenging environment for protein folding and stabilization. It has no ATP and is highly exposed to fluctuations in the external environment (Allen *et al*., 2009).

Localization of recombinant protein in cytoplasm results in a high accumulation of proteins at risk of degradation by proteases and often present in the form of inclusion bodies. In the other hand, the secretion of these proteins into the periplasm or culture medium increases protein solubility and stability (Kleiner-Grote *et al*., 2018). However, the drawback of *E. coli* expression system, especially for industrial purposes, is its inability to easily secrete recombinant protein into the medium. It does not mean that *E. coli* lacks of secretion system. In fact, *E. coli* harbours several types of secretion systems and in general, the mechanism can be divided into two: (1) one-step mechanism, where the molecules are transported directly from cytoplasm to extracellular space. (2) a two-step mechanism, where the molecules are translocated to periplasmic space and subsequently to the outer membrane (OM), prior to being secreted to extracellular space (Kaper & Nataro, 2016). The two-step mechanism requires a pathway known as general secretory (Sec) or twin-arginine translocation (Tat) pathways (Kleiner-Grote *et al*., 2018). The majority of recombinant protein production utilizes either Sec- or Tat- as their secretion mechanism (Burdette *et al*., 2018). The routing into one of these alternative protein export systems requires the fusion of a Sec- or Tat-specific signal peptide to the amino-terminal end of the desired target protein. For translocation using the Sec-pathway, the proteins are post-translationally (SecA/SecB-dependent) or co-translationally (SRP-pathway) targeted to the Sec translocase, a protein complex in the IM. In contrast, the Tat-pathway transports folded proteins, often bound to co-factors across the IM.

Although studies to enhance recombinant protein secretion in *E. coli* have been conducted, but in general when targeted expressed protein is aimed for secretion, *E. coli* is not the first option selected as host. Particularly if the target protein(s) are derived from other type of (micro-)organisms, including the Gram- positive bacteria fellow. Not only due to their difference in cell wall structure which might incommode the secretion, but also mechanism itself could be different. For instance, instead of having three-component in Tat system as *E. coli* (TatABC), The Gram-positive bacteria *Bacillus subtilis* contain only two-component (TatAC) (Frain *et al*., 2019). Unrecognized native signal peptides and their cleavage site, could also pile up the possibility of unsuccessful secretion of heterologous recombinant protein in *E. coli*.

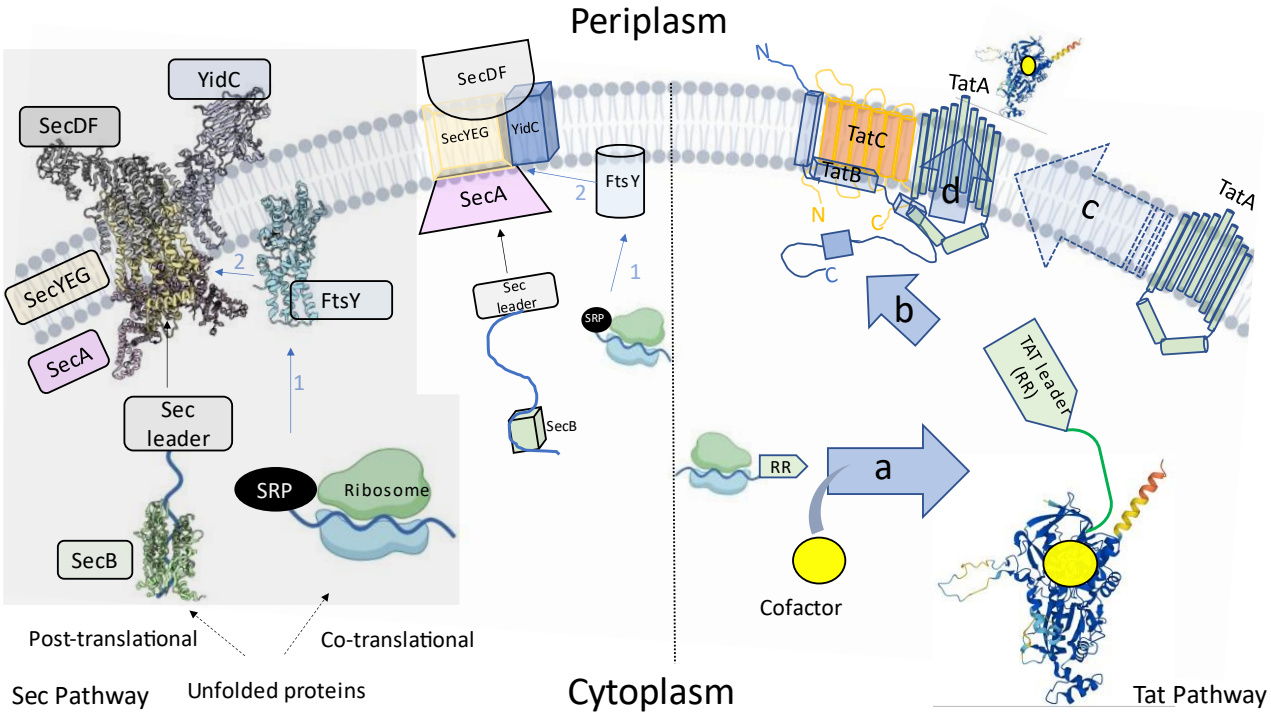

Figure 1-9 Protein secretion pathway in *Escherichia coli.* Crystal structures were obtained from Protein Data Bank (PDB). SecA: 2FSF, SecB: 1QYN, SecYEG 6R7L, FtsY SRP receptor: 5NIY, YidC: 6AL2, and SecDF 2AQP (from *Thermus thermophilus*). Illustration was made with Biorender (https://app.biorender.com/)

1.5.2. Streptomyces lividans expression system

Unlikely to be considered as the first option in recombinant protein production in previous years, *Streptomyces* is actually a versatile and promising platform for this purpose. *Streptomyces* is a Gram-positive, aerobic bacterium and commonly found in soils. Famous for its natural secretion capacity towards numerous hydrolytic enzymes, making *Streptomyces* most attractive feature for recombinant protein production. In addition, *Streptomycetes* are characterized by low endogenous proteolytic activity, grow relatively fast and in inexpensive media, do not produce pyrogenic lipopolysaccharides and endotoxins, are not pathogenic, and they might express G + C-rich genes without codon usage optimization (Anné *et al*., 2012; Sevillano *et al*., 2016). Numbers of heterologous proteins were successfully expressed using this platform including proteins derived from human, Gram-negative, and also Gram-positive bacteria. (Berini *et al*., 2020).

Since *Streptomyces* has not yet been considered as a workhorse in the biotechnological application, commercially available expression hosts and vectors are limited. Nonetheless, the advantage of easily secreted recombinant protein in this platform compensate, if not overcome the mentioned drawback. Among the numbers of *Streptomyces*, *S. lividans* has been reported on its ability to produce secretory proteins. It also harbours a relaxed restriction-modification system, which allows transformation with exogenous DNA without degrading it. Moreover, its genome sequence is known (Gullón & Mellado, 2018).

In contrast with Gram-negative bacteria, Gram-positive bacteria, such *S. lividans*, can release the secreted protein into the medium without the hurdle of the outer membrane. The secretion pathways used to secrete recombinant protein in *S. lividans* are the same as the one mentioned in *E. coli*

secretion system (1.4.1.1), Sec- and Tat- pathway. However, there are differences in the detailed process between *E. coli* and *S. lividans* secretion pathways.

As in *E. coli*, the Sec system is the main translocation route for *S. lividans*. The signal peptide comprising 15 to 40 amino acids (Tsirigotaki *et al*., 2017) have three common regions N (positive charged amino acids), H (hydrophobic amino acids), and C (cleavage site). The role of Sec signal peptide is to guide the nascent preprotein to the secretion channel in the non-folded state, and to trigger the translocase in an allosteric manner (Gelis *et al*., 2007; Gouridis *et al*., 2009). Some revealed differences between Sec pathway in *E. coli* and *S. lividans* are the SecB and YajC.

In *E. coli*, SecB chaperon prevents pre-secretory protein folding by targeting it to the translocase complex in the membrane by cooperating with SecA (Sala *et al*., 2014). Although genes homolog to SecB are found in Gram-positive bacteria, they are not present in either *B. subtilis* and *S. lividans* genome. YajC make a heterotrimeric membrane complex with SecD and SecF in *E. coli*, however genes homolog to YajC are not present in *S. lividans* (Gullón & Mellado, 2018).

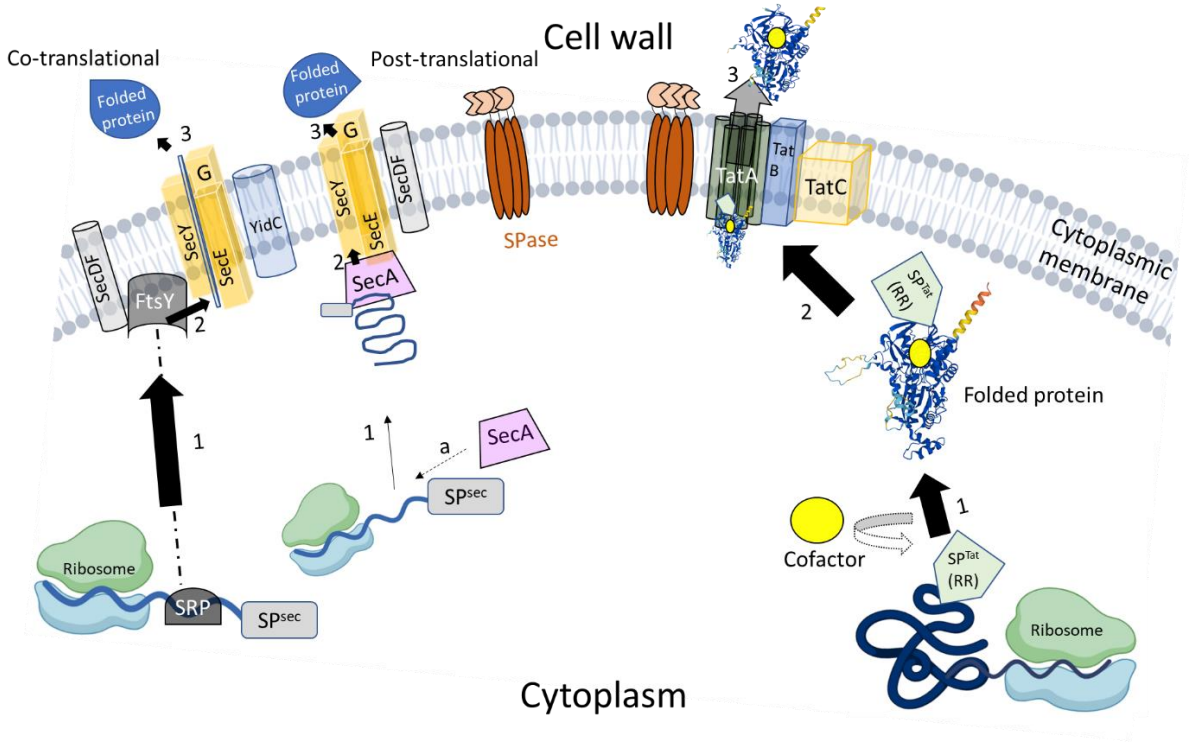

Figure 1-10 Protein secretion pathway in *Streptomyces* (modified from Hamed, Anné, *et al*., 2018). Illustration was made with Biorender (https://app.biorender.com/).

In contrast with the Sec pathway, the Tat system secrets intracellularly folded proteins, which normally contain a co-factor (chapter 1.4.1.1). To avoid mistargeting between Sec and Tat, the signal peptide of Tat-routed protein has N-regions containing a conserved motif S/T-R-R-x-FLK. The H-region is less hydrophobic, and the C-regions contain positively charged amino acids (Hamed *et al*., 2018). Unlike its Gram-positive fellow, *B. subtilis*, where TatB is absent, *S. lividans*' Tat components are like those in Gram-negative bacteria. As to be functional, TatC is essential in combination with 2 TatA protein family members (TatA and B). For the secretion itself, TatB and TatC assemble to form a multivalent receptor complex to which Tat signal peptides bind. Then multiple TatA protomers assemble at TatBC receptors (Cléon *et al*., 2015). The rest involving oligomerization of TatA protomers in a proton motif force (PMF) dependent manner, forming active TatABC translocons (Berks, 2015).

It is a privilege to be in an era where we can have options to select recombinant hosts to produce target protein. Each comes with its advantages and challenges. Thus, choosing the host for heterologous production should be aligned with the research goal. Recombinant expression conducted in this study was to express putative protein(s) (Chapter 3.1), where the other is to observe secretion of characterized protein as well as other putative protein(s) (Chapter 3.2 and 3.3). All the genes used in this study comes from Gram-positive bacteria, particularly actinomycetes. Therefore, *E. coli* expression system was used in the interest of expressing the target protein. While considering the interest in observing secretion, *S. lividans* was applied.

1.6. Owner of the player

Although we rely on recombinant protein production to study the expression and / or secretion of the gene of interest, it is still worthwhile to get to know the bacteria originally harbouring that particular gene(s). The bacteria used for exploring novel AA3 enzymes are known to have complete genome sequences and contain genes encoding peroxidase, laccases, and carbohydrate oxidoreductases. While two bacteria used to study their probability of secreting putative enzyme(s) of interest come from *Streptomyces*.

1.6.1. *Kitasatospora aureofaciens*

Formerly recognized as *Streptomyces aureofaciens* based on 16S rRNA, back to few years ago, Labeda *et al*., 2017 suggested to distinguishing *S. aureofaciens* into genera *Kitasatospora* based on multi-locus sequence analysis. The genus *Kitasatospora* itself was proposed back in 1982, and the name was taken from Kitasato Shibasaburo, a Japanese bacteriologist who was nominated for Nobel prize back in 1901. Resembling morphology as *Streptomyces*, *Kitasatospora* clearly harbours different cell-wall compositions. The aerial and submerged spores contain LL-diaminopimelic acid (DAP), while vegetative and submerged mycelia contain mainly meso-DAP in their cell walls (Takahashi, 2017). In a recent finding, *K. psammotica* is suggested to belong to *K. aureofaciens* based on a comparison of whole genome sequences and phenotypic features (Klaysubun *et al*., 2022).

Apart from being known to harbour Pyranose oxidase (*Ka*POx) in recent year, back in 1948, Benjamin Duggar at Lederle laboratories successfully identified the first tetracycline and chlortetracycline from this bacterium (Pogue *et al*., 2017).

1.6.2. *Amycolatopsis decaplanina*

Belong to the genus *Amycolatopsis*, *A. decaplanina* is the first member of this genus reported to form pseudospongarioa. It produces glycopeptide antibiotic decaplanin, and based on the antimicrobial spectrum, this strain has antibacterial activity against *Staphylococcus aureus*, *Streptomyces murinus*, and *Bacillus subtilis*. However, no antifungal activity was detected (Wink *et al*., 2004). Genus *Amycolatopsis* is known to potentially play a role in lignin degradation, for instance *Amycolatopsis* sp. 75iv2 is known to contain C-type dye-decolorizing peroxidase (Dyp2). This enzyme belongs to the family of heme peroxidase and involve in bacterial lignin degradation (Brown *et al*., 2012). As for *Amycolatopsis* sp. 75iv3 activity of small laccases was identified in study conducted by Levy-Booth *et al*., 2022.

1.6.3. *Streptomyces viridosporus*

In 1978, *S. viridosporus* T7A was known to depolymerize lignin, producing a modified water-soluble, acid-precipitable polymeric lignin (APPL) and releasing several single-ring aromatic phenols. It is also able to modify single-ring aromatic substrate, however, the product was not detected (Abdel-Hamid *et al*., 2013). An extracellular LiP was detected, which can oxidize phenolic compound but

inactive towards non-phenolic compounds. It also showed to have decolorizing activity similar to fungal MnP. Apart from its oxidoreductase activity, hydrolase ability as in cellulase also found in this bacterium.

1.6.4. *Streptomyces alboniger*

Classified as actinomycetia, *S. alboniger* is Gram-positive bacteria known to produce puromycin, an antitumor agent and protein synthesis inhibitor (Sankaran & Pogell, 1975). In a more recent study, eight new butyrolactones (obscurolide-type), two new streptazolin-type compounds, a new metabolite and two new natural products were isolated from the culture broth of *Streptomyces alboniger* YIM20533 (Luo *et al*., 2018). Yet, a report concerning lignocellulose topic has not been reported in this species.

1.6.5. *Streptomyces griseochromogenes*

Originally isolated from soil in Japan in 1958 (Takeuchi *et al*., 1958), the complete genome of *S. griseochromogenes* was reported few years ago in 2017 (Wu *et al*., 2017). Consists of 10,764,674 bp in a linear chromosome, the G+C content is 70.8%, and genomic analysis encode 52 putative gene cluster involved in the biosynthesis of secondary metabolites. The strain *S. griseochromogenes* ATCC 14511T is known to produce nucleoside antibiotic, blasticidin S (Cone *et al*., 2003). Blasticidin S is a peptidyl nucleoside antibiotic and showed strong antagonistic activities against rice pathogenic fungus and used as the first antibiotic to control rice blast in eastern Asia (K. T. Huang *et al*., 1964).

1.7. What have we got so far

The silent war between plants and microbes has been happening for so long that they evolve together to adapt and compete with each other. Plants develop the recalcitrance cell wall that acts as a fortress to protect them from the microbial raid. On the other hand, this condition also influences microbes to adapt and update their alliances and arms to penetrate the fortress. Enzyme acts as microbe's weapon and the ones derived from fungi has been more advanced studied regarding lignocellulose depolymerization. Undeniable potential to be applied in industrial process, yet fungal enzymes are less economically feasible for commercial production. Extreme condition of both temperature and pH make fungal enzymes more susceptible to degradation. Such condition is mostly applied in industrial process. Therefore, commercialization of fungal biodegradation of lignin has yet to succeed beyond a few applications (X.-F. Huang *et al*., 2013).

Apart from fungi, numbers of bacteria also showed to be able to degrade lignin. Studies showed bacterial enzymes for these purposes are more tolerant towards extreme conditions (X.-F. Huang *et al*., 2013). A majority of these bacteria come from the soil, particularly α- and γ-Proteobacteria and Actinobacteria. Proved to contain laccase and peroxidases (DyP and VP), such bacteria should also harbour the auxiliary enzyme producing H2O2 to fuel the peroxidase. Among auxiliary enzymes which can generate H_2O_2, pyranose oxidase (POx, AA3_4) is the only enzyme found in bacteria which fit the profile. To date, only a very limited number of bacterial POx have been characterized and amongst them, POx derived from *K. aureofaciens* is the closest one to its fungal counterpart. The dual activity of both oxidase and dehydrogenase of *Ka*POx also reveals the bacterial system's efficiency. Similar to killing two birds with one stone, *Ka*POx can generate H_2O_2, to fuel the peroxidase and the same enzyme can also reduce the free radical derived from lignin depolymerization. The latter process prevents cell damage and shifts the balance towards depolymerization since free radicals can readily repolymerize.

Utilization of lignocellulose as the most abundant biomass is not limited to the deconstruction of the building blocks and its conversion to renewable energy. The production of value-added materials is another promising application. Bacteria and their enzymes are reported to be able to modify lignin, but lignin valorization by bacteria first requires lignin to be depolymerized into low-molecular-weight (LMW) phenolic compounds (Lee *et al*., 2019). There are still unrevealed mechanisms on how bacteria utilize lignin, hence, studies on this topic will help to close that gap, and obtaining in-depth information on potentially involved enzyme(s) can be one approach to unravel this question. The most straight forward and convenient method to study one enzyme is by recombinant expression followed by purification. Nonetheless, this strategy also comes with its challenges. Depending on the study's purpose and the target protein's character, selecting an appropriate host is very important.

1.8. Where we are: The objective of the study

Amongst the subjects concerning the utilization of lignocellulose, our focus is on the role of bacterial enzyme systems. Emerging studies on bacterial lignin degradation boost the interest in exploring supporting enzymes which might play a role in the process. The discovery and characterization of bacterial pyranose oxidase from *K. aureofaciens* revealed its profile, which fits the role as supporting enzyme in a bacterial lignin degradation process. Therefore, we conducted this study to explore additional bacterial AA3 enzymes. This study is limited to bacteria with fully sequenced genomes, reported to encode peroxidases, laccases and carbohydrate oxidoreductases. Amongst these bacteria, *K. aureofaciens*, *A. decaplanina*, and *S. viridosporus* were selected.

In relation with the mechanism of *Ka*POx, it is suggested this particular enzyme should be secreted extracellularly. The oxidase activity of POx is suitable for providing H_2O_2 for peroxidase activation for lignin depolymerization, while the dehydrogenase activity can play a role in preventing re-polymerization of lignin-derived radicals as well as protecting the cells from damage by those radicals. Both putative biological roles are only plausible if POx is located extracellularly, otherwise the produced H_2O_2 would have to be transported out of the cells for activation of peroxidases. Moreover, the free radicals derived from lignin depolymerization would have to be imported into the cells. Therefore, for the second part of this study, we investigated the subcellular location of *Ka*POx by heterologous expression using Gram-positive bacteria. Fusion constructs with fluorescent protein mRFP were used as a reporter to accommodate the detection of a secreted enzyme.

Studies on more than one enzyme are needed to support the hypothesis of subcellular location of bacterial AA3 enzymes. We explore putative bacterial POx based on sequence similarity to *Ka*POx. The screening was conducted for a limited number of putative bacterial POx harbouring a putative signal peptide. Recombinant enzyme expression was used to determine the subcellular location and potential enzyme activity.

All in all, the characterization of the auxiliary activities system in Actinomycetes will give a serious impulse to the research into the lignin-degrading capacities of bacteria.

Materials and Method

Contents

2. Materials and Methods

The definition of insanity is doing the same thing over and over again and expecting different results. - Albert Einstein

This chapter will be divided into two parts. The Materials chapter will list the media and buffer recipe, consumable, kits, and instruments used. The information about the process will be explained in Methods. To obtain the goals of each project, molecular work, heterologous recombinant expression, purification, and enzyme activity assay are the main parts of the process. Therefore, in Methods chapter, it will be divided into four sub-parts.

2.1. Materials

In this part, I would like to express my gratitude to all scientists who have discovered, built, and optimized the materials mentioned below. Be as it may commercial or for academic purpose only, without their effort, this study will not have the same outcome.

2.1.1 Meritorious equipment

Table 2-1 Equipment used in this study

Technical instrument	Manufacturer	Function
Äkta Explorer	GE Healthcare	Protein purification
Äkta Go	GE Healthcare	Protein purification
Äkta Pure	GE Healthcare	Protein purification
Autoclave, VARIOKLAV 160S	Thermo Scientific	Autoclave
Balances, LC 2200S & AW 224	Sartorius	Balance
Cary Eclipse Fluorescence Spectrometer	Agilent	Fluorescent measurement
Centrifuge, 5424R	Eppendorf	Centrifuge
Centrifuge, 5425	Eppendorf	Centrifuge
Centrifuge, 5810R	Eppendorf	Centrifuge
Centrifuge, Avanti J-26 XP	Beckman Coulter	Centrifuge
Centrifuge, Beckman L-70	Beckman Coulter	Ultracentrifuge
ChemiDoc Imaging System XRS+	Bio-Rad	Visualization of DNA and Protein
Diode Array	Agilent	Spectrum screening
Dionex ICS 5000+	Thermo Scientific	HPLC
Dionex Ultimate 3000	Thermo Scientific	HPLC
Electrophorese unit, PowerPac 300	Bio-Rad	DNA Electrophoresis
Electroporator, MicroPulser	Bio-Rad	Transformation via electroporation
Freezer -80	Sanyo	Store culture
French Press	Newport Scientific, Inc	Cell lyser
Heating block, AccuBlock - Digital Dry Bath	Labnet	Incubation
Hot plate magnetic stirrer	IKA®	magnetic stirring
Ice maker AF80	Scotsman	Ice maker
Incubator Heraeus	Thermo Scientific	Incubate
Incubator shaker	INFORS HT	incubation, cultivation
Lambda 35 UV/Vis Spectrometer	Perkin Elmer	Measure spectrum
Laminar SAFE 2020	Thermo Scientific	Sterile work

Membran-vakuum pump	Vacuubrand GmbH	Vacuum
Microscope Aplhaphot-2 YS2	Nikon	Microscopic visualization
Mili-Q®	Merck	Ultrapure water
Mini PROTEAN Tetra Vertical Electrophoresis Cell	Bio-Rad	Protein electrophoresis
Multimode plate reader, Enspire	Perkin Elmer	Spectrum measurement
Nanodrop 2000c	Thermo Scientific	Quantification of nucleaic acid and protein
pH meter Orion 4 star	Thermo Scientific	measure pH
pH meter Orion star A111	Thermo Scientific	measure pH
PowerPac-HC 250V, 3.0A, 300W	Bio-Rad	Protein electrophoresis
SONOPULS HD60 Ultraschallhomogenisatoren	Bandelin	Cell disruption
Sonorex Ultrasonic bath	Bandelin	Water bath - sonicator
Thermal Cycler C1000	Bio-Rad	PCR
Titramax 1000	Heidoplh	shaker, table top
Trans-Blot® Turbo ™ Transfer system	Bio-Rad	Dry-blotting Western Blot
U-3000 Spectrometer	Hitachi	Measure spectrum
UV transilluminators	Vilber Lourmat	Sterilizing electroporator cuvette
Vortex 3	IKA®	Vortex

2.1.2 Supporting instrument

Table 2-2 List of supporting instruments of some equipment

Instrument	Manufacturer	What does it support
96-well plate clear flat bottom	Corning	Plate reader - Enspire
96-well UV-Transparent microplates	Corning	Plate reader - Enspire
96-well plate black flat bottom	Corning	Plate reader - Enspire
Micro cuvette, QS Quartz, 3 mm	Hellma	Diode Array and Fluorescence Spetrometer
Micro cuvette, QS Quartz, 10 mm	Hellma	Diode Array and Fluorescence Spetrometer

2.1.3. The software

Table 2-3 List of software used in this study

Software	Manufacturer
Image Lab 5.2.1	Bio-Rad Laboratories, Inc
MEGA Version 6 Release: 6140226	MEGA6
Microsoft Office	Microsoft
PyMOL Molecular Graphics System, Version 2.0	Schrödinger, LLC
Unicorn 7.1.0.325	GE Healthcare
Chromaleon 7	Thermo Scientific
Benchling	Benchling

2.1.4. Consumable

Table 2-4 List of consumables used in this study

Consumable	Manufacturer

Vivaspin® Centrifugal Concentrators	Sartorius
Conical centrifuge tubes, Falcon	Becton Dickinson
Electroporation cuvette 1 mm	Thermo Scientific
Microtubes	Eppendorf
Mini-PROTEAN TGX Gels Stain-Free	Bio-Rad
Pipette tips	Thermo Scientific
Syringe	Braun
Membrane filter 0.2 uMm, PVDF	Whatman
Syringe filters, 0.2 um, PVDF, ROTILABO®	Carl ROTH
Disposable petri dish 90 mm	Thermo Labsystems
Micro cuvettes	Greiner Bio-One

2.1.5. Purification column

Table 2-5 List of purification resin / column

Purification column	**Manufacturer**
HisTrap ™ FF column	Cytiva
Ni Resin	New England Biolab
Amylose resin High Flow	New England Biolab
PD-10 Desalting column	GE Healthcare

2.1.6. The express kit

Table 2-6 List of commercial kits used in molecular work

Kits	**Manufacturer**
Monarch Plasmid miniprep Kit	New England Biolabs
Monarch DNA Gel Extraction Kit	New England Biolabs
Monarch PCR and DNA cleanup Kita	New England Biolabs
Monarch Genomic DNA Purification Kit	New England Biolabs

2.1.7. The commercial enzymes

Table 2-7 List of commercial enzymes use in this study

Enyzmes	**Manufacturer**
HiFi DNA Assembly cloning	New England BioLabs
Q5 DNA Polymerase	New England BioLabs
One Taq DNA Polymerase	New England BioLabs
T4 Ligase	New England BioLabs
AatII	New England BioLabs
BamHI	New England BioLabs
EcoRI	New England BioLabs
HindIII	New England BioLabs
NcoI	New England BioLabs
NdeI	New England BioLabs
NotI	New England BioLabs
HpaI	New England BioLabs
PstI	New England BioLabs
XbaI	New England BioLabs
Enterokinase	BioVision

2.1.8. The chemicals

Table 2-8 Chemicals used in this study

Chemicals	**Manufacturer**
Bradford reagent	Bio-Rad
Protein Standard BSA	Sigma-Aldrich
DNA Gel loading dye (6x)	New England Biolab
Ampicilin	Roth
Chloramphenicol	Sigma-Aldrich
Tetracycline	Sigma-Aldrich
Isopropyl B-D-1-thiogalactopyranosidase	Roth
Phenylmethylsulfonyl fluoride	Fluka
Lactose	Fluka
Precision Plus Protein™ Unstained Protein Std.	Bio-Rad
Western C	Bio-Rad
2x Laemmli Sample Buffer	Bio-Rad
1 Kb plus DNA ladder	New England Biolab
Coomassie Brilliant Blue G-250	Fluka
DMSO	Thermo Scientific Acros
D-Maltose	Sigma-Aldrich
L-Arabinose	Sigma-Aldrich
ABTS	AppliChem
DCPIP	Fluka
1,4 Benzoquinone	Sigma-Aldrich
Ferrocenium hexafluorophosphate	Santa Cruz Biotechnology
Thionin	Sigma-Aldrich
Methylene green	Sigma-Aldrich
1,4 Naphtoquinone	Fluka
2,6 Dimethoxy - 1,4 benzoquinone	Sigma-Aldrich
2,6 Dimethylbenzoquinone	Sigma-Aldrich
3,5-Di-tert-butyl 1,2-benzoquinone	Fluka
9,10 Phenantherequinone	Thermo Scientific Acros
Methyl 1,4 benzoquinone	Sigma-Aldrich
Flavin adeninde dinucleotide disodium salt	Roth
Adenosine 5'-triphosphate disodium salt	Sigma-Aldrich
Glucose	Fluka
Xylose	Fluka
Fructose	Roth
Mannose	Fluka
Galactose	Sigma-Aldrich
Trehalose	Merck
Sucrose	Sigma-Aldrich
2-propanol	Roth
Methanol	Roth
Isopropanol	Merck
Choline chloride	Sigma-Aldrich
Cholesterol	Sigma-Aldrich
p-anisyl alcohol	TCl
Benzyl alcohol	Riedl

Cinnamyl alcohol	Sigma-Aldrich
Veratryl alcohol	Acros organics
p-anisaldehyde	Roth
Benzaldehyde	Sigma-Aldrich
Cinnamyladehyde	Roth
Veratryl aldehyde	Acros organics

2.1.9. The microorganisms

The mentioned bacteria below were used during this study. However, only a few reported successful experiments, some of which will not be mentioned further in the next chapters.

Table 2-9 List of bacteria strains used in this study

Cell and strain	**Manufacturer**
Escherichia coli	
DH5a	New England BioLabs
JM109	TaKaRa
JM109 (DE3)	Promega
MC1601	MoBiTec
T7 express	New England BioLabs
BL21 (DE3)	New England BioLabs
BL21 (DE3) pLysS	Promega
Lemo21 (DE3)	University of Toronto
Rosetta ™ (DE3)	Sigma-Aldrich
Bacillus subtilis	
WB800	Gift from BIOTEC Thailand
8901	MoBiTec
Streptomyces lividans	
TK24	Gift from KU Leuven

2.1.10. Plasmid for cloning and expression

Table 2-10 List of plasmids used in this study

Plasmid	**Manufacturer**
pET21D	Novagen
pET22B	Novagen
pMALc2e	Biolabs
pUC19	New England Biolab
pGRO7	TaKaRa
pG-KJE8	TaKaRa
pHT43	Gift from BIOTEC Thailand
pNZ8901	MoBiTec
pIJ486	Gift from KU Leuven

2.1.11. Media and buffer

Table 2-11 Media and its composition

Media	**Composition**	
Luria-Bertani (LB) medium	10 g / L	Peptone from casein

	5 g / L	Yeast extract
	10 g / L	NaCl
	15 g / L	Agar (for solid medium)
Terrific broth (TB) medium	12 g / L	Peptone from casein
	24 g / L	Yeast extract
	5 g / L	Glycerol
	100 mL / L	1 M Potassium phosphate buffer pH 7.5
2×YT medium	16 g / L	Tryptone
	10 g / L	Yeast extract
	5 g / L	NaCl
Antibiotic	100 mg / L	Ampicilin
	20 mg / L	Chloramphenicol
Inducer	5 ug / L	Tetracycline
	0.5 g / L	L-arabinose
	3.4 g / L	Lactose
	0.24 g / L	IPTG
	0.12 g / L	
Super Optimal Broth (SOC)	20 g / L	Tryptone
	5 g / L	Yeast extract
	584 mg / L	NaCl
	186 mg / L	KCl
	2.03 g / L	MgCl2.6H2O
	2.5 g / L	MgSO4.7H2O
Phage medium	0.5 g / L	MgSO4.7H2O
	0.74 g / L	CaCl2. 2H2O
	10 g / L	Glucose
	5 g / L	Tryptone
	5 gr / L	Lab Lemco powder
		Adjust pH to 7.2 with 5N NaOH
Spore element	40 mg / L	ZnCl2
	200 mg / L	FeCl3.6H2O
	10 mg / L	CuCl2.2H2O
	10 mg / L	MnCl2.4H2O
	10 mg / L	Na2B4O7.10H2O
	10 mg / L	(NH4)6Mo7O24.4H2O
		Filter-sterilise
R2 medium	103 g / L	Sucrose
	0.25 g / L	K2SO4
	12.12 g / L	MgCl2.6H2O
	0.1 g / L	Casamino acids
	1 g / L	Yeast extract

	5 g / L	Lab Lemco powder
	100 mL / L	TES buffer
	10 mL / L	KH2PO4 (0.5%) solution
	15 g / L	Agar (for solid medium)
		After autoclave
	2 mL / L	Spore element solution
	1% (V/V)	filter-sterile 36.8% CaCl2.2H2O solution
	0.1% (V/V)	filter-sterile 2mM CuSO4 solution
S-medium	4 g / L	Peptone
	4 g / L	Yeast extract
	0.5 g / L	MgSO4.7H2O
	2 g / L	KH2PO4
	4 g / L	K2HPO4
		After autoclave
	200 mL / L	6.5 % filter-sterilise glucose solution
	0.8 g / L	Glycine

Table 2-12 Buffer used in this study

Buffer		Composition	
TES buffer		0.25 M	TES pH 7.2
PTC buffer		103 g / L	Sucrose
		0.25 g / L	K2SO4
		2.03 g / L	MgCl2.6H2O
		2.94 g / L	CaCl2.2H2O
		80 mL / L	TES buffer
		2 mL / L	Spore element solution
Purification buffer			
Buffer	Concentration / pH	Composition	
Binding (A) / elution (B) buffer	KPP 0.1 M / pH 7	9.343 g / L	K2HPO4
		6.309 g / L	KH2PO4
		5 % (w/v)	glycerol
		5.844 g / L	NaCl
		1.36 g / L	Imidazole for binding buffer
		20.42 g / L	Imidazole for elution buffer
	KPP 0.1 M / pH 7.5	12.813 g / L	K2HPO4
		3.598 g / L	KH2PO4
		5 % (w/v)	glycerol
		5.844 g / L	NaCl
		1.36 g / L	Imidazole for binding buffer
		20.42 g / L	Imidazole for elution buffer
	Tris 0.1 M / pH 8	12.11 g / L	Tris base
			Adjust pH with HCl

		5 % (w/v)	glycerol
		5.844 g / L	NaCl
		1.36 g / L	Imidazole for binding buffer
		20.42 g / L	Imidazole for elution buffer
Column / elution buffer - MBP	0.1 M / pH 7	9.343 g / L	K2HPO4
		6.309 g / L	KH2PO4
		5.844 g / L	NaCl
		5 % (w/v)	glycerol
		3.4 g / L	Maltose (only for elution buffer)

2.2. Methods

2.2.1 Molecular work

***2.2.1.a.* Cloning of Ka97 and Ad18 to pMALc2e**

Targeted genes for the first project were synthesized in pET21D. However, to check their expression when fused to solubility enhancer protein, cloning to pMALc2e was conducted. Here, 2 types of constructs were made, the one with His-tag in C-terminal, and the other one without His-tag in C-terminal. The cloning itself used a conventional method where pMALc2e was digested with *Eco*RI and *Hind*III. The targeted genes were amplified with a primer containing particular restriction enzymes. As to build a construct with His-tag in the C-terminal, an extra round of PCR using different reverse primers was used. The list of the oligonucleotide used for this purpose was listed on Table 2-13.

Table 2-13 List of oligonucleotides for pMALc2e construct

Primer	Template	Sequence 5′ – 3′	Notes
Ad18_XbaI_F	pET21D_Ad18	ccctctagaaataattttgtttaactttaagaaggagatataccatgac	
Ad18_NotI_R		cgagtgcggccgctcagcgacgtaatgctgccggg	Remove His-tag
Ka97_XbaI_F	pET21D_Ka97	ccctctagaaataattttgtttaactttaagaaggagatataccatgc	
Ka97_NotI_R		gagtgcggccgctcactggctgcgaggcggaactg	Remove His-tag
Ad18_EcoRI_F	pET21D_Ad18	accggaattcatgaccgccagcaataccaccaccgaag	
Ad18_HindIII_R		gtgccaagctttcagcgacgtaatgctgccggggcatc	
Ka97_EcoRI_F	pET21D_Ka97	taccggaattcatgccgcaggataatccggcaca	
Ka97_HindIII_R		tgccaagctttcactggctgcgaggcggaactg	
pMal_Ad18_HindIII_R	pMAL_Ad18	tgccaagctttcagtgatgatgatgatgatGctcgagtgcggccgcgcgacgtaatgctgccggggcatc	Add His-tag
pMal_Ka97_HindIII_R	pMAL_Ka97	tgccaagctttcagtgatgatgatgatgatgctcgagtgcggccgcctggctgcgaggcggaactg	Add His-tag

2.2.1.b.* Cloning of *Ka*POx to *Bacillus subtilis* and *Streptomyces lividans

The template used for this study was amplified from the genome of the respective bacteria, *Kitasatospora aureofaciens*. The genomic extraction was conducted following the manufacturer's instruction listed in Chapter 2.1.6. Polymerase Chain Reaction (PCR) was carried out using Q5® High-Fidelity DNA polymerase with the oligonucleotides listed in Table 2-14.

Table 2-14. Oligonucleotides for *Ka*POx construct in *B. subtilis* and *S. lividans*

Name	Sequence (5′ - 3′)	Note
pNZ_SPKaPOx_F	aactgcagaaatggttacattgatagcccgtagatcaac	SPKaPOX to pNZ8901
pNZ_KaPOx_F	aactgcagaaatgattactcgctatacggac	KaPOX to pNZ8901
KaPOxHis_R	ctctctagatcagtgatgatgatgatgatggcttcggacagcgagcacctc	(SP)KaPOX to pNZ8901 / pUC19-P_{vsi}
Pvsi_F	ttttttaagcttggggatgaccaccgcgggag	P_{vsi} to pUC19

Pvsi_R	tttttcatctgcagctctccttcgatcgatg	P_{vsi} to pUC19
SPKaPOx_F	gctgcagatggttacattgatagcccg	SPKaPOX to pUC19-P_{vsi}
KaPOx_F	gagagctgcagatgattactcgctatacggacacc	KaPOX to pUC19-P_{vsi}
mRFP_GA_F	*catcgatcgaaggagag*ctgcagatggcctcctccgaggacgtc	mRFP to pUC19-P_{vsi} without SP^{Sec} with Gibson Assembly
mRFP_GA_R	*agctcggtacccggggatcc*gagctctctagattaggcgccggtggagtggcggc	mRFP to pUC19-P_{vsi} without SP^{Sec} with Gibson Assembly
SPKaPOx_GA_F	cgatcgaaggagagctgcagatggttacattgatagcccgtag	fusion SPKaPOx-mRFP-His in pUC19-P_{vsi}
KaPOx_GA_F	gcttcggacagcgagcacctc	fusion KaPOx-mRFP-His in pUC19-P_{vsi}
KaPOX_GA_R	*cggggatccgagctctctaga***ccgccgctgccgcc**gcttcggacagcgagcacctcg	fusion (SP) KaPOx-linker in pUC19-P_{vsi}
mRFP_F	atggcctcctccgaggacgtcatcaag	
mRFP_lkk_GA_F	**agcggcggcagcggcggt**atggcctcctccgaggacgtc	fusion (SP) KaPOx-mRFP-His in pUC19-P_{vsi}
mRFPHis_GA_R	*ggggatccgagctctctagatca*gtgatgatgatgatgatgggcgccggtggagtggcgcc	fusion (SP) KaPOx-mRFP-His in pUC19-P_{vsi}
eGFP_F	agagctgcagatggtgagcaagggcgaggag	eGFP to pUC-P_{vsi}
eGFP_R	gagctctctagatcattacttgtacagctcgtccatgccgagagtgatccc	eGFP to pUC-P_{vsi}
eGFP_GA_F	*cgagttgggggactttgccg*gtgagcaagggcgaggagct	SPeGFP to pUC-P_{vsi}
eGFP_GA_R	*ggggatccgagctctctaga*ttacttgtacagctcgtccatgc	SPeGFP to pUC-P_{vsi}
eGFP_A	atgtgtcagcggcgccgagttgggggactttgccgatggtgagcaagggcgaggag	SP^{KaPOx} to eGFP
eGFP_B	tcacttgggccctcggcgccgcgaacggctcggtccagtgatgtgtcagcggcgccgagt	SP^{KaPOx} to eGFP
eGFP_C	tcaacaattttgcacaggttcaaccgcactccatcacttgggccctcggcgccgcg	SP^{KaPOx} to eGFP
eGFP_D	gagagctgcagatggttacattgatagcccgtagatcaacaattttgcacaggttc	SP^{KaPOx} to eGFP

Bold: linker, Underlined: Restriction enzyme site; Italic: Complementary sequence

Primers pNZ_SP*Ka*POx_F and *Ka*POxHis_R were used to amplify *spkapox* (the *Ka*POx gene harboring the putative signal peptide sequence and a C-terminal His-tag), while primers pNZ_*Ka*POx_F and *Ka*POxHis_R were used to amplify *kapox* (the *Ka*POx gene with a C-terminal His-tag). Restriction endonucleases *Pst*I and *Xba*I were used to digest both PCR products (*spkapox* and *kapox*) and pNZ8901 prior to ligation using T4 Ligase. The ligated products were transformed to *E. coli* MC1061 for propagation and transformed into *B. subtilis* NZ8901 as circular plasmids isolated from *E. coli* MC1061.

Vector construction for *S. lividans* TK24 expression system was conducted in several steps due to the lack of a promoter in the pIJ486 backbone. The constitutive promoter (P_{vsi}) from the subtilisin inhibitor gene (*vsi*) was amplified using primers P_{vsi}_F and P_{vsi}_R from pIJ486-*sp^{sec}-mRFP* (gift from KU Leuven), digested by *Hind*III and *Pst*I and ligated to pUC19 digested with the same restriction endonucleases to generate pUC19-P_{vsi}. Both primer pairs SP*Ka*POx_F with *Ka*POxHis_R and *Ka*POx_F with *Ka*POxHis_R were used to amplify *spkapox* and *kapox*, respectively, from the *K. aureofaciens* genome. Restriction endonucleases *Pst*I and *Xba*I were used to digest both PCR products and pUC19-P_{vsi} prior to ligation to generate pUC19-P_{vsi}-*spkapox* and pUC19-P_{vsi}-*kapox*. Constructs with the reporter gene *mrfp* were generated through Gibson Assembly® (New England Biolab). We modified the pIJ486-*sp^{sec}-mrfp* into pIJ486-*mrfp* by removing the signal peptide sequence, *sp^{sec}*. Primer mRFP_GA_F (carrying an overhang of the P_{vsi} 3′ end sequence) and mRFP_GA_R (carrying an overhang of the pUC19 sequence) were used to amplify *mrfp* from pIJ486-*sp^{sec}-mrfp*. Vector pUC19-P_{vsi} was linearized with *Pst*I, and Gibson Assembly® was used to insert the amplification product to generate pUC19-P_{vsi}-*mrfp*. The primer pair (SP)*Ka*POx_GA_F and *Ka*POx_GA_R was used to generate the PCR products (*sp)kapox* with an overhang of the P_{vsi} sequence on its 5′ end, a linker and an overhang with the mRFP sequence in its 3′ end. The primer pair mRFP_lkk_GA_F and mRFPHis_GA_R was used to generate *mrfp* with a linker on its 5′ end and a His-tag with a complementary sequence to pUC19 on its 3′ end. The PCR products (*sp*)*kapox-linker* and *linker-mrfp-his*, together with pUC-P_{vsi} linearized with *Pst*I, were used as a template for the Gibson Assembly® reaction, to generate pUC19-P_{vsi}-(*sp*)*kapox-mrfp*. All intermediate constructs

in pUC19-P_{vsi} were digested with restriction enzymes *Hind*III and *Xba*I and ligated into pIJ486 digested with the same restriction enzymes. All constructs used in this study are listed in Table 2-15.

Table 2-15 Vectors used in this study

Name	Recombinant Gene	Host	Origin
pUC19	-	*E. coli*	NEB
pNZ8901	-	*E. coli*/*B. subtilis*	MoBiTec
pNZ8901-*spkapox*	*Ka*POx with signal peptide (*SPKaPOx*)	*E. coli*/*B. subtilis*	This study
pNZ8901-*kapox*	*KaPOx*	*E. coli*/*B. subtilis*	This study
pIJ486	-	*S. lividans* TK24	*KU Leuven*
pIJ486-*sp^{sec}-mrfp*	*mRFP* with signal peptide	*S. lividans* TK24	*KU Leuven*
pUC19-P_{vsi}	Promoter VSI (P_{vsi})	*E. coli*	This study
pUC19-P_{vsi}-*mrfp*	P_{vsi}, *mrfp*	*E. coli*	This study
pUC19-P_{vsi}-*spkapox*	P_{vsi}, *SPKaPOx*	*E. coli*	This study
pUC19-P_{vsi}-*kapox*	P_{vsi}, *KaPOx*	*E. coli*	This study
pUC19-P_{vsi}-*spkapox-mrfp*	P_{vsi}, *SPKaPOx*, *mrfp*	*E. coli*	This study
pUC19-P_{vsi}-*kapox-mrfp*	P_{vsi}, *KaPOx*, *mrfp*	*E. coli*	This study
pIJ486-*mrfp*	P_{vsi}, *mrfp*	*S. lividans* TK24	This study
pIJ486-sp*kapox*	P_{vsi}, *SPKaPOx*	*S. lividans* TK24	This study
pIJ486-*kapox*	P_{vsi}, *KaPOx*	*S. lividans* TK24	This study
pIJ486-sp*kapox-mrfp*	P_{vsi}, *SPKaPOx*, *mrfp*	*S. lividans* TK24	This study
pIJ486-*kapox-mrfp*	P_{vsi}, *KaPOx*, *mrfp*	*S. lividans* TK24	This study

2.2.1.c. Cloning of 2 putative pyranose oxidase genes from *Streptomyces alboniger* and *Streptomyces griseochromogenes* to *Streptomyces lividans*

The targeted genes were amplified from the genome of the respective *Streptomyces* strain. Due to high G+C content, DMSO with final concentration 6% (V/V) was required in PCR process. The same strategy as mentioned in Chapter 2.2.1.b was used to clone targeted genes to *S. lividans.* Vector pUC19-P_{vsi} was used as a transit vector prior to cloning to expression vector pIJ486. For each target genes, two constructs were made, the one containing putative signal peptide (SP) and the one without putative signal peptide (ΔSP). A little bit of modification of pUC19-P_{vsi} was made for cloning targeted gene derived from *S. griseochromogenes*. In this case the restriction site of pUC19-P_{vsi} at the C-terminal was changed into *Nco*I. Oligonucleotides used in this study were listed in Table 2-16

Table 2-16 Oligonucleotides for *Sa*POx and *Sg*POx in *S. lividans*2-

Primer	Template	Sequence 5′-3′
PvsI_Albo_PstI_F	genome *S. alboniger*	gagagctgcagatgaacgccagcgctgcgcccactc
PvsI_SP_Albo_PstI_F	genome *S. alboniger*	ggagagctgcagatgccggcaggcggcggccccat
PvsI_Albo_XbaI_R	genome *S. alboniger*	agctctctagatcagtgatgatgatgatgatggtgtccggggtggcccttgacgatg
PvsI_S.Griseo_NcoI_F	genome *S. griseochromogenes*	agctgcccatgggcatgaccgaagcgcagcattacgacgtcattg
PvsI_SP_S.Griseo_NcoI_F	genome *S. griseochromogenes*	gctgcccatgggcatgacccgcctcgtacgggtcccc
PvsI_S.Griseo_XbaI_R	genome *S. griseochromogenes*	agctctctagatcagtgatgatgatgatgatgtcgcagtcgctccgcgatgtgg
PvsI_NcoI_R	pUC19-Pvsi	catgcccatgggcagctctccttcgatcgatgcggt

2.2.1.d. Transformation

Transformation to *E. coli* was conducted via chemically competent cells. (Green & Sambrook, 2012). Electroporation was used for transformation in *B. subtilis* following the instructions in the supplier's manual (MoBiTec GmbH). Transformation of *S. lividans* TK24 was carried out through protoplast preparation and transformation (Vrancken *et al*., 2010), using thiostrepton (50 μg /mL) as a selection marker.

2.2.2. Cultivation and recombinant protein production

2.2.2.a *Escherichia coli*

Luria-Bertani broth medium containing the required antibiotic(s) was used to prepare the seed culture prior to fermentation. Incubation for seed culture was conducted at 37 °C for 16 hours in production process, TB medium containing the required antibiotic(s) was used for *E. coli* harbouring pET21D. While LB containing 0.2% glucose and ampicillin 100 μg/mL was used for *E. coli* harbouring pMALc2e. Glucose is necessary in the growth medium to repress the maltose genes, one of which is an amylase that can degrade the amylose on the affinity resin. Final OD_{600} at 0.1 was used to inoculate the production medium. Induction using either lactose or IPTG was conducted once OD_{600} reached ~0.5. Induction was carried out at 16 °C for 16 hours at 200 rpm.

Harvesting of *E. coli* biomass was carried out on ice for the entire process. Centrifugation with rotor JA-10 (Beckman) at 6000 rpm, 4 °C, 1 hour was used to separate medium and *E. coli* biomass. The supernatant was discarded and the biomass was washed with washing buffer (25 mM KPP buffer pH 7 containing 100 mM NaCl). The washing step was conducted by resuspending the cell pellet with washing buffer, followed by centrifuge at 4000 rpm, 4 °C, for 1 hour. The pelleted biomass can be stored at -30 °C.

2.2.2.b. *Bacillus subtilis*

B. subtilis harboring recombinant vector pNZ8901 and its derivatives were grown in 50 mL 2xYT medium containing chloramphenicol 5 μg/mL at 37 °C, 200 rpm. Recombinant protein production was induced by adding 1% (*v*/*v*) subtilin preparation when OD_{600} reached 0.8. The subtilin preparation was produced from *B. subtilis* NZ8963 (MoBiTec GmbH) according to the supplier´s manual.

Cultures were harvested at 24 h and 48 h after induction. Then, 50 mL culture was centrifuged and the supernatant was separated from the pellet and stored with the addition of protease inhibitor (10 μg/mL phenyl methyl sulfonyl fluoride; PMSF). The pellet was washed three times with phosphate buffer pH 7. Pellets can be stored at -30 °C while the supernatant will directly process further for purification.

2.2.2.c. *Streptomyces lividans*

Cultivation of *S. lividans* TK24 was conducted in baffled flasks containing 50 mL phage medium with 10 μg/mL thiostrepton at 30 °C, 150 rpm. No induction was required due to the use of the constitutive P_{vsi} promoter. Samples of 1 mL were obtained every 24 h and centrifuged (4000× *g*, 10 min, 4 °C). Supernatants were separated and stored at 4 °C with 10 μg/mL PMSF. The wet cell weight of the pellets was determined, and samples were washed three times with 1 mL phosphate buffer pH 7 containing 25 mM NaCl.

Treatment with lysozyme (0.5 mg/mL for one hour at 37 °C) and sonication was applied for cell disruption. The sonication process was carried on ice using a Bandelin Sonopuls HD 60 (Bandelin electronic GmbH, Berlin, DE) set at 80 V and 30%-cycle for 3 × 1 min, with two-minute intervals The

lysed samples were centrifuged at 13,000 rpm for 5 min at 4 °C, and extracts were stored with 10 μg/mL PMSF.

2.2.3. Purification and protein analysis

2.2.3.a. His-tag purification

Escherichia coli. For recombinant protein produced in *E. coli*, all samples were derived from intracellular. Binding buffer A (Table 12, chapter 2.1.11) and 1 mM PMSF were used to resuspend the cell pellet. Cell disruption was carried out using French press or sonicator Bandelin Sonopuls HD 60. Cell was disrupted until the viscosity of cell lysate reduced. Cell lysate and debris were separated using centrifugation (rotor JA-25.50 at 20,000 rpm, 4 °C, for 1 hour).

The targeted protein containing 6×His was purified using 5 mL pre-packed Ni-NTA column. The protein loading and washing step flow rate was set at 2 mL / minute. Elution using a gradient step was carried at 3 mL / minute for 20 minutes. Eluted samples were collected in fractions and checked for the presence of the targeted band using SDS-PAGE (Chapter 2.2.3.c). Fractions showing the targeted bands at respective size, were pooled for further buffer-changing process. Vivaspin concentrator was used for buffer exchange as well as concentrating protein. Buffer exchange was carried out to remove imidazole in the purified fraction.

Bacillus subtilis. Two types of samples were purified for protein production in *B. subtilis*. One from the supernatant and the other one from the cell pellet. Recombinant His-tagged protein was purified on 1 mL Ni-NTA columns (Merck, Darmstadt, Germany) following the manufacturers recommendations using Buffer A (50 mM Tris-HCl pH 7.5, 30 mM NaCl, and 30 mM Imidazole) as binding and washing buffer and Buffer B (50 mM Tris-HCl pH 7.5, 30 mM NaCl, and 250 mM Imidazole) as elution buffer.

The sample from supernatant was directly loaded into the column once calibrated with respective binding buffer. As for samples from the cell pellets, they required a cell lysis process prior to purification. The cells were pre-treated with lysozyme (0.5 mg/mL for one hour at 37 °C) and disrupted by sonication on ice using a Bandelin Sonopuls HD 60 (Bandelin electronic GmbH, Berlin, DE) set at 80 V and 30%-cycle for 3 × 1 min, with two-minute intervals. PMSF was added at 10 μg/mL.

2.2.3.b. Maltose binding protein affinity tag

In this study, *E. coli* is the only host to produce recombinant protein harboring MBP fusion. The same strategy as mentioned in Chapter 2.2.3.a for *E. coli* was also applied here with some modifications. Column buffer was used for conditioning the column and lysed the cell (Table 12, Chapter 2.1.11). Loading of protein was carried out at 1 mL / minute and the same flow rate was used for the washing step. Column buffer was also used for the washing step. Unlike His-tag purification which used gradient elution, in MBP purification, 1 step elution using 1 mM Maltose (final concentration) was applied.

The eluted fraction was pooled and treated with enterokinase to cleave MBP from the targeted protein. Prior to further purification using anion exchange chromatography (AEX) for MBP removal, buffer exchange using PD-10 column was applied. In PD-10 column, 20 mM Tris-HCl buffer pH 9 was used, thus, the target protein remained in this buffer condition prior to AEX. The elution buffer for AEX was 20 mM Tris-HCl pH 9 with 500 mM NaCl.

2.2.3.c. SDS-PAGE and Western blot

Samples were mixed with 2x SDS buffer mix (Sigma), denatured at 95 °C for 3 min and separated on Mini-PROTEAN®TGX Stain-Free™ Precast Gels 4–20% (Bio-Rad, Hercules, CA, USA) at 150 volts for 50 min. Precision Plus Protein™ Western C™ (Bio-Rad) was used as a molecular weight standard. Proteins were transferred to a 0.2 μm Nitrocellulose membrane by dry-blotting in a Trans-Blot® Turbo™ (Bio-Rad) at 1.3 A, and 25 V for 7 min. Proteins were detected using a BSA-free anti-Penta-His-tag mouse monoclonal IgG (Qiagen, Hilden, Germany) as the primary antibody and Polyclonal Rabbit-anti-mouse Immunoglobulin/HRP (Agilent, Santa Clara, CA, USA) as secondary antibody according to the manufacturer´s recommendations. Clarity Western ECL (Bio-Rad) was used as substrate. Stain-free SDS-PAGE gel and Western blot were visualized in a ChemiDoc™ XRS+ (BioRad).

2.2.4. Enzymatic activity, secretion, and detection

2.2.4.a. Plate reader

Oxidoreductase activity. Oxidoreductase was determined using EnSpire® multimode plate reader (PerkinElmer, Waltham, MA, USA). For dehydrogenase activity, assay was performed towards various electron donor and acceptor listed on Table 2-17. Analysis using plate reader followed the reduction of electron acceptor. The wavelength respective for each electron acceptor was also listed on Table 2-17. For UV-wavelength observation, the 96-well UV-plate was used.

Table 2-17 List of electron donor, electron acceptor, and its wavelength

Electron donor	Final concentration	Electron acceptor	Final concentration	Wavelength (nm)
Monosaccharides		2,6-Dichlorophenolindophenol (DCPIP)	0.3 mM	600
L-arabinose	160 mM	Thionine	0.3 mM	600
Fructose	160 mM	Methyl green	0.3 mM	600
Galactose	160 mM	Ferrocenium hexafluorophosphate (Fc)	0.16 mM	300
Glucose	160 mM	1,4 Benzoquinone (BQ)	0.83 mM	290
Mannose	160 mM	1,4-Naphthoquinone	0.83 mM	343
Sorbose	160 mM	2,6-Dimethoxybenzoquinone	0.83 mM	290
Xylose	160 mM	2,6-Dimethylbenzoquinone	0.83 mM	290
Disaccharides		3,5-Di-tert-butyl 1,2-benzoquinone	0.83 mM	420
Lactose	40 mM	9,10 Phenantherequinone	0.83 mM	327
Maltose	160 mM	Methyl-1,4 Benzoquinone	0.83 mM	290
Sucrose	160 mM			
Trehalose	160 mM			
Sugar alcohol				
Xylitol	80 mM			
Sorbitol	80 mM			

Alcohol / Aryl alcohol				
Ethanol	300 mM			
Isopropanol	300 mM			
Methanol	300 mM			
Anisyl alcohol	17 mM			
Benzyl alcohol	60 mM			
Cinnamyl alcohol	17 mM			
Veratryl alcohol	17 mM			
2,4 dimethoxybenzyl alcohol	17 mM			
2-methoxybenzyl alcohol	17 mM			
2-hydroxybenzyl alcohol	17 mM			
4-hydroxybenzyl alcohol	8 mM			
Others				
Cholesterol	20 μM			
Choline	1.7 mM			

For the oxidase activity, atmospheric oxygen was used as an electron acceptor. Oxidase activity was quantified using 1 mM 2,2'-Azino-bis (3-ethylbenzothiazoline-6-sulfonic acid; ABTS) and Horseradish Peroxidase (Sigma Aldrich; 143 U/mL). Oxidase activity was determined at 420 nm, following the reduction of ABTS into its radical form.

Fluorescence quantification. This analysis was used to study on localization of targeted protein fused with a fluorescent protein, mRFP. Detection of fluorescence of mRFP was conducted by exciting the samples at 584 nm and analyzing the emission at 603 nm. A special 96-well black plate was used for the measurement of the fluorescence signal.

2.2.4.b. HPLC

Detection of oxidized electron donor was conducted using HPLC. In general, enzymatic activity was confirmed when substrate depletion was observed, and / or product peak(s) occurred. Monosaccharides were detected as electron donor using Dionex ICS 5000+ system with CarboPac™ Dionex PA1 column. This system was coupled with an electrochemical detector (ED) to conduct more sensitive analysis, such as low substrate depletion. The eluent used was 100 mM NaOH (A) and 100 mM NaOH + 1M $CH_3COOHNa$ (B). The flow rate was run at 0.25 mL / minute at 25 °C. Running conditions was showed in Table 2-18.

Table 2-18 Running condition for more sensitive detection in Dionex ICS 5000+

Time (minutes)	A (%)	B (%)
Start (0)	100	0
35	90	10

45	80	20
50	50	50
60	100	0

Another alternative to measuring the depletion of monosaccharides can also conduct using the column Aminex HPX-87H coupled with RI detector. The eluent used was 5 mM H_2SO_4 with isocratic flowrate at 0.6 mL / min at 50 °C.

As for aromatic alcohol, Dionex Ultimate 3000 with UV detector and C-18 column was used. The UV-wavelength was set subjected to respective substrates. In this case both benzyl alcohol and anisyl alcohol were measured with UV setting 224 nm. The condition used in this study also enables us to observe electron acceptor 1,4 BQ and its reduced form, hydroquinone. Thus, UV 290 nm was also used Two types of eluents were prepared for this run, MiliQ water with 0.1 % Trifluoro Acetic Acid (A) and Acetonitrile 100% + 0.1% Trifluoro Acetic Acid (B). The flow rate was set to 0.8 mL / minute at 30°C. The run condition was set as shown in Table 2-19.

Table 2-19 Running condition for aryl alcohol detection

Time (minutes)	A (%)	B (%)
Start (0)	95	5
15	60	40
18	24	76
18	95	5
25	95	5

Oxidized anisyl alcohol will generate anisyl aldehyde as a product. The following condition listed on Table 2-20 can be applied to detect this product. Eluent used for this run was 20 mM Na-phosphate pH 3 (A) and Acetonitrile 100% (B). The mobile phase was set at 1 mL / min at 25 °C.

Table 2-20 Running condition for anisyl aldehyde detection

Time (minutes)	A (%)	B (%)
Start (0)	95	5
5	75	25
10	95	5
15	25	75
20	95	5
35	95	5

2.2.4.c. Fluorescence spectrometer

Other than EnSpire® multimode plate reader, Cary Eclipse Fluorescence Spectrometer can also be applied for fluorescence measurement, especially when the volume sample was limited. A special

quartz cuvette was required to conduct this measurement. This study used a fluorescent spectrometer to detect free FAD in putative bacterial AA3 samples. As much as 60 μL of the sample was needed and the setting for this purpose was as follow:

Table 2-21 Measurement of free FAD in fluorescence spectrometer

Excitation	450 nm
Emission	485 – 1000 nm
Ex slit	10 nm
Em slit	20 nm
Voltage	650 V
Speed	2400 nm / min
Average time	0.05 seconds
Interval	2 nm

Determination of FAD using this approach can only be possible when FAD can be removed from the enzyme-FAD complex. One method to release the FAD from the enzyme was by precipitating the enzyme itself and measuring the free-FAD in the supernatant. Therefore, this approach could work when FAD is not covalently bound to the enzyme, otherwise, covalently-bound FAD will be precipitated together with the enzyme. Precipitation can be conducted by incubating enzyme with known concentration and 5% final concentration of trichloro acetic acid (TCA). The solution should mix well for 5 minutes and followed with centrifugation for 2 minutes at 13,500 rpm. Supernatant was used to measure the FAD occupancy in that particular enzyme concentration.

Result and Discussion

Contents

3. Results and discussion

It's not the destination, it's the journey - Ralph Waldo Emerson

3.1. Heterologous expression of bacterial flavin-dependent oxidreductases and their activities.

3.1.1. Expression of putative GMC flavoprotein oxidoreductase in *Escherichia coli*

In this study, we limited the number of model organisms from Actinomycetes with fully sequenced genomes, which were shown to harbour genes encoding peroxidases, laccases, and carbohydrate oxidoreductases. Phylogenetic tree for these model organisms was constructed, namely from the genera *Streptomyces*, *Amycolatopsis*, and *Kitasatospora* (Figure 3-1). Putative enzymes for recombinant expression were selected based on constructed phylogenetic tree. In general, putative flavoprotein oxidoreductases from bacterial sources cluster with either pyranose oxidase or with cholesterol oxidases/dehydrogenases. Both are flavin-dependent enzymes and share common structural fold as glucose-methanol-choline (GMC) superfamily (Sützl *et al.*, 2019; Wongnate & Chaiyen, 2013). Referred to phylogenomic study (Sützl *et al.*, 2019), pyranose oxidase is only one of GMC proteins present in both fungi and bacteria (Bauer *et al.*, 2022), and to date, there is only limited information on bacterial pyranose oxidase (Herzog *et al.*, 2019; Kostelac *et al.*, 2022; Mendes *et al.*, 2016). The approach used in this study was not necessarily targeting other bacterial pyranose oxidase, but rather exploring other AA3 enzymes with open possibility of discovering another pyranose oxidase.

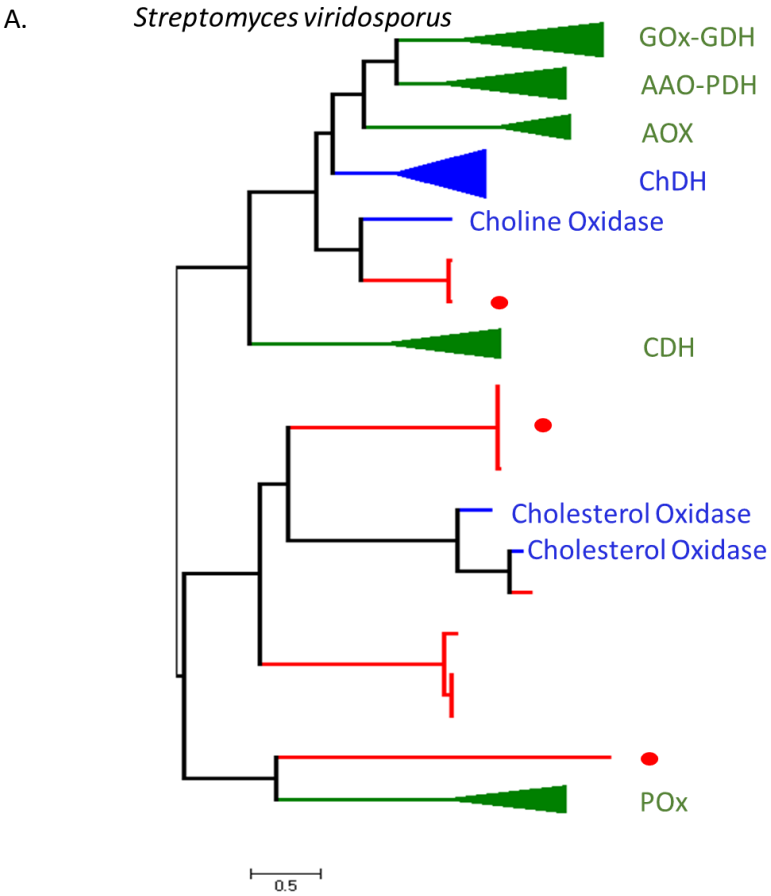

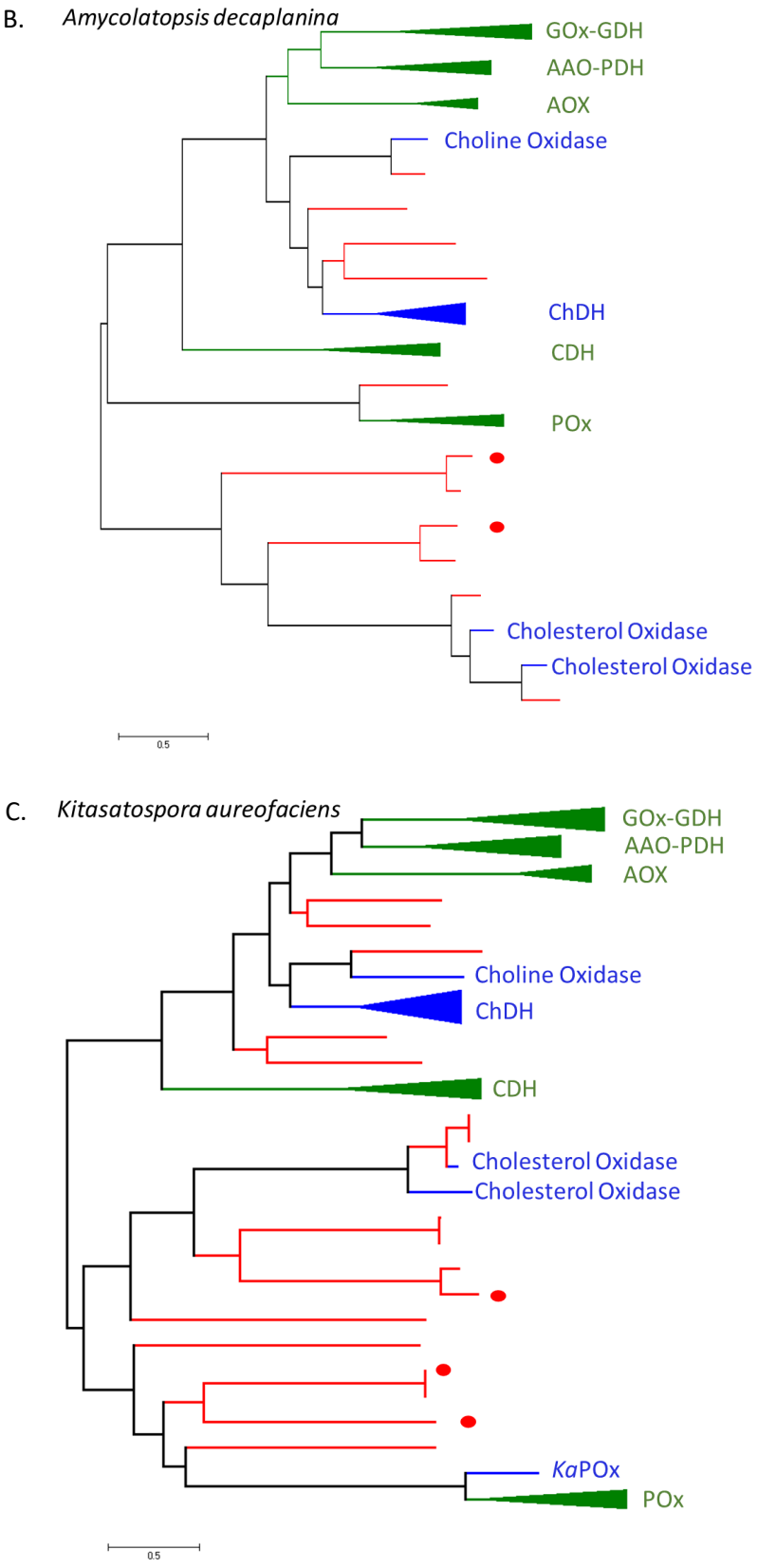

Figure 3-1 Phylogenetic tree of Glucose - Methanol - Choline (GMC) Oxidoreductases derived from *Streptomyces viridosporus* (A), *Amycolatopsis decaplanina* (B), and *Kitasatospora aureofaciens* (C). Characterized fungal genes showed in green, characterized bacterial gene showed in blue, and uncharacterized bacterial gene showed in red. Selected genes showed by the red dot.

In total 8 uncharacterized putative GMC family oxidoreductase were selected (Table 3-1).

Table 3-1 Selected bacterial GMC Oxidoreductase genes

Species	Code	Protein	size (Kda)	pI
K. aureofaciens	Ka12	GMC-oxidoreductase	61.4	6.5
	Ka75	Multispecies GMC family oxidoreductase	65.6	5.74
	Ka97	Multispecies GMC family oxidoreductase	65	9.16
A. decaplanina	Ad18	GMC family oxidoreductase	62	8.74
	Ad47	GMC family oxidoreductase	59.7	5.69
S. viridosporus	Sv27	GMC family oxidoreductase	52.8	5.13
	Sv45	GMC family oxidoreductase	59.6	6.3
	Sv64	GMC family oxidoreductase	65.2	9.07

3.1.1.1. Expression in pET system

Recombinant enzyme expression was conducted using *Escherichia coli* T7 express as host and pET21D with its T7 promoter as expression vector. Due to limited information on substrate specificity, success rate on expressed enzyme was determined by SDS-PAGE (Figure 3-2).

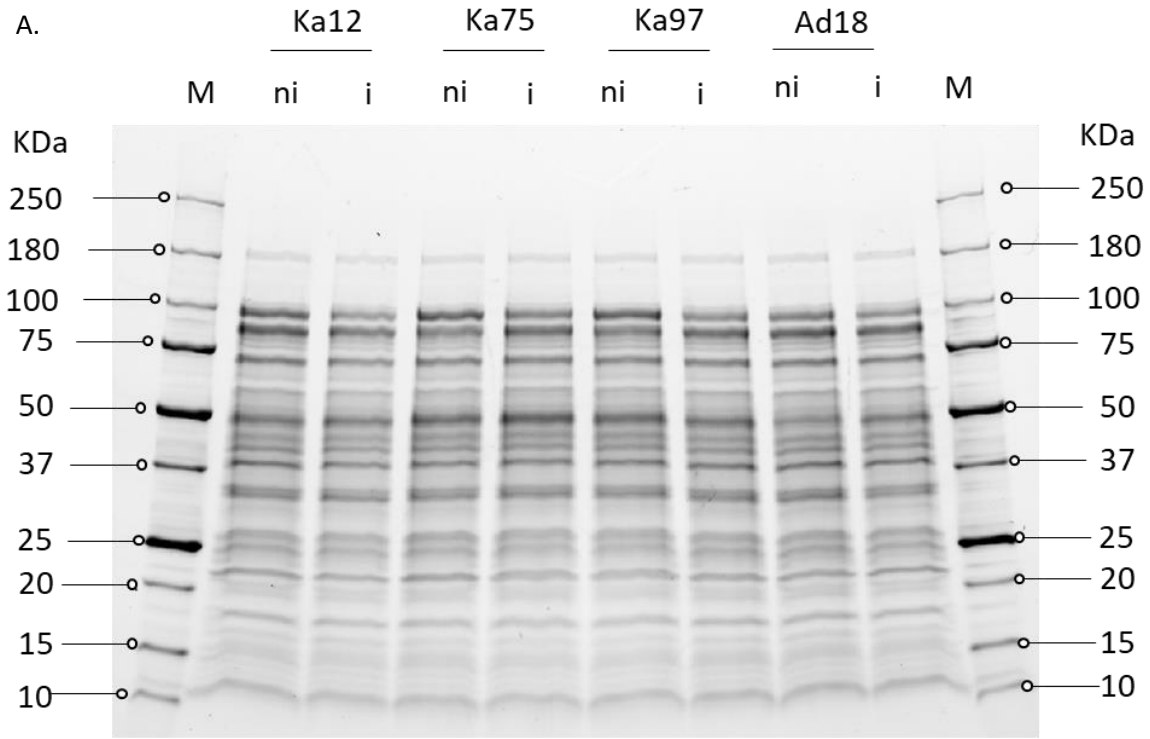

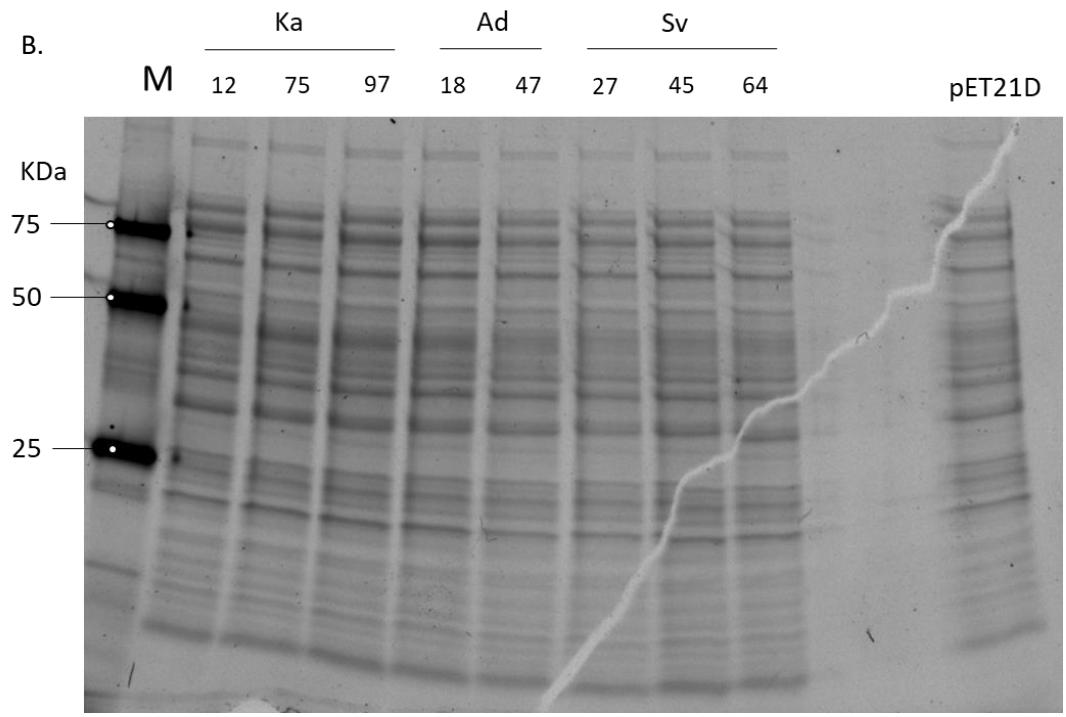

Figure 3-2 SDS PAGE profile of 8 selected GMC oxidoreductase genes. Comparison on non-induced (ni) and induced (i) was showed in (A) for Ka12, Ka75, Ka97, and Ad18. Profile of all induced samples was showed in (B) together with empty vector (pET21D). Marker was showed in M.

The SDS-PAGE outcome showed no significant bands in the expected sizes compared to negative control (non-induce culture or empty vector). This suggested there was no over-expression or there was hardly even recombinant expression. A more sensitive analysis such as Western blot, was required (Figure 3-3) to ensure whether the expression occurred.

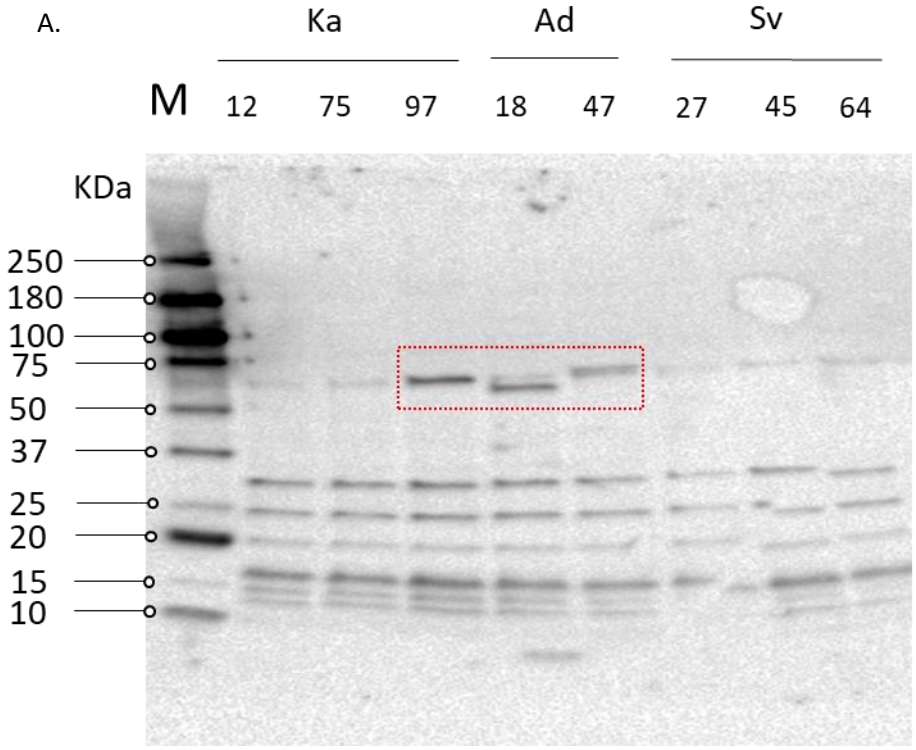

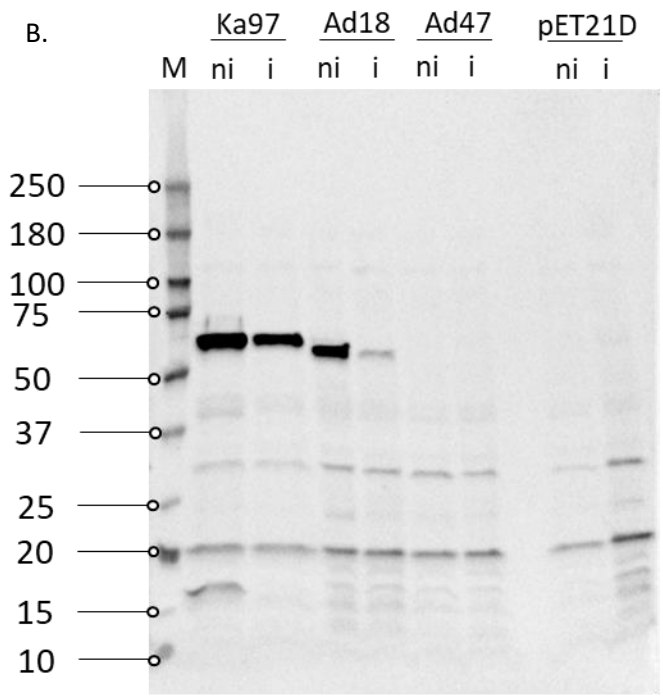

Figure 3-3 Western blot profile using His-Tag antibody of all selected genes (A). Expected target bands from 3 samples (Ka97, Ad48, and Ad47) were showed in red box. Comparison between non-induced (ni) and induced (i) of those 3 respected samples were showed in (B) with empty vector pET21D as negative control.

The generated signal from Western blot (Figure 3-3A) suggested 3 out of 8 samples were expressing the target genes, however further Western blot analysis (Figure 3-3B) revealed only 2 of them, namely Ka97 and Ad18 expressed the targeted gene. Interestingly, expression of the recombinant enzymes happened regardless of induction treatment. Moreover, the non-induced culture showed more expression compared with the induced one which was unexpected and raised some questions.

In general, the inducible system is preferred in the biotechnological applications (Kallunki et al., 2019), and for *E. coli* the most commonly used is pET system. Expression of pET system depends on T7 RNA Polymerase availability, and the presence of T7 RNA polymerase is driven through *lacUV5* or *lac* promoter (Dubendorfft & Studier, 1991; Rosenberg *et al*., 1987.; Studier & Moffatt, 1986; Tabor, 2000; Tabor & Richardson, 1985). The pET system employed either T7 or T7*lac* promoter, the latter possessing *lac*O, which binds to *lac*I repressor, and was used in pET21D (this study). Therefore, expression using this system required IPTG or lactose as inducer. Nonetheless, leakage due to basal expression of T7 RNA polymerase is commonly occurred (Du *et al*., 2021; Dubendorfft & Studier, 1991; Krefft *et al*., 2022). Hence, regarding our case, detected targeted band in non-induced sample was not too surprising, although not expected nor intended.

A leaky expression can be explained and also occurred in other studies, yet it cannot explain why non-induced culture generated more expression compared to induced one. We can only speculate that induction boosts up the expression level, however these two putative enzymes were not easily folded in *E. coli*, which builds up stress on host cells (Frank *et al*., 2012; James *et al*., 2021). Therefore, most of the expressed yet unproperly folded recombinant enzymes were degraded (Widmann & Christen, 2000). On the other hand, for non-induced culture, leaky expression occurred on a basal level, where presumably the stress reaction of the cells was only moderate and folding to a functional conformation could occur more frequently (Frank *et al*., 2012; Tegel *et al*., 2011). Inclusion body is one

of the indications where protein is not properly folded (Terol *et al*., 2021; Mitraki & King, 1989; Strandberg & Enfors, 1991), a quick look at this issue is shown in Figure 3-4.

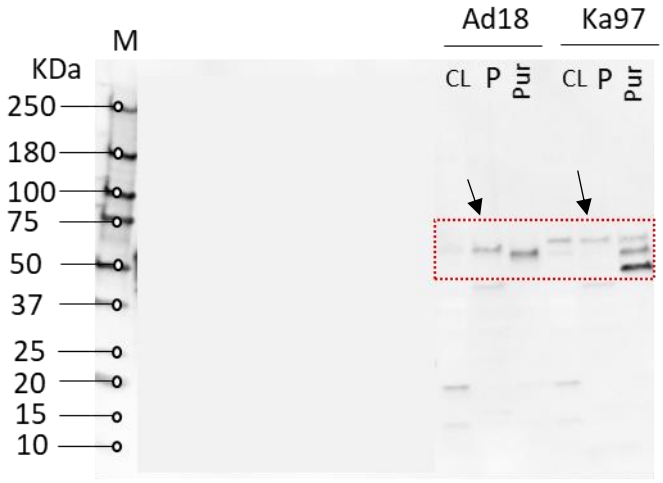

Figure 3-4 Western blot profile of Ad18 and Ka97 to see inclusion body. Cell lysate = CL, Pellet = P, and Purified fraction = Pur. Inclusion body showed in pellet (P) sample marked with arrow.

Western blot profile for investigation of inclusion bodies revealed both Ka97 and Ad18 underwent aggregation. Based on the signal given by the His-tag antibody, Ad18 showed more aggregation compared to Ka97. Successfully purified Ka97, however, is prone to partial degradation.

It is also reported (Dvorak *et al*., 2015; Wurm *et al*., 2016), that IPTG induction, although delivering strong expression, however, increases the probability of mis-folding of expressed protein, as the accumulation of translated peptide chains is actually too high. Since there was no difference in expression level between IPTG and lactose as an inducer (Figure 3-5), therefore induction with lactose was chosen in this report to prevent a higher probability of mis-folding.

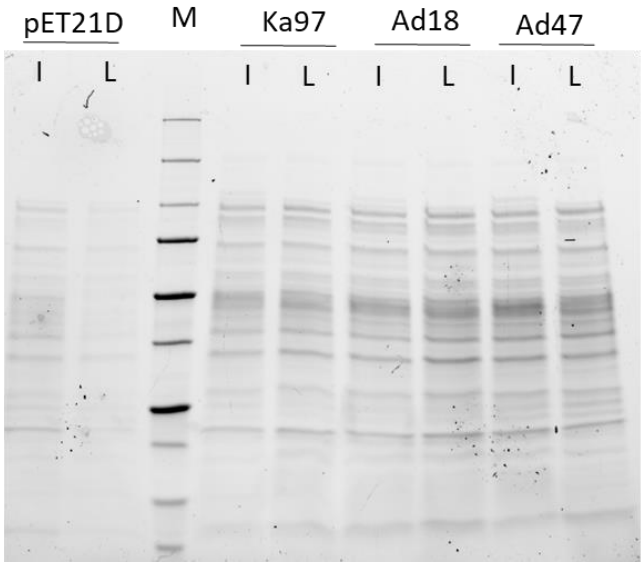

Figure 3-5 Comparison of expressed protein using IPTG (I) as inducer and lactose (L). Marker showed in M and empty vector (pET21D) as control.

3.1.1.1.a. Purification with IMAC

The expression vector pET21D encodes an optional His-tag on the C-terminus of expressed proteins, thus, purification using Immobilized Metal Affinity Chromatography (IMAC) was considered

a straight forward method to gain pure protein. The purified protein is required for further enzyme characterization, especially when the intracellular expression is conducted, such as in this study. There are lots of indigenous intracellular proteins derived from host cells which can interfere with enzymatic activity assay, for instance the presence of *E. coli* nitro / quinone reductase (NfsA), which has proposed role of protecting cells from oxidative stress by converting quinones to hydroquinones (Day *et al*., 2021; Hall *et al*., 2020). Quinone is also one of several potential substrates for our recombinant proteins. Ergo, purification was required to rule out a false positive result.

Aside from availability of general protocols for IMAC protein purification, some proteins might require modification and optimization of the purification process (Boivin *et al*., 2013; Lee *et al*., 2007). For instance, the composition of lysis / binding buffer used (Wingfield, 2015); method of crude extract preparation, such as cell disruption process by chemical disruption (utilizing detergent), french press, glass beads, or sonicator (Becker *et al*., 1996). One of the putative enzymes, Ka97, was employed to examine which cell disruption method is suitable in this study. Western blot profile of purified Ka97 generated from either french press or sonication method was shown in Figure 3-6. While different pH and binding buffer compositions used for the purification of Ka97 were shown in Figure 3-7.

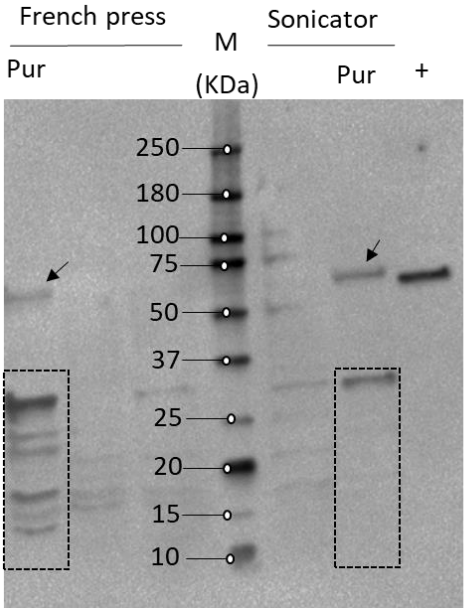

Figure 3-6 Comparison of Western blot profile of Ka97 between cell disruption method. Targeted band of purified enzyme (Pur) showed in black arrow, impurities showed in black box, marker showed as M, and positive western blot control labelled as (+).

Western blot profile of purified Ka97 derived from french press showed more impurities or degraded signal than sonicator. Although more impurities could imply better disruption, nonetheless, the signal of the expected band was better when sonication was applied for cell disruption. Therefore, sonication was selected for the next lysis procedure.

Binding buffers with three different pH was tested on Ka97, and the outcome from SDS-PAGE or Western blot showed pH 7 gave the most promising result compared to pH 8 and pH 7.5, as the targeted band appeared sharpest here. As for the other putative enzyme, Ad18, purification was conducted at pH 7 and 7.5 (Figure 3-8). Based on SDS-profile, pH 7 was also preferred for the next purification.

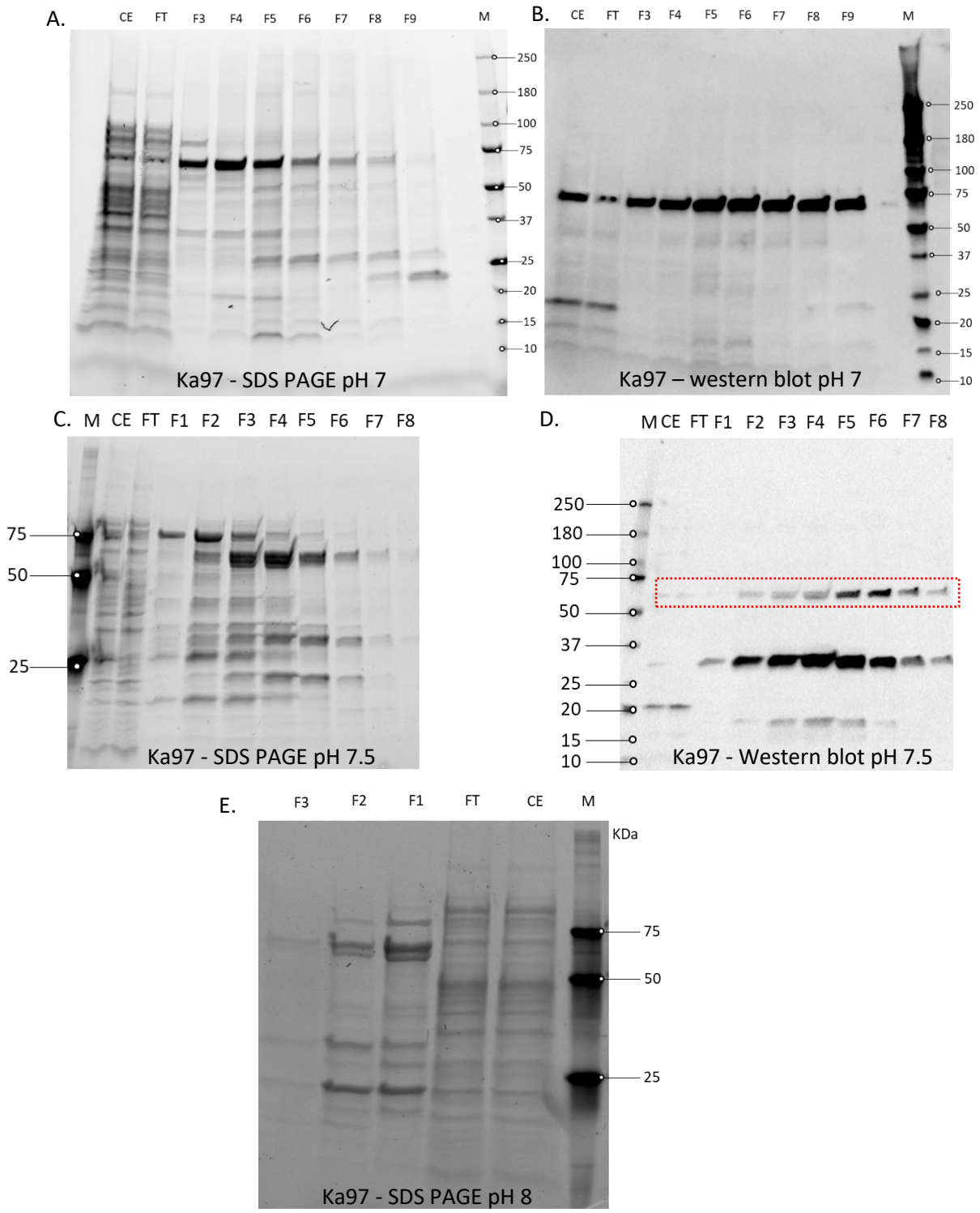

Figure 3-7 Comparison of binding buffer for IMAC purification. Purified Ka97 in 50 mM potassium phosphate (KPP) buffer pH 7 (A for SDS PAGE and B for Western blot), 50 mM KPP buffer pH 7.5 (C for SDS PAGE and D for Western blot), and 50 mM Tris buffer pH 8 (E). Marker was labelled as M in KDa, crude extract (CE), Flow-Through (FT), and purified fraction (F#).

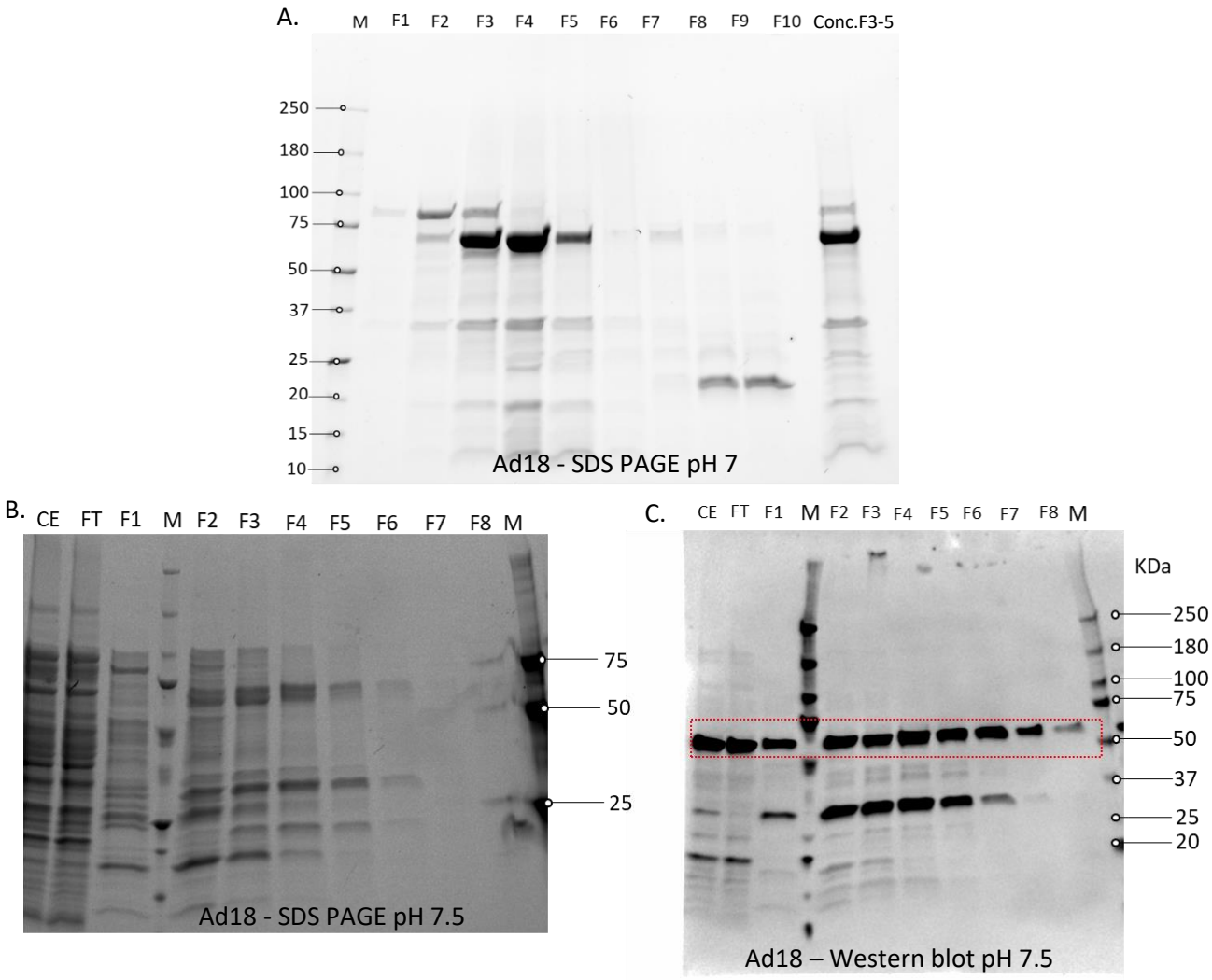

Figure 3-8 Purified Ad18 in 50 mM potassium phosphate (KPP) buffer pH 7 in SDS PAGE (A), and 50 mM KPP buffer pH 7.5 (B for SDS-PAGE and C for western blot). M = Marker (KDa), CE = Crude extract, FT = Flow-Through, and F# = Purified fraction. Targeted band in western blot profile showed in red box.

Poor expression and purification yield of both Ad18 and Ka97 raised the question of whether the expressed and detected enzymes correspond to our target enzymes. Thus, analysis using mass spectrometry was used to verify this question. Mass spectrometry results (supplementary material Figure S1 and Table S1) showed that both expressed and detected enzymes were our targeted enzymes. However, they were not the dominant enzymes found. These findings corresponded with the SDS-PAGE and Western blot results, where recombinant enzyme can be expressed in *E. coli*, however the yield was very low, as it was not visible on SDS-PAGE but only detected with western blot analysis.

Purification of Ka97 from 7.3 gr Wet Cell Weight (WCW) generated 0.4 mg/mL of semi-pure recombinant enzyme whereas the concentration of semi-purified Ad18 using the same purification step was 0.184 mg/mL. These preparations were employed to conduct preliminary substrate screening for both Ka97 and Ad18.

3.1.1.1.b. Enzyme activity

Both Ka97 and Ad18 are annotated as oxidoreductase enzymes, which require suitable electron donors and electron acceptors for their activities. Screening for both substrates was conducted

simultaneously using the acquired semi-purified enzymes mentioned above, and the results showed in Table 3-2 and Figure 3-9.

Table 3-2 Screening of electron acceptor for Ka97 and Ad18

Electron acceptor	*Ka97*	*Ad18*
Oxygen	-	-
2,6-Dichlorophenolindophenol (DCPIP)	-	-
Thionine	-	-
Methyl green	-	-
Ferrocenium hexafluorophosphate (Fc)	+	-
1,4 Benzoquinone (BQ)	-	+
1,4-Naphthoquinone	-	-
2,6-Dimethoxybenzoquinone	-	-
2,6-Dimethylbenzoquinone	-	-
3,5-Di-tert-butyl 1,2-benzoquinone	-	-
9,10 Phenantherequinone	-	-
Methyl-1,4 Benzoquinone	-	-

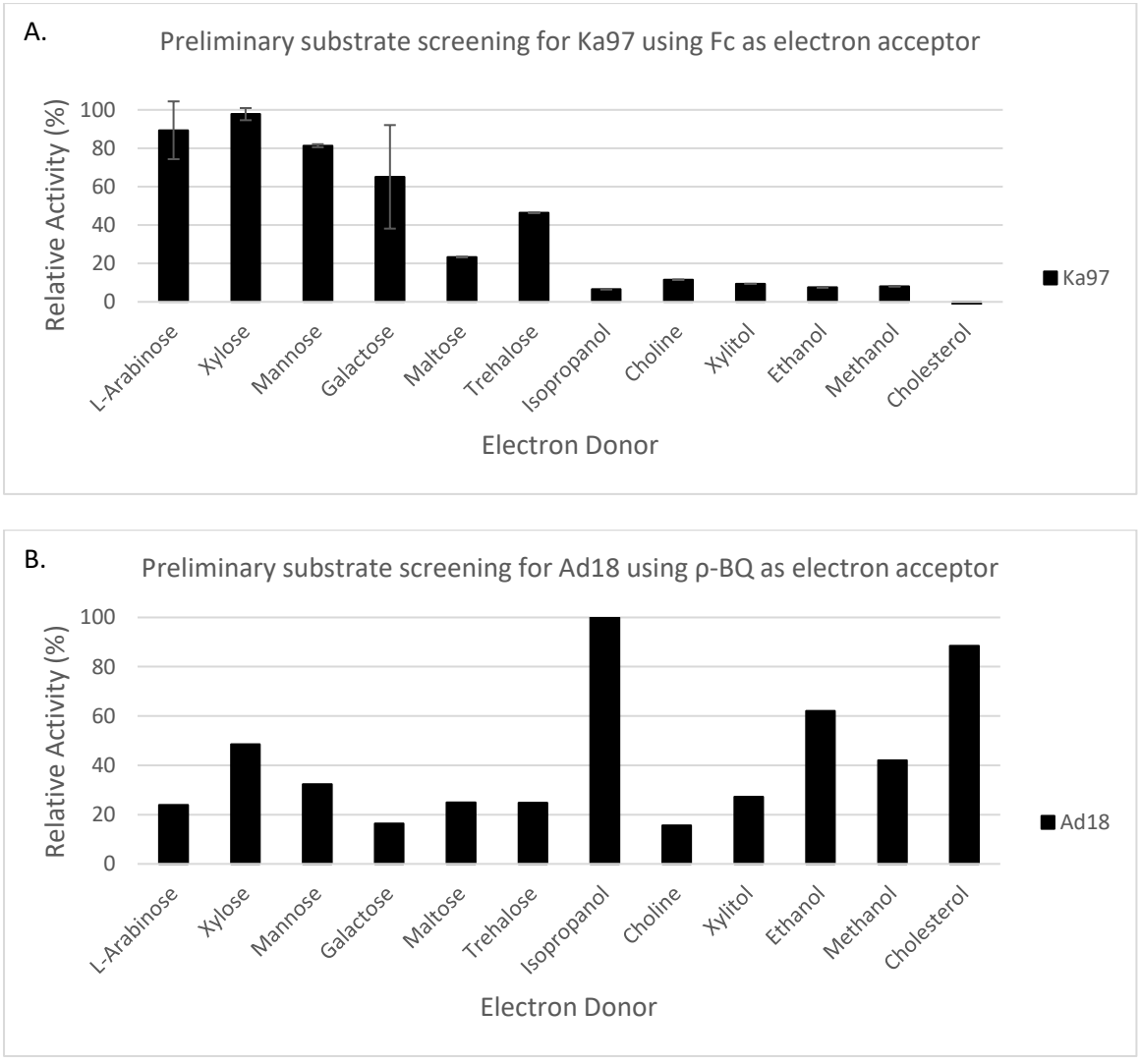

Figure 3-9 Screening of electron donor of Ka97 (A) and Ad18 (B)

Screening on electron acceptor showed that both Ka97 and Ad18 cannot utilize oxygen as an electron acceptor, and preferred other molecules like Ferrocenium (Fc) and *p*-benzoquinone (BQ) for Ka97 and Ad18, respectively. Therefore, both enzymes are considered to have dehydrogenase activity rather than oxidase activity. As for electron donor preferences, Ka97 shows activity towards monosaccharides, especially xylose, arabinose, and mannose. These monosaccharides are known as major hemicellulose components in the plant cell walls (Lojkova *et al*., 2020). When Fc was used as an electron acceptor, the specific activity of Ka97 towards xylose was 2.07 U/mg ± 0.64, followed by L-arabinose at 1.84 U/mg ± 0.21, and for mannose was 1.71 U/mg ± 0.46. Combination of xylose and Fc was used to determine pH optimum of Ka97 (Figure 3-10).

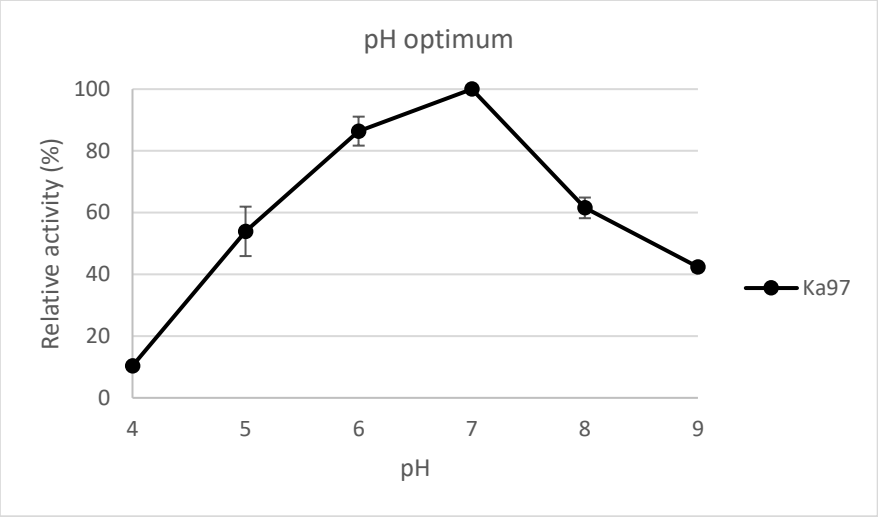

Figure 3-10 Profile of pH optimum for Ka97. Acetate buffer was used to cover pH 4 and 5, potassium phosphate buffer was used for pH 6 and 7, and Tris-HCl buffer was used for pH 8 and 9.

The optimum pH for Ka97 was pH 7 using potassium phosphate buffer and it still had around 87% relative activity in pH 6. In more acidic conditions at pH 5 and 4, the enzyme only had around 50 % and 10% relative activity, respectively.

Screening on electron donors for Ad18 showed that isopropanol, cholesterol, and ethanol were preferred over sugar (Figure 3-9B). Nonetheless, even with isopropanol, which gave the highest relative activity compared to other tested substrates, the enzymatic activity of Ad18 was considered very low. Thus, further substrate screening for Ad18 was conducted and limited to alcohol and aryl alcohol (Figure 3-11).

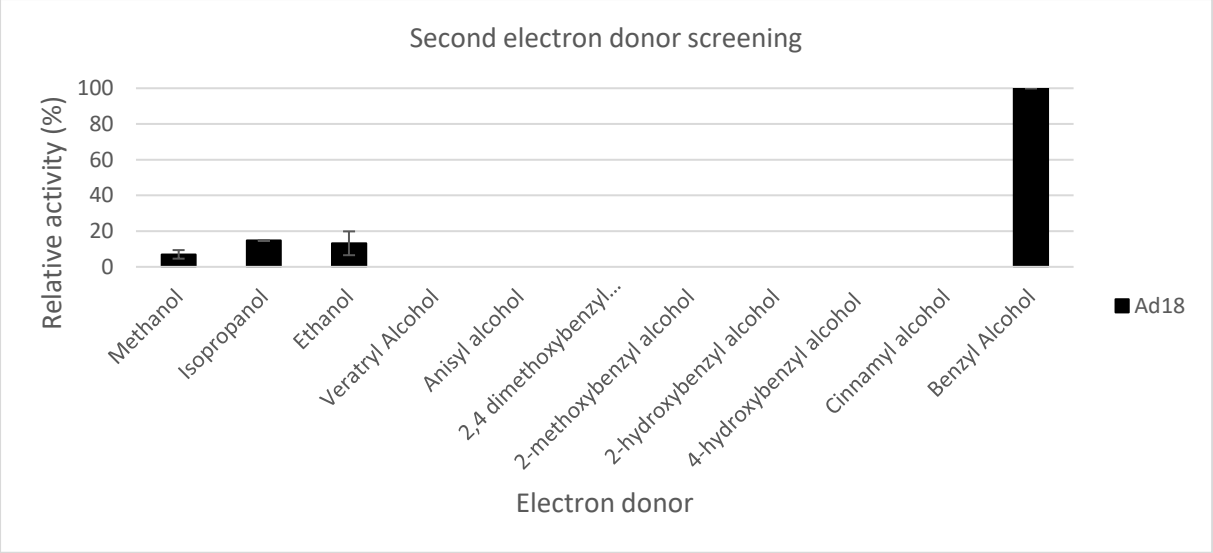

Figure 3-11 Second screening step for electron donor of Ad18

In the second screening step, Ad18 showed promising result towards benzyl alcohol, which is known as model for lignin derived alcohols (Stucchi *et al*., 2020). This screening step was conducted using a spectrophotometer, which followed the reduction of electron acceptor, *p*-benzoquinone to hydroquinone, at UV spectrum 290 nm. Under this condition, only benzyl alcohol can be measured. This was due to the spectrum of benzyl alcohol and its predicted oxidized product, benzyl aldehyde, which do not interfere with the hydroquinone signal, whereas other screened aryl alcohol substrates have a spectrum that overlaps with the hydroquinone signal (supplementary material Figure S2). Nonetheless, when reactions with veratryl alcohol and anisyl alcohol were measured at 330 nm and 310 nm, respectively (Lappe *et al*., 2021; Pedersen, 2018.; Tien & Ma, 1997), still Ad18 it did not show enzymatic activity towards these molecules.

The first screening to determine substrate preferences was based on a spectrophotometer, following the electron acceptor reduction. HPLC analysis was used to monitor depletion of substrate or to observe product formation to verify the enzyme activity on the electron donor (Figure 3-12).

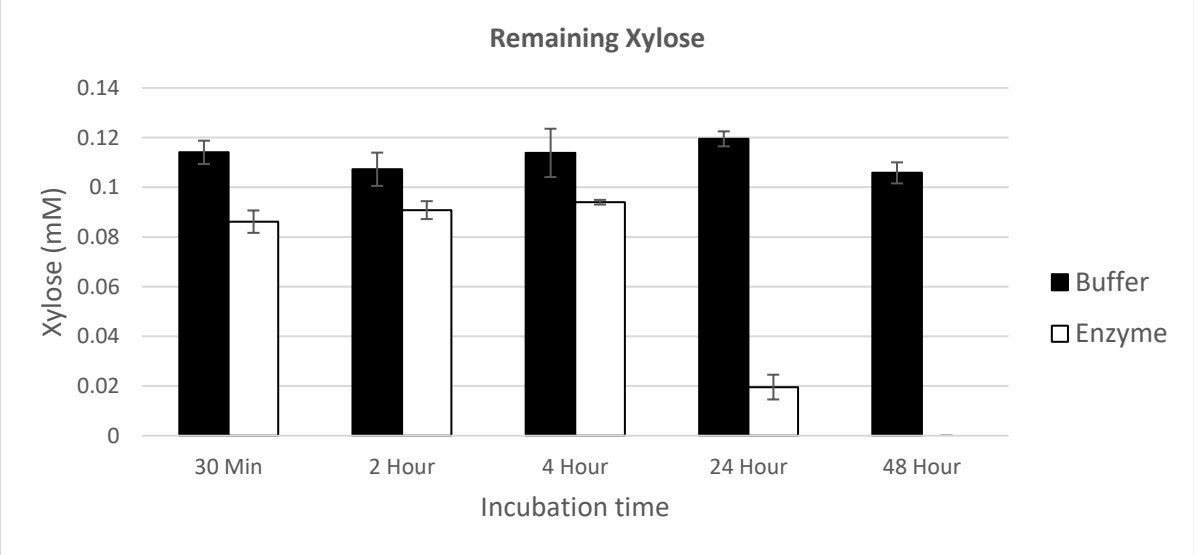

Figure 3-12 HPLC analysis to monitor substrate (xylose) depletion for Ka97

Analysis of enzyme reactions by HPLC was limited to the most promising substrate worked for each enzyme, xylose for Ka97, and benzyl alcohol for Ad18. Unfortunately, we could not detect either depletion or product formation of benzyl alcohol upon reaction with Ad18. However, we could follow the depletion of xylose when Ka97 was present in the reaction. Therefore, Ka97 was verified to have enzymatic activity towards xylose in the presence of ferrocenium as an electron acceptor.

Despite the fact that Ka97 was observed to react with xylose based on spectrophotometer and HPLC, it was noted that Ka97 required more than 24 hours to fully oxidize 0.1 mM xylose. A high concentration of xylose was also required to determine the reaction velocity, indicating several possibilities: (1) xylose is not the natural substrate of Ka97, (2) the amount of properly folded and active Ka97 was very low. In order to investigate the latter possibilities, Flavin Adenine Dinucleotide (FAD), a co-factor of AA3 enzymes, was measured.

The spectrum of FAD could not be detected in purified Ka97 and Ad18. This was not too surprising because amount and purity level of purified enzymes were low. However, FAD can exist not only in protein-bound form, but also as free FAD (Islam *et al*., 2013). Since FAD is auto-fluorescent, a more sensitive analysis to detect free FAD using fluorescence spectrophotometer could be employed as shown in Figure 3-13 (Kolenc & Quinn, 2019). Free FAD measurement was conducted by precipitating the protein; therefore, this measurement is feasible when FAD is not covalently bound to protein. In this study, free FAD from Ka97 and Ad18 can be detected with this analysis, which suggested the FAD was not covalently bound to the proteins. The concentration of free FAD detected in 1 mg / mL of Ka97 and Ad18 was 0.126 µM, and 0.37 µM, respectively. A very rough estimation on the FAD occupancy for Ka97 was 0.8% and 2.9% for Ad18. Although the FAD occupancy could not be determined precisely, it can give the overview that the incorporation of FAD into the enzyme was low, which explained the low activity of Ka97 and Ad18. Yet, detected free FAD through this analysis confirmed Ka97 and Ad18 are AA3 enzymes with non-covalently linked FAD.

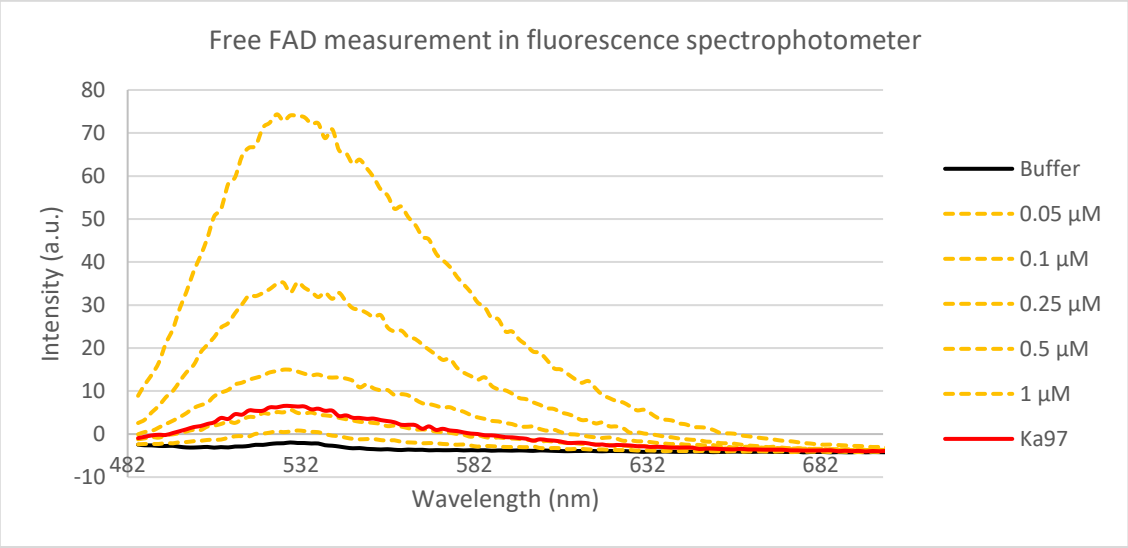

Figure 3-13 Free FAD measurement with fluorescence spectrophotometer. Free FAD with various concentration (yellow dotted line) was used as standard curve, buffer (black line) was used as negative control, and sample from Ka97 showed in red line.

The pET expression system in *E. coli* could generally express 2 out of 8 putative AA3 enzymes screened in this study. This system did not deliver over-expression of Ka97 and Ad18, but obtained purified enzymes were adequate to conduct enzymatic assay which focused on screening of substrate

specificity. Based on generated data from the analysis conducted above, the main challenge in this study was the expression yield and FAD occupancy of recombinant enzymes. For both these challenges, improperly folded expressed protein was thought to be the issue (Terpe, 2006). Therefore, another expression system, pMALc2e, was tested (Gopal & Kumar, 2013).

3.1.1.2. pMAL expression system

Commercially available expression vector pMAL, employs the maltose binding protein (MBP) which is fused to the targeted protein. Maltose binding protein enable proper folding of target protein and also increases solubility (Lebendiker & Danieli, 2017; Pennati *et al*., 2014). A prediction for protein solubility was conducted using SoluProt 1.0 (https://loschmidt.chemi.muni.cz/soluprot/), where a value above 0.5 indicates soluble expression. Predicted solubility of Ka97 and Ad18 were compared between pET system and pMAL system as shown in Table 3-3.

Table 3-3 Predicted solubility of Ka97 and Ad18

	Solubility	
	pET	pMAL
Ka97	0.220	0.909
Ad18	0.207	0.911

The outcome from SoluProt suggested that both Ka97 and Ad18 were not soluble when expressed in *E. coli*, however when fused with MBP, they were predicted to be soluble, as the value increased from 0.2 to 0.9 for both enzymes. Expression for these constructs was analysed in SDS-PAGE (Figure 3-14).

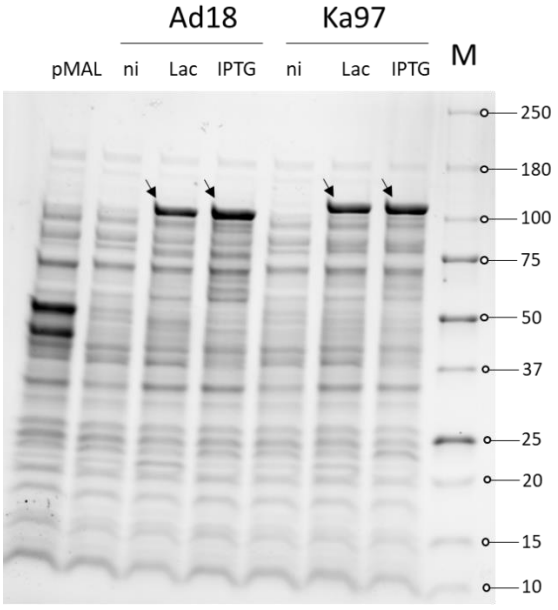

Figure 3-14 SDS-PAGE profile of Ka97 and Ad18 fused with maltose binding protein. Targeted protein pointed with black arrow. Empty vector (pMAL) and non-induction (ni) were used as negative control. Induction was conducted using lactose (lac) and IPTG. Marker was labelled as M.

The result from SDS-PAGE showed that by fusing with MBP, the solubility of both targeted proteins increased and, in the end, generated a higher expression level compared to expression using pET system. Maltose binding protein has a molecular weight of 40 KDa, thus, the fusion protein of Ka97 has

a total size of 107.9 KDa and for Ad18 was 104.5 KDa. In order to test enzyme activity, a purification step using amylose resin was conducted.

3.1.1.2.a. Purification of MBP fused protein

In principle, two steps purification was required to obtain pure protein from pMALc2e construct. The first purification step is removing other impurities from the fusion protein, in which affinity chromatography using MBP takes place. Prior to the second purification step, the purified fusion protein was cleaved by a suitable protease, breaking the linkage between MBP and the target protein. The second purification step is to remove the cleaved MBP (Figure 3-15).

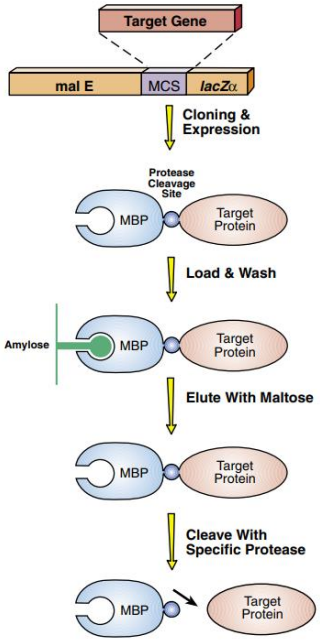

Figure 3-15 Purification scheme of pMALc2e construct
(http://wolfson.huji.ac.il/purification/PDF/Expression_Systems/NEB_Maltose.pdf)

In the first purification, amylose resin was used to bind with MBP, then a buffer containing maltose was used for elution. Evaluation of yield and purity level after purification was conducted using SDS-PAGE as shown in Figure 3-16.

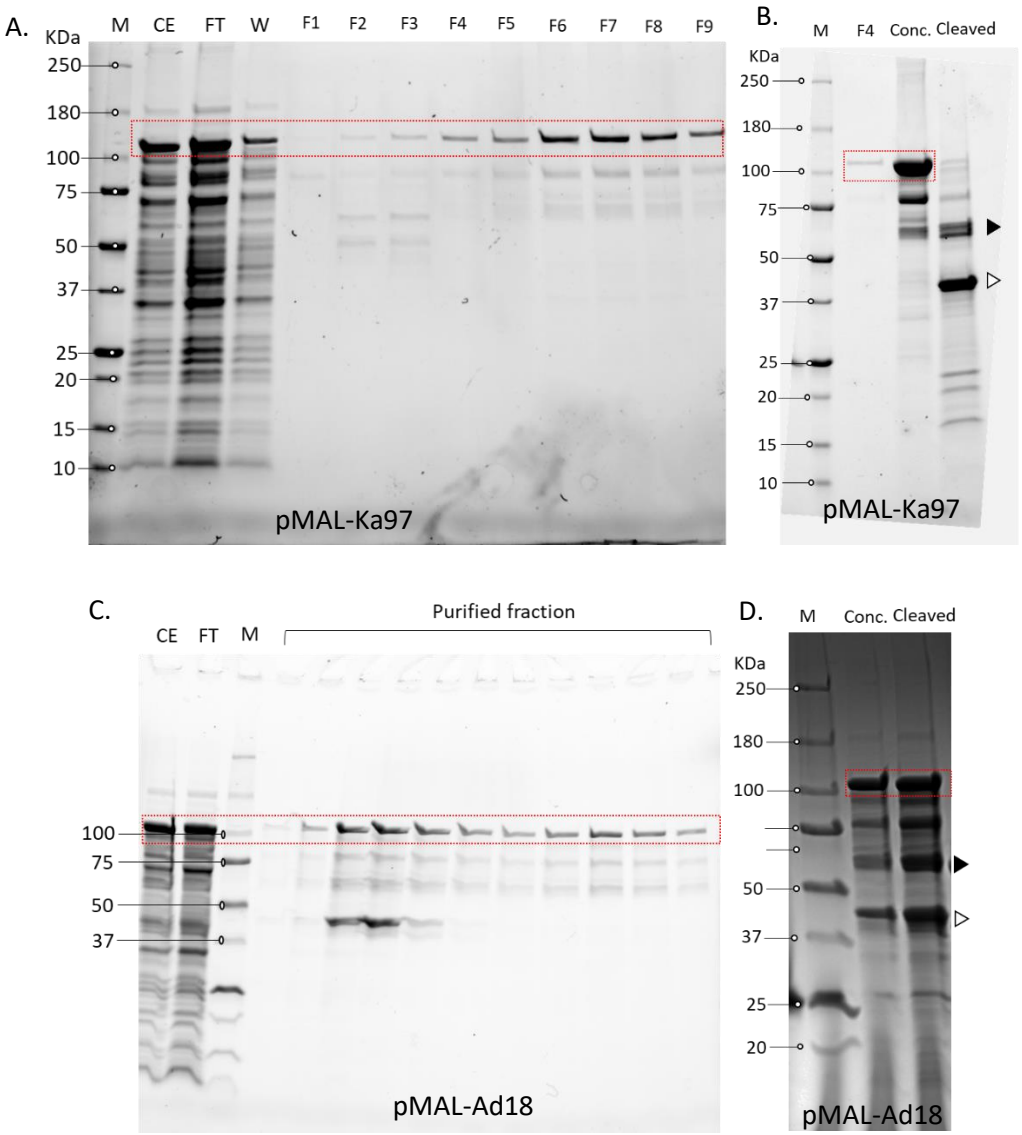

Figure 3-16 SDS-PAGE profile of purified and cleaved fusion protein. Purified fusion protein of MBP-Ka97 (A) and MBP-Ad18 (C). Cleaved fusion protein MBP-Ka97 (B) and MBP-Ad18 (D). Concentrated of purified fraction labelled as Conc. Fusion protein treated with enterokinase labelled as Cleaved. Fusion protein indicated in red box, targeted protein indicated in black arrow, and MBP indicated in white arrow. M = marker, FT = Flow through, W=Wash, and F# = purified fraction.

Results from SDS-PAGE showed that fusion protein MBP-Ka97/Ad18 was successfully purified with much better purity compared to non-fused counterparts derived from pET system. The detected band of the expected size in FT indicated the loaded fusion proteins exceeded the binding capacity of the column, or binding affinity between MBP and resin was reduced due to passenger protein (Costa *et al*., 2014; Pryor & Leiting, 1997). The suspected MBP band (40 KDa) on the purified fraction (Figure 3-16C) and concentrated sample (Figure 13-6D), indicated fusion MBP-Ad18 was truncated prior to enterokinase treatment. When treated with enterokinase (Figure 3-16D, cleaved), both Ad18 and MBP showed a more intense band, yet enterokinase failed to cleave all fusion MBP-Ad18.

Unlike Ad18, fusion protein MBP-Ka97 did not show the MBP band in the purified fraction (Figure 3-16A, F1-9), nor in a concentrated sample (Figure 3-16B, Conc.). When treated with enterokinase (Figure 3-16 B), most of the fusion MBP-Ka97 was cleaved into ~65 KDa and ~40 KDa, which were the theoretical size of Ka97 and MBP, respectively. However, the intensity of Ka97 band

was less than MBP, which could be a sign of the occurring degradation of Ka97 once cleaved from MBP. Moreover, additional new bands around 18 – 22 KDa occurred after enterokinase treatment, supporting this hypothesis.

At this step, we decided to focus on Ka97 because gained data so far suggested that Ka97 showed more promising enzymatic activity and purification process was considered more successful compared to Ad18, despite issues such as degradation occurring. Therefore, further purification to remove MBP was only conducted for Ka97 (Figure 3-17).

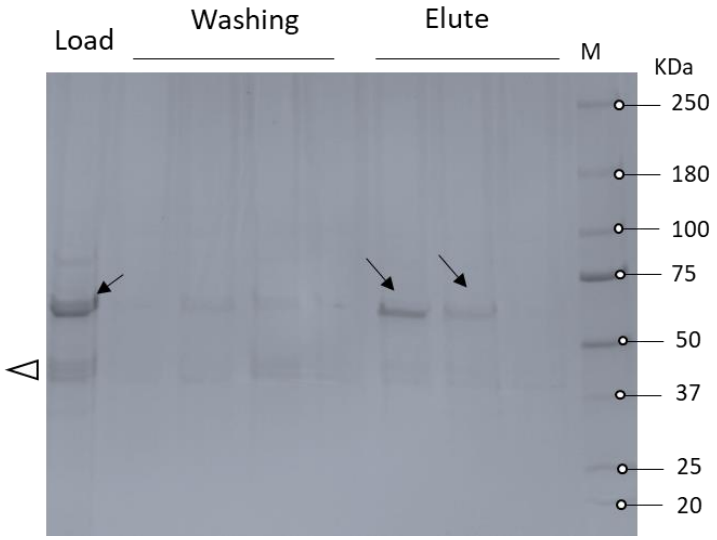

Figure 3-17 SDS-PAGE profile of second purification for pMAL-Ka97. Two bands prior to purification showed in Load were Ka97 (indicated in black arrow) and MBP (white triangle). Purified Ka97 band was shown in Elute, mark with black arrow. Marker labelled as M.

Anion exchange chromatography (AEX) was used for second step purification, and outcome from SDS-PAGE showed Ka97 was the dominant band after elution. Unfortunately, when the assay to determine enzyme activity was conducted, we could not detect any activity. Prior to the second purification, the enzyme activity assay was also conducted for fusion protein MBP-Ka97, and cleaved MBP-Ka97. From these 3 conditions, only cleaved MBP-Ka97 without further purification could deliver activity towards xylose. This enzyme activity was measured in spectrophotometer and resulted in 0.65 U/mL ± 0.05, the highest value observed so far.

We speculate that the presence of MBP at the N terminal position in the fusion proteins might hinder the enzyme-substrate encounter. This issue was also reported in another study (Dälken *et al*., 2010), where un-cleaved fusion MBP-Granzyme B resulted in inactive enzyme. Inactive fusion proteins with MBP are, however, not omnipresent and tend to depend on the passenger protein. For instance, CD45 fused MBP restores its activity due to the interaction between MBP and the passenger protein (Lorenzo *et al*., 1997). Another study on the influences of MBP on the activity of the fused enzyme (Momin *et al*., 2019) showed the possibility that the passenger sequence could promote interlaced dimers of the MBP. This possibility appears not likely in our case, but cannot be ruled out entirely.

In the case of no enzyme activity after AEX, the conditions used in this purification step might result in inactive Ka97 (Goheen & Gibbins, 2000; Goheen & Hilsenbeck, 1998). Additionally, the yield of enzyme tends to become lower with more required purification steps (Amersham Pharmacia Biotech, 1999). It is worth mentioning that post-cleavage of the fusion protein MBP-Ka97, the passenger protein was less stable and showed a tendency for degradation, which was explained previously in Figure 3-

16B, and also observed in occurring precipitation. Precipitation of proteins after MBP was cleaved off was also observed in other studies (Duong-Ly & Gabelli, 2015; Nominé *et al*., 2001; Raran-Kurussi & Waugh, 2012; Saavedra-Alanis *et al*., 1994), when the proteins were hard to express due to a tendency for insolubility or mis-folding issues in the first place.

This finding supported our hypothesis that most of the expressed Ka97 in *E. coli* was not properly folded and eventually led to an inactive enzyme. Expression as a fusion with MBP increased the solubility which is shown in Figure 3-14, yet, no activity could be detected from the intact fusion protein. In addition, once MBP was cleaved, Ka97 was unstable and precipitated. All acquired data suggested solubility itself could not guarantee the active and proper folding of the target protein (Nominé *et al*., 2001; Sachdev & Chirgwin, 1998). Therefore, besides interference of the N-terminal MBP with the enzyme-substrate encounter, the remaining folding problems of Ka97 in its fusion form could be an explanation for the lack of activity of MBP-Ka97.

The effort to enhance the folding of Ka97 into an active conformation either in its native form or as an MBP-Ka97 fusion protein was conducted by adding chaperon-encoding plasmids, namely pGro7 and pG-KJE8 (Nishihara *et al*., 1998, 2000; Takara Bio Inc). Unfortunately, no difference in both expression and enzyme activity after the co-expression of chaperones could be observed.

3.1.2. Comparison to other characterized pyranose oxidases

We were interested in the phylogenetic distance between these 2-novel putative AA3 enzymes with other characterized bacterial AA3 enzymes. To date, only a few bacterial AA3 enzymes have been characterized and all of them are pyranose oxidases, namely *As*POx from *Pseudoarthrobacter siccitolerans* (Mendes *et al*., 2016), *Ka*POx from *Kitasatospora aureofaciens* (Herzog *et al*., 2019), and *Sc*POx from *Streptomyces canus* (Kostelac *et al*., 2022). A phylogenetic tree comparing Ka97 and Ad18 with characterized bacterial AA3 enzymes is shown in Figure 3-18.

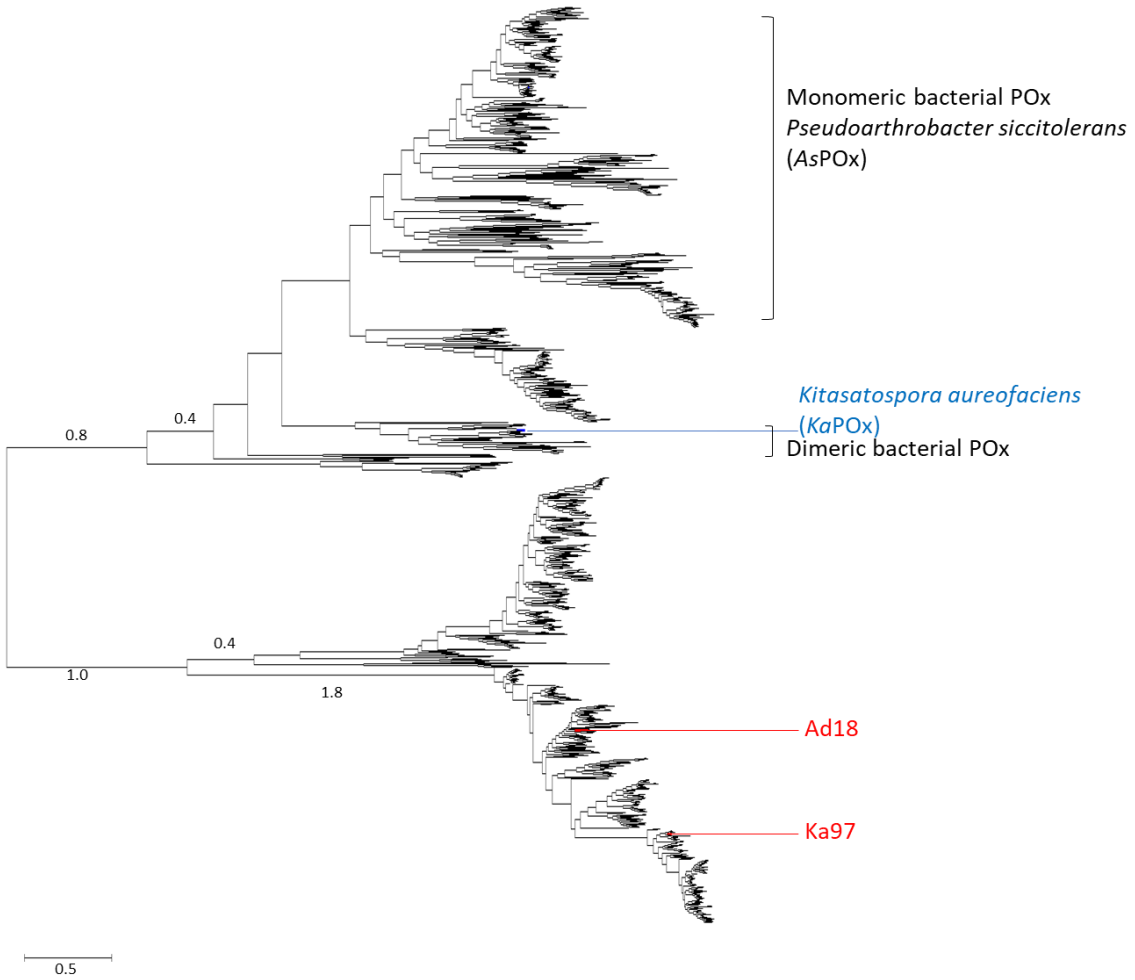

Figure 3-18 Phylogenetic tree comparing Ka97 and Ad18 with characterized bacterial pyranose oxidase (POx).

The phylogenetic tree showed that Ka97 and Ad18 are not very distant from each other, but are located in a different clade compared to other known bacterial POx.

3.2. Subcellular localization of Pyranose 2-Oxidase from *Kitasatospora aureofaciens*

3.2.1. Signal peptide prediction

The *Kitasatospora aureofaciens* (*K. aureofaciens*) genomic sequence upstream of the coding region of *Ka*POx was analyzed using ORF Finder: https://www.ncbi.nlm.nih.gov/orffinder/ (accessed on November 2019), and two Met residues were discovered upstream and in frame with the previously annotated start codon (Figure 3-19). These additional sequences amount to 63 amino acids starting from the first and 44 amino acids starting from the second encoded Met residue. These sequences were analyzed using TatP-1.0 (Bendtsen *et al*., 2005) https://services.healthtech.dtu.dk/service.php?TatP-1.0 (accessed on November 2019). The longer sequence comprising 63 AA was classified as unlikely to be a Tat signal peptide, but part of the 44 AA sequence was found to score above the cut-off in all but one category. The potential signal peptide cleavage site was predicted to be between positions 36 and 37 (Figure 3-20).

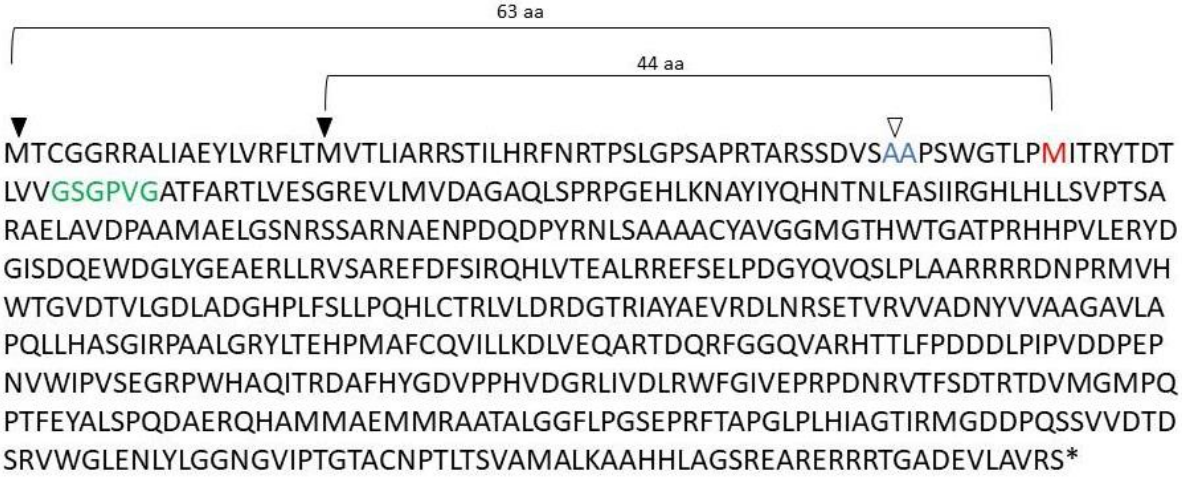

Figure 3-19 Results from ORF Finder showing two Methionine (M) in frame in the upstream region (filled triangles), followed by the previously annotated start codon (M in red). The putative cleavage site is shown in blue with an open triangle. The Rossman fold motif is shown in green.

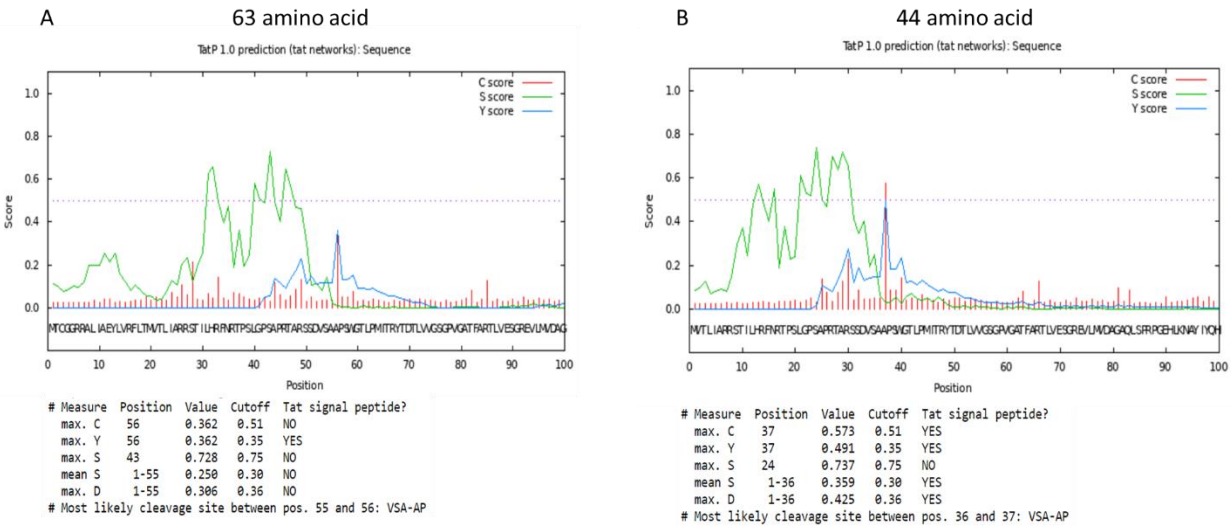

Figure 3-20 Signal peptide prediction using TatP-1.0 for the additional upstream 63 amino acids (A) and 44 amino acids (B).

3.2.2. Heterologous expression of *KaPOx* with a putative signal peptide

Here we expressed pyranose oxidase from *K. aureofaciens* (*Ka*POx), a bacterial enzyme from the family Auxiliary Activities 3 (AA3), in the two Gram-positive bacterial expression systems *B. subtilis* and *S. lividans*. We used constructs containing *Ka*POx, as previously expressed intracellularly in *E. coli* and characterized (Herzog *et al*., 2019), as well as constructs containing the genomic sequence encoding additional 44 amino acids upstream of and in frame with the previously characterized coding sequence and also starting with an ATG.

3.2.2.a. Bacillus subtilis

To investigate whether the 44 AA upstream of the originally annotated ATG of *Ka*POx constitute a functional signal peptide as predicted, constructs with and without this additional sequence (SPKaPOxHis and KaPOxHis, respectively) were prepared and heterologously expressed as described. Expression in *Bacillus.subtilis (B. subtilis)* did not result in detectable levels of secreted protein with either construct, but the His-tagged protein was detectable in the cell extract by Western blotting (Figure 3-21). Protein purification by affinity chromatography was possible from the cell extract, but not from the supernatant. Yields of purified protein were considerably lower from the extract of cultures expressing the SP*Ka*POxHis construct (Figure 3-21).

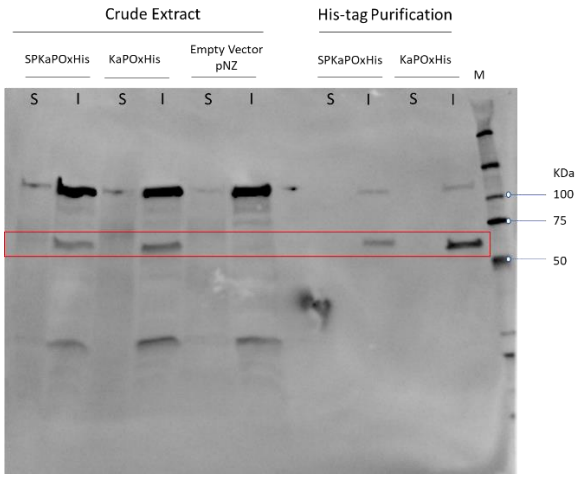

Figure 3-21 Western blot of samples from *B. subtilis* expression system harbouring SP*Ka*POxHis, *Ka*POxHis, and the empty pNZ vector in un-purified form (crude extract) and purified form (His-tag purification). Sample from supernatant are indicated as S, samples from the cell extract are indicated as I, the Western blot marker is marked as M. Expected molecular weight of targeted protein was 60 KDa (shown in red box).

3.2.2.b. Streptomyces lividans

Expression in *S. lividans* was carried out using the constitutive promoter P_{vsi} and pIJ486 as plasmid backbone (Figure 3-22). Secreted *Ka*POx could be detected in the supernatant of *S. lividans* carrying the construct with the putative SP by enzymatic assay at a volumetric activity of 0.01 U/mL (dehydrogenase activity; Figure 3-23) as early as 48 h after start of the cultivation.

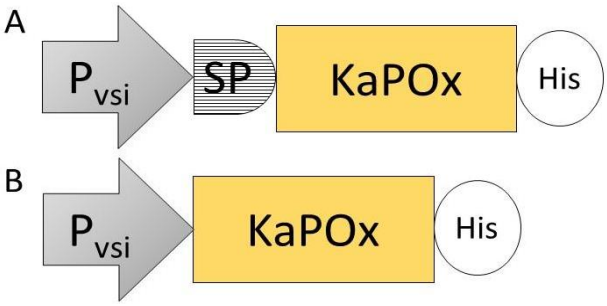

Figure 3-22 Expression constructs SP*Ka*POxHis (**A**) and *Ka*POxHis (**B**), containing the constitutive promoter of the *S. venezuelae* subtilisin inhibitor gene (P_{vsi}), the putative signal peptide (SP) identified upstream of the mature domain of pyranose oxidase from *K. aureofaciens* (KaPOx) and a C-terminal 6× His-tag (His).

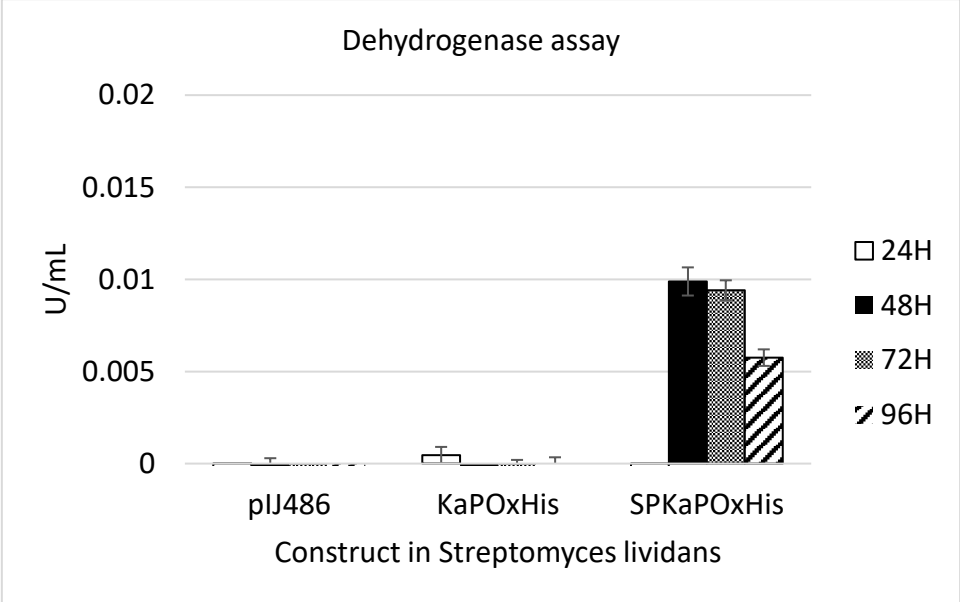

Figure 3-23 Dehydrogenase activity assay of *S. lividans* supernatant obtained from cultures harboring the empty vector pIJ486, pIJ486-KaPOxHis, and pIJ486-SPKaPOxHis. Samples were taken from the supernatant at 24, 48, 72 and 96 h (H) as indicated.

The construct with the putative signal peptide showed dehydrogenase activity towards glucose as the electron donor and ferrocenium hexafluorophosphate as the electron acceptor. The volumetric dehydrogenase activity was low at 0.01 U/mL, and oxidase activity could not be detected. Herzog *et al*. (2019) showed a 6.6-fold dehydrogenase activity with ferrocenium hexafluorophosphate compared to oxidase activity with molecular oxygen as electron acceptor for recombinant *Ka*POx produced in *E. coli*. Considering the low dehydrogenase activity of secreted *Ka*POx produced in *S. lividans*, we conclude that oxidase activity is probably below the detection limit.

3.2.3. Fusion protein

Translational fusions of the fluorescent mono-Red Fluorescent Protein (mRFP) C-terminally of *Ka*POx with a 6×His-Tags added C-terminally of mRFP were constructed (Figure 3-24). Both fusion constructs (SP*Ka*POxmRFPHis and *Ka*POxmRFPHis) were expressed in *S. lividans* under the control of the P_{vsi} promoter (Figure 3-25)

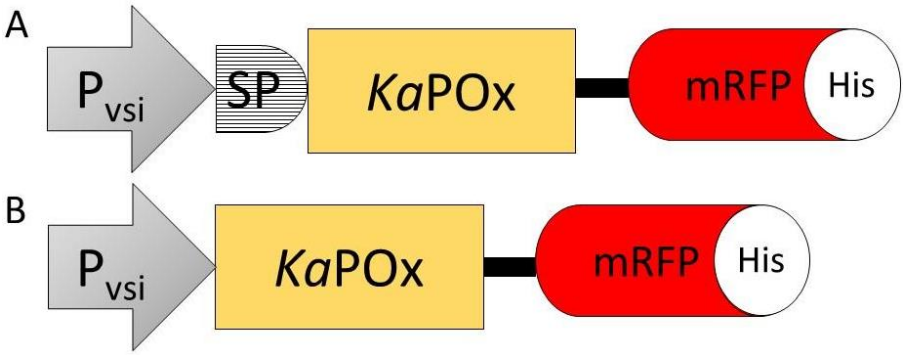

Figure 3-24 Constructs SP*Ka*POxmRFPHis (A) and *Ka*POxmRFPHis (B) containing the constitutive *S. venezuelae* P_{vsi} promoter (P_{vsi}), the putative signal peptide (SP), the *Ka*POx mature domain, the mRFP fluorescent protein (mRFP) and a C-terminal 6×His-Tag (His).

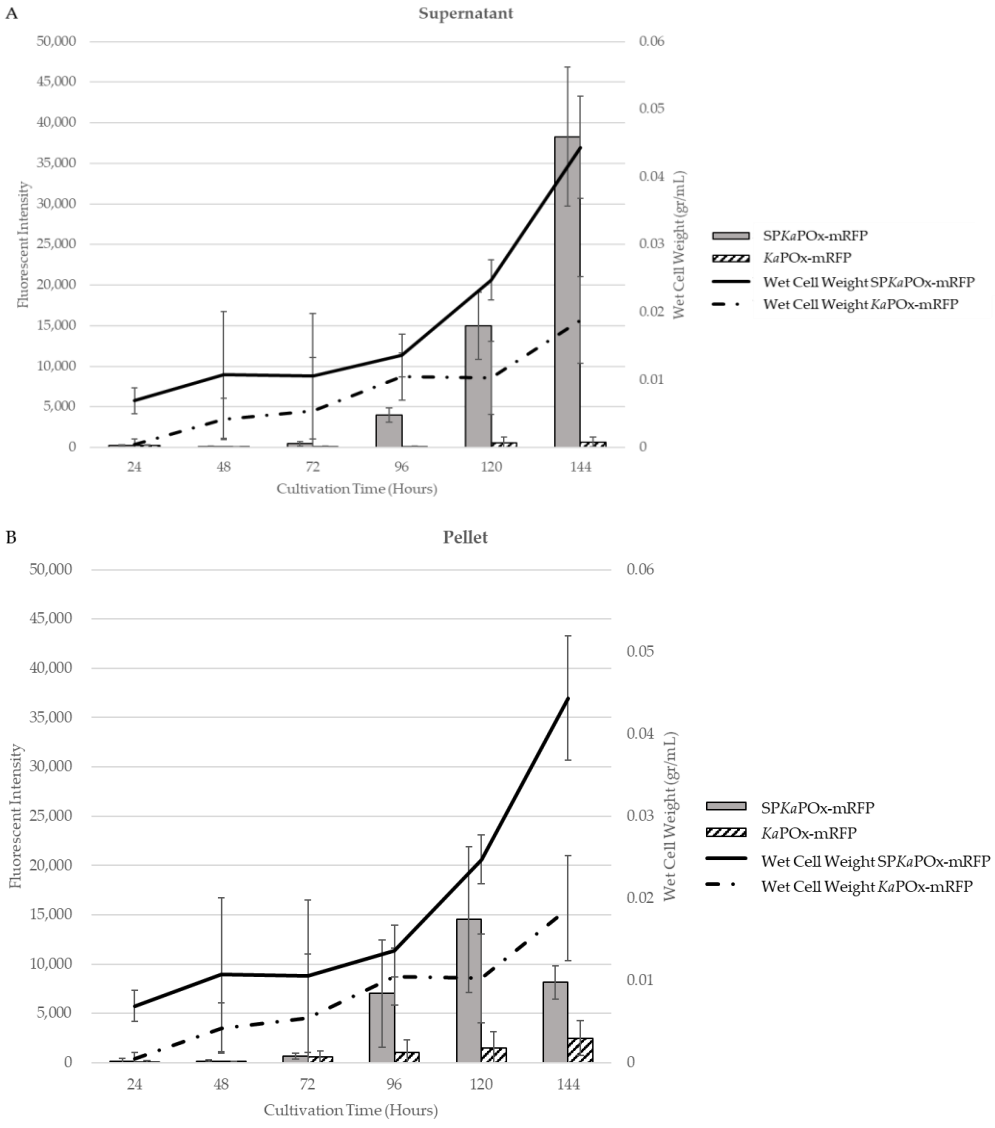

Figure 3-25 Growth curve (in wet cell weight) and mRFP fluorescence intensity from cultures expressing the fusion constructs SP*Ka*POxmRFPHis and *Ka*POxmRFPHis in the supernatants (A) and the pellet fractions (B). Fluorescent intensity values are adjusted for the reco recorded wet cell weight and are the mean results of three cultures.

Fluorescence was detected in the cell pellets starting at 72 h in cultures of both constructs. The intensity increased until the end of cultivation at a very low level for cultures harboring *Ka*POxmRFPHis; for cultures harboring SP*Ka*POxmRFPHis a stronger increase was measured until 120 h, followed by a decline at 144 h. In the culture supernatants, SP*Ka*POxmRFPHis showed a very low level of fluorescence at 72 h that constantly increased in intensity until 144 h, and was always higher than the intensity in the cell pellet except very early after initial detection (Figure 3-25) The supernatant from *Ka*POxmRFPHis showed a much lower fluorescence, detectable only at 120 and 144 h, which was another 48 h later after detected earliest in pellet at 72 h (Figure 3-25). The intensity of *Ka*POxmRFPHis in supernatant remained very low until the last sampling point, and significantly lower than in the cell pellets at all time points (Figure 3-25).

Wet cell weight (WCW) was monitored over time, and the obtained values were used to normalize the measured fluorescence intensity. A different growth behavior for cells harboring the different constructs was observed: cultures harboring *Ka*POxmRFPHis showed a constant but slow increase in wet cell weight, with a final value after 144 h, approximately half of that recorded for cultures of SP*Ka*POxmRFPHis, in which a marked increase after 96 h was observable.

Notably, the fluorescence intensity in the cell pellets of SP*Ka*POxmRFPHis cultures peaked at 120 h and decreased for the last sampling point at 144 h. Also notable is the different growth behavior of the cultures expressing the two different constructs: the wet cell weight of SP*Ka*POxmRFPHis and *Ka*POxmRFPHis cultures was comparable until 96 h, but increased markedly slower after this in *Ka*POxmRFPHis cultures to a maximal value of 0.08 g/mL compared to SP*Ka*POxmRFPHis cultures, which reached 0.140 g/mL. This is concomitant with the appearance of the fluorescent fusion protein in significant amounts in the supernatant. These observations suggest that, while (over)expression of both fusion constructs constitutes a metabolic burden for the cells, secretion driven by the signal peptide (and observable in the fluorescent intensity) avoids or alleviates cellular stress through the cytoplasmic accumulation of the heterologous fusion protein, resulting in healthier growth and higher biomass formation than in the cells producing fusion protein lacking the putative signal peptide, where the expressed fusion protein accumulates throughout growth.

During six days or 144 h of cultivation, the increase of wet cell weight as well as fluorescence intensity relative to WCW, increased gradually without fluctuations or abrupt changes. When monitored for longer periods (until 192 h, not shown) an onset of "plateauing" of secretory fluorescence is observable in SP*Ka*POxmRFPHis cultures, while wet cell weight continues to increase for all cultures and only starts to show a lower increase rate at the last sampling point. This suggests that the cells had not yet reached the stationary phase. Since no sudden increases in extracellular fluorescence with concomitant stagnation or loss of wet cell weight were observed, we conclude that the extracellular fluorescence is a consequence of secretion, not cell death and lysis.

It is notable that the fluorescent signal from the fusion constructs was detectable later than the enzymatic activity in the previous experiments (72 h vs. 48 h). The fusion proteins are larger at 86.5 KDa than the *Ka*POx mature domain (59.9 KDa). A late secretion for heterologous enzymes in *S. lividans* was reported for the 95 KDa xyloglucanase (Sianidis *et al*., 2006), where secretion peaked at ~120H of cultivation time. It appears plausible that *Ka*POx is secreted earlier compared to fusion proteins containing the fluorescent reporter.

3.2.4. Enzymatic activity

Enzymatic activity assays were also done on the samples from supernatants and pellets of cultures harboring both constructs. Both oxidase and dehydrogenase activity could be detected in the

pellets starting at 96 h (oxidase activity is not shown, as the values were consistently very low). In the supernatants, no activity was measurable for cultures of *Ka*POxmRFPHis. Cultures containing SP*Ka*POxmRFPHis showed low activity at 120 and 144 h (Figure 3-26A). Enzymatic activities in the cell pellet increased slowly on a low level for *Ka*POxmRFPHis cultures. In SP*Ka*POxmRFPHis cultures, activity was higher at 96 and 120 h and declined in the last sample at 144 h. It is notable that the measured activities in the pellet fractions were higher in all corresponding samples than those in the supernatants.

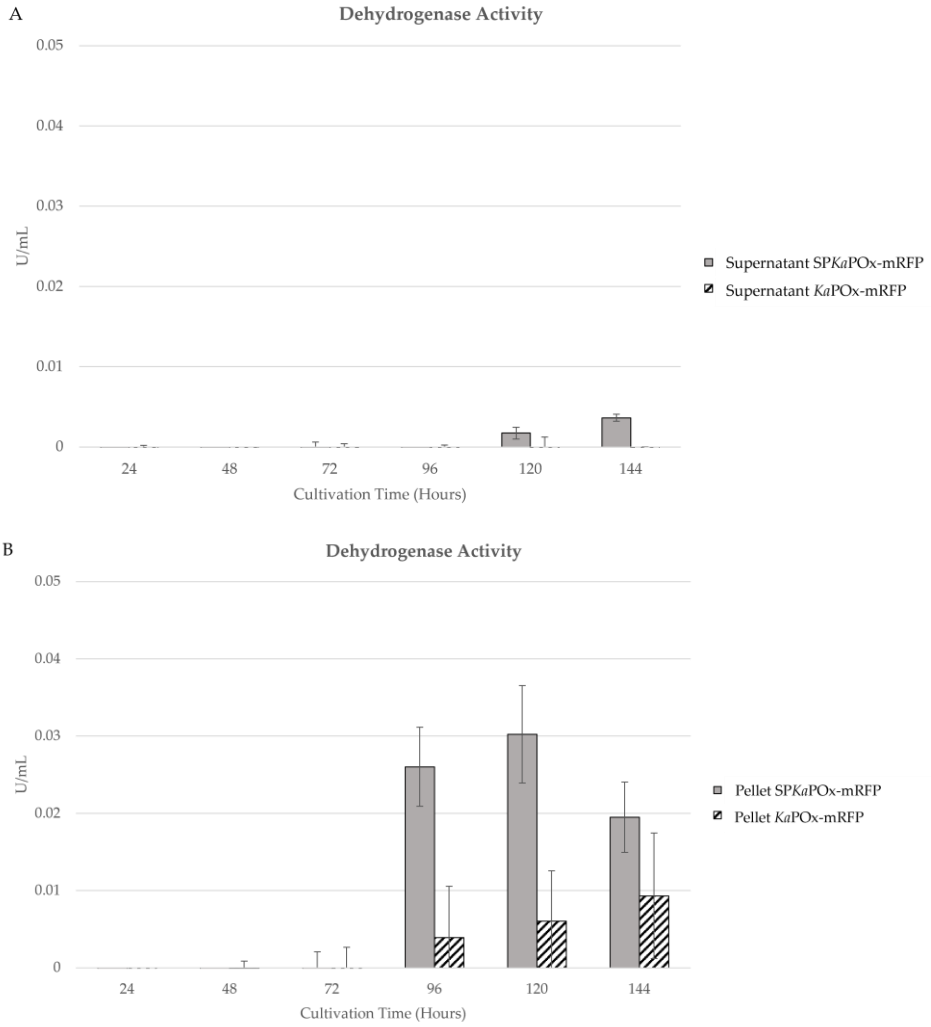

Figure 3-26 Enzymatic activity (dehydrogenase) in samples of the supernatant (A) and the pellet fractions (B) of cultures harboring SP*Ka*POxmRFPHis and *Ka*POxmRFPHis. Activity values are normalized for the recorded wet cell weight, as in Figure 3-25.

Measured enzymatic activity (dehydrogenase) in both cell pellets and supernatants of SP*Ka*POxmRFPHis and *Ka*POxmRFPHis cultures had marked discrepancies into the results of the fluorescence measurements. *Ka*POxmRFPHis cultures followed the same pattern as observed previously, with the accumulation of active enzyme in the pellet fraction and essentially no detectable activity in the supernatants. SP*Ka*POxmRFPHis cultures also showed intracellular accumulation of activity, peaking at 120 h, as did the fluorescence measurement. In the supernatants, however, the activities, while following the same pattern as in the secretory fluorescence (constant increase until 144

h), remained much lower than the measured intracellular activities. Taken by itself, this appears to argue against the secretion of active enzymes to meaningful levels.

The presence of fusion protein was detected in supernatant samples of SP*Ka*POxmRFPHis cultures by Western blot using an anti-His-tag antibody. A band corresponding to intact fusion protein is visible in the samples obtained after 72 h and after 96 h of cultivation. In both samples, a notably more intense band corresponding to a molecular weight of 27 KDa is present (Figure 3-27B). Western blot analysis of SP*Ka*POxHis derived from the supernatant is shown in Figure 3-27A.

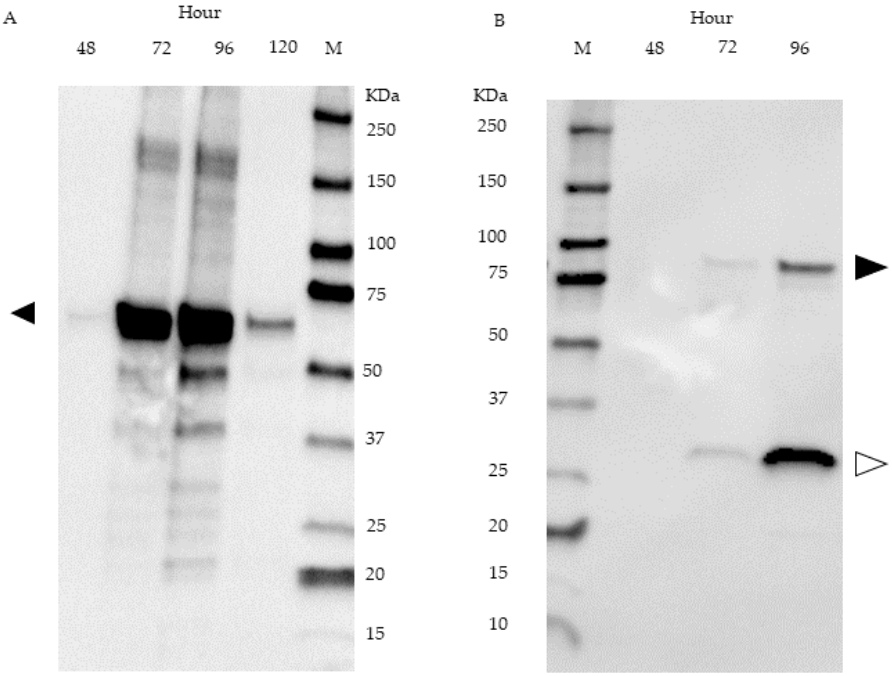

Figure 3-27 Western blot of supernatant samples from *S. lividans* cultures harboring SP*Ka*POxHis at 48, 72, 96 and 120 h (A) and SP*Ka*POxmRFPHis at 48, 72 and 96 h (B). A size marker is shown in lane M. The expected molecular weight of intact fusion protein and of the mRFP domain is 86.5 KDa (black arrow) and 26.6 KDa (white arrow), respectively.

Western blot analysis of supernatant samples revealed intact fusion protein in the supernatant, faintly in samples taken after 72 h and more prominently in samples taken after 96 h. At both time points, a more intense band corresponding to the molecular weight of mRFP (± 27 KDa) is also detected (Figure 27B). We conclude that the lower band represents the product of proteolytic cleavage of the secreted fusion protein, namely mRFP, which is detected via the attached His-tag (the rest of the protein, i.e., the *Ka*POx mature domain, is not detectable, as it does not contain a His-tag). Since mRFP is a small, compact protein composed mostly of β-sheets, it is conceivable that it is released from the fusion protein by extracellular proteases, but stays otherwise intact and fluorescent (thus detectable in the fluorescence measurements), whereas the larger oxidoreductase domain of the fusion protein may be further degraded and rendered inactive. In this case, we can presumably detect all of the secretory fluorescence, but only a fraction of the activity. The appearance of the His-tagged mRFP domain in the supernatant by another pathway, namely cell lysis and subsequent proteolysis, or intracellular proteolysis followed by cell lysis and release, is not plausible at these time points, as this would have been obvious in other parameters. According to the structural model of *Ka*POx (Herzog *et al*., 2019), the C-terminus is exposed on the surface of the Rossman domain, facing away from the active site as well

as the dimerization interface. An interference of the mRFP domain with dimerization and/or activity appears unlikely, but cannot be entirely ruled out.

Regarding the failure to detect enzymatic activity (either kind) in the experiments with *B. subtilis*, it has to be noted that the used strain NZ8901 is not optimized for extracellular protease activity (Bongers *et al*., 2005), which is known to be a major detrimental factor for the expression of heterologous proteins in this organism (Harwood & Cranenburgh, 2008; Neef *et al*., 2021). Since these early experiments were only done with SP*Ka*POxHis- and *Ka*POxHis-constructs, which do not allow fluorescent detection (and do not provide a more stable mRFP-domain that can be detected via the His-tag), it is conceivable that secretion driven by the putative signal peptide did, in fact, happen, but remained undetectable due to rapid proteolysis. Additionally, while the gene sequence was adapted to *B. subtilis* codon usage, a certain incompatibility between the signal peptide and mature domain sequences of SP*Ka*POx and the *B. subtilis* secretory machinery has to be considered. *K. aureofaciens*, which belongs to the phylum Actinobacteria and is closely related to Streptomycetaceae (Hsiao & Kirby, 2008), was previously classified as *Streptomyces aureofaciens* (Labeda *et al*., 2017), *B. subtilis* belongs to the Firmicutes, and differences between the Tat translocase complexes of *B. subtilis* (comprising two subunits, TatA and TatC) and those of *S. lividans* and other *Streptomyces* spp., which comprise three subunits (TatA, TatB and TatC), were reported (Anné *et al*., 2014; Kolkman *et al*., 2008). It is conceivable that the *B. subtilis* Tat system does not properly process the native SP from *KaPOx*.

In bacteria, Auxiliary Activities Family 3 sequences are generally closely related to fungal POx sequences rather than to sequences from other subfamilies (Herzog *et al*., 2019; Sützl *et al*., 2019). We have shown here that the pyranose oxidase from *K. aureofaciens* is very likely a secretory enzyme, which supports the discussed biological function as an Auxiliary Activity with biological roles in hydrogen peroxide provision and/or quinone redox cycling, as outlined in the Introduction. This raises the question of whether more bacterial POx-like enzymes are secretory enzymes (and whether their annotations in genome data need to be re-examined and perhaps revised). We performed a BLAST search (tblastn) using *Ka*POx as the query sequence, selected the 25 sequences with the highest similarity and query coverage where upstream sequences were available, plus the characterized enzymes from *P. siccitolerans* and *S. canus*, and examined these upstream sequences for putative signal peptide sequences as described. The results are summarized in Table 3-4: 15 out of 27 sequences extended in frame upstream of the annotated start codon. In four cases, these additional sequences were less than twelve amino acids long. In two cases (both *Streptomyces* spp.), TatP-1.0 predicted the sequence to be a signal peptide with a score of 5 out of 5. One sequence (from *Actinoalloteichus* sp., of the family Pseudonocardiaceae) of 100 additional amino acids gave more than one additional sequence, one of which was classified as possibly constituting a signal peptide. The upstream sequence of the gene from *P. siccitolerans* was predicted with a score of 3 out of 5; two more sequences (from *Streptomyces* and an *Arthrobacter* species) resulted in a score of 2 out of 5. The sequences that contain putative upstream signal peptides are distributed across several branches of a phylogenetic tree constructed from extant bacterial POx-like sequences (supplementary material Figure S3), and an allocation along taxonomic categories is not possible. It appears plausible that bacterial GMC-oxidoreductases, while generally similar to fungal POx sequences, have diversified to a range of biological functions, with some as secretory enzymes with an auxiliary activity in lignocellulose degradation, and others with a cytoplasmic location and a different biological role. Clearly these results are preliminary, and further investigations into the biochemical properties of bacterial POx-like sequences, their subcellular localization and biological function are necessary.

Table 3-4 Prediction of putative Tat signal peptide using TatP-1.0

No	Species	E Value	Per. Ident	Upstream	Length (AA)	TatP-1.0	Note
1	*Kitasatospora aureofaciens*	0	95.24	v	44	Predicted	This study
2	*Mycobacterium lacus*	0	65.19	n.d			
3	*Actinomyces* sp. Lu 9419	6.00×10^{-175}	56.75	v	101	n.d	
4	*Amycolatopsis japonica*	3.00×10^{-168}	55.29	n.d			
5	*Frankia alni* ACN14a	7.00×10^{-152}	51.06	n.d			
6	*Streptomyces sudanensis*	9.00×10^{-140}	49.01	n.d			
7	*Streptomyces davawennsis* JCM 4913	3.00×10^{-135}	48.99	v	55	n.d	
8	*Streptomyces alboniger*	8.00×10^{-139}	48.91	v	56	Predicted	TatP-1.0 score 5 out of 5
9	*Streptomyces* sp. MRC013	1.00×10^{-138}	48.74	n.d			
10	*Phytohabitans suffuscus*	4.00×10^{-102}	48.15	n.d		n.d	
11	*Streptomyces cinnabarinus*	2.00×10^{-135}	48.08	v	12	n.d	
12	*Streptomyces cyaneogriseus* subsp. *noncyanogenus*	2.00×10^{-93}	48.04	v	52	n.d	TatP-1.0 score 2 out of 5
13	*Streptomyces huasconensis*	4.00×10^{-136}	47.76	v	64	Predicted	TatP-1.0 score 5 out of 5
14	*Streptomyces tuirus*	6.00×10^{-143}	46.94	v	32	n.d	
15	*Streptomyces lusitanus*	3.00×10^{-139}	46.48	n.d			
16	*Phytohabitans flavus*	3.00×10^{-125}	46.23	n.d			
17	*Nocardiopsis* sp. Mg02	4.00×10^{-106}	38.95	v	10	n.d	
19	*Microbacterium* sp. 10M-3C3	5.00×10^{-63}	38.25	v	50	n.d	
20	*Microbacterium atlanticum*	2.00×10^{-60}	37.59	v	41	n.d	
21	*Microbacterium* sp. KUDC0405	1.00×10^{-48}	37.59	v	5	n.d	
22	*Microbacterium testaceum* StLB037	6.00×10^{-62}	37.55	n.d			
23	*Micromonospora carbonacea*	7.00×10^{-76}	37.1	n.d			
24	*Arthrobacter* sp. DNA4	6.00×10^{-59}	37.08	v	35	n.d	TatP-1.0 score 2 out of 5
25	*Actinoalloteichus* sp. AHMU CJ021	1.00×10^{-59}	37.06	v	100	Predicted	More than 1 possibility for TatP-1.0 prediction
26	*Microbacterium* sp. XT11	7.00×10^{-63}	37.02	v	10	n.d	

27	*Streptomyces canus*	9.00×10^{-61}	33.71	n.d			
28	*Pseudarthrobacter siccitolerans*	6.00×10^{-64}	34.89	v	60	Predicted	TatP-1.0 score 3 out of 5

Most fungal POx enzymes have been purified from hyphal extracts *(Ai et al., 2014; Danneel et al*., 1993; Leitner *et al*., 2001; Machida & Nakanishi, 1984), although Daniel *et al*., 1994 proposed an extracellular localization based on microscopic studies. Nishimura *et al*., 1996 expressed a cDNA from *Trametes* (*Coriolus*) *versicolor* in *E. coli* and reported that the first 38 amino acids were missing in the translated protein. Hallberg *et al*., 2004 reported that the N-terminal part of *Trametes ochracea* (*multicolor*) pyranose oxidase has an unordered conformation and is not resolvable in the crystal structure. These two enzymes show 96% identity, and both their N-terminal parts show similarities to a (bacterial) Tat signal peptide as analyzed by computational tools (TatP-1.0; supplementary material Figure S4). Pyranose oxidase has long been discussed as having been acquired by fungi from bacteria via Horizontal Gene Transfer (HGT) (Sützl *et al*., 2019). The fact that most fungal POx does not appear to be secretory enzymes (or that the Tat-SP-like sequence at the N-terminus of the *T. ochracea* and *T. versicolor* POx is not functional in fungi) does not necessarily contradict this—most lignocellulose-degrading fungi possess other enzymes for these biological functions. It is possible that different bacterial pyranose oxidase sequences were acquired by fungi on separate occasions and have diversified post-HGT for other roles.

3.3. Heterologous expression and secretion of bacterial AA3 enzymes derived from *Streptomyces alboniger* and *Streptomyces griseochromogenes*

3.3.1. Signal peptide prediction

The discovery of putative signal peptides preceding the annotated *Ka*POx (Chapter 3.2.), led us to explore other similar enzymes which could be predicted to be secreted by its putative signal peptide. An online computational tool tblastn (https://blast.ncbi.nlm.nih.gov/Blast.cgi) was employed to find regions of similarity between *Ka*POx (WP_046385855) and translated nucleotide in databases. The search for other bacterial AA3 enzymes similar to *Ka*POx was limited to 4 genera of Actinomycetes (*Kitasatospora*, *Amycolatopsis*, *Frankia*, and *Streptomyces*). In total we found 21 putative AA3 enzymes, as shown in Table 3-5.

Table 3-5 Computational analysis for Tat pathway prediction using *Ka*POx as query sequence

Species	tblastn				Upstream	TatP-1.0	
	Query cover	**E-value**	**% ID**	**Acc. No.**	start codon	**Upstream**	**Mature peptide**
Kitasatospora							
K. setae KM 6054	17%	1.7	39.62%	AP010968.1	yes	no	yes
K. albolonga YIM 101047	18%	5.1	32.05%	CP020563.1	yes	no	no
Kitasatospora sp. MMS16 - BH015	90%	3E-12	24.76%	CP025394.1	yes	no	no
Kitasatospora sp 152608	6%	3.2	41.03%	KU127235.1	no	no	no
Amycolatopsis							
A. mediterranei U32	87%	1E-57	34.51%	CP002000.1	no	no	no
A. mediterranei S699	87%	1E-57	34.51%	CP002896.1	no	no	no
A. japonica strain MG417-CF17	90%	9E-170	55.29%	CP008953.1	no	no	no
A. keratiniphila strain HCCB 10007	5%	4.5	40.62%	CP003410.1	yes	no	no
A. orientalis strain B-37	66%	2E-12	28.14%	CP016174.1	yes	no	no
Frankia							
Frankia alni strain ACN14A	87%	5E-150	50.96%	CT573213.2	no	no	no
Streptomyces							
**S. alboniger* strain ATCC1246	92%	4E-138	48.19%	CP023695.1	yes	yes	no
S. davawensis strain JCM 4913	86%	1E-133	48.99%	HE971709.1	yes	no	no

S. cyanogriseus subsp. noncyanogenus strain NMWT 1	91%	6E-92	46.42%	CP010849.1	yes	no	no
S. noursei ATCC 11455	91%	2E-60	34.94%	CP011533.1	no	no	no
S. albidoflavus strain J1074	88%	4E-55	34.84%	CP004370.1	yes	yes	no
+*S. chartreusis* strain ATCC 14922	96%	8E-55	33.52%	CP023689.1	yes	yes	no
S. aquilus strain GGCR-6	87%	5E-50	33.33%	CP034463.1	no	no	no
S. lincolnensis strain ATCC 2936	86%	3E-44	32.89%	CP016438.1	yes	no	no
S. venezuelae strain ATCC 15439	60%	7E-12	36.42%	CP013129.1	no	no	no
**S. griseochromogenes* strain ATCC 14511	42%	0.000002	37.66%	CP016279.1	yes	yes	no
S. gilvosporeus strain F607	53%	0.000006	43.94%	CP020569.1	yes	no	no
S. aquilus strain GGCR-6	17%	1.7	39.62%	AP010968.1	yes	no	yes

* This study

+ Updated locus location

A further investigation of the presence of upstream start codon(s) preceding the annotated sequences, was conducted using ORF Finder (online at https://www.ncbi.nlm.nih.gov/orffinder/) (Figure 3-28). The results of this analysis eliminated 8 candidate enzymes, which did not harbour upstream coding sequences in frame. Prediction of the functionality of additional sequences as Tat signal peptides using TatP-1.0 (https://services.healthtech.dtu.dk/service.php?TatP-1.0) was applied to the remaining 13 candidate enzymes.

A

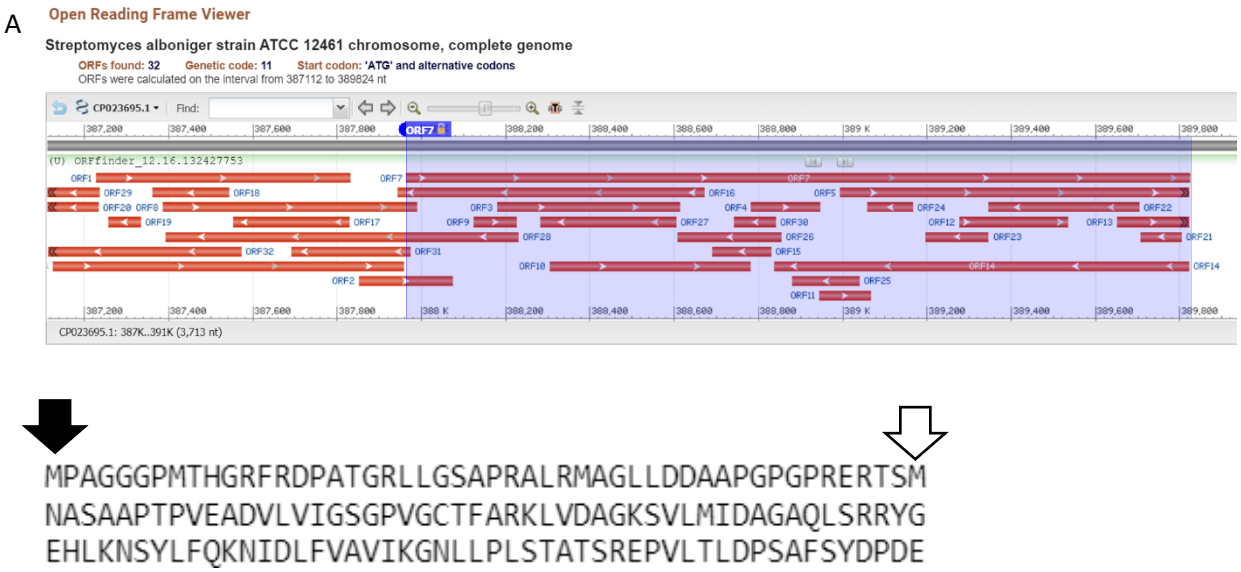

MPAGGGPMTHGRFRDPATGRLLGSAPRALRMAGLLDDAAPGPGPRERTSM
NASAAPTPVEADVLVIGSGPVGCTFARKLVDAGKSVLMIDAGAQLSRRYG
EHLKNSYLFQKNIDLFVAVIKGNLLPLSTATSREPVLTLDPSAFSYDPDE

Figure 3-28 Prediction of upstream sequence by ORF Finder *S. alboniger* (A) and *S. griseochromogenes* (B). Black arrow showed predicted upstream start codon and white arrow showed start codon of annotated sequence.

Among the genera *Kitasatospora*, *Amycolatopsis* and *Streptomyces*, the annotated gene from *Amycolatopsis* gave the lowest probability of secretion, either by an absence of a putative signal peptide, or by a low prediction score. In this study, we limited the following steps to enzymes that harbour a putative signal peptide with a high prediction score for a functional Tat pathway-secretion. This left us with three candidate enzymes from *Streptomyces alboniger* (*Sa*GMC), *Streptomyces albidoflavus*, and *Streptomyces griseochromogenes* (*Sg*GMC), shown in Figure 3-29. The scores from TatP-1.0 are summarized in Table 3-6. Due to the unavailability of *S. albidoflavus* from DSMZ, Leibniz Institute, we proceeded with the two candidate enzymes from *S. alboniger* and *S. griseochromogenes*.

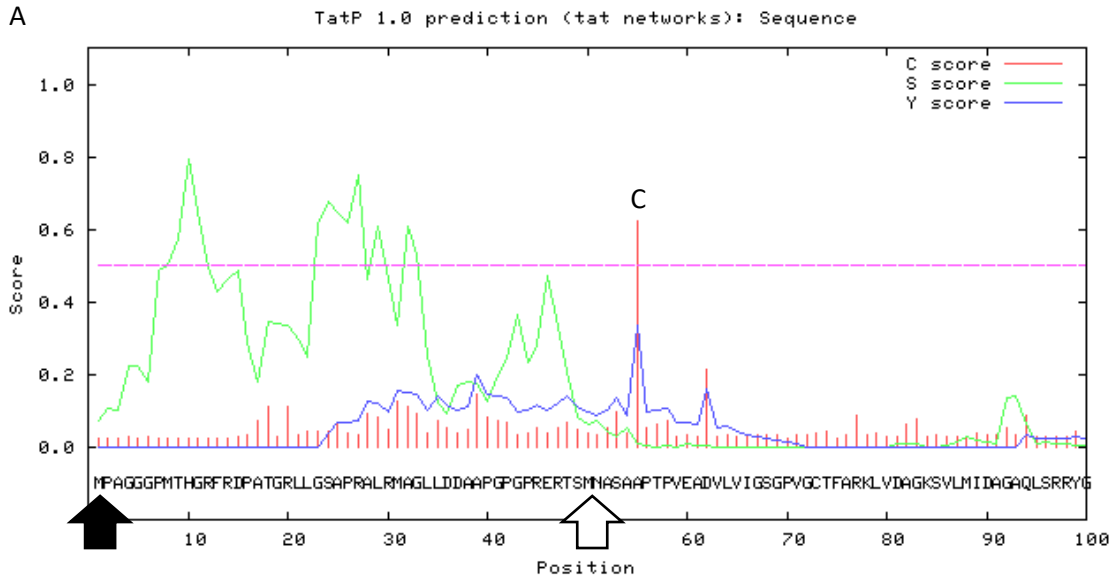

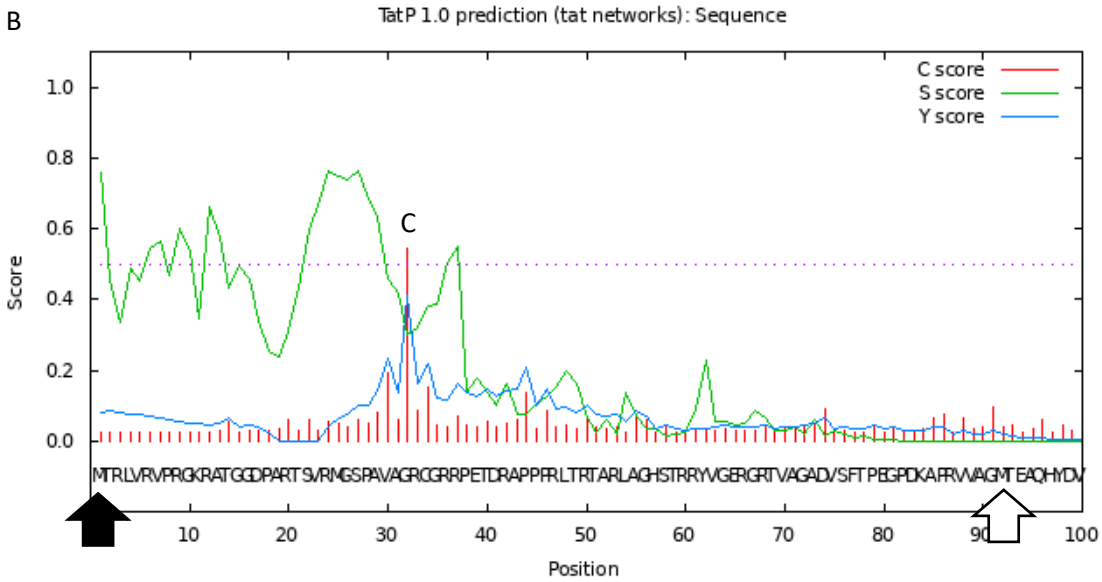

Figure 3-29 Analysis using TatP-1.0 for Putative GMC from *S. alboniger* (A) and *S. griseochromgenes* (B). Cleavage site marked with C, upstream start codon shown in black arrow, and annotated start codon showed in white arrow.

Table 3-6 Scores generated from TatP-1.0 for several possible signal peptide sequences

Species	Amino acid length	Max. C	Max. Y	Max. S	Mean S	Max. D
S. alboniger	100 AA	Yes	No	Yes	Yes	No
	59 AA	No	No	Yes	Yes	No
	56 AA	Yes	Yes	Yes	Yes	Yes
S. griseochromogenes	100 AA	Yes	Yes	Yes	Yes	Yes
	91 AA	Yes	Yes	Yes	Yes	Yes
	67 AA	No	No	No	No	No

3.3.2. Molecular cloning.

Targeted genes were listed in Table 3-7 and successfully amplified genes were shown in Figure 3-30. The high GC content in all targeted sequences required modification of the PCR reactions. The use of 6% (v/v) DMSO in the PCR reaction was shown to be crucial for successful amplification(Obradovic et al., 2013). DMSO at 3% (v/v) concentration was also recommended when conducting colony PCR in this study.

Table 3-7 Targeted genes for heterologous expression in *S. lividans*

Species	**Gene**	**GC Content (%)**
S. alboniger	sp-*sa*gmc	70.06
	*sa*gmc	69.19
S. griseochromogenes	sp-*sg*gmc	67.26
	*sg*gmc	66.10

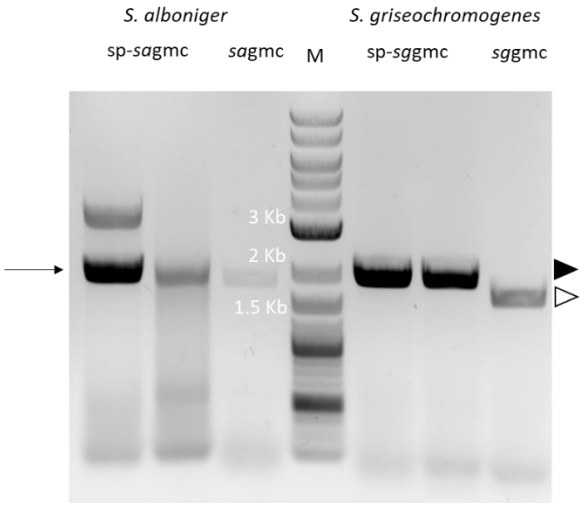

Figure 3-30 Amplified target genes from *S. alboniger* and *S. griseochromogenes*. Genes containing putative signal peptide sequences labelled as *sp*. Ladder is shown as M. Targeted band is shown in black arrow for sequence from *S. alboniger* containing signal peptide (sp-*sa*gmc). Targeted band from *S. griseochromogenes* showed in black and white triangle for sp-*sg*gmc and *sg*gmc, respectively.

Due to limited information on the production of the targeted enzymes in their native host and also the absence of data about the activity of these enzymes, heterologous expression in *S. lividans* followed by Western blot analysis was employed for simpler detection of targeted enzymes. Both enzymes selected for this study are derived from *Streptomyces*, thus, it is expected that *S. lividans* could deliver targeted enzymes to the extracellular location due to recognition of their putative signal peptide sequence and its cleavage site. In addition, our previous study (Chapter 3.2.) showed that *S. lividans* successfully delivered *Ka*POx into the culture supernatant when its signal peptide was present. Expression in *S. lividans* system was conducted using the constitutive promoter P_{vsi} and pIJ486 as the plasmid backbone (Figure 3-31), where constructs without putative signal peptide sequences were used as a negative control.

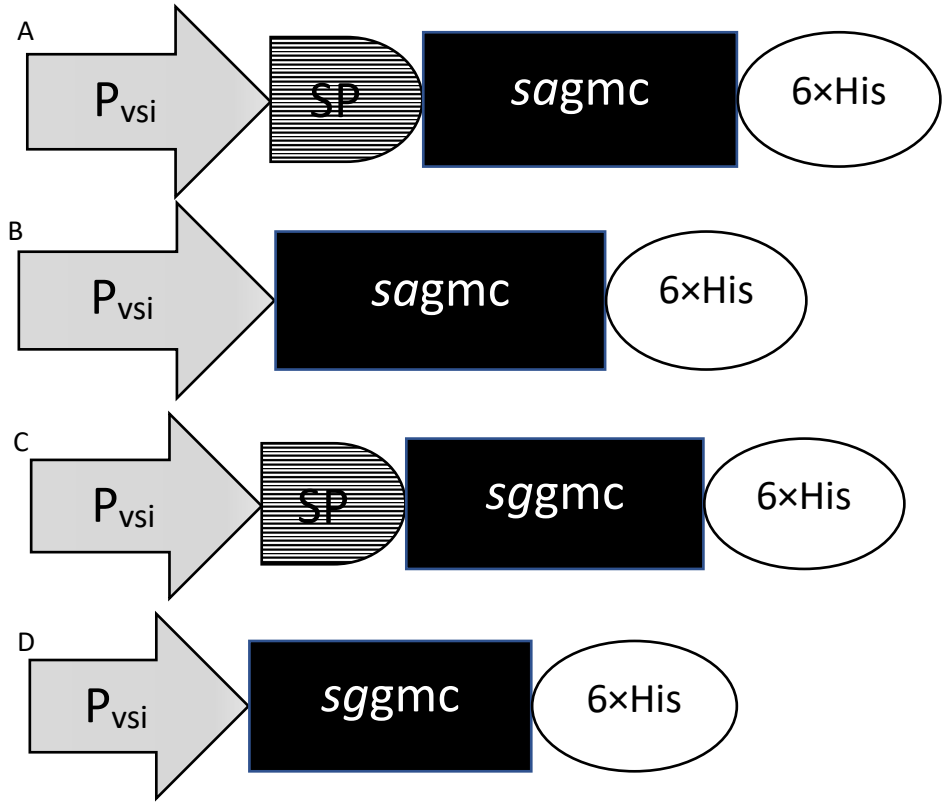

Figure 3-31. Constructs of targeted genes in pIJ486 with C-terminal 6×His-Tag. Putative signal peptide sequence of each genes showed as SP and constitutive promoter from *S. venezuelae* (P_{vsi}) was used.

3.3.3. Recombinant protein production

Heterologous expression in *S. lividans* was conducted for 3 days (Figure 3-32). Cultures harbouring the construct sp-*sa*gmc showed the highest protein concentration at 48 hours in both supernatant (0.3 mg/mL ± 0.087) and cell lysate (1.5 mg/mL ± 0.323) and a decline afterwards. Strains harbouring the construct *sa*gmc showed the highest protein concentration in the cell lysate at 66 hours (1.953 mg/mL ± 0.381) but protein concentration in the supernatant increased gradually starting from 48 hours and reached a peak at 72 hours (0.113 mg/mL ± 0.023). Quantification of protein concentration was coupled with observation of cell growth. Wet cell weight (WCW) was used to measure cell growth and its trajectory was used as an indicator of cell lysis.

A

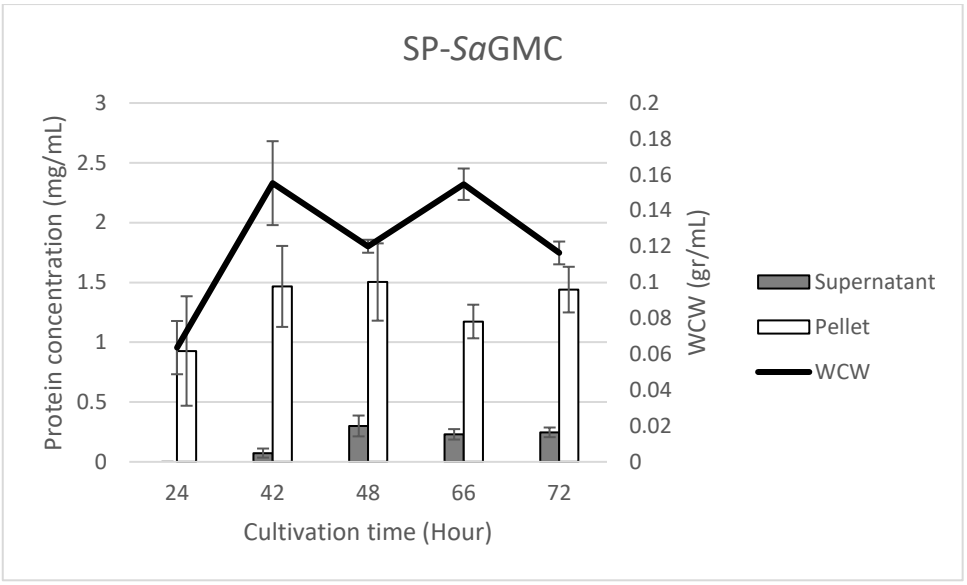

B

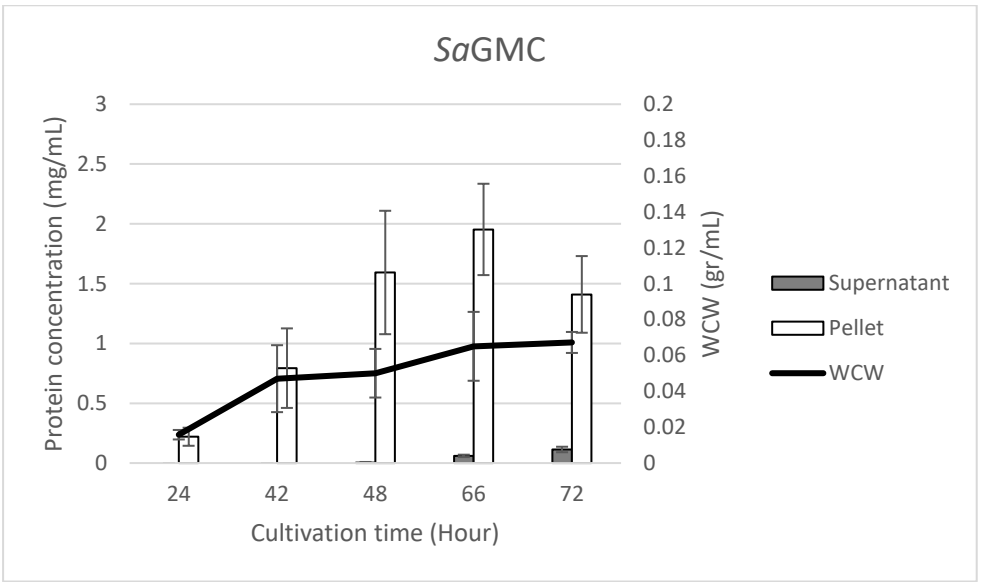

Figure 3-32 Recombinant protein production of targeted gene from *S. alboniger*. Construct with putative signal peptide sequence (SP-*Sa*GMC) showed in (A), construct without putative signal peptide (*Sa*GMC) showed in (B).

The observed WCW of pIJ-sp-*sa*gmc showed an increasing trend from 48 hours (0.120 gr/mL ± 0.0036) until 66 hours (0.155 gr/mL ± 0.0088). It started to decline at 72 hours (0.116 gr/mL ± 0.0064), followed by decreased protein concentration in the cell lysate. These data suggest no cell lysis occurred at 48 hours for pIJ-sp-*sa*gmc.

In comparison with its negative control, the WCW of pIJ-sp-*sa*gmc was 2.4-fold higher at 48 hours. The protein concentration in the cell lysates of both constructs were similar, 1.5 mg/mL and 1.59 mg/mL for pIJ-sp-*sa*gmc and pIJ-*sa*gmc, respectively. The amount of WCW should go in line with protein concentration. Therefore, it was possible, the less amount of protein concentration at cell lysate of pIJ-*sp-sa*gmc was due to secretion of protein(s) to supernatant. It should be emphasized that secreted protein(s) mentioned were not subjected to our target protein specifically. In that particular time point (48 hours), 20% of the protein in the cell lysate of pIJ-sp-*sa*gmc was released to the supernatant. Nevertheless, it was notable that the total amount of protein from cell lysate and supernatant of pIJ-sp-

*sa*gmc still did not comply with the difference on WCW of both constructs. In this matter, the presence of native protease derived from the host cell should put into account.

Strains harbouring the construct without the signal peptide, pIJ-*sa*gmc, showed a reduced growth not only at 48 hours, but throughout the cultivation, compared to strains harbouring pIJ-sp-*sa*gmc. The expression of pIJ-sp-*sa*gmc reached 0.155 gr/mL ± 0.0088 in 66 hours as its highest while pIJ-*sa*gmc only reached 0.067 gr/mL ± 0.0059 in 72 hours. This outcome corroborates the notion of the previous study (Chapter 3.2), where secretion driven by the signal peptide prevents cytoplasmic accumulation of the expressed recombinant protein, resulting in higher biomass production through avoidance of a stress reaction on the accumulation of non-secreted protein.

Heterologous expression of the other candidate enzyme (Figure 3-33) showed the highest protein concentration for pIJ-sp-*sg*gmc at 42 hours in cell lysate (2.18 mg/mL ± 0.239) and 66 hours in the supernatant (0.37 mg/mL ± 0.026). The highest protein concentration in cell lysate was comparable with its cell growth, as this construct also reached maximum growth at 42 hours (0.182 gr/mL ± 0.0138).

A

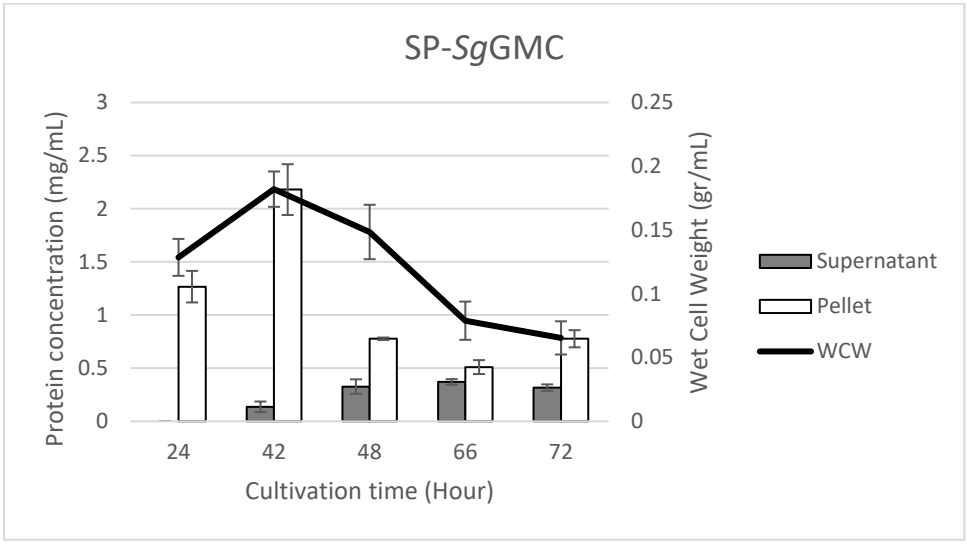

B

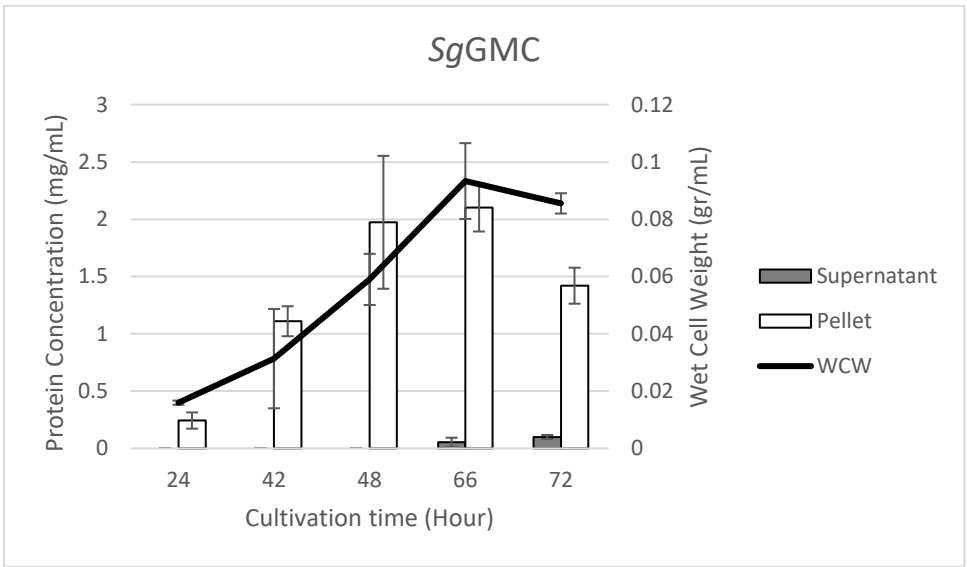

Figure 3-33 Recombinant protein production of targeted gene from *S.griseochromogenes*. Construct with putative signal peptide sequence (SP-*Sg*GMC) shown in (A), construct without putative signal peptide (*Sg*GMC) shown in (B).

Measurement of protein concentration for the negative control, pIJ-*sg*gmc, showed the highest protein concentration in the cell lysate at 66 hours (2.103 mg/mL ± 0.210) and 72 hours in the supernatant (0.1 mg/mL ± 0.017). The highest WCW for this construct was observed at the same time point when the highest protein concentration was measured in cell lysate, 66 hours (0.093 gr/mL ± 0.0132).

The growth pattern for pIJ-*sg*gmc was different compared to pIJ-sp-*sg*gmc. The maximum WCW for pIJ-*sg*gmc was 1.96-fold less than pIJ-sp-*sg*gmc and it was reached at 66 hours, while for pIJ-sp-*sg*gmc, the highest WCW was reached at 42 hours.

The same pattern of cell growth was observed when comparing the different constructs for both enzymes, *Sa*GMC and *Sg*GMC. When the putative signal peptide sequence was present, more biomass was generated, independent from the secreted targeted enzymes. Strains harbouring constructs without putative signal peptides generated less biomass and required longer cultivation times to do so.

3.3.4. Recombinant enzyme detection

3.3.4.a. Western blot

Due to limited information on enzyme activity, detection using 6×His-Tag antibody was used to confirm recombinant enzyme expression (Figure 3-34).

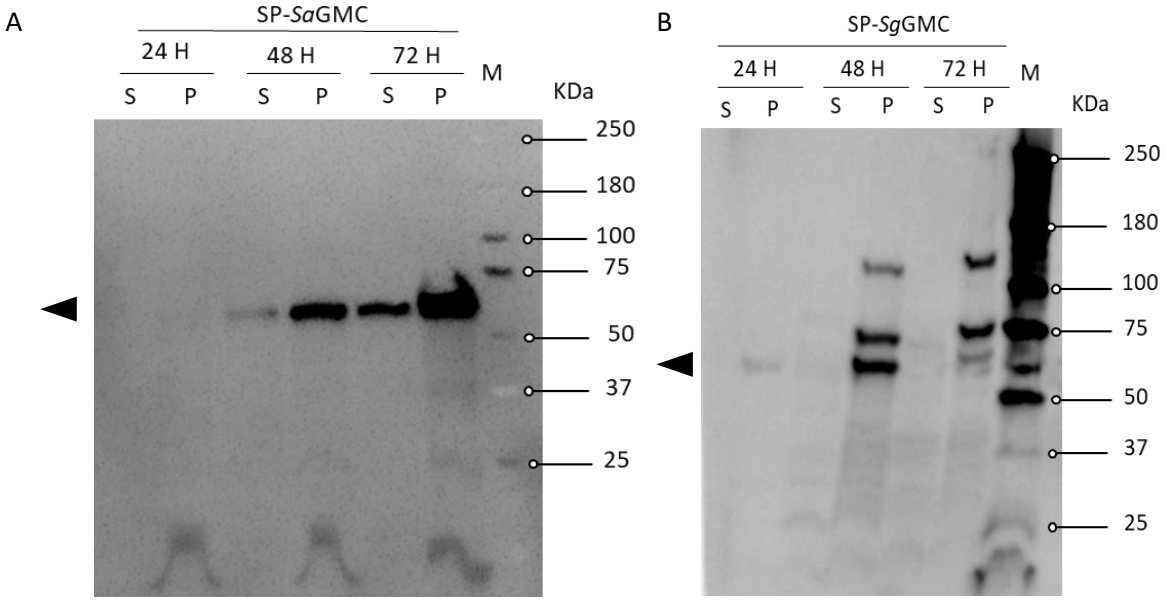

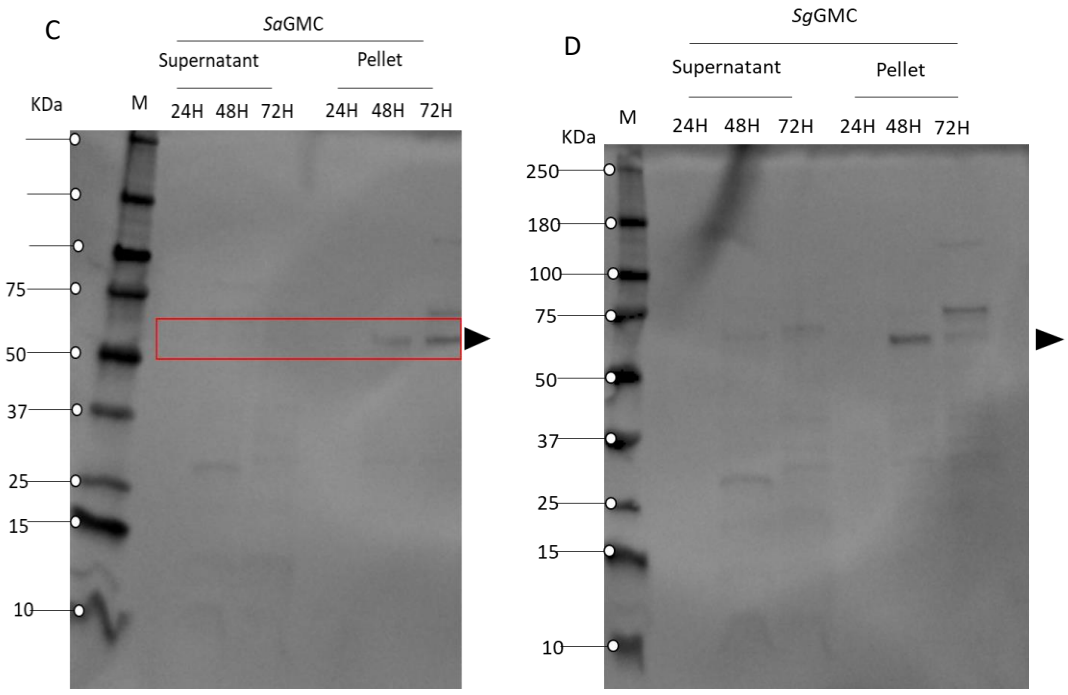

Figure 3-34 Western blot analysis of expressed recombinant protein. Target protein from *S. alboniger* harboring putative signal peptide (SP-*Sa*GMC) shown in A; without putative signal peptide shown in C. Target protein from *S. griseochromogenes* harboring putative signal peptide (SP-*Sg*GMC) shown in B; without putative signal peptide shown in D. Marker shown in M, sample from supernatant shown as S, and pellet / cell lysate shown as P. Time point shown in hour (H). Expected size of targeted protein marked in black triangle.

3.3.4.b. Streptomyces alboniger

For samples harbouring putative signal peptide sequence from *S. alboniger* (SP-*Sa*GMC), Western blot analysis could detect a signal from the supernatant and cell lysate starting from 48 hours. Although all samples were adjusted to the same concentration prior to protein loading for this analysis, there was a different intensity in the supernatant and cell lysate at this time point. This was not surprising because samples used for Western blot were not purified and the protein concentration data are in agreement with this result, where intracellular protein concentration was higher compared to secreted ones. Apart from proofing the secretion of target protein, a more intense Western blot signal from intracellular sample compared to extracellular also suggest a possible traffic jam in protein secretion. A study on *S. lividans* secretion using reporter fluorescent protein (Hamed, Vrancken, *et al*., 2018) mentioned that cellular factors might prevent the secretion process, regardless of the amount of synthesized recombinant protein. In addition, Hamed *et al*., 2018, also reported a significant amount of recombinant protein accumulated in the cytoplasm, irrespective of the secretion level, when the expressing strain was cultivated in nutritious medium, which was the case in our study. Their report concluded that high-level synthesis / secretion directly impacts the endogenous secretome, which suggested a possible stress response where the severity is subjected to growth medium.

The construct without putative signal peptide sequence (*Sa*GMC) showed the signal of predicted target protein only in the cell lysate at 48 and 72 hours. There was no Western blot signal detected in the supernatant for this construct. This outcome supports the computational analysis that the upstream sequence of the putative GMC from *S. alboniger* is a functional signal peptide.

Mass spectrometry analysis was conducted to confirm the results from Western blot and eliminate uncertainties regarding the possibility of cell lysis, and whether the detected signal from Western blot really represents our targeted enzyme (Figure 3-35).

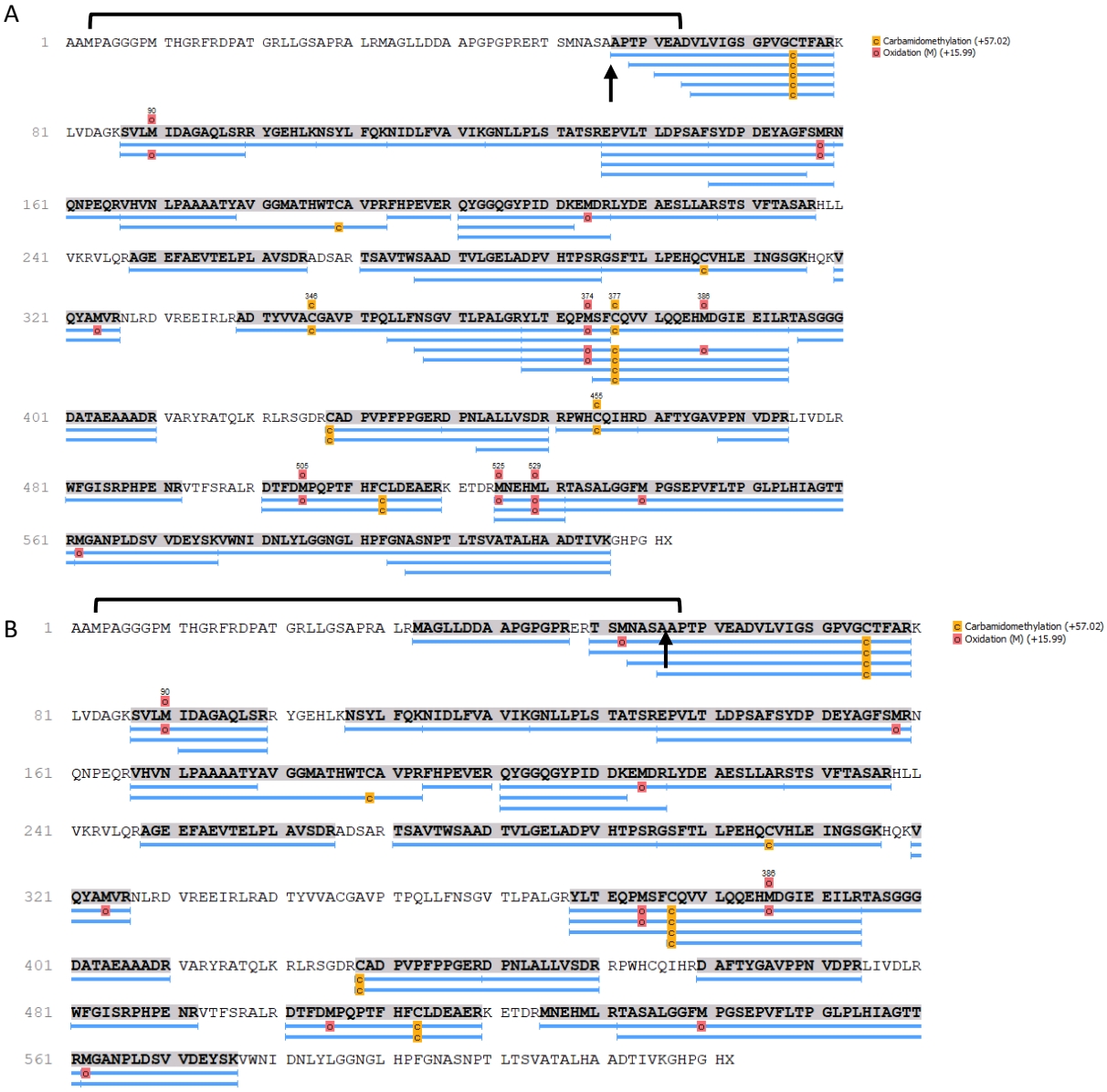

Figure 3-35 Mass spectrometry of SP-*Sa*GMC from supernatant (A) and cell lysate (B). Putative signal peptide sequence showed under black bracket (⌐¬), cleavage site was showed with black arrow, and detected peptides in mass spectrometry was underlined in blue.

The most likely cleavage site for SP-*Sa*GMC, based on the TatP-1.0 prediction shown in Figure 3-29, is between position 54 and 55 (ASA-AP). Mass spectrometry from the supernatant of SP-*Sa*GMC (Figure 3-35A) showed that detected peptides started only after this putative signal peptide sequence, right after the predicted cleavage position. As comparison, the results from cell lysate showed peptide fragments from the putative signal peptide sequence (Figure 3-35B, fragment under the black bracket, underline in blue). This outcome from mass spectrometry analysis confirmed three things: the detected band from Western blot analysis represents our targeted protein (1); this enzyme is secreted due to the presence of a signal peptide sequence (2); and the detected signal in the supernatant sample was not

due to cell lysis (3). Furthermore, the absence of fragments from the signal peptide sequence in the supernatant indicates that secretion occurred including proper signal peptide cleavage (Auclair *et al*., 2012; Li *et al*., 2006; Sevillano *et al*., 2016).

3.3.4.b. Streptomyces griseochromogenes

The targeted protein from *S. griseochromogenes* harbouring a putative signal peptide sequence did not yield any Western blot signal in the supernatant (Figure 3-34B). The protein could be detected in the cell lysate of SP-*Sg*GMC starting from 24 hours and reach its highest intensity at 48 hours before it was depleted at 72 hours. The product of the construct without signal peptide could not be detected in the supernatant at any time point, but in the cell lysate, a band of the expected size was detected in samples from 48 and 72 hours. The intensity at 48 hours was much higher than at 72 hours for *Sg*GMC (Figure 3-34D).

Outcomes from mass spectrometry analysis agree with Western blot analysis, where no peptides of SP-*Sg*GMC were found in the supernatant. Samples from the cell lysate showed peptide fragments from the target protein but they were not particularly prominent. Mass spectrometry data verify that no secretion occurred for SP-*Sg*GMC but 25 supporting peptides confirmed its intracellular accumulation. In this case, we could only assume several factors explaining the lack of secretion of SG to the supernatant: (1) low expression of SP-SG due to as of now unknown reasons, hence the secreted target protein was well below the limit of detection, (2) the putative signal peptide of SG was not a functional signal peptide after all, despite the prediction from TatP-1.0, or (3) the expression host *S. lividans* failed to recognize and cleave the signal peptide. In the latter assumptions, accumulation in the cytoplasmic was expected, and could also trigger the proteolytic degradation(Vicente *et al*., 2016). If this was the case, then it might also explain the pattern appeared in Figure 3-33A where protein concentration of SP-SG inside the cell decreased rapidly from 42 hours to 72 hours.

Computational prediction using TatP-1.0 depends on the length of amino acid sequence input. Table 3-6 showed that the putative SP from *Sg*GMC was only predicted as a signal peptide when at least 91 amino acids preceding the annotated start codon were used. When 67 amino acids prior to the annotated start codon (where there is also a methionine residue) were calculated, it was not predicted to be a signal peptide. Tat signal sequences tend to be longer than Sec signal sequences (P. A. Lee *et al*., 2006), and the average length of Sec signal peptide is 35 to 40 amino acids for *Streptomyces* (Anné *et al*., 2014; Hamed, Anné, *et al*., 2018; Tsirigotaki *et al*., 2017). An established Tat signal peptide from Xylanase C (XlnC) is 49 amino acids long (Faury *et al*., 2004; Li *et al*., 2006), and our previous study on *Ka*POx localization showed a signal peptide of 44 amino acids. The Tat signal peptide prediction of 91 amino acids is significantly longer and may simply be a coincidental similarity.

3.3.5. Sequence and structure comparison

Successful secretion of SP-*Sa*GMC in *S. lividans* encouraged us to explore more about this enzyme. We investigated its position in the phylogenetic tree compared with other characterized and uncharacterized Auxiliary Activities 3 enyzmes (Figure 3-36).

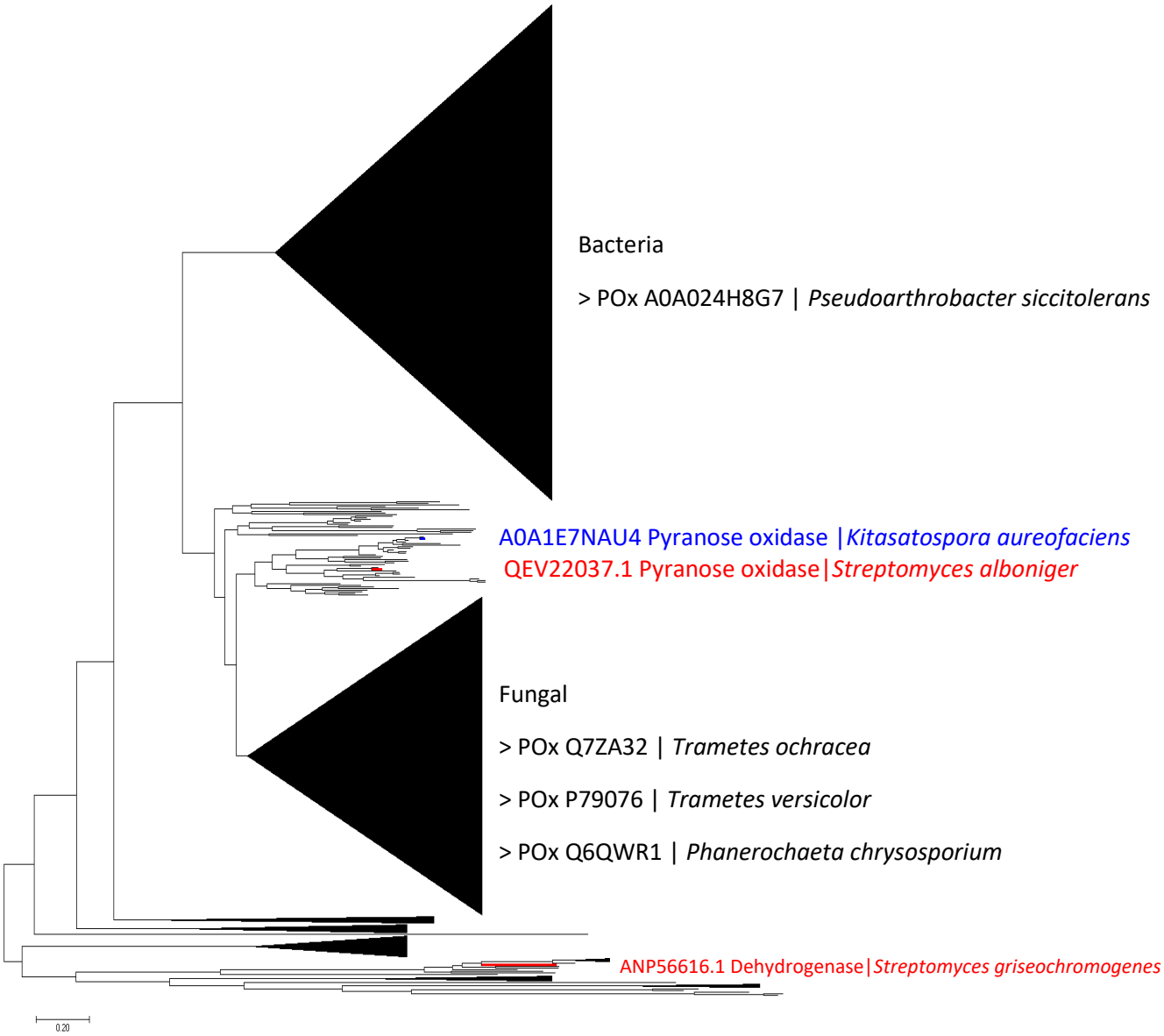

Figure 3-36 Phylogenetic tree of Pyranose oxidase from *S. alboniger*.

The constructed phylogenetic tree revealed the annotated pyranose oxidase from *S. alboniger* (*Sa*GMC, QEV22037.1 in red) close to the characterized pyranose oxidase from *K. aureofaciens* (*Ka*POx, in blue) and quite distinct from *Sg*GMC (ANP56616.1 in red). Their alignment also supports this result (Figure 3-37, Table 3-8).

```
Sg          -----MTEAQHYDVIVIGTGAGGGTIAHRLADTGKRILLLERGDYLPRERDNWDSTAVFV 55
KaPOx       ------MITRYTDTLVVGSGPVGATFARTLVESGREVLMVDAGAQLSPRPGEHLKN---- 50
Sa          MNASAAPTPVEADVLVIGSGPVGCTFARKLVDAGKSVLMIDAGAQLSRRYGEHLKN---- 56
                       *.:*:*:*  * *:*: *.::*: :*::: *  *  . .:  ..

Sg          KGKYRAPEFWFDKNGNQFPP-------------------------------------- 75
KaPOx       -------AYIYQHNTNLFASIIRGHLHLLSVPTSARAELAVDPAAMAELGSN-RSSARNA 102
Sa          -------SYLFQKNIDLFVAVIKGNLLPLSTATSREPVLTLDPSAFSYDPDEYAGFSMRN 109
                      : :::* : *

Sg          --------------EVNYYVGGNTKFYGAALFRMRPEDFGELRHHDGISPAWPLRYEDFE 121
KaPOx       ENPDQDPYRNLSAAAACYAVGGMGTHWTGATPRHHPVL----ERYDG------ISDQEWD 152
Sa          QNPEQRVHVNLPAAAATYAVGGMATHWTCAVPRFHPEV----ERQYG-GQGYPIDDKEMD 164
                          . * ***  ..:  *  * :*      .:  *      :  :: :

Sg          PYYTQAEHLYLVHGRHGEDPTEGPTSAQYAYPPVQHEPRIEQLSH--DLEKQGLHPFHLP 179
KaPOx       GLYGEAERLLRVSAREF-----------DFSIRQH-LVTEALRREFSELPDGYQVQSLP 199
Sa          RLYDEAESLLARSTSVF-----------TASARHL-LVKRVLQRAGEEFA---EVTELP 208
              * :** *                          :     . * :  .      .   **

Sg          IGVNLTQD-ERGRAVHTSACIRCDRVDGFPCLVGAKSDAQVICVDPALRHANVEMITHAD 238
KaPOx       LAARRRR--DNPRMVHWT---------GVDTVLGDLADG----------HPLFSLLPQHL 238
Sa          LAVSDRADSARTSAVTWS---------AADTVLGELADPVHTP-----SRGSFTLLPEHQ 254
            :..       .   *  :         .   ::*  :*           :  . :: .

Sg          VRRLETDTTGRSVTKVVATVG--DGDPSTVEFGADIVVVACGAVNSAVLLLRSADDRHPQ 296
KaPOx       CTRLVLDRDGT--RIAYAEVRDLNR-SETVRVVADNYVVAAGAVLAPQLLHASGIRP--- 292
Sa          CVHLEINGSGKHQKVQYAMVRNLRDVREEIRLRADTYVVACGAVPTPQLLFNSGVTL--- 311
              :*  :  *       * *       . :.. **  ***.*** :  **  *.

Sg          GLANSSDVVGRYYMRHNNMALMAVSREPNDT-------------------------KFQ 330
KaPOx       ------AALGRYLTEHP-MAFCQVILLKDLVEQARTDQR---FGGQ---------VAR-- 331
Sa          ------PALGRYLTEQP-MSFCQVVLQQEHMDGIEEILRTASGGGDATAEAAADRVARYR 364
                   .:***  .:  *::  *    :                              :

Sg          --KTLALHDWYLGSDDWDYPLGGIQ-------MLGKSDSEQIHGEAPRWAGAVAPDMPFE 381
KaPOx       -------HTTLFPDDDLPIPVDDPEPNVWIPVSEGRPWHAQITRDAFHY-G----DVPPH 379
Sa          ATQLKRLRSGDRCADPVPFPPGERDPNLALLVSDRRPWHCQIHRDAFTY-G----AVPPN 419
                   :      *    * .  :          :    **  :*  : *     :* .

Sg          VLAHHAVDFWLCGEDLPVAENRVTLDRDDGIHLALDEKNNIAGLER-LRHKLQGMLEHLG 440
KaPOx       VDGRLIVDLRWFGIVEPRPDNRVTFSDTRTDVMGMPQPTFEYALSPQDAERQHAMMAEMM 439
Sa          VDPRLIVDLRWFGISRPHPENRVTFSRALRDTFDMPQPTFHFCLDEAERKETDRMNEHML 479
            *  :  **:   *   *  :****:.      : : : .    *.    .. . *  .:

Sg          M-----HEHHLLSRSLYLHKGMPIGATAHQAGTVRFGGDPASSALDVNCKAHDLDNLYVV 495
KaPOx       RAATALGGFLPGSEPRFTAPG----LPLHIAGTIRMGDDPQSSVVDTDSRVWGLENLYLG 495
Sa          RTASALGGFMPGSEPVFLTPG----LPLHIAGTTRMGANPLDSVVDEYSKVWNIDNLYLG 535
                   .   *.  :   *       * *** *:* :* .*.:*  .:. .::***:

Sg          DTSFFPSIGAVNPSLTAIANALRVGDHIAERLR-----------------  528
KaPOx       GNGVIPTGTACNPTLTSVAMALKAAHHLAGSREARERRRTGADEVLAVRS*  545
Sa          GNGLHPFGNASNPTLTSVATALHAADTIVKGHPGHX--------------  571
            .... *   * **:**::* **:... :.
```

Figure 3-37 Blast P of *Sa*GMC (Sa) and *Sg*GMC (Sg) using *Ka*POx as query sequence. Rossmann fold motif showed in red box.

Table 3-8 Blast P score of *Sa*GMC and *Sg*GMC with *Ka*POx as query sequence

Species	Protein	Query Cover	E value	Per Identity	Accession length
S. alboniger	*Sa*GMC	94 %	3e-167	50.54%	620
S. griseochromogenes	*Sg*GMC	74%	4e-16	25.26 %	528

These two analyses above suggested *Sg*GMC is phylogenetically rather distinct from *Sa*GMC and *Ka*POx, which both are secreted in the presence of their native signal peptide in *S. lividans* and which are much closer located in the phylogenetic tree. Here, we also compared the structure of *Sa*GMC and *Ka*POx based on AlphaFold model (Figure 3-38).

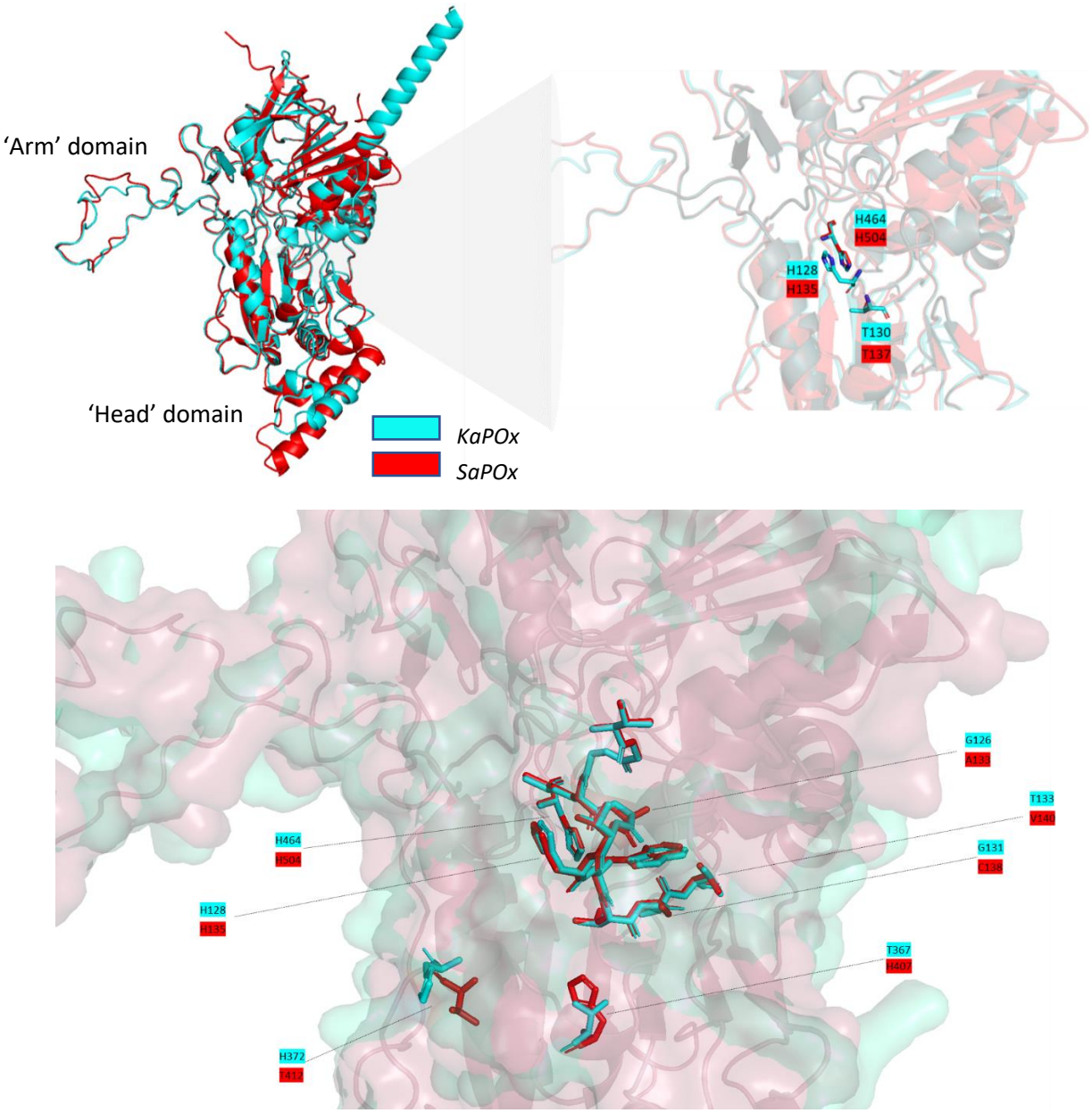

Figure 3-38 Structure of *Ka*POx dan *Sa*GMC

The superimposed model of *Ka*POx and *Sa*GMC does not look exactly similar, especially in arm domain and head domain. However, it also does not look too distinct, especially in the critical residues which are considered responsible for catalytic activity and attachment of FAD. The histidine residue at position 464 (H464) and Threonine at position 130 (T130) in *Ka*POx are known as FAD-coordinating catalytic residue (Herzog *et al*., 2019). These residues corresponded to H504 and T137 in *Sa*GMC. Pyranose oxidase from *K. aureofaciens* is known to have a covalent link to FAD, as do several pyranose oxidases from fungi, like *Trameters ochracea* (*To*POx) (Halada *et al*., 2003). For *To*POx, H167 is known to establish the covalent 8α-(N3)-histidyl link (Halada *et al*., 2003) to FAD, and this residue corresponds to H128 in the *Ka*POx model. H128 in *Ka*POx corresponds to H135 in *Sa*GMC. Another similar motif found between *Ka*POx and *Sa*GMC is the FAD-coordinating *si*-side helix and loop, where 122-VGGMGTHWTGAT-133 in *Ka*POx is highly similar to 129-VGGMATHWTCAV-140 (different residues underlined). Nevertheless, there are some disparities in residues responsible for the gating segment of the substrate recognition loop between *Ka*POx and *Sa*GMC. In *Ka*POx, H372 corresponds to T412 of *Sa*GMC, and T367 of *Ka*POx corresponds to H407 of *Sa*GMC as well as to H450 in *To*POx (Herzog *et al*., 2019; Spadiut *et al*., 2010).

3.3.6. Enyzme activity

Auxiliary activity 3 enzymes are known to have diverse substrate specificities (Sützl *et al*. 2018), but their mechanism of action remains the same. In the first half reaction, the co-factor FAD oxidizes the first substrate, known as the electron donor. For the second half reaction, the reduced FAD reduces the second substrate, the electron acceptor, such as oxygen (oxidase activity) or other molecules (dehydrogenase activity), becoming re-oxidized in the process. Considering the high similarity in important residues between *Ka*POx and *Sa*GMC, the assumption that *Sa*GMC shows a similar substrate specificity with *Ka*POx is plausible. Thus, the screening of *Sa*GMC activity in this study was limited to sugars, especially monosaccharides.

3.3.6.a. Plate reader

A high-throughput assay using a plate reader was conducted to screen several monosaccharides and a number of disaccharides, which may be suitable electron donors for *Sa*GMC (Figure 3-39).

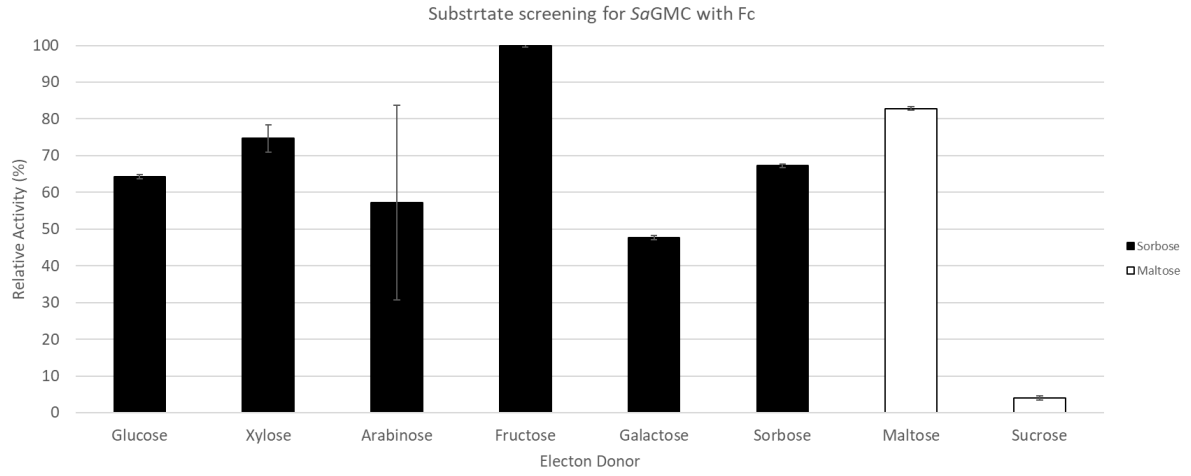

Figure 3-39 Substrate screening for *Sa*GMC using plate reader.

When ferrocenium hexafluorophosphate (Fc) was used as an electron acceptor, the enzyme showed the highest activity towards fructose, followed by maltose, xylose, sorbose, and glucose. Disaccharides were represented by maltose and sucrose, where *Sa*GMC showed preferences towards maltose compared to sucrose. Maltose is formed from 2 units of glucose with an α-(1-4) glycosidic bond (Ouellette & Rawn, 2018), while sucrose is a non-reducing sugar composed of glucose and fructose linked at C1 on the glucosyl subunit and C2 on the fructosyl subunit (Stick & Williams, 2009). When glucose was used as a substrate, *Sa*GMC showed 64.3% relative activity compared to fructose. Therefore, activity towards maltose due to some impurity of glucose cannot be entirely ruled out.

An assay using molecular oxygen as an electron acceptor was also conducted, however there was no activity detected, suggesting *Sa*GMC mainly has dehydrogenase activity. Other than Fc, 2,6-Dichlorophenolindophenol (DCPIP) and *p*-Benzoquinone (BQ) were also screened as electron acceptors (Figure 3-40).

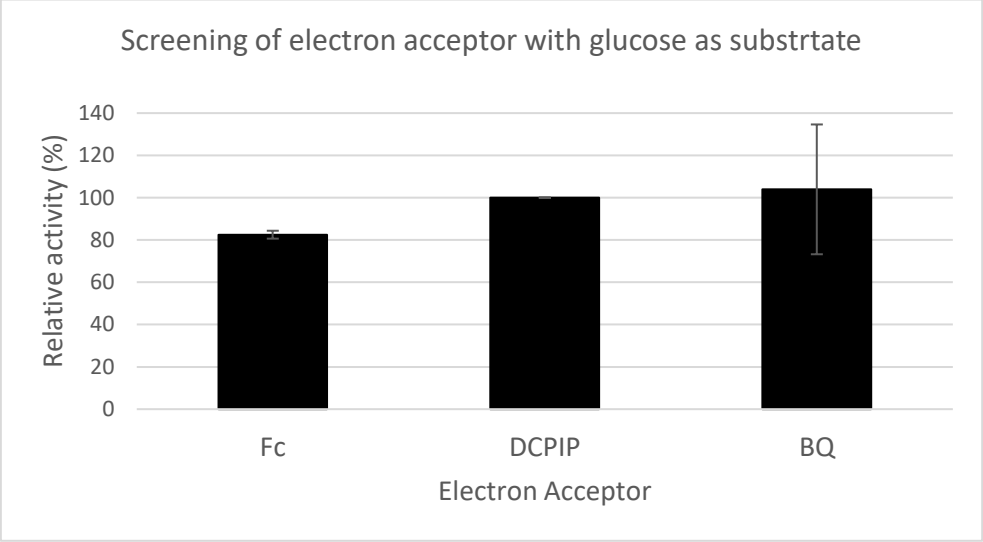

Figure 3-40 Screening of electron acceptor of *Sa*GMC

There were no clear preferences for a particular electron acceptor for *Sa*GMC, only DCPIP gave a slightly higher activity compared to Fc. While Fc and BQ require UV detection of their reduction, DCPIP can be detected at 600 nm and the colorless reduced state can be easily followed by visual inspection. Therefore, *Sa*GMC activity was determined using DCPIP (Figure 3-41).

Figure 3-41 Decolorization of DCPIP after overnight incubation.

In this study, the plate reader determines the enzyme activity by following the electron acceptor reduction, not by following the oxidation of the electron donor or the product formation. In the case of *Sa*GMC, the high concentration of electron donor required and the slow enzymatic reaction suggested that another analysis was required to support this preliminary substrate screening. Therefore, high performance liquid chromatography (HPLC) was conducted for further verification.

3.3.6.b. High Performance Liquid Chromatography (HPLC)

Analysis using HPLC enabled observation towards substrate depletion and / or product formation. Results from HPLC analysis showed that when fructose was used as substrate, a new peak formed (Figure 3-42). Proper negative controls were used to verify this outcome, including reaction mix without enzymes, reaction mix without substrate, and reaction mix with supernatant from cultures harboring an empty expression vector. Compared to these controls, only the reaction in the presence of *Sa*GMC showed the formation of this new peak. However, due to limitations of positive control and availability of standards, we could not determine the identity of the molecule constituting the newly formed peak.

Figure 3-42 HPLC of *Sa*GMC with fructose as substrate

Another substrate that showed the formation of a new peak was glucose (Figure 3-43A). All negative controls mentioned above were also applied and none showed a novel peak formation. The retention time of the product peak was the same as the retention time of 2-keto D-glucose (Figure 3-43B). Therefore, we conclude that *Sa*GMC oxidizes glucose at the C-2 position, generating 2-keto D-glucose as the product. A quantification of 2-keto D- glucose was done using a standard curve, and it revealed SA could generate 0.25 mM ± 0.02 of 2-keto D-glucose after 16 hours of incubation. We could not precisely determine the turnover number in this analysis, but confirmed the enzyme activity by observing product formation.

A

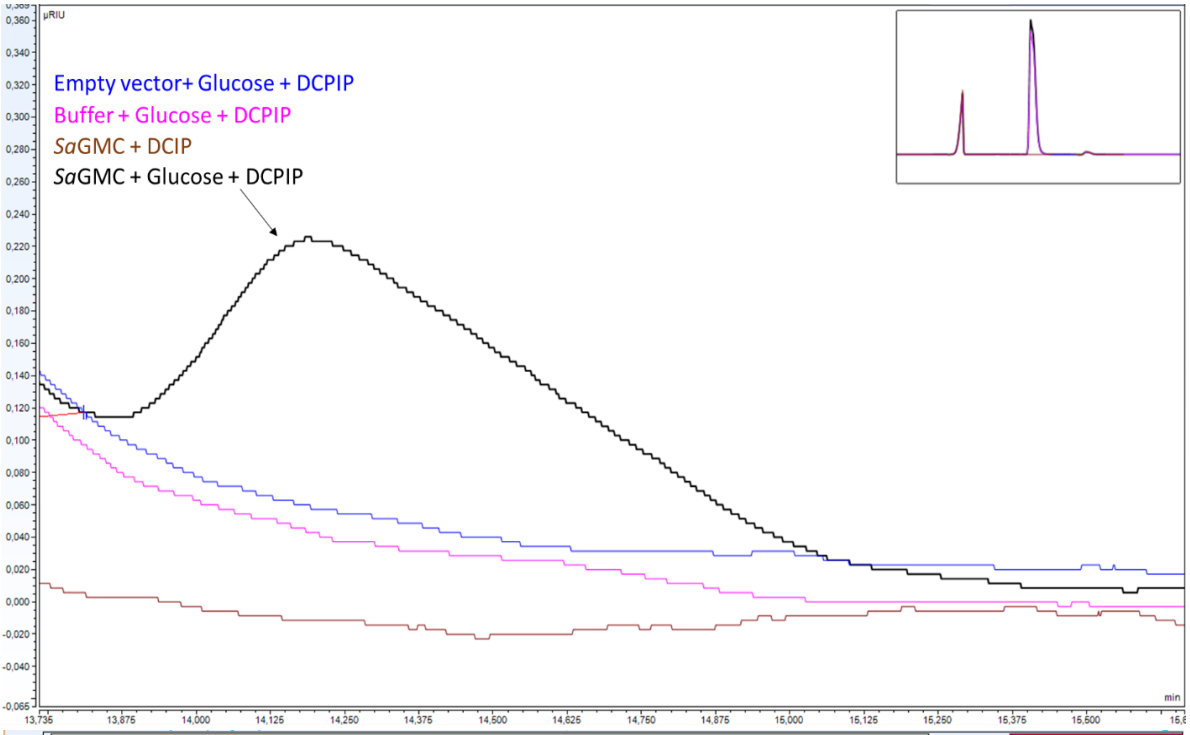

B

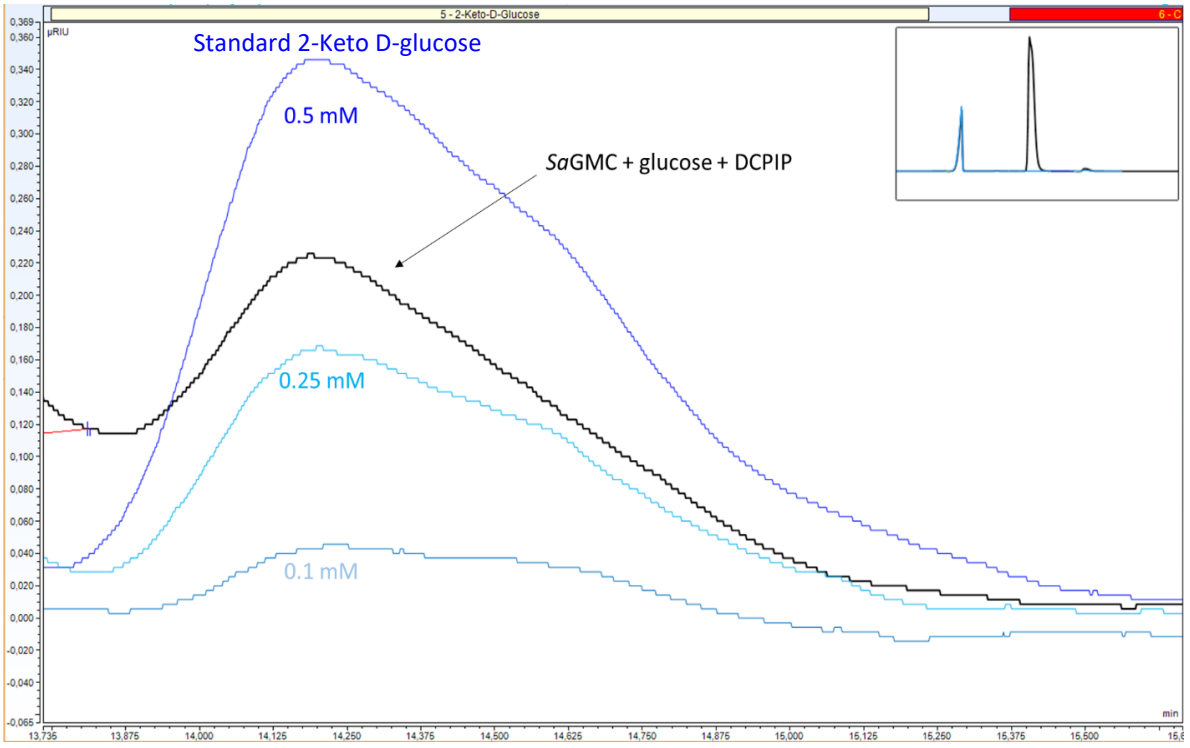

Figure 3-43 HPLC of *Sa*GMC towards glucose. Formation of product peak with presence of *Sa*GMC compared to negative controls (A) and confirmation of product formed is 2-keto D-glucose (B).

In general, HPLC analysis can determine substrate depletion followed by product formation, assuming both substrate and product can be detected using the same condition. In this study, substrate depletion was difficult to quantify because the initial substrate concentration used was 100 mM, which is considered high. The product concentration of 2-keto D-glucose was only 1mM, thus it was difficult to determine the minor substrate depletion from this reaction.

Despite the low activity of *Sa*GMC towards monosaccharides, we confirmed that glucose is oxidized to 2-keto D-glucose, therefore *Sa*GMC can be considered a pyranose oxidase/dehydrogenase. However, the high glucose concentration and low conversion rate indicate that glucose may not be the natural substrate for this enzyme from *S. alboniger*, *Sa*POx (previously written as *Sa*GMC).

Summary, conclusion, and outlook

More to find than can ever be found, more to do than can ever be done –
Circle of life by Elton John and T. Rice

4. Summary, conclusion, and outlook

Numerous industrial applications utilize lignocellulosic biomass as building blocks for their products. The physiological conditions of deconstruction and valorisation of this biomass by white-rot fungi has been more thoroughly studied compared to the bacterial counterparts. Indeed, lignin degrading fungi are more visible compared to bacteria. Therefore, the majority of studies involving bacterial lignin degradation mostly rely on '-omics' studies, which was also partly applied in this study as well. Instead of conducting more studies on the 'main player' enzymes such as laccase and peroxidases, this study focuses on 'the helper' enzyme(s), specifically from Auxiliary Activity family 3.

In the first study (Chapter 3.1), a selection of potential genes from bacteria was conducted to elucidate if there are other enzymes that can function as AA3 enzymes derived from bacteria. Based on genomic study, the selected bacteria were known to harbour genes annotated as lignin-degrading enzymes. The next step was expressing selected genes by heterologous recombinant expression in *E. coli*. From 8 genes candidate, only 2 genes were successfully expressed. The yield and purity level of these successfully expressed enzymes were poor, suggesting improper folding might be a reason. Another strategy to fuse target enzymes with maltose binding protein (MBP) resulted in much better expression. Nonetheless, once MBP was removed from the target enzymes by proteolytic cleavage, precipitation occurred. In addition, the activity of the fusion proteins could not be detected. Despite the limitation on enzyme availability, screening to reveal substrate preferences could be conducted. One of the target enzymes named Ad18, derived from *Amycolatopsis decaplanina*, showed activity in the presence of benzyl alcohol and 1,4-benzoquinone when measured spectrophotometrically using a plate reader. However, when the reaction on 1,4-benzoquinones was conducted using HPLC, it showed no depletion of this substrate. The second enzyme, Ka97, derived from *Kitasatospora aureofaciens*, its activity was observed when ferrocenium hexafluorophosphate (Fc) was used as electron acceptor with D-xylose, L-arabinose and D-mannose as electron donor. This activity was also observed using a plate reader. Further verification using HPLC confirmed the depletion of D-xylose in the presence of Ka97 in the reaction.

Whether the tested potential substrates were the natural substrate of these enzymes could not be verified. Kinetic measurements could also not be conducted due to poor purity and the limited availability of enzymes. D-xylose, L-arabinose, and D-mannose are major hemicellulose components in plant cell walls, and the activity of Ka97 towards these monosaccharides in the presence of Fc as an electron acceptor was established. Confirmation that Ka97 and Ad18 are AA3 enzymes was done by detecting the cofactor FAD in its free form by fluorescence spectrometer. This approach was required due to low FAD incorporation in both enzymes. Whether low FAD loading leads to improper enzyme folding or vice versa was not clear. All in all, we successfully expressed these two enzymes, confirmed they are AA3 enzymes, and one of them was verified to be active towards D-xylose and Fc.

Since the major challenge here was the expression of the enzymes, it would be very intriguing to compare expressions of these genes in another host. All the putative genes selected here originated from *Actinomycetes*, thus, using a host which is phylogenetically closer to *Actinomycetes* such as *S. lividans* might solve the problem regarding protein folding and expression.

For the second study on the subcellular location of bacterial AA3 enzymes, the previously characterized pyranose oxidase derived from *Kitasatospora aureofaciens*, *Ka*POx, was used. A physiological role in peroxidase activation and redox cycling in lignin depolymerization suggests an extracellular localization of bacterial POx, which is shown in this study. This finding gives a better understanding on how bacteria, in particular *K. aureofaciens*, could be involved in lignin degradation.

In this study, the selection of an appropriate host for recombinant enzyme expression turned out to be crucial. Although both host organisms are Gram-positive bacteria, *B. subtilis* was unable to deliver the recombinant enzyme to the supernatant in meaningful amounts, but *S. lividans* was able to secret the targeted recombinant enzyme. Verification of secreted *Ka*POx is of importance for further study of this enzyme family. It suggests the possibility of secretion of other bacterial auxiliary enzymes, which can be employed in industrial applications. Nonetheless, more studies and data are required to obtain a better overview on this matter.

The third study was conducted to strengthen the obtained information on secreted bacterial AA3 enzymes. Exploration on the other bacterial pyranose oxidase harbouring putative signal peptides was narrowed down to candidates *Sa*GMC (derived from *S. Alboniger*, annotated as pyranose oxidase) and *Sg*GMC (derived from *S. Griseochromogenes*, annotated as dehydrogenase). The recombinant protein production of both enzyme candidates showed *Sa*GMC is secreted extracellular when the additional upstream amino acid sequence constituting a signal peptide is present. Further investigation on enzyme activity of *Sa*GMC showed activity towards fructose and glucose, where the latter was confirmed to generate 2-keto D-glucose as its oxidation product. Therefore, in the end, we could confirm *Sa*GMC as *Sa*POx. We are aware that a more detailed characterization of *Sa*POx is required for a better understanding of this enzyme, but the confirmation that *Sa*POx is a secretory enzyme strengthens the point made in the second study regarding the secretion of *Ka*POx.

Based on the secretion study conducted for the last two projects, the growth pattern of the host cell (*S. lividans*) was similar. Cell lines harbouring constructs of targeted enzymes with native signal peptides generated more biomass compared to constructs without signal peptide. This confirmed the hypothesis of a cellular stress reaction due to the accumulation of overexpressed proteins that could not be secreted. Based on our study, we conclude that compared to the other bacterial host such as *E. coli* and *B. subtilis*, *S. lividans* is the best option for studies on recombinant secreted enzymes derived from *Actinomycetes*. Yet, there is still room for improvement to optimize the secretion and delivery of active enzyme using *S. lividans* as a host.

References

Those who do not remember the past are condemned to repeat it – George Santayana

5. References

Abdel-Hamid, A. M., Solbiati, J. O., & Cann, I. K. O. (2013). Insights into Lignin Degradation and its Potential Industrial Applications. *Advances in Applied Microbiology*, *82*, 1–28. https://doi.org/10.1016/B978-0-12-407679-2.00001-6

Ai, M. Q., Wang, F. F., Zhang, Y. Z., & Huang, F. (2014). Purification of pyranose oxidase from the white rot fungus Irpex lacteus and its cooperation with laccase in lignin degradation. *Process Biochemistry*, *49*(12), 2191–2198. https://doi.org/10.1016/j.procbio.2014.10.001

Albrecht, M., & Lengauer, T. (2003). Pyranose oxidase identified as a member of the GMC oxidoreductase family. *Bioinformatics*, *19*(10), 1216–1220. https://doi.org/10.1093/bioinformatics/btg140

Allen, W. J., Phan, G., & Waksman, G. (2009). Structural Biology of Periplasmic Chaperones. *Advances in Protein Chemistry and Structural Biology*, *78*, 51–97. https://doi.org/10.1016/S1876-1623(08)78003-9

Amersham Pharmacia Biotech. (1999). *Protein Purification Handbook Edition AB*.

Anné, J., Maldonado, B., van Impe, J., van Mellaert, L., & Bernaerts, K. (2012). Recombinant protein production and streptomycetes. *Journal of Biotechnology*, *158*(4), 159–167. https://doi.org/10.1016/j.jbiotec.2011.06.028

Anné, J., Vrancken, K., van Mellaert, L., van Impe, J., & Bernaerts, K. (2014). Protein secretion biotechnology in Gram-positive bacteria with special emphasis on Streptomyces lividans. In *Biochimica et Biophysica Acta - Molecular Cell Research* (Vol. 1843, Issue 8, pp. 1750–1761). Elsevier. https://doi.org/10.1016/j.bbamcr.2013.12.023

Auclair, S. M., Bhanu, M. K., & Kendall, D. A. (2012). Signal peptidase I: Cleaving the way to mature proteins. In *Protein Science* (Vol. 21, Issue 1, pp. 13–25). https://doi.org/10.1002/pro.757

Bach, H., Mazor, Y., Shaky, S., Shoham-Lev, A., Berdichevsky, Y., Gutnick, D. L., & Benhar, I. (2001). Escherichia coli maltose-binding protein as a molecular chaperone for recombinant intracellular cytoplasmic single-chain antibodies. *Journal of Molecular Biology*, *312*(1), 79–93. https://doi.org/10.1006/jmbi.2001.4914

Baig, F., Fernando, L. P., Salazar, M. A., Powell, R. R., Bruce, T. F., & Harcum, S. W. (2014). Dynamic Transcriptional Response of Escherichia coli to Inclusion Body Formation. *Biotechnol. Bioeng*, *111*, 980–999. https://doi.org/10.1002/bit.25169/abstract

Baminger, U., Subramaniam, S. S., Renganathan, V., & Haltrich, D. (2001). Purification and Characterization of Cellobiose Dehydrogenase from the Plant Pathogen Sclerotium (Athelia) rolfsii. *Applied and Environmental Microbiology*, *67*(4), 1766–1774. https://doi.org/10.1128/AEM.67.4.1766-1774.2001

Bannwarth, M., Bastian, S., Heckmann-Pohl, D., Giffhorn, F., & Schulz, G. E. (2004). Crystal structure of pyranose 2-oxidase from the white-rot fungus Peniophora sp. *Biochemistry*, *43*(37), 11683–11690. https://doi.org/10.1021/bi048609q

Bauer, J. A., Zámocká, M., Majtán, J., & Bauerová-Hlinková, V. (2022). Glucose Oxidase, an Enzyme "Ferrari": Its Structure, Function, Production and Properties in the Light of Various Industrial and Biotechnological Applications. In *Biomolecules* (Vol. 12, Issue 3). MDPI. https://doi.org/10.3390/biom12030472

Becker, J. M., Caldwell, G. A., & Zachgo Eve Ann. (1996). *Biotechnology* (second). https://doi.org/https://doi.org/10.1016/B978-012084562-0/50072-2

Becker, J., & Wittmann, C. (2019). A field of dreams: Lignin valorization into chemicals, materials, fuels, and health-care products. In *Biotechnology Advances* (Vol. 37, Issue 6). Elsevier Inc. https://doi.org/10.1016/j.biotechadv.2019.02.016

Bendtsen, J. D., Nielsen, H., Widdick, D., Palmer, T., & Brunak, S. (2005). Prediction of twin-arginine signal peptides. *BMC Bioinformatics*, *6*. https://doi.org/10.1186/1471-2105-6-167

Berg, B., & McClaugherty, C. (2014). *Plant Litter*. Springer Berlin Heidelberg. https://doi.org/10.1007/978-3-642-38821-7

Berini, F., Marinelli, F., & Binda, E. (2020). Streptomycetes: Attractive Hosts for Recombinant Protein Production. In *Frontiers in Microbiology* (Vol. 11). Frontiers Media S.A. https://doi.org/10.3389/fmicb.2020.01958

Berks, B. C. (2015). The Twin-Arginine Protein Translocation Pathway. *Annual Review of Biochemistry*, *84*, 843–864.

Bhatwa, A., Wang, W., Hassan, Y. I., Abraham, N., Li, X. Z., & Zhou, T. (2021). Challenges associated with the formation of recombinant protein inclusion bodies in escherichia coli and strategies to address them for industrial applications. In *Frontiers in Bioengineering and Biotechnology* (Vol. 9). Frontiers Media S.A. https://doi.org/10.3389/fbioe.2021.630551

Bodor, A., Bounedjoum, N., Vincze, G. E., Erdeiné Kis, Á., Laczi, K., Bende, G., Szilágyi, Á., Kovács, T., Perei, K., & Rákhely, G. (2020). Challenges of unculturable bacteria: environmental perspectives. In *Reviews in Environmental Science and Biotechnology* (Vol. 19, Issue 1). Springer. https://doi.org/10.1007/s11157-020-09522-4

Boivin, S., Kozak, S., & Meijers, R. (2013). Optimization of protein purification and characterization using Thermofluor screens. In *Protein Expression and Purification* (Vol. 91, Issue 2, pp. 192–206). https://doi.org/10.1016/j.pep.2013.08.002

Bongers, R. S., Veening, J. W., van Wieringen, M., Kuipers, O. P., & Kleerebezem, M. (2005). Development and characterization of a subtilin-regulated expression system in Bacillus subtilis: Strict control of gene expression by addition of subtilin. *Applied and Environmental Microbiology*, *71*(12), 8818–8824. https://doi.org/10.1128/AEM.71.12.8818-8824.2005

Brown, M. E., Barros, T., & Chang, M. C. Y. (2012). Identification and Characterization of a Multifunctional Dye Peroxidase from a Lignin-Reactive Bacterium. *ACS Chemical Biology*, *7*(12), 2074–2081. https://doi.org/10.1021/cb300383y

Brown, M. E., & Chang, M. C. Y. (2014). Exploring bacterial lignin degradation. In *Current Opinion in Chemical Biology* (Vol. 19, Issue 1, pp. 1–7). https://doi.org/10.1016/j.cbpa.2013.11.015

Brown, M. E., Walker, M. C., Nakashige, T. G., Iavarone, A. T., & Chang, M. C. Y. (2011). Discovery and characterization of heme enzymes from unsequenced bacteria: Application to microbial lignin degradation. *Journal of the American Chemical Society*, *133*(45), 18006–18009. https://doi.org/10.1021/ja203972q

Bugg, T. D. H., Ahmad, M., Hardiman, E. M., & Singh, R. (2011). The emerging role for bacteria in lignin degradation and bio-product formation. In *Current Opinion in Biotechnology* (Vol. 22, Issue 3, pp. 394–400). https://doi.org/10.1016/j.copbio.2010.10.009

Burdette, L. A., Leach, S. A., Wong, H. T., & Tullman-Ercek, D. (2018). Developing Gram-negative bacteria for the secretion of heterologous proteins. In *Microbial Cell Factories* (Vol. 17, Issue 1). BioMed Central Ltd. https://doi.org/10.1186/s12934-018-1041-5

Cavener, D. R. (1992). GMC oxidoreductases: A newly defined family of homologous proteins with diverse catalytic activities. *Journal of Molecular Biology*, *223*(3), 811–814. https://doi.org/10.1016/0022-2836(92)90992-S

Cléon, F., Habersetzer, J., Alcock, F., Kneuper, H., Stansfeld, P. J., Basit, H., Wallace, M. I., Berks, B. C., & Palmer, T. (2015). The TatC component of the twin-arginine protein translocase functions as an obligate oligomer. *Molecular Microbiology*, *98*(1), 111–129. https://doi.org/10.1111/mmi.13106

Cone, M. C., Yin, X., Grochowski, L. L., Parker, M. R., & Zabriskie, T. M. (2003). The Blasticidin S Biosynthesis Gene Cluster from Streptomyces griseochromogenes: Sequence Analysis, Organization, and Initial Characterization. *ChemBioChem*, *4*(9), 821–828. https://doi.org/10.1002/cbic.200300583

Costa, S., Almeida, A., Castro, A., & Domingues, L. (2014). Fusion tags for protein solubility, purification, and immunogenicity in Escherichia coli: The novel Fh8 system. In *Frontiers in Microbiology* (Vol. 5, Issue FEB). Frontiers Research Foundation. https://doi.org/10.3389/fmicb.2014.00063

Cragg, S. M., Beckham, G. T., Bruce, N. C., Bugg, T. D. H., Distel, D. L., Dupree, P., Etxabe, A. G., Goodell, B. S., Jellison, J., McGeehan, J. E., McQueen-Mason, S. J., Schnorr, K., Walton, P. H., Watts, J. E. M., & Zimmer, M. (2015). Lignocellulose degradation mechanisms across the Tree of Life. In *Current Opinion in Chemical Biology* (Vol. 29, pp. 108–119). Elsevier Ltd. https://doi.org/10.1016/j.cbpa.2015.10.018

Crawford, D. L. (1978). Lignocellulose Decomposition by Selected Streptomyces Strainst. In *Appl. and environ. Microbiol.*

Csarman, F., Wohlschlager, L., & Ludwig, R. (2020). Cellobiose dehydrogenase. In *Enzymes* (Vol. 47, pp. 457–489). Academic Press. https://doi.org/10.1016/bs.enz.2020.06.002

Dälken, B., Jabulowsky, R. A., Oberoi, P., Benhar, I., & Wels, W. S. (2010). Maltose-binding protein enhances secretion of recombinant human granzyme B accompanied by in vivo processing of a precursor MBP fusion protein. *PLoS ONE*, *5*(12). https://doi.org/10.1371/journal.pone.0014404

Daniel, G., Volc, J., Kubatova, E., & Nilsson', T. (1992). Ultrastructural and Immunocytochemical Studies on the H202-Producing Enzyme Pyranose Oxidase in Phanerochaete chrysosporium Grown under Liquid Culture Conditions. In *Appl. and environ. Microbiol.* (Vol. 58, Issue 11). https://journals.asm.org/journal/aem

Daniel, G., Volc, J., & Kubatova2, E. (1994). Pyranose Oxidase, a Major Source of H202 during Wood Degradation by Phanerochaete chrysosporium, Trametes versicolor, and Oudemansiella mucida. In *Appl. and environ. Microbiol.* (Vol. 60, Issue 7). http://aem.asm.org/

DANNEEL, H. -J, RÖSSNER, E., ZEECK, A., & GIFFHORN, F. (1993). Purification and characterization of a pyranose oxidase from the basidiomycete Peniophora gigantea and chemical analyses of its reaction products. *European Journal of Biochemistry*, *214*(3), 795–802. https://doi.org/10.1111/j.1432-1033.1993.tb17982.x

Daou, M., Piumi, F., Cullen, D., Record, E., & Faulds, C. B. (2016). Heterologous production and characterization of two glyoxal oxidases from Pycnoporus cinnabarinus. *Applied and Environmental Microbiology*, *82*(16), 4867–4875. https://doi.org/10.1128/AEM.00304-16

Dashtban, M., Schraft, H., Syed, T. A., & Qin, W. (2010). Fungal biodegradation and enzymatic modification of lignin. *International Journal of Molecular Biology*, *1*(1), 36–50.

Davis, J. R., Goodwin, L., Teshima, H., Detter, C., Tapia, R., Han, C., Huntemann, M., Wei, C. L., Han, J., Chen, A., Kyrpides, N., Mavrommatis, K., Szeto, E., Markowitz, V., Ivanova, N., Mikhailova, N., Ovchinnikova, G., Pagani, I., Pati, A., … Sello, J. K. (2013). Genome sequence of Streptomyces viridosporus strain T7A ATCC 39115, a lignin-degrading actinomycete. *Genome Announcements*, *1*(4). https://doi.org/10.1128/genomeA.00416-13

Day, M. A., Jarrom, D., Christofferson, A. J., Graziano, A. E., Ross Anderson, J. L., Searle, P. F., Hyde, E. I., & White, S. A. (2021). The structures of E. coli NfsA bound to the antibiotic nitrofurantoin; to 1,4-benzoquinone and to FMN. *Biochemical Journal*, *478*(13), 2601–2617. https://doi.org/10.1042/BCJ20210160

de Gonzalo, G., Colpa, D. I., Habib, M. H. M., & Fraaije, M. W. (2016). Bacterial enzymes involved in lignin degradation. In *Journal of Biotechnology* (Vol. 236, pp. 110–119). Elsevier B.V. https://doi.org/10.1016/j.jbiotec.2016.08.011

de Marco, A., Ferrer-Miralles, N., Garcia-Fruitós, E., Mitraki, A., Peternel, S., Rinas, U., Trujillo-Roldán, M. A., Valdez-Cruz, N. A., Vázquez, E., & Villaverde, A. (2019). Bacterial inclusion bodies are industrially exploitable amyloids. In *FEMS Microbiology Reviews* (Vol. 43, Issue 1, pp. 53–72). Oxford University Press. https://doi.org/10.1093/femsre/fuy038

de Oliveira, B. v., Teixeira, G. S., Reis, O., Barau, J. G., Teixeira, P. J. P. L., do Rio, M. C. S., Domingues, R. R., Meinhardt, L. W., Paes Leme, A. F., Rincones, J., & Pereira, G. A. G. (2012). A potential role for an extracellular methanol oxidase secreted by Moniliophthora perniciosa in Witches' broom disease in cacao. *Fungal Genetics and Biology*, *49*(11), 922–932. https://doi.org/10.1016/j.fgb.2012.09.001

de Strooper, B., & Karran, E. (2016). The Cellular Phase of Alzheimer's Disease. In *Cell* (Vol. 164, Issue 4, pp. 603–615). Cell Press. https://doi.org/10.1016/j.cell.2015.12.056

DeAngelis, K. M., Allgaier, M., Chavarria, Y., Fortney, J. L., Hugenholtz, P., Simmons, B., Sublette, K., Silver, W. L., & Hazen, T. C. (2011). Characterization of trapped lignin-degrading microbes in tropical forest soil. *PLoS ONE*, *6*(4). https://doi.org/10.1371/journal.pone.0019306

Du, F., Liu, Y. Q., Xu, Y. S., Li, Z. J., Wang, Y. Z., Zhang, Z. X., & Sun, X. M. (2021). Regulating the T7 RNA polymerase expression in E. coli BL21 (DE3) to provide more host options for recombinant protein production. *Microbial Cell Factories*, *20*(1). https://doi.org/10.1186/s12934-021-01680-6

Dubendorfft, J. W., & Studier, F. W. (1991). Controlling Basal Expression in an Inducible T7 Expression System by Blocking the Target T7 Promoter with Zac Repressor. In *J. Mol. Biol* (Vol. 219).

Duong-Ly, K. C., & Gabelli, S. B. (2015a). Affinity Purification of a Recombinant Protein Expressed as a Fusion with the Maltose-Binding Protein (MBP) Tag. In *Methods in Enzymology* (Vol. 559, pp. 17–26). Academic Press Inc. https://doi.org/10.1016/bs.mie.2014.11.004

Duong-Ly, K. C., & Gabelli, S. B. (2015b). Affinity Purification of a Recombinant Protein Expressed as a Fusion with the Maltose-Binding Protein (MBP) Tag. In *Methods in Enzymology* (Vol. 559, pp. 17–26). Academic Press Inc. https://doi.org/10.1016/bs.mie.2014.11.004

Dvorak, P., Chrast, L., Nikel, P. I., Fedr, R., Soucek, K., Sedlackova, M., Chaloupkova, R., Lorenzo, V., Prokop, Z., & Damborsky, J. (2015). Exacerbation of substrate toxicity by IPTG in Escherichia coli BL21(DE3) carrying a synthetic metabolic pathway. *Microbial Cell Factories*, *14*(1). https://doi.org/10.1186/s12934-015-0393-3

Faury, D., Saidane, S., Li, H., & Morosoli, R. (2004). Secretion of active xylanase C from Streptomyces lividans is exclusively mediated by the Tat protein export system. *Biochimica et Biophysica Acta (BBA) - Proteins and Proteomics*, *1699*(1–2), 155–162. https://doi.org/10.1016/j.bbapap.2004.02.008

Felice, A. K. G., Schuster, C., Kadek, A., Filandr, F., Laurent, C. V. F. P., Scheiblbrandner, S., Schwaiger, L., Schachinger, F., Kracher, D., Sygmund, C., Man, P., Halada, P., Oostenbrink, C., & Ludwig, R. (2021). Chimeric Cellobiose Dehydrogenases Reveal the Function of Cytochrome Domain Mobility for the Electron Transfer to Lytic Polysaccharide Monooxygenase. *ACS Catalysis*, *11*(2), 517–532. https://doi.org/10.1021/acscatal.0c05294

Fernandes, T. A. R., Silveira, W. B. da, Passos, F. M. L., & Zucchi, T. D. (2014). Laccases from Actinobacteria — What We Have and What to Expect. *Advances in Microbiology*, *04*(06), 285–296. https://doi.org/10.4236/aim.2014.46035

Ferreira, P., Carro, J., Serrano, A., & Martínez, A. T. (2015). A survey of genes encoding H2O2-producing GMC oxidoreductases in 10 Polyporales genomes. *Mycologia*, *107*(6), 1105–1119. https://doi.org/10.3852/15-027

Frain, K. M., Robinson, C., & van Dijl, J. M. (2019). Transport of Folded Proteins by the Tat System. In *Protein Journal* (Vol. 38, Issue 4, pp. 377–388). Springer Science and Business Media, LLC. https://doi.org/10.1007/s10930-019-09859-y

Frank, E. G., McDonald, J. P., Karata, K., Huston, D., & Woodgate, R. (2012). A strategy for the expression of recombinant proteins traditionally hard to purify. *Analytical Biochemistry*, *429*(2), 132–139. https://doi.org/10.1016/j.ab.2012.07.016

Gacias-Amengual, N., Wohlschlager, L., Csarman, F., & Ludwig, R. (2022). Fluorescent Imaging of Extracellular Fungal Enzymes Bound onto Plant Cell Walls. *International Journal of Molecular Sciences*, *23*(9). https://doi.org/10.3390/ijms23095216

Gelis, I., Bonvin, A. M. J. J., Keramisanou, D., Koukaki, M., Gouridis, G., Karamanou, S., Economou, A., & Kalodimos, C. G. (2007). *Structural basis for signal sequence recognition by the 204-kDa translocase motor SecA determined by NMR*.

Gibson, L. J. (2012). The hierarchical structure and mechanics of plant materials. In *Journal of the Royal Society Interface* (Vol. 9, Issue 76, pp. 2749–2766). Royal Society. https://doi.org/10.1098/rsif.2012.0341

Goheen, S. C., & Gibbins, B. M. (2000). Protein losses in ion-exchange and hydrophobic interaction high-performance liquid chromatography. In *Journal of Chromatography A* (Vol. 890). www.elsevier.com/locate/chroma

Goheen, S. C., & Hilsenbeck, J. L. (1998). High-performance ion-exchange chromatography and adsorption of plasma proteins. In *Journal of Chromatography A* (Vol. 816).

Gopal, G. J., & Kumar, A. (2013). Strategies for the production of recombinant protein in escherichia coli. *Protein Journal*, *32*(6), 419–425. https://doi.org/10.1007/s10930-013-9502-5

Gouridis, G., Karamanou, S., Gelis, I., Kalodimos, C. G., & Economou, A. (2009). Signal peptides are allosteric activators of the protein translocase. *Nature*, *462*(7271), 363–367. https://doi.org/10.1038/nature08559

Granato, E. T., Meiller-Legrand, T. A., & Foster, K. R. (2019). The Evolution and Ecology of Bacterial Warfare. In *Current Biology* (Vol. 29, Issue 11, pp. R521–R537). Cell Press. https://doi.org/10.1016/j.cub.2019.04.024

Green, Mi. R., & Sambrook, J. (2012). *Molecular Cloning: A Laboratory Manual, 4th edition. Click here for more information or to buy the book* (4th ed.). John Inglis. www.cshlpress.org

Gregersen, N., Bross, P., Vang, S., & Christensen, J. H. (2006). Protein misfolding and human disease. In *Annual Review of Genomics and Human Genetics* (Vol. 7, pp. 103–124). https://doi.org/10.1146/annurev.genom.7.080505.115737

Gullón, S., & Mellado, R. P. (2018). The cellular mechanisms that ensure an efficient secretion in Streptomyces. In *Antibiotics* (Vol. 7, Issue 2). MDPI AG. https://doi.org/10.3390/antibiotics7020033

Halada, P., Leitner, C., Sedmera, P., Haltrich, D., & Volc, J. (2003). Identification of the covalent flavin adenine dinucleotide-binding region in pyranose 2-oxidase from Trametes multicolor. *Analytical Biochemistry*, *314*(2), 235–242. https://doi.org/10.1016/S0003-2697(02)00661-9

Hall, K. R., Robins, K. J., Williams, E. M., Rich, M. H., Calcott, M. J., Copp, J. N., Little, R. F., Schwörer, R., Evans, G. B., Patrick, W. M., & Ackerley, D. F. (2020). Intracellular complexities of acquiring a new enzymatic function revealed by mass-randomisation of active site residues. *ELife*, *9*, 1–40. https://doi.org/10.7554/eLife.59081

Hall, S. J., Silver, W. L., Timokhin, V. I., & Hammel, K. E. (2015). Lignin decomposition is sustained under fluctuating redox conditions in humid tropical forest soils. *Global Change Biology*, *21*(7), 2818–2828. https://doi.org/10.1111/gcb.12908

Hallberg, B. M., Leitner, C., Haltrich, D., & Divne, C. (2004). Crystallization and preliminary X-ray diffraction analysis of pyranose 2-oxidase from the white-rot fungus Trametes multicolor. *Acta Crystallographica. Section D, Biological Crystallography*, *60*(Pt 1), 197–199. https://doi.org/10.1107/S0907444903024922

Hamed, M. B., Anné, J., Karamanou, S., & Economou, A. (2018). Streptomyces protein secretion and its application in biotechnology. In *FEMS Microbiology Letters* (Vol. 365, Issue 22). Oxford University Press. https://doi.org/10.1093/femsle/fny250

Hamed, M. B., Vrancken, K., Bilyk, B., Koepff, J., Novakova, R., van Mellaert, L., Oldiges, M., Luzhetskyy, A., Kormanec, J., Anné, J., Karamanou, S., & Economou, A. (2018). Monitoring protein secretion in Streptomyces using fluorescent proteins. *Frontiers in Microbiology*, *9*(DEC). https://doi.org/10.3389/fmicb.2018.03019

Harwood, C. R., & Cranenburgh, R. (2008). Bacillus protein secretion: an unfolding story. In *Trends in Microbiology* (Vol. 16, Issue 2, pp. 73–79). https://doi.org/10.1016/j.tim.2007.12.001

Hassan, N., Tan, T. C., Spadiut, O., Pisanelli, I., Fusco, L., Haltrich, D., Peterbauer, C. K., & Divne, C. (2013). Crystal structures of Phanerochaete chrysosporium pyranose 2-oxidase suggest that the N-terminus acts as a propeptide that assists in homotetramer assembly. *FEBS Open Bio*, *3*, 496–504. https://doi.org/10.1016/j.fob.2013.10.010

Hecht, H. J., Kalisz, H. M., Hendle, J., Schmid, R. D., & Schomburg, D. (1993). Crystal Structure of Glucose Oxidase from Aspergillus niger Refined at 2·3 Å Reslution. *Journal of Molecular Biology*, *229*(1), 153–172. https://doi.org/10.1006/JMBI.1993.1015

Herzog, P. L., Sützl, L., Eisenhut, B., Maresch, D., Haltrich, D., Obinger, C., & Peterbauer, C. K. (2019). *Versatile Oxidase and Dehydrogenase Activities of Bacterial Pyranose 2-Oxidase Facilitate Redox Cycling with Manganese Peroxidase In Vitro*. https://doi.org/10.1128/AEM

Hibbing, M. E., Fuqua, C., Parsek, M. R., & Peterson, S. B. (2010). Bacterial competition: Surviving and thriving in the microbial jungle. In *Nature Reviews Microbiology* (Vol. 8, Issue 1, pp. 15–25). https://doi.org/10.1038/nrmicro2259

Houston, K., Tucker, M. R., Chowdhury, J., Shirley, N., & Little, A. (2016). The plant cell wall: A complex and dynamic structure as revealed by the responses of genes under stress conditions. In *Frontiers in Plant Science* (Vol. 7, Issue AUG2016). Frontiers Media S.A. https://doi.org/10.3389/fpls.2016.00984

Hsiao, N. H., & Kirby, R. (2008). Comparative genomics of Streptomyces avermitilis, Streptomyces cattleya, Streptomyces maritimus and Kitasatospora aureofaciens using a Streptomyces coelicolor microarray system. *Antonie van Leeuwenhoek, International Journal of General and Molecular Microbiology*, *93*(1–2), 1–25. https://doi.org/10.1007/s10482-007-9175-1

Huang, K. T., Misato, T., & Asuyama, H. (1964). Effect of blasticidins on protein synthesis of *Piricularia oryzae*. *The Journal of Antibiotics*, *17*, 65–70.

Huang, X.-F., Santhanam, N., Badri, D. v, Hunter, W. J., Manter, D. K., Decker, S. R., Vivanco, J. M., & Reardon, K. F. (2013). Isolation and Characterization of Lignin-Degrading Bacteria from Rainforest Soils. *Biotechnology and Bioengineering*, *110*, 1616–1626. https://doi.org/10.1002/bit.24833/abstract

Islam, M. S., Honma, M., Nakabayashi, T., Kinjo, M., & Ohta, N. (2013). pH dependence of the fluorescence lifetime of FAD in solution and in cells. *International Journal of Molecular Sciences*, *14*(1), 1952–1963. https://doi.org/10.3390/ijms14011952

Ithal, N., Recknor, J., Nettleton, D., Maier, T., Baum, T. J., & Mitchum, M. G. (2007). Developmental Transcript Profiling of Cyst Nematode Feeding Cells in Soybean Roots e-Xtra *. *Molecular Plant-Microbe Interactions MPMI*, *510*(5), 510–525. https://doi.org/10.1094/MPMI

James, J., Yarnall, B., Koranteng, A., Gibson, J., Rahman, T., & Doyle, D. A. (2021). Protein over-expression in Escherichia coli triggers adaptation analogous to antimicrobial resistance. *Microbial Cell Factories*, *20*(1). https://doi.org/10.1186/s12934-020-01462-6

Janssen, F. W., & Ruelius, H. W. (1968). Carbohydrate oxidase, a novel enzyme from polyporus obtusus. *Biochimica et Biophysica Acta (BBA) - Enzymology*, *167*(3), 501–510. https://doi.org/10.1016/0005-2744(68)90040-5

Janusz, G., Pawlik, A., Sulej, J., Świderska-Burek, U., Jarosz-Wilkolazka, A., & Paszczyński, A. (2017a). Lignin degradation: Microorganisms, enzymes involved, genomes analysis and evolution. In *FEMS Microbiology Reviews* (Vol. 41, Issue 6, pp. 941–962). Oxford University Press. https://doi.org/10.1093/femsre/fux049

Janusz, G., Pawlik, A., Sulej, J., Świderska-Burek, U., Jarosz-Wilkolazka, A., & Paszczyński, A. (2017b). Lignin degradation: Microorganisms, enzymes involved, genomes analysis and evolution. In *FEMS Microbiology Reviews* (Vol. 41, Issue 6, pp. 941–962). Oxford University Press. https://doi.org/10.1093/femsre/fux049

Jin, T., Chuenchor, W., Jiang, J., Cheng, J., Li, Y., Fang, K., Huang, M., Smith, P., & Xiao, T. S. (2017). Design of an expression system to enhance MBP-mediated crystallization. *Scientific Reports*, *7*. https://doi.org/10.1038/srep40991

Kallunki, T., Barisic, M., Jäättelä, M., & Liu, B. (2019). How to choose the right inducible gene expression system for Mammalian studies? In *Cells* (Vol. 8, Issue 8). MDPI. https://doi.org/10.3390/cells8080796

Kaper, J. B., & Nataro, J. P. (2016). Escherichia coli in the Americas. In *Escherichia Coli in the Americas*. Springer International Publishing. https://doi.org/10.1007/978-3-319-45092-6

Kapust, R. B., & Waugh, D. S. (1999). Escherichia coli maltose-binding protein is uncommonly effective at promoting the solubility of polypeptides to which it is fused. *Protein Science*, *8*, 1668–1674.

Kersten, P. J., & Cullen, D. (1993). Cloning and characterization of a cDNA encoding glyoxal oxidase, a H202-producing enzyme from the lignin-degrading basidiomycete Phanerochaete chrysosporium (hydrogen peroxide/peroxidase/fungus/galactose oxidase). In *Proc. Natl. Acad. Sci. USA* (Vol. 90). https://www.pnas.org

Klaysubun, C., Srisuk, N., & Duangmal, K. (2022). Kitasatospora humi sp. nov., isolated from a tropical peat swamp forest soil, and proposal for the reclassification of Kitasatospora psammotica as a later heterotypic synonym of Kitasatospora aureofaciens. *International Journal of Systematic and Evolutionary Microbiology*, *72*(5). https://doi.org/10.1099/ijsem.0.005356

Kleiner-Grote, G. R. M., Risse, J. M., & Friehs, K. (2018). Secretion of recombinant proteins from E. coli. In *Engineering in Life Sciences* (Vol. 18, Issue 8, pp. 532–550). Wiley-VCH Verlag. https://doi.org/10.1002/elsc.201700200

Koch, C., Neumann, P., Valerius, O., Feussner, I., & Ficner, R. (2016). Crystal structure of alcohol oxidase from Pichia pastoris. *PLoS ONE*, *11*(2). https://doi.org/10.1371/journal.pone.0149846

Kolenc, O. I., & Quinn, K. P. (2019). Evaluating cell metabolism through autofluorescence imaging of NAD(P)H and FAD. In *Antioxidants and Redox Signaling* (Vol. 30, Issue 6, pp. 875–889). Mary Ann Liebert Inc. https://doi.org/10.1089/ars.2017.7451

Kolkman, M. A. B., van der Ploeg, R., Bertels, M., van Dijk, M., van der Laan, J., van Dijl, J. M., & Ferrari, E. (2008). The twin-arginine signal peptide of Bacillus subtilis YwbN can direct either Tat- or Sec-dependent secretion of different cargo proteins: Secretion of active subtilisin via the B. subtilis Tat

pathway. *Applied and Environmental Microbiology*, *74*(24), 7507–7513. https://doi.org/10.1128/AEM.01401-08

Kostelac, A., Sützl, L., Puc, J., Furlanetto, V., Divne, C., & Haltrich, D. (2022). Biochemical Characterization of Pyranose Oxidase from Streptomyces canus—Towards a Better Understanding of Pyranose Oxidase Homologues in Bacteria. *International Journal of Molecular Sciences*, *23*(21), 13595. https://doi.org/10.3390/ijms232113595

Kracher, D., Scheiblbrandner, S., Felice, A. K. G., Breslmayr, E., Preims, M., Ludwicka, K., Haltrich, D., Eijsink, V. G. H., & Ludwig, R. (2016). Extracellular electron transfer systems fuel cellulose oxidative degradation. *Science*. 352(6289): 1098-101.doi: 10.1126/science.aaf3165

Krefft, D., Prusinowski, M., Maciszka, P., Skokowska, A., Zebrowska, J., & Skowron, P. M. (2022). T7-lac promoter vectors spontaneous derepression caused by plant-derived growth media may lead to serious expression problems: a systematic evaluation. *Microbial Cell Factories*, *21*(1). https://doi.org/10.1186/s12934-022-01740-5

Kujawa, M., Volc, J., Halada, P., Sedmera, P., Divne, C., Sygmund, C., Leitner, C., Peterbauer, C., & Haltrich, D. (2007). Properties of pyranose dehydrogenase purified from the litter-degrading fungus Agaricus xanthoderma. *FEBS Journal*, *274*(3), 879–894. https://doi.org/10.1111/j.1742-4658.2007.05634.x

Labeda, D. P., Dunlap, C. A., Rong, X., Huang, Y., Doroghazi, J. R., Ju, K. S., & Metcalf, W. W. (2017). Phylogenetic relationships in the family Streptomycetaceae using multi-locus sequence analysis. *Antonie van Leeuwenhoek, International Journal of General and Molecular Microbiology*, *110*(4), 563–583. https://doi.org/10.1007/s10482-016-0824-0

Lagaert, S., Beliën, T., & Volckaert, G. (2009). Plant cell walls: Protecting the barrier from degradation by microbial enzymes. In *Seminars in Cell and Developmental Biology* (Vol. 20, Issue 9, pp. 1064–1073). Elsevier Ltd. https://doi.org/10.1016/j.semcdb.2009.05.008

Lappe, A., Jankowski, N., Albrecht, A., & Koschorreck, K. (2021). Characterization of a thermotolerant aryl-alcohol oxidase from Moesziomyces antarcticus oxidizing 5-hydroxymethyl-2-furancarboxylic acid. *Applied Microbiology and Biotechnology*, *105*(21–22), 8313–8327. https://doi.org/10.1007/s00253-021-11557-8

Lebendiker, M., & Danieli, T. (2017). Purification of proteins fused to maltose-binding protein. In *Methods in Molecular Biology* (Vol. 1485, pp. 257–273). Humana Press Inc. https://doi.org/10.1007/978-1-4939-6412-3_13

Lee, J.J., Brulev, D.F., & Kang, K.A. (2007). Effect of pH and imidazole on protein C purification from Cohn fraction iv-1 by IMAC. DOI:10.1007/978-0-387-71764-7_9.

Lee, P. A., Tullman-Ercek, D., & Georgiou, G. (2006). The bacterial twin-arginine translocation pathway. In *Annual Review of Microbiology* (Vol. 60, pp. 373–395). https://doi.org/10.1146/annurev.micro.60.080805.142212

Lee, S., Kang, M., Bae, J. H., Sohn, J. H., & Sung, B. H. (2019). Bacterial Valorization of Lignin: Strains, Enzymes, Conversion Pathways, Biosensors, and Perspectives. In *Frontiers in Bioengineering and Biotechnology* (Vol. 7). Frontiers Media S.A. https://doi.org/10.3389/fbioe.2019.00209

Leitner, C., Volc, J., & Haltrich, D. (2001). Purification and Characterization of Pyranose Oxidase from the White Rot Fungus *Trametes multicolor*. *Applied and Environmental Microbiology*, *67*(8), 3636–3644. https://doi.org/10.1128/AEM.67.8.3636-3644.2001

Levasseur, A., Drula, E., Lombard, V., Coutinho, P. M., & Henrissat, B. (2013a). Expansion of the enzymatic repertoire of the CAZy database to integrate auxiliary redox enzymes. *Biotechnology for Biofuels*, *6*(1). https://doi.org/10.1186/1754-6834-6-41

Levasseur, A., Drula, E., Lombard, V., Coutinho, P. M., & Henrissat, B. (2013b). Expansion of the enzymatic repertoire of the CAZy database to integrate auxiliary redox enzymes. *Biotechnology for Biofuels*, *6*(1). https://doi.org/10.1186/1754-6834-6-41

Levasseur, A., Piumi, F., Coutinho, P. M., Rancurel, C., Asther, M., Delattre, M., Henrissat, B., Pontarotti, P., Asther, M., & Record, E. (2008). FOLy: An integrated database for the classification and functional annotation of fungal oxidoreductases potentially involved in the degradation of lignin and related

aromatic compounds. *Fungal Genetics and Biology*, *45*(5), 638–645. https://doi.org/10.1016/j.fgb.2008.01.004

Levy-Booth, D. J., Navas, L. E., Fetherolf, M. M., Liu, L. Y., Dalhuisen, T., Renneckar, S., Eltis, L. D., & Mohn, W. W. (2022). Discovery of lignin-transforming bacteria and enzymes in thermophilic environments using stable isotope probing. *ISME Journal*, *16*(8), 1944–1956. https://doi.org/10.1038/s41396-022-01241-8

Li, H., Faury, D., & Morosoli, R. (2006). Impact of amino acid changes in the signal peptide on the secretion of the Tat-dependent xylanase C from Streptomyces lividans. *FEMS Microbiology Letters*, *255*(2), 268–274. https://doi.org/10.1111/j.1574-6968.2005.00081.x

Liu, Q., Luo, L., & Zheng, L. (2018). Lignins: Biosynthesis and biological functions in plants. In *International Journal of Molecular Sciences* (Vol. 19, Issue 2). MDPI AG. https://doi.org/10.3390/ijms19020335

Lojkova, L., Vranová, V., Formánek, P., Drápelová, I., Brtnicky, M., & Datta, R. (2020). Enantiomers of carbohydrates and their role in ecosystem interactions: A review. *Symmetry*, *12*(3). https://doi.org/10.3390/sym12030470

Lorenzo, H. K., Farber, D., Germain, V., Acuto, O., & Alzari, P. M. (1997). The MBP fusion protein restores the activity of the furst phosphatase domain of CD45. *FEBS Letters*, *411*, 231–235.

Lozano Terol, G., Gallego-Jara, J., Sola Martínez, R. A., Martínez Vivancos, A., Cánovas Díaz, M., & de Diego Puente, T. (2021). Impact of the Expression System on Recombinant Protein Production in Escherichia coli BL21. *Frontiers in Microbiology*, *12*. https://doi.org/10.3389/fmicb.2021.682001

Luo, N., Yang, Y. bin, Yang, X. Q., Miao, C. P., Li, Y. Q., Xu, L. H., Ding, Z. T., & Zhao, L. X. (2018). The streptazolin- and obscurolide-type metabolites from soil-derived: Streptomyces alboniger YIM20533 and the mechanism of influence of γ-butyrolactone on the growth of Streptomyces by their non-enzymatic reaction biosynthesis. *RSC Advances*, *8*(61), 35042–35049. https://doi.org/10.1039/c8ra06690f

Machida, Y., & Nakanishi, T. (1984). Purification and properties of pyranose oxidase from coriolus versicolor. *Agricultural and Biological Chemistry*, *48*(10), 2463–2470. https://doi.org/10.1080/00021369.1984.10866537

Mairhofer, J., Scharl, T., Marisch, K., Cserjan-Puschmann, M., & Striedner, G. (2013). Comparative transcription profiling and in-depth characterization of plasmid-based and plasmid-free Escherichia coli expression systems under production conditions. *Applied and Environmental Microbiology*, *79*(12), 3802–3812. https://doi.org/10.1128/AEM.00365-13

Malhotra, A. (2009). Chapter 16 Tagging for Protein Expression. *Methods in Enzymology*, *463*(C), 239–258. https://doi.org/10.1016/S0076-6879(09)63016-0

Marschall, L., Sagmeister, P., & Herwig, C. (2017). Tunable recombinant protein expression in E. coli: promoter systems and genetic constraints. In *Applied Microbiology and Biotechnology* (Vol. 101, Issue 2, pp. 501–512). Springer Verlag. https://doi.org/10.1007/s00253-016-8045-z

Martinez, A. T., Speranza, M., Ruiz-Duenas, F. J., Ferreira, P., Camarero, S., Guillen, F., Martinez, M. J., Gutierrez, An., & del Rio, J. C. (2005). *Biodegradation of lignocellu-losics: microbial, chemical, and enzymatic aspects of the fungal attack of lignin Lignocellulosic materials*. www.im.microbios.org

Masai, E., Katayama, Y., & Fukuda, M. (2007). Genetic and biochemical investigations on bacterial catabolic pathways for lignin-derived aromatic compounds. In *Bioscience, Biotechnology and Biochemistry* (Vol. 71, Issue 1, pp. 1–15). https://doi.org/10.1271/bbb.60437

Mayolo-Deloisa, K., González-González, M., & Rito-Palomares, M. (2020). Laccases in Food Industry: Bioprocessing, Potential Industrial and Biotechnological Applications. In *Frontiers in Bioengineering and Biotechnology* (Vol. 8). Frontiers Media S.A. https://doi.org/10.3389/fbioe.2020.00222

Mendes, S., Banha, C., Madeira, J., Santos, D., Miranda, V., Manzanera, M., Ventura, M. R., van Berkel, W. J. H., & Martins, L. O. (2016). Characterization of a bacterial pyranose 2-oxidase from Arthrobacter siccitolerans. *Journal of Molecular Catalysis B: Enzymatic*, *133*, S34–S43. https://doi.org/10.1016/j.molcatb.2016.11.005

Miedes, E., Vanholme, R., Boerjan, W., & Molina, A. (2014). The role of the secondary cell wall in plant resistance to pathogens. In *Frontiers in Plant Science* (Vol. 5, Issue AUG). Frontiers Research Foundation. https://doi.org/10.3389/fpls.2014.00358

Miklos, A. C., Li, C., Sorrell, C. D., Lyon, L. A., & Pielak, G. J. (2011). Evaluation of three industrial Escherichia coli strains in fed-batch cultivations during high-level SOD protein production. *BMC Biophysics*, *4*(1). https://doi.org/10.1186/2046-1682-4-13

Miller, N. J., & Rice-Evans, C. A. (1997). Factors influencing the antioxidant activity determined by the ABTS.+ radical cation assay. *Free Radical Research*, *26*(3), 195–199. https://doi.org/10.3109/10715769709097799

Mitraki, A., & King, J. (1989). *Protein folding intermediates and inclusion body formation*. http://www.nature.com/naturebiotechnology

Momin, A. A., Hameed, U. F. S., & Arold, S. T. (2019). Passenger sequences can promote interlaced dimers in a common variant of the maltose-binding protein. *Scientific Reports*, *9*(1). https://doi.org/10.1038/s41598-019-56718-y

Mori, K., Nakajima, M., Kojima, K., Murakami, K., Ferri, S., & Sode, K. (2011). Screening of Aspergillus-derived FAD-glucose dehydrogenases from fungal genome database. *Biotechnology Letters*, *33*(11), 2255–2263. https://doi.org/10.1007/s10529-011-0694-5

Neef, J., van Dijl, J. M., & Buist, G. (2021). Recombinant protein secretion by Bacillus subtilis and lactococcus lactis: Pathways, applications, and innovation potential. In *Essays in Biochemistry* (Vol. 65, Issue 2, pp. 187–195). Portland Press Ltd. https://doi.org/10.1042/EBC20200171

Nishihara, K., Kanemori, M., Kitagawa, M., Yanagi, H., & Yura, T. (1998). Chaperone Coexpression Plasmids: Differential and Synergistic Roles of DnaK-DnaJ-GrpE and GroEL-GroES in Assisting Folding of an Allergen of Japanese Cedar Pollen, Cryj2, in Escherichia coli. In *Applied and environmental microbiology* (Vol. 64, Issue 5). https://journals.asm.org/journal/aem

Nishihara, K., Kanemori, M., Yanagi, H., & Yura, T. (2000). Overexpression of Trigger Factor Prevents Aggregation of Recombinant Proteins in Escherichia coli. In *Applied and environmental microbiology* (Vol. 66, Issue 3).

Nishimura, I., Okada, K., & Koyama, Y. (1996). Cloning and expression of pyranose oxidase cDNA from Coriolus versicolor in Escherichia coli. In *Journal of Biotechnology* (Vol. 52).

Nominé, Y., Ristriani, T., & Laurent, C. (2001). A strategy for optimizing the monodispersity of fusion proteins: application to purification of recombinant HPV E6 oncoprotein. In *Protein Engineering* (Vol. 14, Issue 4).

Obradovic, J., Jurisic, V., Tosic, N., Mrdjanovic, J., Perin, B., Pavlovic, S., & Djordjevic, N. (2013). Optimization of PCR conditions for amplification of GC-rich EGFR promoter sequence. *Journal of Clinical Laboratory Analysis*, *27*(6), 487–493. https://doi.org/10.1002/jcla.21632

Odier,', E., Janin, G., & Monties3, A. B. (1981). Poplar Lignin Decomposition by Gram-Negative Aerobic Bacteria. In *Applied and environmental microbiology*.

Ouellette, R. J., & Rawn, J. D. (2018). Carbohydrates. *Organic Chemistry*, 889–928. https://doi.org/10.1016/B978-0-12-812838-1.50028-1

Pedersen, N. J. (n.d.). *Oxidation of veratryl alcohol with lignin peroxidase and nanoscale photosystems*.

Pennati, A., Deng, J., & Galipeau, J. (2014). Maltose-binding protein fusion allows for high level bacterial expression and purification of bioactive mammalian cytokine derivatives. *PLoS ONE*, *9*(9). https://doi.org/10.1371/journal.pone.0106724

Pessione, E. (2021). The Less Expensive Choice: Bacterial Strategies to Achieve Successful and Sustainable Reciprocal Interactions. In *Frontiers in Microbiology* (Vol. 11). Frontiers Media S.A. https://doi.org/10.3389/fmicb.2020.571417

Peterbauer, C. K., & Volc, J. (2010). Pyranose dehydrogenases: Biochemical features and perspectives of technological applications. In *Applied Microbiology and Biotechnology* (Vol. 85, Issue 4, pp. 837–848). https://doi.org/10.1007/s00253-009-2226-y

Piano, V., Palfey, B. A., & Mattevi, A. (2017). Flavins as Covalent Catalysts: New Mechanisms Emerge. In *Trends in Biochemical Sciences* (Vol. 42, Issue 6, pp. 457–469). Elsevier Ltd. https://doi.org/10.1016/j.tibs.2017.02.005

Pisanelli, I., Kujawa, M., Spadiut, O., Kittl, R., Halada, P., Volc, J., Mozuch, M. D., Kersten, P., Haltrich, D., & Peterbauer, C. (2009). Pyranose 2-oxidase from Phanerochaete chrysosporium-Expression in E. coli and

biochemical characterization. *Journal of Biotechnology*, *142*(2), 97–106. https://doi.org/10.1016/j.jbiotec.2009.03.019

Plomion, C., Leprovost, G., & Stokes, A. (2001). Wood formation in trees. In *Plant Physiology* (Vol. 127, Issue 4, pp. 1513–1523). American Society of Plant Biologists. https://doi.org/10.1104/pp.010816

Pogue, J. M., Dudley, M. N., Eranki, A., & Kaye, K. S. (2017). Tetracyclines and Chloramphenicol. *Infectious Diseases, 2-Volume Set*, 1256-1260.e1. https://doi.org/10.1016/B978-0-7020-6285-8.00146-5

Pryor, K. D., & Leiting, B. (1997). High-Level Expression of Soluble Protein in Escherichia coli Using a His 6-Tag and Maltose-Binding-Protein Double-Affinity Fusion System. In *protein expression and purification* (Vol. 10).

Ramón, A., Señorale-Pose, M., & Marín, M. (2014). Inclusion bodies: Not that bad... In *Frontiers in Microbiology* (Vol. 5, Issue FEB). Frontiers Research Foundation. https://doi.org/10.3389/fmicb.2014.00056

Raran-Kurussi, S., & Waugh, D. S. (2012a). The Ability to Enhance the Solubility of Its Fusion Partners Is an Intrinsic Property of Maltose-Binding Protein but Their Folding Is Either Spontaneous or Chaperone-Mediated. *PLoS ONE*, *7*(11). https://doi.org/10.1371/journal.pone.0049589

Raran-Kurussi, S., & Waugh, D. S. (2012b). The Ability to Enhance the Solubility of Its Fusion Partners Is an Intrinsic Property of Maltose-Binding Protein but Their Folding Is Either Spontaneous or Chaperone-Mediated. *PLoS ONE*, *7*(11). https://doi.org/10.1371/journal.pone.0049589

Rashid, G. M. M., Taylor, C. R., Liu, Y., Zhang, X., Rea, D., Fülöp, V., & Bugg, T. D. H. (2015). Identification of Manganese Superoxide Dismutase from Sphingobacterium sp. T2 as a Novel Bacterial Enzyme for Lignin Oxidation. *ACS Chemical Biology*, *10*(10), 2286–2294. https://doi.org/10.1021/acschembio.5b00298

Rinas, U., Garcia-Fruitós, E., Corchero, J. L., Vázquez, E., Seras-Franzoso, J., & Villaverde, A. (2017). Bacterial Inclusion Bodies: Discovering Their Better Half. In *Trends in Biochemical Sciences* (Vol. 42, Issue 9, pp. 726–737). Elsevier Ltd. https://doi.org/10.1016/j.tibs.2017.01.005

Rosenberg, A. H., Lade, B. N., Chui, D., Lin, S.-W., Dunn, J. J., & Studier, F. W. (n.d.). *vectors for selective expression of cloned DNAs by T7 RNA polymerase*.

Saavedra-Alanis, V. M., Rysavy, P., Rosenbergs, L. E., & Kalousekb, F. (1994). Rat Liver Mitochondrial Processing Peptidase. *The Journal of Biological Chemistry*, *269*(12), 9284–9288.

Sachdev, D., & Chirgwin, J. M. (1998). Solubility of Proteins Isolated from Inclusion Bodies Is Enhanced by Fusion to Maltose-Binding Protein or Thioredoxin. In *protein expression and purification* (Vol. 12).

Sala, A., Bordes, P., & Genevaux, P. (2014). Multitasking SecB chaperones in bacteria. In *Frontiers in Microbiology* (Vol. 5, Issue DEC). Frontiers Media S.A. https://doi.org/10.3389/fmicb.2014.00666

Salaheddin, C., Takakura, Y., Tsunashima, M., Stranzinger, B., Spadiut, O., Yamabhai, M., Peterbauer, C. K., & Haltrich, D. (2010). *Characterisation of recombinant pyranose oxidase from the cultivated mycorrhizal basidiomycete Lyophyllum shimeji (hon-shimeji)*. http://www.microbialcellfactories.com/content/9/1/57

Salvachúa, D., Werner, A. Z., Pardo, I., Michalska, M., Black, B. A., Donohoe D ⊚, B. S., Haugen, S. J., Katahira, R., Notonier, S., Ramirez D ⊚, K. J., Amore, A., Purvine, S. O., Zink, E. M., Abraham, P. E., Giannone, R. J., Poudel, S., Laible, P. D., Hettich, R. L., & Beckham, G. T. (2020). Outer membrane vesicles catabolize lignin-derived aromatic compounds in Pseudomonas putida KT2440. *PNAS*, *117*(17), 9302–9310. https://doi.org/10.1073/pnas.1921073117/-/DCSupplemental

Sankaran, L., & Pogell, B. M. (1975). Biosynthesis of Puromycin in Streptomyces alboniger: Regulation and Properties of O-Demethylpuromycin 0-Methyltransferase. In *antimicrobial agents and chemotherapy* (Vol. 8, Issue 6). American Society for Microbiology. https://journals.asm.org/journal/aac

Sato, K., Nishina, Y., & Shiga, K. (2013). Decomposition of the fluorescence spectra of two FAD molecules in electron-transferring flavoprotein from Megasphaera elsdenii. In *Journal of Biochemistry* (Vol. 154, Issue 1, pp. 61–66). https://doi.org/10.1093/jb/mvt027

Scheiblbrandner, S., & Ludwig, R. (2020). Cellobiose dehydrogenase: Bioelectrochemical insights and applications. In *Bioelectrochemistry* (Vol. 131). Elsevier B.V. https://doi.org/10.1016/j.bioelechem.2019.107345

Schnekenburger, M., & Diederich, M. (2015). Nutritional Epigenetic Regulators in the Field of Cancer: New Avenues for Chemopreventive Approaches. *Epigenetic Cancer Therapy*, 393–425. https://doi.org/10.1016/B978-0-12-800206-3.00018-5

Schwinn, K., Ferré, N., & Huix-Rotllant, M. (2020). UV-visible absorption spectrum of FAD and its reduced forms embedded in a cryptochrome protein. *Physical Chemistry Chemical Physics*, *22*(22), 12447–12455. https://doi.org/10.1039/d0cp01714k

Sevillano, L., Vijgenboom, E., van Wezel, G. P., Díaz, M., & Santamaría, R. I. (2016). New approaches to achieve high level enzyme production in Streptomyces lividans. *Microbial Cell Factories*, *15*(1). https://doi.org/10.1186/s12934-016-0425-7

Sianidis, G., Pozidis, C., Becker, F., Vrancken, K., Sjoeholm, C., Karamanou, S., Takamiya-Wik, M., van Mellaert, L., Schaefer, T., Anné, J., & Economou, A. (2006). Functional large-scale production of a novel Jonesia sp. xyloglucanase by heterologous secretion from Streptomyces lividans. *Journal of Biotechnology*, *121*(4), 498–507. https://doi.org/10.1016/j.jbiotec.2005.08.002

Sigoillot, J. C., Berrin, J. G., Bey, M., Lesage-Meessen, L., Levasseur, A., Lomascolo, A., Record, E., & Uzan-Boukhris, E. (2012). Fungal Strategies for Lignin Degradation. In *Advances in Botanical Research* (Vol. 61, pp. 263–308). Academic Press Inc. https://doi.org/10.1016/B978-0-12-416023-1.00008-2

Silva Coelho-Moreira, J. da, Maria, G., Castoldi, R., Silva Mariano, S. da, Dorneles, F., Bracht, A., & Marina, R. (2013). Involvement of Lignin-Modifying Enzymes in the Degradation of Herbicides. In *Herbicides - Advances in Research*. InTech. https://doi.org/10.5772/55848

Singh, A., Upadhyay, V., Singh, A., & Panda, A. K. (2020). Structure-Function Relationship of Inclusion Bodies of a Multimeric Protein. *Frontiers in Microbiology*, *11*. https://doi.org/10.3389/fmicb.2020.00876

Singh, A., Upadhyay, V., Upadhyay, A. K., Singh, S. M., & Panda, A. K. (2015). Protein recovery from inclusion bodies of Escherichia coli using mild solubilization process. In *Microbial Cell Factories* (Vol. 14, Issue 1). BioMed Central Ltd. https://doi.org/10.1186/s12934-015-0222-8

Singhvi, P., Saneja, A., Srichandan, S., & Panda, A. K. (2020). Bacterial Inclusion Bodies: A Treasure Trove of Bioactive Proteins. In *Trends in Biotechnology* (Vol. 38, Issue 5, pp. 474–486). Elsevier Ltd. https://doi.org/10.1016/j.tibtech.2019.12.011

Spadiut, O., Tan, T. C., Pisanelli, I., Haltrich, D., & Divne, C. (2010). Importance of the gating segment in the substrate-recognition loop of pyranose 2-oxidase. *FEBS Journal*, *277*(13), 2892–2909. https://doi.org/10.1111/j.1742-4658.2010.07705.x

Stewart, E. J. (2012). Growing unculturable bacteria. In *Journal of Bacteriology* (Vol. 194, Issue 16, pp. 4151–4160). https://doi.org/10.1128/JB.00345-12

Stick, R. v., & Williams, S. J. (2009). Disaccharides, Oligosaccharides and Polysaccharides. *Carbohydrates: The Essential Molecules of Life*, 321–341. https://doi.org/10.1016/B978-0-240-52118-3.00009-0

Stirling, P. C., Lundin, V. F., & Leroux, M. R. (2003). Getting a grip on non-native proteins. In *EMBO Reports* (Vol. 4, Issue 6, pp. 565–570). https://doi.org/10.1038/sj.embor.embor869

Strandberg, L., & Enfors, S.-O. (1991). Factors Influencing Inclusion Body Formation in the Production of a Fused Protein in Escherichia coli. In *applied and environmental microbiology* (Vol. 57, Issue 6).

Stucchi, M., Cattaneo, S., Cappella, A., Wang, W., Wang, D., Villa, A., & Prati, L. (2020). Catalytic Oxidation of Methoxy Substituted Benzyl Alcohols as Model for Lignin Valorisation. *Catalysis Today*, *357*, 15–21. https://doi.org/10.1016/j.cattod.2019.03.022

Studier, F. W., & Moffattf, B. A. (1986). Use of Bacteriophage T7 RNA Polymerase to Direct Selective High-level Expression of Cloned Genes. In *J. MoZ. Biol* (Vol. 189).

Sützl, L., Foley, G., Gillam, E. M. J., Bodén, M., & Haltrich, D. (2019). The GMC superfamily of oxidoreductases revisited: Analysis and evolution of fungal GMC oxidoreductases. *Biotechnology for Biofuels*, *12*(1). https://doi.org/10.1186/s13068-019-1457-0

Sützl, L., Laurent, C. V. F. P., Abrera, A. T., Schütz, G., Ludwig, R., & Haltrich, D. (2018). Multiplicity of enzymatic functions in the CAZy AA3 family. In *Applied Microbiology and Biotechnology* (Vol. 102, Issue 6, pp. 2477–2492). Springer Verlag. https://doi.org/10.1007/s00253-018-8784-0

Sygmund, C., Kittl, R., Volc, J., Halada, P., Kubátová, E., Haltrich, D., & Peterbauer, C. K. (2008). Characterization of pyranose dehydrogenase from Agaricus meleagris and its application in the C-2 specific conversion of d-galactose. *Journal of Biotechnology*, *133*(3), 334–342. https://doi.org/10.1016/j.jbiotec.2007.10.013

Tabor, S. (2000). *Expression Using the T7 RNA Polymerase/Promoter System*. https://doi.org/10.1002/0471142727.mb1602s11

Tabor, S., & Richardson, C. C. (1985). A bacteriophage T7 RNA polymerase/promoter system for controlled exclusive expression of specific genes (T7 DNA polymerase/T7 gene 5 protein/proteolysis/13-lactamase/rifampicin). In *Proc. Nati. Acad. Sci. USA* (Vol. 82). https://www.pnas.org

Takahashi, Y. (2017). Genus Kitasatospora, taxonomic features and diversity of secondary metabolites. In *Journal of Antibiotics* (Vol. 70, Issue 5, pp. 506–513). Nature Publishing Group. https://doi.org/10.1038/ja.2017.8

Takara Bio Inc. (n.d.). *Chaperone Plasmid Set For Research Use v201701Da*. http://www.takara-bio.com

Takeuchi, S., Hirayama, K., Ueda, K., Sakai, H., & Yonehara, H. (1958). Blasticidin S, a new antibiotic. *Journal Antibiotic*, *11*, 1–5.

Tan, T. C., Spadiut, O., Wongnate, T., Sucharitakul, J., Krondorfer, I., Sygmund, C., Haltrich, D., Chaiyen, P., Peterbauer, C. K., & Divne, C. (2013). The 1.6 Å Crystal Structure of Pyranose Dehydrogenase from Agaricus meleagris Rationalizes Substrate Specificity and Reveals a Flavin Intermediate. *PLoS ONE*, *8*(1). https://doi.org/10.1371/journal.pone.0053567

Taylor, C. R., Hardiman, E. M., Ahmad, M., Sainsbury, P. D., Norris, P. R., & Bugg, T. D. H. (2012). Isolation of bacterial strains able to metabolize lignin from screening of environmental samples. *Journal of Applied Microbiology*, *113*(3), 521–530. https://doi.org/10.1111/j.1365-2672.2012.05352.x

Tegel, H., Ottosson, J., & Hober, S. (2011). Enhancing the protein production levels in Escherichia coli with a strong promoter. *FEBS Journal*, *278*(5), 729–739. https://doi.org/10.1111/j.1742-4658.2010.07991.x

Terpe, K. (2006). Overview of bacterial expression systems for heterologous protein production: From molecular and biochemical fundamentals to commercial systems. In *Applied Microbiology and Biotechnology* (Vol. 72, Issue 2, pp. 211–222). https://doi.org/10.1007/s00253-006-0465-8

Thambugala, K. M., Daranagama, D. A., Phillips, A. J. L., Kannangara, S. D., & Promputtha, I. (2020). Fungi vs. Fungi in Biocontrol: An Overview of Fungal Antagonists Applied Against Fungal Plant Pathogens. In *Frontiers in Cellular and Infection Microbiology* (Vol. 10). Frontiers Media S.A. https://doi.org/10.3389/fcimb.2020.604923

Tien, M., & Ma, D. (1997). Oxidation of 4-Methoxymandelic Acid by Lignin Peroxidase mediation by veratryl alcohol*. In *the journal of biological chemistry* (Vol. 272, Issue 14). http://www-jbc.stanford.edu/jbc/

Tsirigotaki, A., de Geyter, J., Šoštarić, N., Economou, A., & Karamanou, S. (2017). Protein export through the bacterial Sec pathway. In *Nature Reviews Microbiology* (Vol. 15, Issue 1, pp. 21–36). Nature Publishing Group. https://doi.org/10.1038/nrmicro.2016.161

van Bloois, E., Torres Pazmiño, D. E., Winter, R. T., & Fraaije, M. W. (2010). A robust and extracellular heme-containing peroxidase from Thermobifida fusca as prototype of a bacterial peroxidase superfamily. *Applied Microbiology and Biotechnology*, *86*(5), 1419–1430. https://doi.org/10.1007/s00253-009-2369-x

Vicente, R. L., Gullón, S., Marín, S., & Mellado, R. P. (2016). The three streptomyces lividans HtrA-Like proteases involved in the secretion stress response act in a cooperative manner. *PLoS ONE*, *11*(12). https://doi.org/10.1371/journal.pone.0168112

Volc, J., Kubátová, E., Daniel, G., Sedmera, P., & Haltrich, D. (2001). Screening of basidiomycete fungi for the quinone-dependent sugar C-2/C-3 oxidoreductase, pyranose dehydrogenase, and properties of the enzyme from Macrolepiota rhacodes. *Archives of Microbiology*, *176*(3), 178–186. https://doi.org/10.1007/s002030100308

Vrancken, K., van Mellaert, L., & Anné, J. (2010). Cloning and expression vectors for a Gram-positive host, Streptomyces lividans. *Methods in Molecular Biology (Clifton, N.J.)*, *668*, 97–107. https://doi.org/10.1007/978-1-60761-823-2_6

Wade, W. (2002). Unculturable bacteriaÐthe uncharacterized organisms that cause oral infections. In *81±83 section of odontology* (Vol. 95).

Walker, W. H., Hemmerich, P., & Massey, V. (1967). Reduktive Photoalkylierung des Flavinkerns und Flavinkatalysierte Photodecarboxylierung von Phenylacetat Studien in der Flavinreihe. 15. Mitteilung [1]. *Helvetica Chimica Acta*, *50*(8), 2269–2279. https://doi.org/10.1002/hlca.19670500812

Weiland-Bräuer, N. (2021). Friends or foes—microbial interactions in nature. In *Biology* (Vol. 10, Issue 6). MDPI AG. https://doi.org/10.3390/biology10060496

Whittaker, M. M., Kersten, P. J., Cullen, D., & Whittaker, J. W. (1999). Identification of Catalytic Residues in Glyoxal Oxidase by Targeted Mutagenesis*. In *the journal of biological chemistry* (Vol. 274, Issue 51). http://www.jbc.org

Widmann, M., & Christen, P. (2000). Comparison of folding rates of homologous prokaryotic and eukaryotic proteins. *Journal of Biological Chemistry*, *275*(25), 18619–18622. https://doi.org/10.1074/jbc.C000156200

Wilhelm, R. C., Singh, R., Eltis, L. D., & Mohn, W. W. (2019). Bacterial contributions to delignification and lignocellulose degradation in forest soils with metagenomic and quantitative stable isotope probing. *ISME Journal*, *13*(2), 413–429. https://doi.org/10.1038/s41396-018-0279-6

Wingfield, P. T. (2015). Overview of the purification of recombinant proteins. *Current Protocols in Protein Science*, *2015*, 6.1.1-6.1.35. https://doi.org/10.1002/0471140864.ps0601s80

Wink, J., Gandhi, J., Kroppenstedt, R. M., Seibert, G., Sträubler, B., Schumann, P., & Stackebrandt, E. (2004). Amycolatopsis decaplanina sp. nov., a novel member of the genus with unsual morphology. *International Journal of Systematic and Evolutionary Microbiology*, *54*(1), 235–239. https://doi.org/10.1099/ijs.0.02586-0

Wongnate, T., & Chaiyen, P. (2013). The substrate oxidation mechanism of pyranose 2-oxidase and other related enzymes in the glucose-methanol-choline superfamily. *FEBS Journal*, *280*(13), 3009–3027. https://doi.org/10.1111/febs.12280

Wu, L., Chen, G., & Feng, G. (2017). Complete genome sequence of Streptomyces griseochromogenes ATCC 14511T, a producer of nucleoside compounds and diverse secondary metabolites. *Journal of Biotechnology*, *249*, 16–19. https://doi.org/10.1016/j.jbiotec.2017.03.017

Wurm, D. J., Veiter, L., Ulonska, S., Eggenreich, B., Herwig, C., & Spadiut, O. (2016). The E. coli pET expression system revisited—mechanistic correlation between glucose and lactose uptake. *Applied Microbiology and Biotechnology*, *100*(20), 8721–8729. https://doi.org/10.1007/s00253-016-7620-7

Xu, Z., Peng, B., Kitata, R. B., Nicora, C. D., Weitz, K. K., Pu, Y., Shi, T., Cort, J. R., Ragauskas, A. J., & Yang, B. (2022). Understanding of bacterial lignin extracellular degradation mechanisms by Pseudomonas putida KT2440 via secretomic analysis. *Biotechnology for Biofuels and Bioproducts*, *15*(1), 117. https://doi.org/10.1186/s13068-022-02214-x

Yamada, Y., Wang, J., Kawagishi, H., & Hirai, H. (2014). Improvement of ligninolytic properties by recombinant expression of glyoxal oxidase gene in hyper lignin-degrading fungus Phanerochaete sordida YK-624. *Bioscience, Biotechnology and Biochemistry*, *78*(12), 2128–2133. https://doi.org/10.1080/09168451.2014.946398

Yoshida, H., Sakai, G., Mori, K., Kojima, K., Kamitori, S., & Sode, K. (2015). Structural analysis of fungus-derived FAD glucose dehydrogenase. *Scientific Reports*, *5*. https://doi.org/10.1038/srep13498

Zámocký, M., Hallberg, M., Ludwig, R., Divne, C., & Haltrich, D. (2004). Ancestral gene fusion in cellobiose dehydrogenases reflects a specific evolution of GMC oxidoreductases in fungi. *Gene*, *338*(1), 1–14. https://doi.org/10.1016/j.gene.2004.04.025

Zeng, Y., Himmel, M. E., & Ding, S. Y. (2017). Visualizing chemical functionality in plant cell walls Mike Himmel. In *Biotechnology for Biofuels* (Vol. 10, Issue 1). BioMed Central Ltd. https://doi.org/10.1186/s13068-017-0953-3

Appendix

6. Appendix

To a great mind, nothing is little – Arthur Conan Doyle

6.1. Supplementary material

A

AA_KaWP97_in_pET21D:
log(e) = -139.3

(validate)

```
  1 MPQDNPAQNQHDPSEADGYDYDVLVIGSGFGGSVSALRLTEKGYRVGVLEAGRRFTRATL  60
 61 PKNSWDLKNYLWAPALGCYGIQRVHLLGNVMVLAGAGVGGGSLNYANTLYVPPKQFFEDR 120
121 QWGHITDWQDELKPYYDQARRMLGVRLNPTMTPSDVHLKAAAEKMGVGDTFHLAPVGVFF 180
181 GDGEDSDGTAKAAPGAEVSDPYFGGAGPARRACTECGECMTGCRHGAKNTLTENYLHLAE 240
241 RAGAVIHPMTSVVTVTEDSRGGFAVGTLPTDDKRKGRGRTFTARRVIVAAGTYGTQTLLH 300
301 KMRDSGLLPLISPRLGELTRTNSEALVGAQTDDRRYRKAHGAPKADFTRGVAITSSVHPN 360
361 AVTHIEPVRYGKGSNAMGSLSVLQVPIPKRAPRALAWAANCARHPLLLLRSLSNRRWSER 420
421 TIIGLVMQSLDNSLTTYRKPGGLGKGLLTARQGHGAPNPQQIPEATEAATLLAQEINGFA 480
481 GSNVGELMGTPLTAHFLGGCPIGEDADHGVIDPYHRLYGHPGISVVDGSAVSANLGVNPS 540
541 LTITAQAERAMSFWPNKGEEDTRPAPGRPYRRLAPVAPSHPAVPEKAFAALRLPLLPVPA 600
601 VPPRSQAAALEHHHHHH                                             617
```

B

AdWP18_pET21D_amino_acid:
log(e) = -34.9

(validate)

```
  1 MTASNTTTEDDFDYDVIVVGSGFGGSVAALRLTEKGYRVAVIEAGRRFADDEFAKTSWDL  60
 61 RRYVWAPQVGCFGIQRIHMLKDVMVLAGAGVGGGSLVYANTLYRPLKPFYVDPQWSHITD 120
121 WESELGPHYDQASRMLGVVTNPSVTPSDVVMKGVAEDMGVPDSYHPTPVGVYFGKPGERA 180
181 EDPYFGGAGPARTGCTECGACMTGCRVGAKNTLVKNYLYLAEKDGAKVIPLTTVSAISPL 240
241 NAGGYEVSIKKTGTTSRKFRHKLTAAQVVLAAGTWGTQNLLHSMRDTAKLPKLSPRLGEL 300
301 TRTNSEAIIGAARTSVDEERNFSRGVAITSSIHPDDNTHIEPVRYGKGSNAMSLLQTIAT 360
361 EGDSAVPRWRQAVNFMFKHPVQTVRLLNGYRWSERTVILLVMQSLDNSITTYTKRGLFGR 420
421 RKYTSKQGHGEPNPSFIPAGHEANLRTAERIGGMAGGTWGEIFDIPLTAHFIGGAPIGTA 480
481 ADNGVIDPYHRVFNYPGLSIVDGSAITANLGVNPSLTITAQAERAFSLWPNKGEQDSRPS 540
541 QDSPYTRLEPIAPKNPAVPADAPAALRRAAALEHHHHHH                       579
```

Figure S1 Mass Spectrometry analysis for Ka97 (A) and Ad18 (B)

Table S1 Mass Spectrometry analysis for Ka97 and Ad18 compared with *E. coli* database

Sample	Rank	Log(E)	Log(I)	Unique	Mr	Accession
Ka97	1	-429.4	7.07	45	74.2	Bifunctional_Polymyxin_Resistance_Protein_Arna_Os=Escherichia_Coli
	2	**-139.3**	**5.96**	**17**	**66.1**	**Aa_Kawp97_In_Pet21d**
	3	-91.4	5.16	12	69.1	Chaperone_Protein_Dnak_Os=Escherichia_Coli_(Strain_B_/_Bl21-De3)
	4	-89.6	5.43	13	71	Atp-Dependent_Zinc_Metalloprotease_Ftsh_Os=Escherichia_Coli
	5	-86.5	5.71	9	62.1	Sp|K1c9_Human| Keratin
	6	-77.5	5.34	10	65.8	Sp|K2c1_Human| Keratin,
	7	-60.8	5.26	8	68.1	Peptidylprolyl_Isomerase_Os=Escherichia_Coli_(Strain_B_/_Bl21-De3)
	8	-60.4	6.69	8	24.4	Trypsin; Ec 3.4.21.4; Flags: Precursor; Sp|Tryp_Pig|
Ad18	1	-274.9	6.42	33	56.1	Ecoli_Alkyl_Hydroperoxide_Reductase_Subunit_F_Os=Escherichia_Coli
	2	-139.3	5.86	15	51.5	Ecoli_Soluble_Pyridine_Nucleotide_Transhydrogenase_Os=Escherichia_Coli
	3	-89.8	5.34	12	66.9	Ecoli_Glutamine--Fructose-6-Phosphate_Aminotransferase_[Isomerizing]
	4	-73.9	5.11	10	69.3	Sp|Albu_Human|
	5	-66.3	5.27	8	57.3	Sp|P0a6f5|Ch60_Ecoli_60_Kda_Chaperonin_Os=Escherichia_Coli
	6	-59.5	4.99	9	53.3	Ecoli_Udp-N-Acetylmuramoyl-L-Alanyl-D-Glutamate
	7	-49	4.72	8	74.2	Ecoli_Bifunctional_Polymyxin_Resistance_Protein_Arna_Os=Escherichia_Coli

	8	**-34.9**	**4.62**	**6**	**62.7**	**Adwp18_pET21d_Amino_Acid**
	9	-30.5	4.66	5	55.2	ATPa_Ecoli_Atp_Synthase_Subunit_Alpha_Os=Escherichia_Coli
	10	-30.3	4.68	5	62.9	Ecoli_Acetolactate_Synthase_Isozyme_3_Large_Subunit
	11	-24.3	4.45	4	54.8	Ecoli_Guanosine-5'-Triphosphate,3'-Diphosphate_Pyrophosphatase
	12	-23.3	4.43	4	51.2	Sp|P76403|Yegq_Ecoli_Uncharacterized_Protease_Yegq_Os=Escherichia_Coli
	13	-23	4.52	4	53.6	Murc_Ecoli_Udp-N-Acetylmuramate--L-Alanine_Ligase_Os=Escherichia_Coli
	14	-16.9	4.57	3	71.1	Dpo3x_Ecoli_Dna_Polymerase_Iii_Subunit_Tau_Os=Escherichia_Coli
	15	-16.9	4.75	3	24.4	Sp|Tryp_Pig|

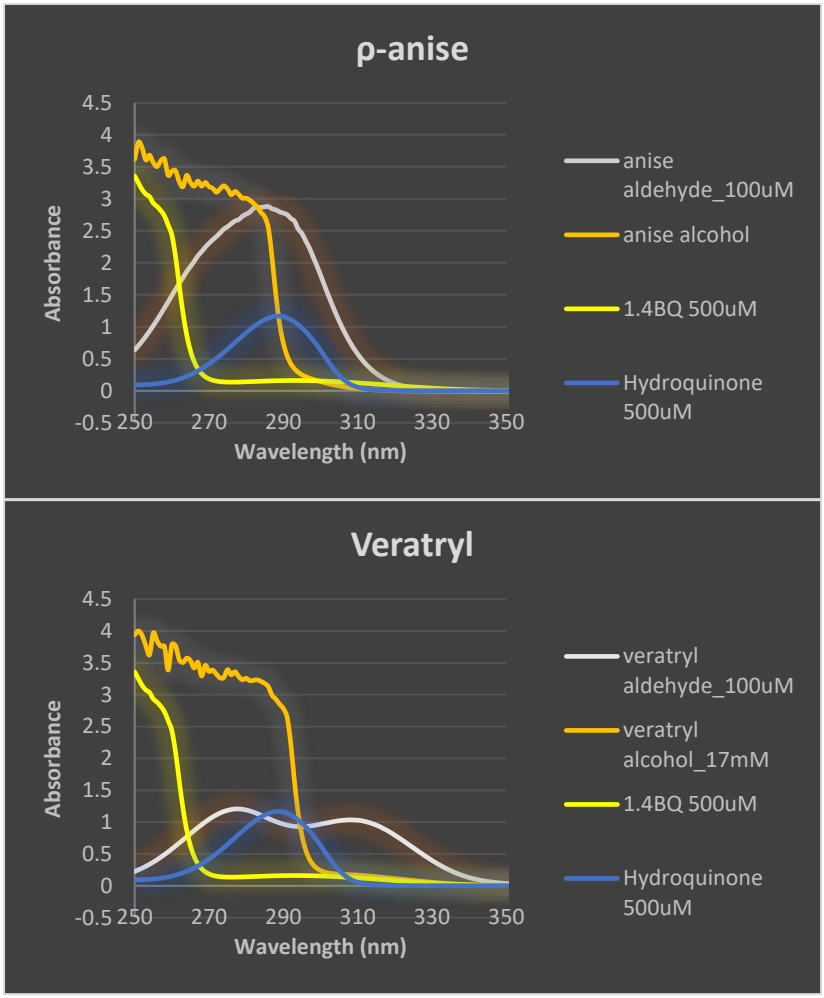

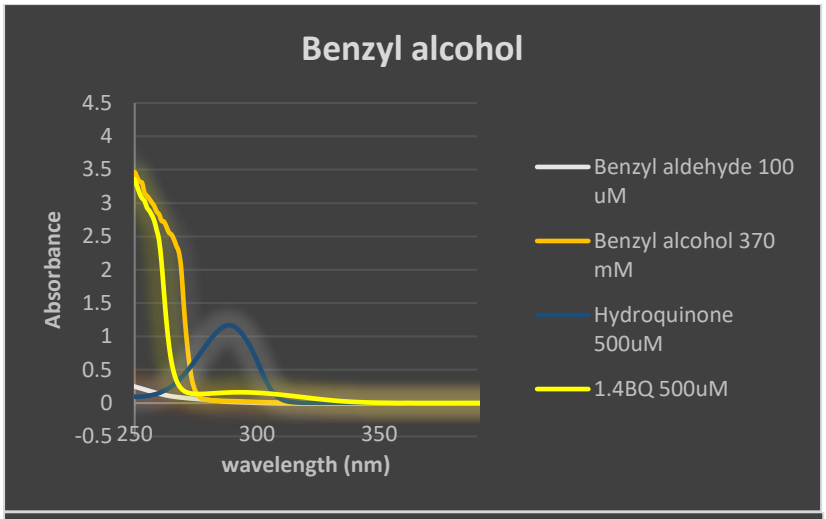
Benzyl alcohol
Absorbance
4.5
4
3.5
3
2.5
2
1.5
1
0.5
0
-0.5
250
300
350
wavelength (nm)
Benzyl aldehyde 100 uM
Benzyl alcohol 370 mM
Hydroquinone 500uM
1.4BQ 500uM

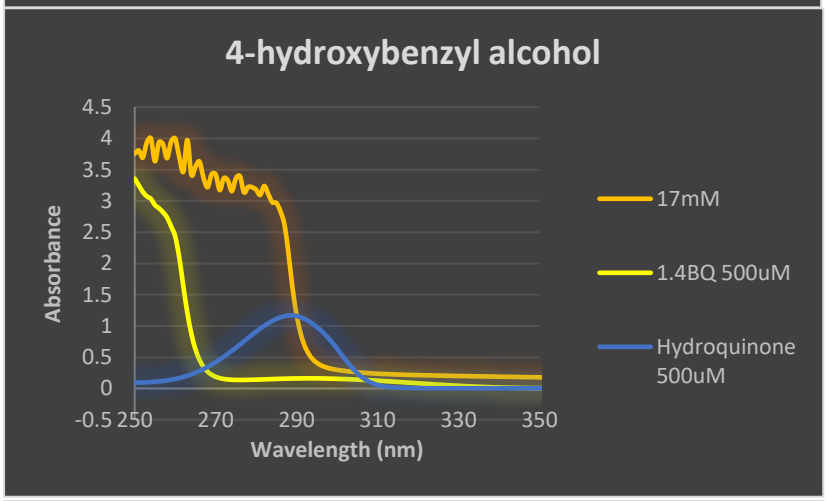
4-hydroxybenzyl alcohol
Absorbance
4.5
4
3.5
3
2.5
2
1.5
1
0.5
0
-0.5
250
270
290
310
330
350
Wavelength (nm)
17mM
1.4BQ 500uM
Hydroquinone 500uM

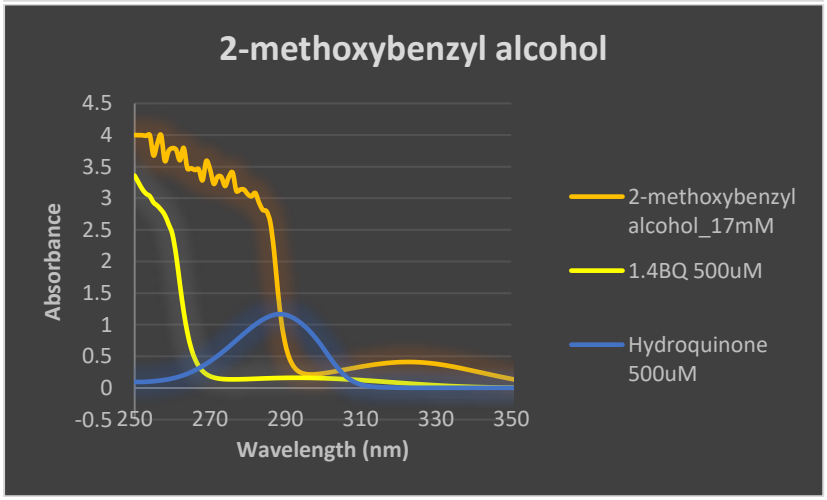
2-methoxybenzyl alcohol
Absorbance
4.5
4
3.5
3
2.5
2
1.5
1
0.5
0
-0.5
250
270
290
310
330
350
Wavelength (nm)
2-methoxybenzyl alcohol_17mM
1.4BQ 500uM
Hydroquinone 500uM

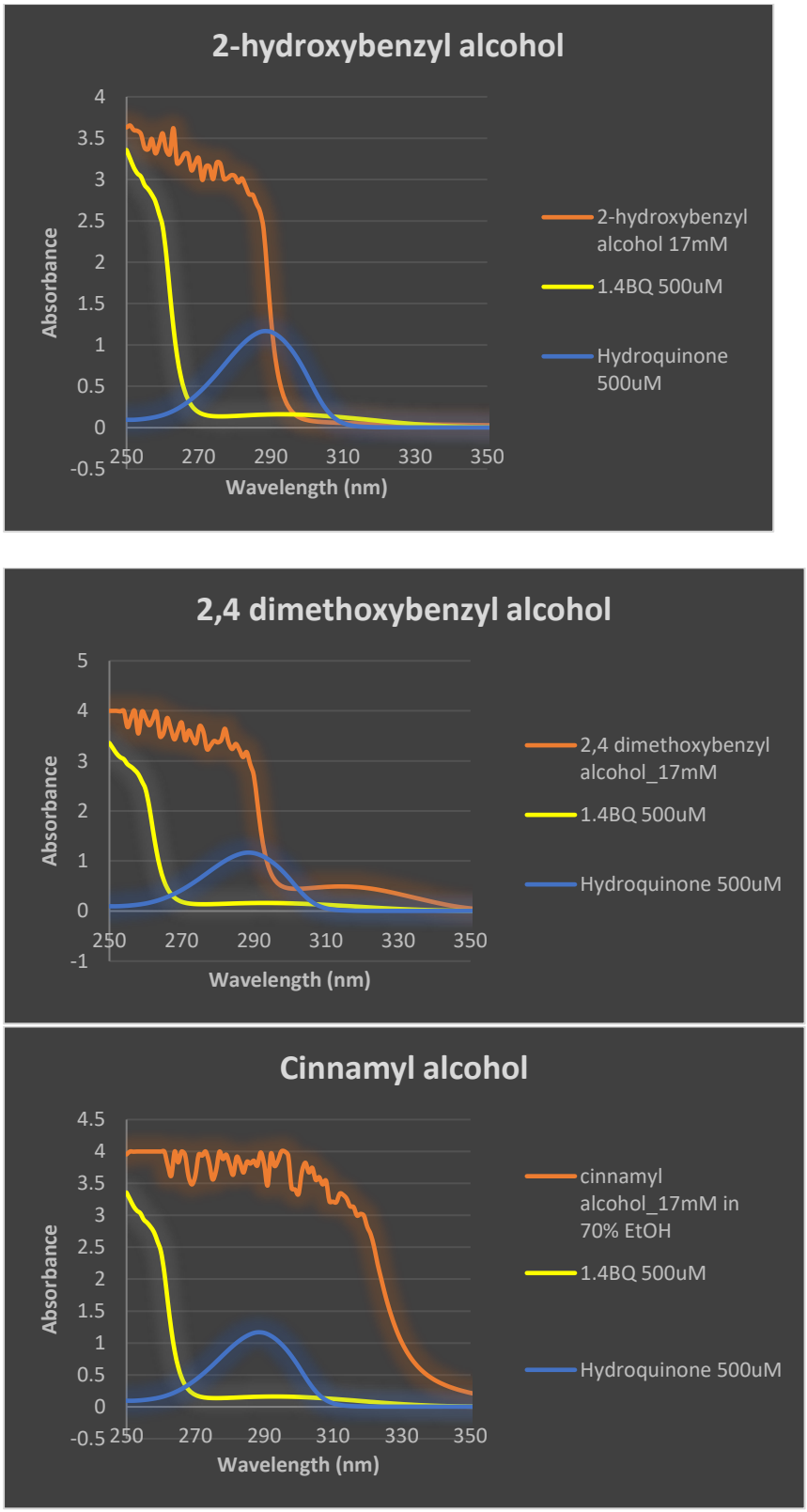

Figure S2 Spectrum of various alcohol (orange line, 17mM unless stated otherwise) and their potential oxidized products, aldehyde, (gray line, 100μM) with 1,4 Benzoquinone (yellow line, 500 μM) and Hydroquinone (blue line, 500 μM).

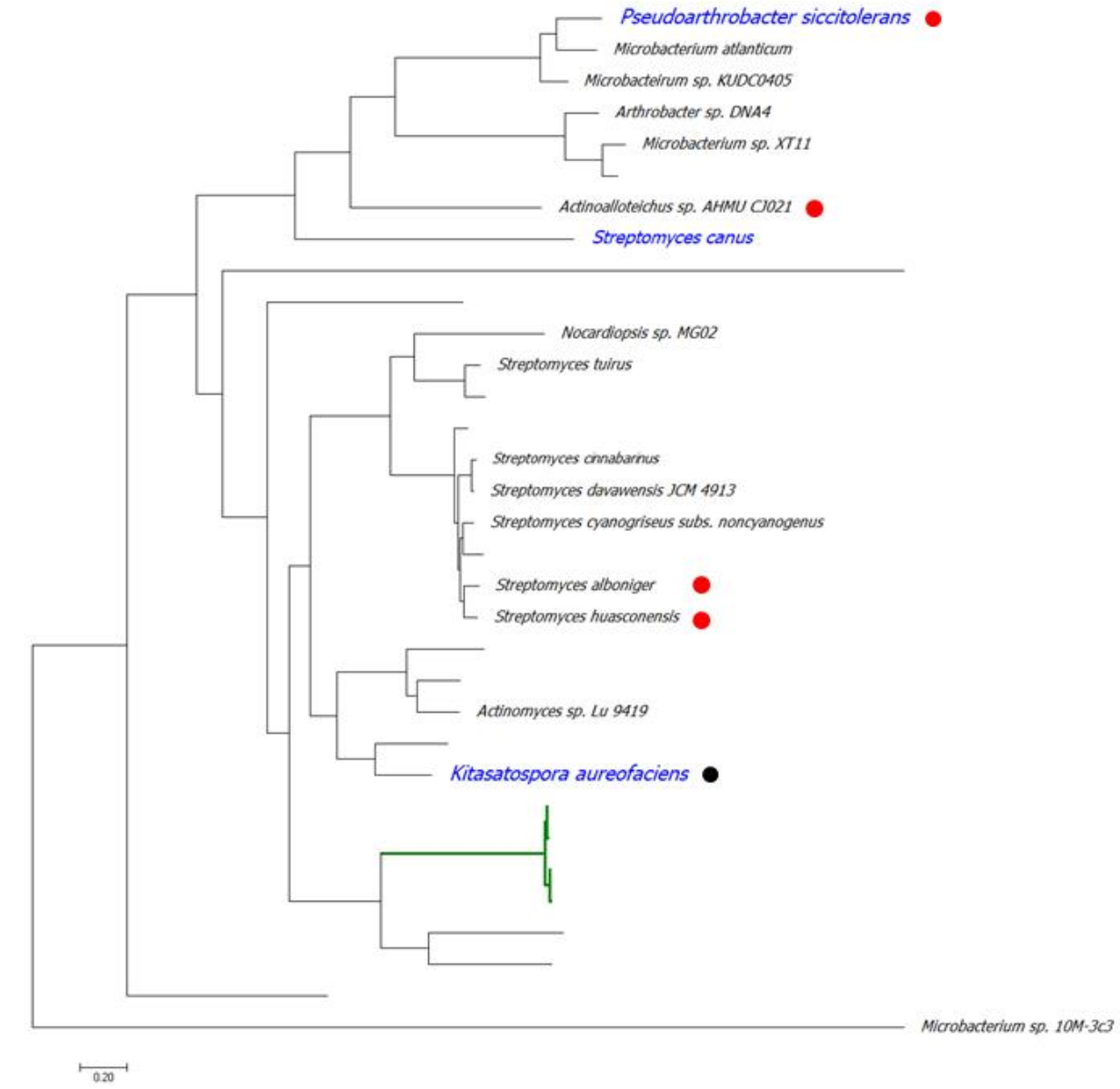

Figure S3 Phylogenetic tree of bacterial AA3 enzymes similar to *Ka*POx. Multiple alignment was conducted using Mafft (https://mafft.cbrc.jp/) with iterative refinement method for < 200 sequence with global homology. Tree was constructed using NGPhylogeny (https://ngphylogeny.fr/) with TrimAl as alignment curation and PhyML for tree inference.

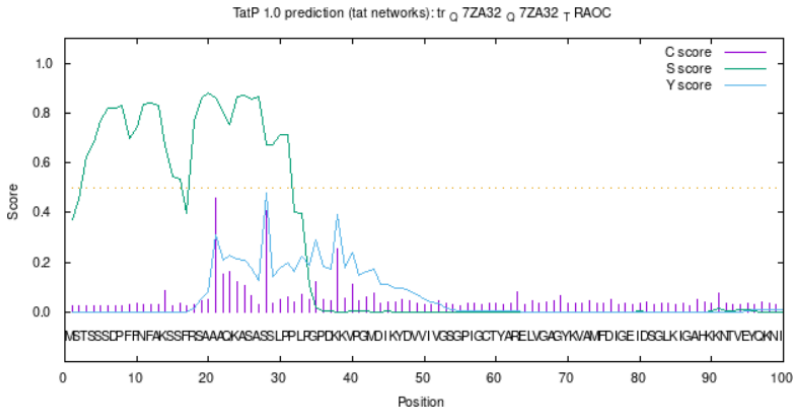

data

```
>tr_Q7ZA32_Q7ZA32_TRA  length = 100
# Measure  Position  Value  Cutoff  Tat signal peptide?
  max. C    21       0.456   0.51   NO
  max. Y    28       0.480   0.35   YES
  max. S    20       0.883   0.75   YES
  mean S     1-27    0.735   0.30   YES
  max. D     1-27    0.607   0.36   YES
# Most likely cleavage site between pos. 27 and 28: ASA-SS
# Potential Tat signal peptide but No Tat motif was found
# Used regex: RR.[FGAVML][LITMVF]
//
```

Figure S4: Signal peptide prediction using TatP-1.0 for Pyranose Oxidase from *Trametes ochracea* (POx Q7ZA32

6.2. List of abbreviation

AA	Auxiliary Activity
AADH	Aryl alcohol dehydrogenase
AAO	Aryl alcohol oxidase
ABTS	2,2'-azino-bis(3-ethylbenzothiazoline-6-sulfonic acid)
AOx	Alcohol oxidase
B. subtilis	*Bacillus subtilis*
BQ	1,4 Benzoquinone
CAZy	Carbohydrate Active Enzyme
CDH	Cellobiose dehydrogenase
CYT	cytochrome
DCIP / DCPIP	2,6-Dichlorophenolindophenol
E. coli	*Escherichia coli*
FAD	Flavin Adenine Dinucleotide
Fc	Ferrocenium hexafluorophosphate
GDH	Glucose dehydrogenase
GMC	Glucose Methanol Choline
GOx	Glucose oxidase
HPLC	High-Performance Liquid Chromatography
Ka / *K. aureofaciens*	*Kitasatospora aureofaciens*
MBP	Maltose Binding Protein
PCR	Polymerase Chain Reaction
PDH	Pyranose dehydrogenase
POD	Peroxidases
POx	Pyranose Oxidase
S. coelicolor	*Streptomyces coelicolor*
S. lividans	*Streptomyces lividans*
S. viridopsprus	*Streptomyces viridosporus*
Sa / *S. alboniger*	*Streptomyces alboniger*
Sg / *S. griseochromogenes*	*Streptomyces griseochromogenes*
SP	Signal Peptide

6.3. List of tables and figures

List of Tables

List of Figures

6.4. Published paper

International Journal of *Molecular Sciences*

MDPI

Article

Localization of Pyranose 2-Oxidase from *Kitasatospora aureofaciens*: A Step Closer to Elucidate a Biological Role

Ludovika Jessica Virginia [1,2] and Clemens Peterbauer [1,2,*]

[1] Food Biotechnology Laboratory, Department of Food Science and Technology, BOKU—University of Natural Resources and Life Sciences, Muthgasse 11, 1190 Vienna, Austria
[2] Doctoral Programme BioToP—Biomolecular Technology of Proteins, BOKU—University of Natural Resources and Life Sciences, Muthgasse 11, 1190 Vienna, Austria
* Correspondence: clemens.peterbauer@boku.ac.at; Tel.: +43-1-47654-75212

Abstract: Lignin degradation in fungal systems is well characterized. Recently, a potential for lignin depolymerization and modification employing similar enzymatic activities by bacteria is increasingly recognized. The presence of genes annotated as peroxidases in Actinobacteria genomes suggests that these bacteria should contain auxiliary enzymes such as flavin-dependent carbohydrate oxidoreductases. The only auxiliary activity subfamily with significantly similar representatives in bacteria is pyranose oxidase (POx). A biological role of providing H_2O_2 for peroxidase activation and reduction of radical degradation products suggests an extracellular localization, which has not been established. Analysis of the genomic locus of POX from *Kitasatospora aureofaciens* (*Ka*POx), which is similar to fungal POx, revealed a start codon upstream of the originally annotated one, and the additional sequence was considered a putative Tat-signal peptide by computational analysis. We expressed *Ka*POx including this additional upstream sequence as well as fusion constructs consisting of the additional sequence, the *Ka*POx mature domain and the fluorescent protein mRFP1 in *Streptomyces lividans*. The putative signal peptide facilitated secretion of KaPOx and the fusion protein, suggesting a natural extracellular localization and supporting a potential role in providing H_2O_2 and reducing radical compounds derived from lignin degradation.

Keywords: pyranose oxidase; *Streptomyces lividans*; Secretion; *Kitasatospora aureofaciens*; fluorescent

check for updates

Citation: Virginia, L.J.; Peterbauer, C. Localization of Pyranose 2-Oxidase from *Kitasatospora aureofaciens*: A Step Closer to Elucidate a Biological Role. *Int. J. Mol. Sci.* 2023, *24*, 1975. https://doi.org/10.3390/ijms24031975

Academic Editors: Rebecca Pogni and Maria Camilla Baratto

Received: 22 December 2022
Revised: 11 January 2023
Accepted: 16 January 2023
Published: 19 January 2023

1. Introduction

Lignocellulose, a composite of the polymers lignin, cellulose, hemicellulose and pectin, provides structural integrity and resistance to pathogens and herbivores to plants. The paracristallinity of cellulose, the complexity of the hemicellulose matrix and the linkage to lignin are major barriers against the enzymatic degradation of lignocellulose [1]. The lignin fraction is a heterogenous alkyl-aromatic polymer formed from three aromatic alcohols with different degrees of methoxylation. Lignification happens through monomer and polymer crosslinking via radicals produced by oxidases and is characterized by a large number of different interunit linkages, resulting in a remarkable recalcitrance to degradation [1,2].In nature, degradation of lignocellulose is feasible at physiological conditions by a number of organisms. The process of lignin degradation is mostly described in white-rot and brown-rot fungi [3,4], which mineralize lignin through a cocktail of oxidative enzymes, namely polyphenol oxidases (laccases) and peroxidases (lignin, manganese and versatile peroxidases), as well as auxiliary enzymes such as H_2O_2-generating oxidases. These peroxide-providing enzymes can belong to the Glucose-Methanol-Choline (GMC) oxidoreductase family of flavoenzymes (Auxiliary Activities Family 3), such as aryl alcohol oxidases, pyranose oxidases or cellobiose dehydrogenases, or to the copper radical oxidases (Auxiliary Activities Family 5), such as glyoxal oxidase [2]. Additionally, peroxide providing enzymes may be involved in the oxidative depolymerization of cellulose and

hemicellulose through lytic polysaccharide monoxygenases (LPMOs), for which hydrogen peroxide is also an essential co-substrate [5]. Most flavoprotein oxidases, such as aryl alcohol oxidases and pyranose oxidases, also have a significant dehydrogenase activity using (substituted) quinones as electron acceptors, often with a higher efficiency than molecular oxygen [6–8]. This dehydrogenase activity may also be involved in lignin depolymerization, as has been shown in vitro for combinations of fungal laccase and pyranose oxidase [9] as well as lignin peroxidase and pyranose oxidase [6,10], where addition of pyranose oxidase increased the degree of depolymerization markedly, presumably by reducing the resulting lignin breakdown products and preventing their immediate repolymerization.

While the enzymatic system(s) for depolymerization of lignin in fungi are well investigated, this is not the case for bacteria, although a potential for lignin depolymerization and modification using similar enzymatic activities such as laccases and peroxidases is increasingly recognized [1,11–13]. To date, there are only few reports on flavoprotein oxidoreductases that can be considered Auxiliary Activities for lignocellulose degradation. Pyranose oxidases were characterized from *Pseudarthrobacter siccitolerans* [14], *Kitasatospora aureofaciens* [6] and *Streptomyces canus* [15]. The sequence of POx derived from *K. aureofaciens* (*Ka*POx) is closely related to fungal POx [16] and shows both oxidase and dehydrogenase activity with comparable substrate preferences to fungal enzymes. The oxidase activity of POx is suitable for providing H_2O_2 for peroxidase activation for lignin depolymerization, while the dehydrogenase activity can play a role in preventing re-polymerization of lignin-derived radicals as well as protecting the cells from damage by those radicals. Both putative biological roles are only plausible if POx is located extracellularly, otherwise the produced hydrogen peroxide would have to be transported out of the cells for activation of peroxidases, and free radicals derived from lignin depolymerization would have to be imported into the cells. Both bacterial genes were identified by sequence similarities and were expressed in *E. coli* for characterization, but their natural subcellular localization has not been established. It should be noted that a copper radical oxidase with catalytic similarities to glyoxal oxidase (for which similar biological functions are discussed) has been described as a secretory enzyme in *Streptomyces coelicolor* and *Streptomyces lividans* [17]. We investigated the subcellular location of *Ka*POx by heterologous expression using Gram-positive bacterial expression systems and included additional sequences upstream of the annotated ATG that may constitute a functional signal peptide. To accommodate the detection of secreted enzyme, fusion constructs with a fluorescent protein (mono-Red Fluorescent Protein, mRFP) were used as reporter.

2. Results

2.1. Signal Peptide Prediction

The *K. aureofaciens* genomic sequence upstream of the coding region of *Ka*POx was analyzed using ORF Finder: https://www.ncbi.nlm.nih.gov/orffinder/ (accessed on 11 November 2019), and two Met residues were discovered upstream and in frame with the previously annotated start codon (Figure 1). These additional sequences amount to 63 amino acids starting from the first and 44 amino acids starting from the second encoded Met residue. These sequences were analyzed using TatP-1.0 [18]: https://services.healthtech.dtu.dk/service.php?TatP-1.0 (accessed on 11 November 2019). The longer sequence comprising 63 AA was classified as unlikely to be a Tat signal peptide, but part of the 44 AA sequence was found to score above the cut-off in all but one category. The potential signal peptide cleavage site was predicted to be between positions 36 and 37 (Supplemental Material, Figure S1).

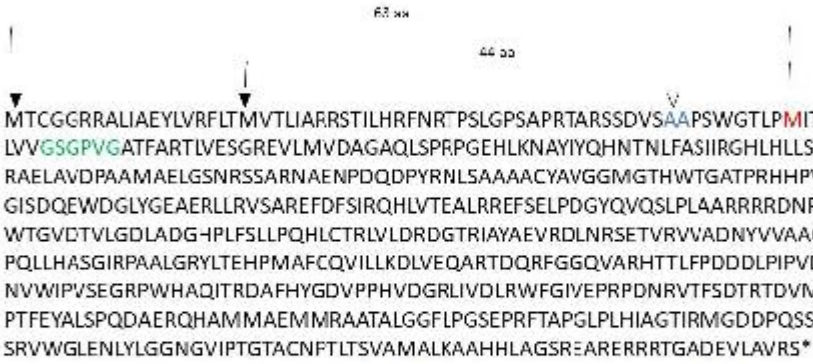

Figure 1. Results from ORF Finder showing two Methionine (M) in frame in the upstream region (filled triangles), followed by the previously annotated start codon (M in red). The putative cleavage site is shown in blue with an open triangle. The Rossman fold motif is shown in green.

2.2. Heterologous Expression of *Ka*POx with a Putative Signal Peptide

To investigate whether the 44 AA upstream of the originally annotated ATG of *Ka*POx constitute a functional signal peptide as predicted, constructs with and without this additional sequence (SP*Ka*POxHis and KaPOxHis, respectively) were prepared and heterologously expressed as described (Figure 2). Expression in *B. subtilis* did not result in detectable levels of secreted protein with either construct, but the His-tagged protein was detectable in the cell extract by Western blotting (Supplementary Figure S2). Protein purification by affinity chromatography was possible from the cell extract, but not from the supernatant. Yields of purified protein were considerably lower from the extract of cultures expressing the SP*Ka*POxHis construct (Figure S2). Expression in *S. lividans* was carried out using the constitutive promoter P_{vsi} and pIJ486 as plasmid backbone (Figure 2). Secreted *Ka*POx could be detected in the supernatant of *S. lividans* carrying the construct with the putative SP by enzymatic assay at a volumetric activity of 0.01 U/mL (dehydrogenase activity; Figure 3) as early as 48 h after start of the cultivation.

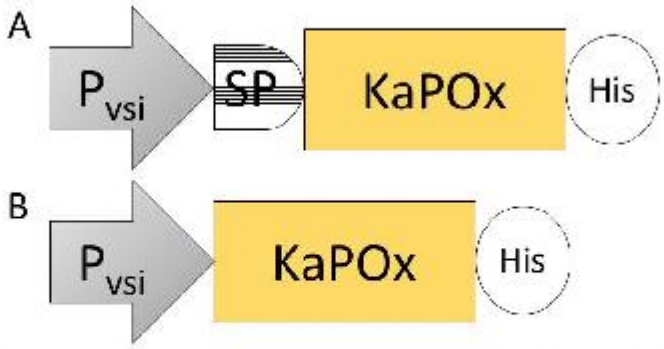

Figure 2. Expression constructs SP*Ka*POxHis (**A**) and *Ka*POxHis (**B**), containing the constitutive promoter of the *S. venezuelae* subtilisin inhibitor gene (P_{vsi}), the putative signal peptide (SP) identified upstream of the mature domain of pyranose oxidase from *K. aureofaciens* (KaPOx) and a C-terminal 6× His-tag (His).

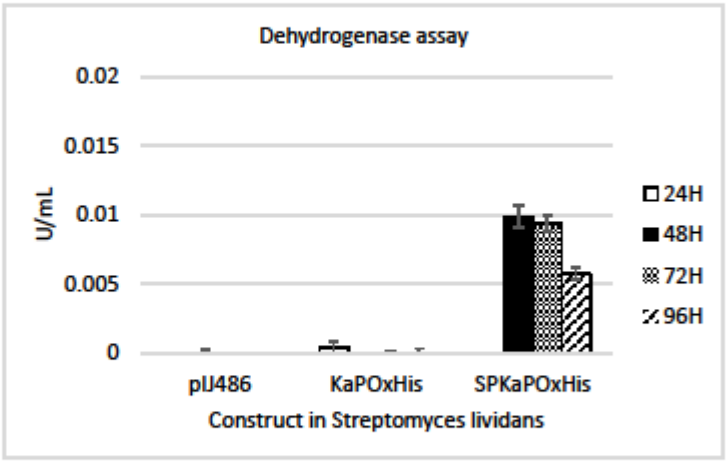

Figure 3. Dehydrogenase activity assay of *S. lividans* supernatant obtained from cultures harboring the empty vector pIJ486, pIJ486-*Ka*POxHis, and pIJ486-SP*Ka*POxHis. Samples were taken from the supernatant at 24, 48, 72 and 96 h (H) as indicated.

2.3. *Fusion Protein Approach*

Translational fusions of the fluorescent mono-Red Fluorescent Protein (mRFP) C-terminally of *Ka*POx with a 6× His-Tags added C-terminally of mRFP were constructed (Figure 4).

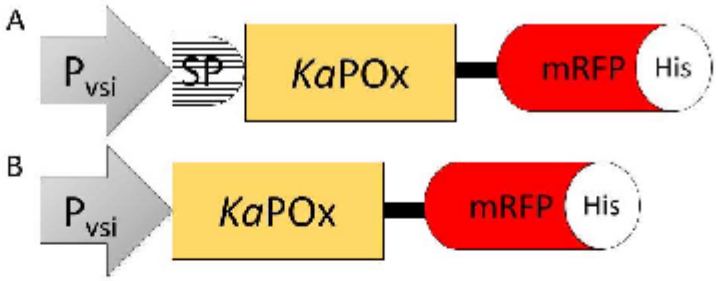

Figure 4. Constructs SP*Ka*POxmRFPHis (**A**) and *Ka*POxmRFPHis (**B**) containing the constitutive *S. venezuelae* P_{vsi} promoter (P_{vsi}), the putative signal peptide (SP), the *Ka*POx mature domain, the mRFP fluorescent protein (mRFP) and a C-terminal 6×His-Tag (His).

Both fusion constructs (SP*Ka*POxmRFPHis and *Ka*POxmRFPHis) were expressed in *S. lividans* under the control of the P_{vsi} promoter. In the culture supernatants, SP*Ka*POxmRFPHis showed a very low level of fluorescence at 72 h that increased constantly in intensity until 144 h. The supernatant from *Ka*POxmRFPHis showed a much lower fluorescence, detectable only at 120 and 144 h (Figure 5).

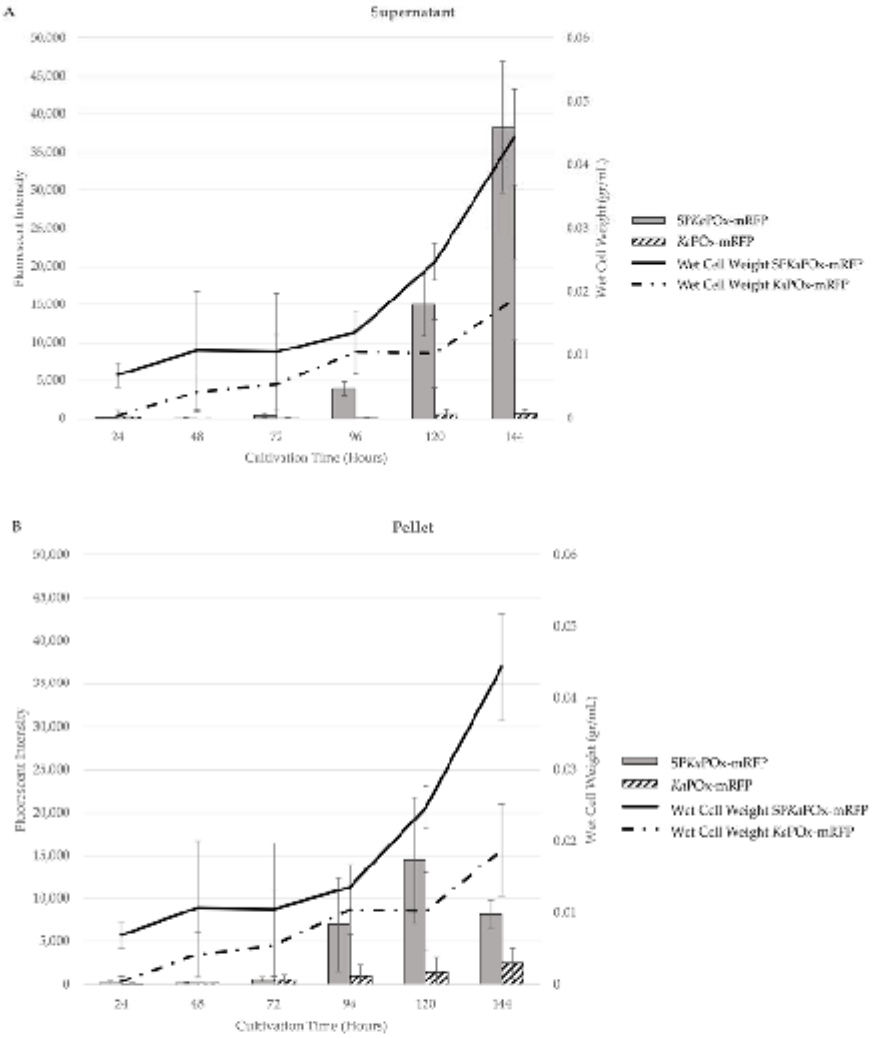

Figure 5. Growth curve (in wet cell weight) and mRFP fluorescence intensity from cultures expressing the fusion constructs SP*Ka*POxmRFPHis and *Ka*POxmRFPHis in the supernatants (**A**) and the pellet fractions (**B**). Fluorescent intensity values are adjusted for the recorded wet cell weight and are the mean results of three cultures.

Fluorescence was also detected in the cell pellets starting at 72 h in cultures of both constructs. Intensity increased until the end of cultivation at a very low level for cultures harboring *Ka*POxmRFPHis; for cultures harboring SP*Ka*POxmRFPHis a stronger increase was measured until 120 h, followed by a decline at 144 h. Wet cell weight (WCW) was monitored over time, and the obtained values were used to normalize the measured fluorescence intensity. A different growth behavior for cells harboring the different constructs was observed: cultures harboring *Ka*POxmRFPHis showed a constant but slow increase

in wet cell weight, with a final value after 144 h, approximately half of that recorded for cultures of SP*Ka*POxmRFPHis, in which a marked increase after 96 h was observable.

Enzymatic activity assays were also done on the samples from supernatants and pellets of cultures harboring both constructs. Both oxidase as well as dehydrogenase activity could be detected in the pellets starting at 96 h (oxidase activity is not shown, as the values were consistently very low). In the supernatants, no activity was measurable for cultures of *Ka*POxmRFPHis. Cultures containing SP*Ka*POxmRFPHis showed low activity at 120 and 144 h (Figure 6A). Enzymatic activities in the cell pellet increased slowly on a low level for *Ka*POxmRFPHis cultures. In SP*Ka*POxmRFPHis cultures, activity was higher at 96 and 120 h and declined in the last sample at 144 h. It is notable that the measured activities in the pellet fractions were higher in all corresponding samples than those in the supernatants.

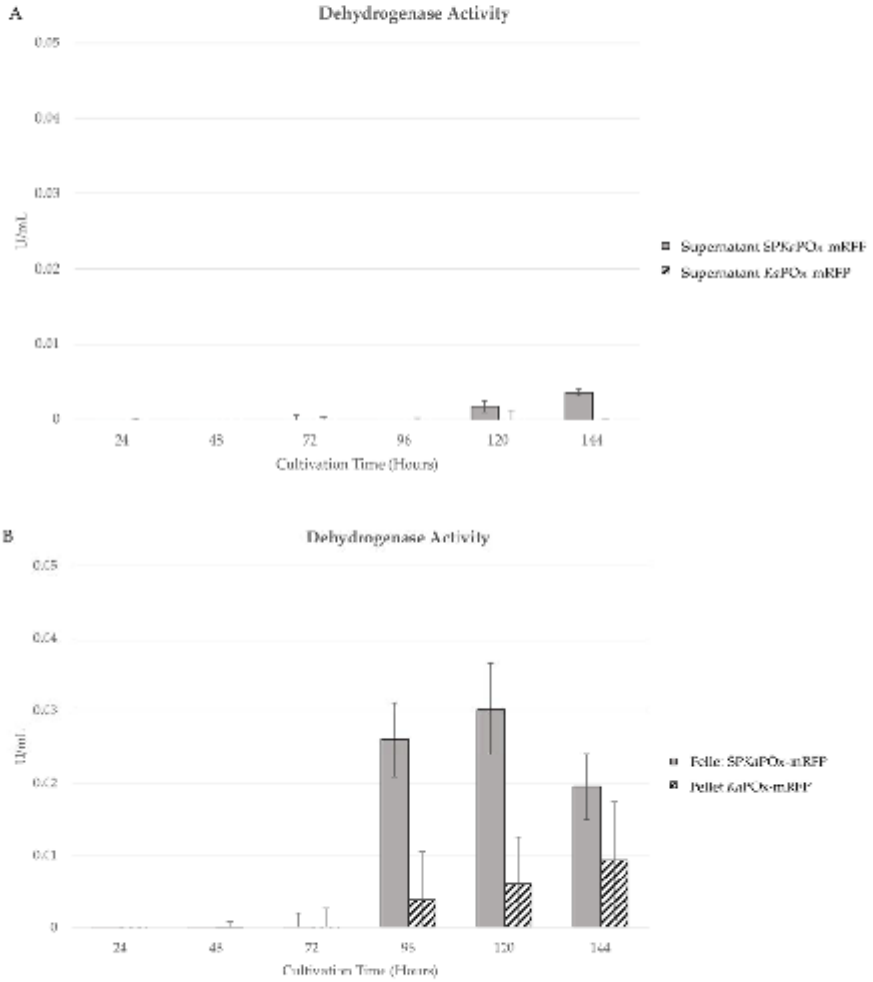

Figure 6. Enzymatic activity (dehydrogenase) in samples of the supernatant (**A**) and the pellet fractions (**B**) of cultures harboring SP*Ka*POxmRFPHis and *Ka*POxmRFPHis. Activity values are normalized for the recorded wet cell weight, as in Figure 5.

The presence of fusion protein was detected in supernatant samples of SP*Ka*POxmRFPHis cultures by Western blot using an anti-His-tag antibody. A band corresponding to intact fusion protein is visible in the samples obtained after 72 h and after 96 h of cultivation. In both samples, a notably more intense band corresponding to a molecular weight of 27 kDa is present (Figure 7B). Western blot analysis of SP*Ka*POxHis derived from the supernatant is shown in Figure 7A.

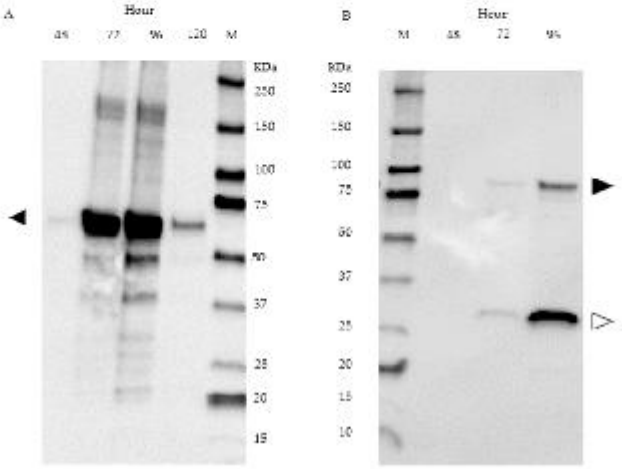

Figure 7. Western blot of supernatant samples from *S. lividans* cultures harboring SP*Ka*POxHis at 48, 72, 96 and 120 h (**A**) and SP*Ka*POxmRFPHis at 48, 72 and 96 h (**B**). A size marker is shown in lane M. The expected molecular weight of intact fusion protein and of the mRFP domain is 86.5 KDa (black arrow) and 26.6 KDa (white arrow), respectively.

3. Discussion

Here we expressed pyranose oxidase from *K. aureofaciens* (*Ka*POx), a bacterial enzyme from the family Auxiliary Activities 3 (AA3), in the two Gram-positive bacterial expression systems *B. subtilis* and *S. lividans*. We used constructs containing *Ka*POx, as previously expressed intracellularly in *E. coli* and characterized [6], as well as constructs containing the genomic sequence encoding additional 44 amino acids upstream of and in frame with the previously characterized coding sequence and also starting with an ATG. This upstream sequence was tentatively classified to constitute a Tat signal peptide by computational tools. We could not detect secretory enzyme in cultivations of both constructs expressed in *B. subtilis* but could purify the tagged protein from the cell extracts of both cultures. When using *S. lividans* as expression host, secretory enzyme with dehydrogenase activity towards glucose as the electron donor and ferrocenium hexafluorophosphate as the electron acceptor was detected in cultures harboring the construct with the putative signal peptide. The volumetric dehydrogenase activity was low at 0.01 U/mL, and oxidase activity could not be detected. Herzog et al. (2019) showed a 6.6-fold dehydrogenase activity with ferrocenium hexafluorophosphate compared to oxidase activity with molecular oxygen as electron acceptor for recombinant *Ka*POx produced in *E. coli*. We conclude that, considering the low dehydrogenase activity of secreted *Ka*POx produced in *S. lividans*, oxidase activity is probably below the detection limit.

We subsequently prepared fusion constructs with the gene encoding the fluorescent reporter protein mRFP downstream of the *Ka*POx-encoding gene (with and without the upstream sequence encoding the putative SP). Fluorescence could be detected in the supernatant after 72 h in cultures expressing the fusion construct with the putative SP, increasing significantly until 144 h and always higher than the intensity in the cell pellet

except very early after initial detection (Figure 5A). When constructs without the putative SP were used, a fluorescent signal was detected in the pellet at 72 h, but only another 48 h later in the supernatant, where the intensity remained very low until the last sampling point, and significantly lower than in the cell pellets at all time points (Figure 5B). It is notable that the fluorescence intensity in the cell pellets of SP*Ka*POxmRFPHis cultures reached a peak at 120 h and decreased for the last sampling point at 144 h. Also notable is the different growth behavior of the cultures expressing the two different constructs: the wet cell weight of SP*Ka*POxmRFPHis and *Ka*POxmRFPHis cultures was comparable until 96 h, but increased markedly slower after this in *Ka*POxmRFPHis cultures to a maximal value of 0.08 g/mL compared to SP*Ka*POxmRFPHis cultures, which reached 0.140 g/mL. This is concomitant with the appearance of fluorescent fusion protein in significant amounts in the supernatant. These observations suggest that, while (over)expression of both fusion constructs constitutes a metabolic burden for the cells, secretion driven by the signal peptide (and observable in the fluorescent intensity) avoids or alleviates cellular stress through cytoplasmic accumulation of the heterologous fusion protein, resulting in healthier growth and higher biomass formation than in the cells producing fusion protein lacking the putative signal peptide, where the expressed fusion protein accumulates throughout growth.

During six days or 144 h of cultivation, increase of wet cell weight as well as fluorescence intensity relative to WCW increased gradually without fluctuations or abrupt changes. When monitored for longer periods (until 192 h, not shown) an onset of "plateauing" of secretory fluorescence is observable in SP*Ka*POxmRFPHis cultures, while wet cell weight continues to increase for all cultures and only starts to show a lower increase rate at the last sampling point. This suggests that the cells had not yet reached the stationary phase. Since no sudden increases in extracellular fluorescence with concomitant stagnation or loss of wet cell weight were observed, we conclude that the extracellular fluorescence is a consequence of secretion, not cell death and lysis.

It is notable that the fluorescent signal from the fusion constructs was detectable later than the enzymatic activity in the previous experiments (72 h vs. 48 h). The fusion proteins are larger at 86.5 KDa than the *Ka*POx mature domain (59.9 KDa). A late secretion for heterologous enzymes in *S. lividans* was reported by Sianidis et al. (2006) [19] for the 95 KDa xyloglucanase, where secretion peaked at ~120H of cultivation time. It appears plausible that *Ka*POx is secreted earlier compared to fusion proteins containing the fluorescent reporter.

We also measured enzymatic activity (dehydrogenase) in both cell pellets and supernatants of SP*Ka*POxmRFPHis and *Ka*POxmRFPHis cultures and observed a marked discrepancy to the results of the fluorescence measurements. *Ka*POxmRFPHis cultures followed the same pattern as observed previously, with accumulation of active enzyme in the pellet fraction and essentially no detectable activity in the supernatants. SP*Ka*POxmRFPHis cultures also showed intracellular accumulation of activity, peaking at 120 h, as did the fluorescence measurement. In the supernatants, however, the activities, while following the same pattern as in the secretory fluorescence (constant increase until 144 h), remained much lower than the measured intracellular activities. Taken by itself, this appears to argue against secretion of active enzymes to meaningful levels. Western blot analysis of supernatant samples revealed intact fusion protein in the supernatant, faintly in samples taken after 72 h and more prominently in samples taken after 96 h. At both time points, a more intense band corresponding to the molecular weight of mRFP (± 27 KDa) is also detected (Figure 7B). We conclude that the lower band represents the product of proteolytic cleavage of secreted fusion protein, namely mRFP, which is detected via the attached His-tag (the rest of the protein, i.e., the *Ka*POx mature domain, is not detectable, as it does not contain a His-tag). Since mRFP is a small, compact protein composed mostly of β-sheets, it is conceivable that it is released from the fusion protein by extracellular proteases, but stays otherwise intact and fluorescent (thus detectable in the fluorescence measurements), whereas the larger oxidoreductase domain of the fusion protein may be further degraded and rendered inactive. In this case, we can presumably detect all of the secretory fluores-

cence, but only a fraction of the activity. The appearance of the His-tagged mRFP domain in the supernatant by another pathway, namely cell lysis and subsequent proteolysis, or intracellular proteolysis followed by cell lysis and release, is not plausible at these time points, as this would have been obvious in other parameters. According to the structural model of *Ka*POx [6], the C-terminus is exposed on the surface of the Rossman domain, facing away from the active site as well as the dimerization interface. An interference of the mRFP domain with dimerization and/or activity appears therefore unlikely, but cannot be entirely ruled out.

Regarding the failure to detect enzymatic activity (either kind) in the experiments with *B. subtilis*, it has to be noted that the used strain NZ8901 is not optimized for extracellular protease activity [20], which is known to be a major detrimental factor for the expression of heterologous proteins in this organism [21,22]. Since these early experiments were only done with SP*Ka*POxHis- and *Ka*POxHis-constructs, which do not allow fluorescent detection (and do not provide a more stable mRFP-domain that can be detected via the His-tag), it is conceivable that secretion driven by the putative signal peptide did, in fact, happen, but remained undetectable due to rapid proteolysis. Additionally, while the gene sequence was adapted to *B. subtilis* codon usage, a certain incompatibility between the signal peptide and mature domain sequences of SP*Ka*POx and the *B. subtilis* secretory machinery has to be considered. *K. aureofaciens*, which belongs to the phylum Actinobacteria and is closely related to Streptomycetaceae [23], was previously classified as *Streptomyces aureofaciens* [24]. *B. subtilis* belongs to the Firmicutes, and differences between the Tat translocase complexes of *B. subtilis* (comprising two subunits, TatA and TatC) and those of *S. lividans* and other *Streptomyces* spp., which comprise three subunits (TatA, TatB and TatC), were reported [25,26]. It is conceivable that the native SP from *KaPOx* is not properly processed by the *B. subtilis* Tat system.

In bacteria, Auxiliary Activities Family 3 sequences are generally closely related to fungal POx sequences rather than to sequences from other subfamilies [6,27]. We have shown here that the pyranose oxidase from *K. aureofaciens* is very likely a secretory enzyme, which supports the discussed biological function as an Auxiliary Activity with biological roles in hydrogen peroxide provision and/or quinone redox cycling, as outlined in the Introduction. This raises the question whether more bacterial POx-like enzymes are secretory enzymes (and whether their annotations in genome data needs to be re-examined and perhaps revised). We performed a BLAST search (tblastn) using *Ka*POx as the query sequence, selected the 25 sequences with highest similarity and query coverage where upstream sequences were available, plus the characterized enzymes from *P. siccitolerans* and *S. canus*, and examined these upstream sequences for putative signal peptide sequences as described. The results are summarized in Table 1: 15 out of 27 sequences extended in frame upstream of the annotated start codon. In four cases, these additional sequences were less than twelve amino acids long. In two cases (both *Streptomyces* spp.), TatP-1.0 predicted the sequence to be a signal peptide with a score of 5 out of 5. One sequence (from *Actinoalloteichus* sp., of the family Pseudonocardiaceae) of 100 additional amino acids gave more than one additional sequence, one of which was classified as possibly constituting a signal peptide. The upstream sequence of the gene from *P. siccitolerans* was predicted with a score of 3 out of 5; two more sequences (from *Streptomyces* and an *Arthrobacter* species) resulted in a score of 2 out of 5. The sequences that contain putative upstream signal peptides are distributed across several branches of a phylogenetic tree constructed from extant bacterial POx-like sequences (Supplementary material Figure S4), and an allocation along taxonomic categories is not possible. It appears plausible that bacterial GMC-oxidoreductases, while generally similar to fungal POx sequences, have diversified to a range of biological functions, with some as secretory enzymes with an auxiliary activity in lignocellulose degradation, and others with a cytoplasmic location and a different biological role. Clearly these results are preliminary, and further investigations into the biochemical properties of bacterial POx-like sequences, their subcellular localization and biological function are necessary.

Table 1. Prediction of putative Tat signal peptide using TatP-1.0.

No.	Species	E Value	Per. Ident	Upstream	Length (AA)	TatP-1.0	Note
1	*Kitasatospora aureofaciens*	0	95.24	v	44	Predicted	This study
2	*Mycobacterium lacus*	0	65.19	n.d			
3	*Actinomyces* sp. Lu 9419	6.00×10^{-175}	56.75	v	101	n.d	
4	*Amycolatopsis japonica*	3.00×10^{-168}	55.29	n.d			
5	*Frankia alni* ACN14a	7.00×10^{-152}	51.06	n.d			
6	*Streptomyces sudanensis*	9.00×10^{-140}	49.01	n.d			
7	*Streptomyces daxiawennsis* JCM 4913	3.00×10^{-135}	48.99	v	55	n.d	
8	*Streptomyces alboniger*	8.00×10^{-139}	48.91	v	56	Predicted	TatP-1.0 score 5 out of 5
9	*Streptomyces* sp. MRC013	1.00×10^{-138}	48.74	n.d			
10	*Phytohabitans suffuscus*	4.00×10^{-102}	48.15	n.d		n.d	
11	*Streptomyces cinnabarinus*	2.00×10^{-135}	48.08	v	12	n.d	
12	*Streptomyces cyaneogriseus* subsp. *noncyanogenus*	2.00×10^{-93}	48.04	v	52	n.d	TatP-1.0 score 2 out of 5
13	*Streptomyces huasconensis*	4.00×10^{-136}	47.76	v	64	Predicted	TatP-1.0 score 5 out of 5
14	*Streptomyces tuirus*	6.00×10^{-143}	46.94	v	32	n.d	
15	*Streptomyces lusitanus*	3.00×10^{-139}	46.48	n.d			
16	*Phytohabitans flavus*	3.00×10^{-125}	46.23	n.d			
17	*Nocardiopsis* sp. Mg02	4.00×10^{-106}	38.95	v	10	n.d	
19	*Microbacterium* sp. 10M-3C3	5.00×10^{-63}	38.25	v	50	n.d	
20	*Microbacterium atlanticum*	2.00×10^{-60}	37.59	v	41	n.d	
21	*Microbacterium* sp. KUDC0405	1.00×10^{-48}	37.59	v	5	n.d	
22	*Microbacterium testaceum* StLB037	6.00×10^{-62}	37.55	n.d			
23	*Micromonospora carbonacea*	7.00×10^{-76}	37.1	n.d			
24	*Arthrobacter* sp. DNA4	6.00×10^{-59}	37.08	v	35	n.d	TatP-1.0 score 2 out of 5
25	*Actinoalloteichus* sp. AHMU CJ021	1.00×10^{-59}	37.06	v	100	Predicted	More than 1 possibility for TatP-1.0 prediction
26	*Microbacterium* sp. XT11	7.00×10^{-63}	37.02	v	10	n.d	
27	*Streptomyces canus*	9.00×10^{-61}	33.71	n.d			
28	*Pseudarthrobacter siccitolerans*	6.00×10^{-64}	34.89	v	60	Predicted	TatP-1.0 score 3 out of 5

Most fungal POx enzymes have been purified from hyphal extracts [7,9,28,29], although Daniel et al. (1994) [30] proposed an extracellular localization based on microscopic studies. Nishimura et al. (1996) [31] expressed a cDNA from *Trametes* (*Coriolus*) *versicolor* in *E. coli* and reported that the first 38 amino acids were missing in the translated protein. Hallberg et al. [32] reported that the N-terminal part of *Trametes ochracea* (*multicolor*) pyranose oxidase has an unordered conformation and is not resolvable in the crystal structure [32]. These two enzymes show 96% identity, and both their N-terminal parts show similarities to a (bacterial) Tat signal peptide as analyzed by computational tools (TatP-1.0; Supplementary Material Figure S3). Pyranose oxidase has long been discussed as having been acquired by fungi from bacteria via Horizontal Gene Transfer (HGT) [27]. The fact that most fungal POx do not appear to be secretory enzymes (or that the Tat-SP-like sequence at the N-terminus of the *T. ochracea* and *T. versicolor* POx is not functional in fungi) does not necessarily contradict this—most lignocellulose-degrading fungi possess other enzymes for these biological functions. It is possible that different bacterial pyranose oxidase sequences were acquired by fungi on separate occasions and have diversified post-HGT for other roles.

4. Materials and Methods

4.1. Strains and Plasmids

Escherichia coli JM109 and MC1061 (MoBiTec GmbH, Göttingen, Germany) were used as an intermediate cloning host. *Bacillus subtilis* NZ8901 (MoBiTec GmbH) and *Streptomyces lividans* TK24 were used as an expression host. Vector pUC19 was used for cloning purposes in *E. coli*, pNZ8901 was used as an expression vector in *B. subtilis* and pIJ486 was used as a backbone for expression in *S. lividans*. *S. lividans* TK24 and pIJ486 were a gift from Dr. Mohamed Belal Hamed (KU Leuven) [33,34].

4.2. Media

Standard Luria Bertani (LB) medium containing Ampicillin (100 µg/mL) or Chloramphenicol (10 µg/mL) was used for *E. coli* cultivation. Cultivation of *B. subtilis* was conducted in 2 × YT medium (per liter: 16 g tryptone, 10 g yeast extract, 5 g NaCl) containing chloramphenicol (5 µg/mL) as described in the supplier's manual. *S. lividans* was cultivated as described [35] in phage medium (per liter: 0.5 g $MgSO_4 \cdot 7H_2O$, 0.74 g $CaCl_2 \cdot 2H_2O$, 10 g glucose, 5 g tryptone, 5 g yeast extract, 5 g Lab Lemco powder; the pH was adjusted to 7.2 with 5 N NaOH). For *S. lividans* transformation, R2 medium was used (per liter: 103 g sucrose, 0.25 g K_2SO_4, 12.12 g $MgCl_2 \cdot 6H_2O$, 0.1 g casamino acids, 1 g yeast extract, 5 g of Lab Lemco powder, 100 mL TES buffer, 2 mL trace element solution, 10 mL 0.5% KH_2PO_4 and 2% agar. 10 mL filter-sterile 36.8% $CaCl_2 \cdot 2H_2O$ and 1 mL filter-sterile 2 mM $CuSO_4$ solution were added after sterilization). The trace element solution contained (per liter) 40 mg $ZnCl_2$, 200 mg $FeCl_3 \cdot 6H_2O$, 10 mg $CuCl_2 \cdot 2H_2O$, 10 mg $MnCl_2 \cdot 4H_2O$, 10 mg $Na_2B_4O_7 \cdot 10H_2O$, and 10 mg $(NH_4)6Mo_7O_{24} \cdot 4H_2O$) and was filter-sterilized. Thiostrepton was used as a selective marker and added to a final concentration of 50 µg/mL from a stock solution of 50 mg/mL in DMSO. Chemicals and media components were purchased from Sigma Aldrich (St. Louis, MO, USA).

4.3. DNA Manipulation

Genomic extraction was carried out using Monarch® Genomic DNA Purification Kit, and plasmid DNA was isolated using Monarch® Plasmid Miniprep Kit. Polymerase Chain Reaction (PCR) was carried out using Q5® High-Fidelity DNA polymerase with the oligonucleotides listed in Supplementary Table S1. Monarch® PCR & DNA Cleanup Kit and Monarch® DNA Gel Extraction Kit were used to purify PCR products. All extraction and purification kits and all DNA-modifying enzymes and restriction endonuclease were purchased from New England Biolabs (Ipswich, MA, USA).

4.4. Vector Constructions

Constructions based on the shuttle vector pNZ8901 for the *B. subtilis* expression system were done by amplifying the gene of interest from the genome of *K. aureofaciens* through standard PCR. Primers pNZ_SP*Ka*POx_F and *Ka*POxHis_R were used to amplify *spkapox* (the *Ka*POx gene harboring the putative signal peptide sequence and a C-terminal His-tag), while primers pNZ_*Ka*POx_F and *Ka*POxHis_R were used to amplify *kapox* (the *Ka*POx gene with a C-terminal His-tag). Restriction endonucleases *Pst*I and *Xba*I were used to digest both PCR products (*spkapox* and *kapox*) and pNZ8901 prior to ligation using T4 Ligase. The ligated products were transformed to *E. coli* MC1061 for propagation and transformed into *B. subtilis* NZ8901 as circular plasmids isolated from *E. coli* MC1061.

Vector construction for *S. lividans* TK24 expression system was conducted in several steps due to the lack of a promoter in the pIJ486 backbone. The constitutive promoter (P_{vsi}) from the subtilisin inhibitor gene (*vsi*) was amplified using primers P_{vsi}_F and P_{vsi}_R from pIJ486-*sp*^{sec}-*mRFP* (gift from KU Leuven), digested by *Hind*III and *Pst*I and ligated to pUC19 digested with the same restriction endonucleases to generate pUC19-P_{vsi}. Both primer pairs SP*Ka*POx_F with *Ka*POxHis_R and *Ka*POx_F with *Ka*POxHis_R were used to amplify *spkapox* and *kapox*, respectively, from the *K. aureofaciens* genome. Restriction endonucleases *Pst*I and *Xba*I were used to digest both PCR products and pUC19-P_{vsi} prior to ligation to generate pUC19-P_{vsi}-*spkapox* and pUC19-P_{vsi}-*kapox*. Constructs with the reporter gene *mrfp* were generated through Gibson Assembly® (New England Biolab). We modified the pIJ486-*sp*^{sec}-*mrfp* into pIJ486-*mrfp* by removing the signal peptide sequence, *sp*^{sec}. Primer mRFP_GA_F (carrying an overhang of the P_{vsi} 3′ end sequence) and mRFP_GA_R (carrying an overhang of the pUC19 sequence) were used to amplify *mrfp* from pIJ486-*sp*^{sec}-*mrfp*. Vector pUC19-P_{vsi} was linearized with *Pst*I, and Gibson Assembly® was used to insert the amplification product to generate pUC19-P_{vsi}-*mrfp*. The primer pair (SP)*Ka*POx_GA_F and *Ka*POx_GA_R was used to generate the PCR products (*sp*)*kapox* with an overhang of the P_{vsi} sequence on its 5′ end, a linker and an overhang with the mRFP sequence in its 3′ end. The primer pair mRFP_lkk_GA_F and mRFPHis_GA_R was used to generate *mrfp* with a linker on its 5′ end and a His-tag with a complementary sequence to pUC19 on its 3′ end. The PCR products (*sp*)*kapox-linker* and *linker-mrfp-his*, together with pUC-P_{vsi} linearized with *Pst*I, were used as a template for the Gibson Assembly® reaction, to generate pUC19-P_{vsi}-(*sp*)*kapox-mrfp*. All intermediate constructs in pUC19-P_{vsi} were digested with restriction enzymes *Hind*III and *Xba*I and ligated into pIJ486 digested with the same restriction enzymes. All constructs used in this study were listed in Table 2.

Table 2. Vectors used in this study.

Name	Recombinant Gene	Host	Origin
pUC19	-	*E. coli*	NEB
pNZ8901	-	*E. coli*/*B. subtilis*	MoBiTec
pNZ8901-*spkapox*	*Ka*POx with signal peptide (*SPKaPOx*)	*E. coli*/*B. subtilis*	This study
pNZ8901-*kapox*	*KaPOx*	*E. coli*/*B. subtilis*	This study
pIJ486	-	*S. lividans* TK24	*KU Leuven*
pIJ486-*sp*^{sec}-*mrfp*	*mRFP* with signal peptide	*S. lividans* TK24	*KU Leuven*
pUC19-P_{vsi}	Promoter VSI (P_{vsi})	*E. coli*	This study
pUC19-P_{vsi}-*mrfp*	P_{vsi}, *mrfp*	*E. coli*	This study
pUC19-P_{vsi}-*spkapox*	P_{vsi}, *SPKaPOx*	*E. coli*	This study
pUC19-P_{vsi}-*kapox*	P_{vsi}, *KaPOx*	*E. coli*	This study
pUC19-P_{vsi}-*spkapox-mrfp*	P_{vsi}, *SPKaPOx*, *mrfp*	*E. coli*	This study
pUC19-P_{vsi}-*kapox-mrfp*	P_{vsi}, *KaPOx*, *mrfp*	*E. coli*	This study
pIJ486-*mrfp*	P_{vsi}, *mrfp*	*S. lividans* TK24	This study
pIJ486-spkapox	P_{vsi}, *SPKaPOx*	*S. lividans* TK24	This study
pIJ486-kapox	P_{vsi}, *KaPOx*	*S. lividans* TK24	This study
pIJ486-spkapox-*mrfp*	P_{vsi}, *SPKaPOx*, *mrfp*	*S. lividans* TK24	This study
pIJ486-kapox-*mrfp*	P_{vsi}, *KaPOx*, *mrfp*	*S. lividans* TK24	This study

4.5. Transformation

Chemically competent cells were used to conduct transformation in *E. coli* [36], and electroporation was used for transformation in *B. subtilis* following the instructions in the supplier´s manual (MoBiTec GmbH). Transformation of *S. lividans* TK24 was carried out through protoplast preparation and transformation [35], using thiostrepton (50 µg/mL) as a selection marker.

4.6. Cultivation and Protein Production

B. subtilis harboring recombinant vector pNZ8901 and its derivatives were grown in 50 mL 2xYT medium containing chloramphenicol 5 µg/mL at 37 °C, 200 rpm. Recombinant protein production was induced by adding 1% (*v*/*v*) subtilin preparation when OD_{600} reached 0.8. The subtilin preparation was produced from *B. subtilis* NZ8963 (MoBiTec GmbH) according to the supplier´s manual. Cultures were harvested at 24 h and 48 h after induction. Then, 50 mL culture was centrifuged and the supernatant separated from the pellet and stored with the addition of protease inhibitor (10 µg/mL phenyl methyl sulfonyl fluoride; PMSF). The pellet was washed three times with phosphate buffer pH 7 and suspended in 5 mL buffer following the last washing step. PMSF was added at 10 µg/mL, and the cells were pre-treated with lysozyme (0.5 mg/mL for one hour at 37 °C) and disrupted by sonication on ice using a Bandelin Sonopuls HD 60 (Bandelin electronic GmbH, Berlin, DE) set at 80 V and 30%-cycle for 3 × 1 min, with two-minute intervals. Recombinant His-tagged protein was purified on 1 mL Ni-NTA columns (Merck, Darmstadt, Germany) following the manufacturers recommendations using Buffer A (50 mM Tris-HCl pH 7.5, 30 mM NaCl, and 30 mM Imidazole) as binding and washing buffer and Buffer B (50 mM Tris-HCl pH 7.5, 30 mM NaCl, and 250 mM Imidazole) as elution buffer.

Cultivation of *S. lividans* TK24 was conducted in baffled flasks containing 50 mL phage medium with 10 µg/mL thiostrepton at 30 °C, 150 rpm. No induction was required due to the use of the constitutive P_{vsi} promoter. Samples of 1 mL were obtained every 24 h and centrifuged (4000× *g*, 10 min, 4 °C). Supernatants were separated and stored at 4 °C with 10 µg/mL PMSF. Wet cell weight of the pellets was determined, and samples were washed three times with 1 mL phosphate buffer pH 7 containing 25 mM NaCl. Treatment with lysozyme and sonication was done as described for *B. subtilis* (sonication was done for only 1 min). The lysed samples were centrifuged at 13,000 rpm for 5 min at 4 °C, and extracts were stored with 10 µg/mL PMSF.

4.7. SDS-PAGE and Western Blot

Samples were mixed with 2x SDS buffer mix (Sigma), denatured at 95 °C for 3 min and separated on Mini-PROTEAN®TGX Stain-Free™ Precast Gels 4–20% (Bio-Rad, Hercules, CA, USA) at 150 volt for 50 min. Precision Plus Protein™ Western C™ (Bio-Rad) was used as a molecular weight standard. Proteins were transferred to a 0.2 µm Nitrocellulose membrane by dry-blotting in a Trans-Blot® Turbo™ (Bio-Rad) at 1.3 A, and 25 V for 7 min. Proteins were detected using a BSA-free anti-Penta-His-tag mouse monoclonal IgG (Qiagen, Hilden, Germany) as primary antibody and Polyclonal Rabbit-anti-mouse Immunoglobulin/HRP (Agilent, Santa Clara, CA, USA) as secondary antibody according to the manufacturer´s recommendations. Clarity Western ECL (Bio-Rad) was used as substrate. Visualization of both stain-free SDS-PAGE gel and Western blot was done in a ChemiDoc™ XRS+ (BioRad).

4.8. Enzymatic Activity Assay and Fluorescent Signal Analysis

To determine the *Ka*POx dehydrogenase activity, an enzymatic activity assay was performed using 160 mM glucose as electron donor and ferrocenium hexafluorophosphate 0.16 mM as electron acceptor. For the oxidase activity, atmospheric oxygen was used as electron acceptor. Quantification of oxidase activity was done using 1 mM 2,2′-Azino-bis (3-ethylbenzothiazoline-6-sulfonic acid; ABTS) and Horseradish Peroxidase (Sigma Aldrich;

143 U/mL). Dehydrogenase activity was determined spectrophotometrically at 300 nm, while oxidase activity was determined at 420 nm as described previously [6].

Detection of fluorescence of mRFP was conducted by exciting the samples at 584 nm and analyzing the emission at 603 nm. Both *Ka*POx enzymatic activities as well as mRFP fluorescent signals were measured in an EnSpire® multimode plate reader (PerkinElmer, Waltham, MA, USA).

Supplementary Materials: The supporting information can be downloaded at: https://www.mdpi.com/article/10.3390/ijms24031975/s1.

Author Contributions: Conceptualization, C.P.; Investigation, L.J.V.; Writing—original draft, L.J.V.; Writing—review & editing, C.P.; Supervision, C.P. All authors have read and agreed to the published version of the manuscript.

Funding: This research was funded by the AUSTRIAN SCIENCE FUND FWF, grant W1224, and the Austrian Agency for Education and Internationalisation OeAD via an ASEA-UNINET Ernst-Mach-Grant for L. Jessica Virginia. Open Access Funding by the Austrian Science Fund (FWF).

Institutional Review Board Statement: Not applicable.

Informed Consent Statement: Not applicable.

Data Availability Statement: Not applicable.

Acknowledgments: The financial support for L. Jessica Virginia from the Austrian Agency for Education and Internationalisation (OeAD) through an ASEA-UNINET Ernst-Mach-Grant is gratefully acknowledged. L. Jessica Virginia was a member of the Doctoral Program BioToP—Biomolecular Technology of Proteins (supported by the Austrian Science Fund FWF grant W1224). We are grateful to Mohamed Belal Hamed and Anastassios Economou, KU Leuven, for the gift of plasmids and bacterial strains.

Conflicts of Interest: The authors declare no conflict of interest.

References

1. Cragg, S.M.; Beckham, G.T.; Bruce, N.C.; Bugg, T.D.H.; Distel, D.L.; Dupree, P.; Etxabe, A.G.; Goodell, B.S.; Jellison, J.; McGeehan, J.E.; et al. Lignocellulose degradation mechanisms across the Tree of Life. *Curr. Opin. Chem. Biol.* **2015**, *29*, 108–119. [CrossRef]
2. Polegioni, L.; Tonin, F.; Rosini, E. Lignin-degrading enzymes. *FEBS J.* **2015**, *282*, 1190–1213. [CrossRef]
3. Bugg, T.D.H.; Ahmad, M.; Hardiman, E.M.; Rahmanpour, R. Pathways for degradation of lignin in bacteria and fungi. *Nat. Prod. Rep.* **2011**, *28*, 1883. [CrossRef]
4. Xu, Z.; Lei, P.; Wen, Z.; Jin, M. Recent advances in lignin valorization with bacterial cultures: Microorganisms, metabolic pathways, and bio-products. *Biotechnol. Biofuels* **2019**, *12*, 2–19. [CrossRef]
5. Bissaro, B.; Røhr, Å.K.; Müller, G.; Chylenski, P.; Skaugen, M.; Forsberg, Z.; Horn, S.J.; Vaaje-Kolstad, G.; Eijsink, V.G.H. Oxidative cleavage of polysaccharides by monocopper enzymes depends on H_2O_2. *Nat. Chem. Biol.* **2017**, *13*, 1123–1128. [CrossRef]
6. Herzog, P.L.; Sützl, L.; Eisenhut, B.; Maresch, D.; Haltrich, D.; Obinger, C.; Peterbauer, C.K. Versatile Oxidase and Dehydrogenase Activities of Bacterial Pyranose 2-Oxidase Facilitate Redox Cycling with Manganese Peroxidase In Vitro. *Appl. Environ. Microbiol.* **2019**, *85*, e00390-19. [CrossRef]
7. Leitner, C.; Volc, J.; Haltrich, D. Purification and Characterization of Pyranose Oxidase from the White Rot Fungus *Trametes multicolor*. *Appl. Environ. Microbiol.* **2001**, *67*, 3636–3644. [CrossRef]
8. Pisanelli, I.; Kujawa, M.; Spadiut, O.; Kitt, R.; Halada, P.; Volc, J.; Mozuch, M.D.; Kersten, P.; Haltrich, D.; Peterbauer, C. Pyranose 2-oxidase from *Phanerochaete chrysosporium*–expression in *E. coli* and biochemical characterization. *J. Biotechnol.* **2009**, *142*, 97–106. [CrossRef]
9. Ai, M.Q.; Wang, F.F.; Zhang, Y.Z.; Huang, F. Purification of pyranose oxidase from the white rot fungus *Irpex lacteus* and its cooperation with laccase in lignin degradation. *Proc. Biochem.* **2014**, *49*, 2191–2198. [CrossRef]
10. Wang, F.F.; Huang, F.; Ai, M.Q. Synergetic Depolymerization of Aspen CEL by Pyranose 2-Oxidase and Lignin-degrading Peroxidases. *Bioresources* **2019**, *14*, 3481–3494. [CrossRef]
11. Bugg, T.D.H.; Ahmad, M.; Hardiman, E.M.; Singh, R. The emerging role for bacteria in lignin degradation and bio-product formation. *Curr. Opin. Biotechnol.* **2011**, *22*, 394–400. [CrossRef]
12. Bugg, T.D.H.; James, J.W.; Rashid, G.M.M. Bacterial enzymes for lignin depolymerisation: New biocatalysts for generation of renewable chemicals from biomass. *Curr. Opin. Chem. Biol.* **2020**, *55*, 26–33. [CrossRef]
13. Diaz-Garcia, L.; Bugg, T.D.H.; Jiménez, D.J. Exploring the lignin catabolism potential of soil-derived lignocellulolytic microbial consortia by a gene-centric metagenomic approach. *Microb. Ecol.* **2020**, *80*, 885–896. [CrossRef]

14. Mendes, S.; Banha, C.; Madeira, J.; Santos, D.; Miranda, V.; Manzanera, M.; Ventura, M.R.; van Berkel, W.J.H.; Martins, L.O. Characterization of a bacterial pyranose 2-oxidase from *Arthrobacter siccitolerans*. *J. Mol. Catal. B Enzym.* **2016**, *133*, S34–S43. [CrossRef]
15. Kostelac, A.; Sützl, L.; Puc, J.; Furlanetto, V.; Divne, C.; Haltrich, D. Biochemical Characterization of Pyranose Oxidase from *Streptomyces canus*—Towards a Better Understanding of Pyranose Oxidase Homologues in Bacteria. *Int. J. Mol. Sci.* **2022**, *23*, 13595. [CrossRef]
16. Abrera, A.T.; Sützl, L.; Haltrich, D. Pyranose Oxidase: A versatile sugar oxidoreductase for bioelectrochemical applications. *Bioelectrochemistry* **2020**, *132*, 107409. [CrossRef]
17. Whittaker, M.M.; Whittaker, J.W. *Streptomyces coelicolor* oxidase (SCO2837p): A new free radical metalloenzyme secreted by *Streptomyces coelicolor* A3(2). *Arch. Biochem. Biophys.* **2006**, *452*, 108–118. [CrossRef]
18. Bendtsen, J.D.; Nielsen, H.; Widdick, D.; Palmer, T.; Brunak, S. Prediction of twin-arginine signal peptides. *BMC Bioinform.* **2005**, *6*, 167. [CrossRef]
19. Sianidis, G.; Pozidis, C.; Becker, F.; Vrancken, K.; Sjoeholm, C.; Karamanou, S.; Takamiya-Wik, M.; Mellaert, L.V.; Schaefer, T.; Anne, J.; et al. Functional large-scale production of a novel *Jonesia sp.* xyloglucanase by heterologous secretion from *Streptomyces lividans*. *J. Biotechnol.* **2006**, *121*, 498–507. [CrossRef]
20. Bongers, R.S.; Veening, J.; van Wieringen, M.; Kuipers, O.P.; Kleerebezem, M. Development and Characterization of a Subtilin-Regulated Expression System in *Bacillus subtilis*: Strict Control of Gene Expression by Addition of Subtilin. *Appl. Env. Microbiol.* **2005**, *71*, 8818–8824. [CrossRef]
21. Harwood, C.; Cranenburgh, R. Bacillus protein secretion: An unfolding story. *Trends Microbiol.* **2008**, *16*, 73–79. [CrossRef] [PubMed]
22. Neef, J.; van Dijl, J.M.; Buist, G. Recombinant protein secretion by *Bacillus subtilis* and *Lactococcus lactis*: Pathways, applications and innovation potentials. *Essays Biochem.* **2021**, *65*, 187–195. [CrossRef]
23. Hsiao, N.H.; Kirby, R. Comparative genomics of Streptomyces avermitilis, Streptomyces cattleya, Streptomyces maritimus and Kitasatospora aureofaciens using a Streptomyces coelicolor microarray system. *Antonie Leeuwenhoek* **2007**, *93*, 1–25. [CrossRef]
24. Labeda, D.P.; Dunlap, C.A.; Rong, X.; Huang, Y.; Doroghazi, J.R.; Ju, K.S.; Metcalf, W.W. Phylogenetic relationships in the family Streptomycetaceae using multi-locus sequence analysis. *Antonie Leeuwenhoek* **2017**, *110*, 563–583. [CrossRef] [PubMed]
25. Anne, J.; Vrancken, K.; van Mellaert, L.; van Impe, J.; Bernaerts, K. Protein secretion biotechnology in gram-positive bacteria with special emphasis on *Streptomyces lividans*. *Biochim. Biophys. Acta* **2014**, *1843*, 1750–1761. [CrossRef] [PubMed]
26. Kolkman, M.A.B.; van der Ploeg, R.; Bertels, M.; van Dijk, M.; van der Laan, J.; van Dijl, J.M.; Ferrari, E. The Twin-Arginine Signal Peptide of *Bacillus subtilis* YwbN Can Direct either Tat- or Sec-Dependent Secretion of Different Cargo Proteins: Secretion of Active Subtilisin via the *B. subtilis* Tat Pathway. *Appl. Environ. Microbiol.* **2008**, *74*, 7507–7513. [CrossRef]
27. Sützl, L.; Foley, G.; Gillam, E.M.J.; Bodén, M.; Haltrich, D. The GMC superfamily of oxidoreductases revisited: Analysis and evolution of fungal GMC oxidoreductases. *Biotechnol. Biofuels* **2019**, *12*, 118. [CrossRef]
28. Danneel, H.J.; Rossner, E.; Zeeck, A.; Giffhorn, F. Purification and characterization of a pyranose oxidase from the basidiomycete *Peniophora gigantea* and chemical analyses of its reaction products. *Eur. J. Biochem.* **1993**, *214*, 795–802. [CrossRef]
29. Machida, Y.; Nakanishi, T. Purification and properties of pyranose oxidase from *Coriolus versicolor*. *Agric. Biol. Chem.* **1984**, *48*, 2463–2470. [CrossRef]
30. Daniel, G.; Volc, J.; Kubatova, E. Pyranose oxidase, a major source of H_2O_2 during wood degradation by *Phanerochaete chrysosporium*, *Trametes versicolor*, and *Oudemansiella mucida*. *Appl. Environ. Microbiol.* **1994**, *60*, 2524–2532. [CrossRef]
31. Nishimura, I.; Okada, K.; Koyama, Y. Cloning and expression of pyranose oxidase cDNA from *Coriolus versicolor* in *Escherichia coli*. *J. Biotechnol.* **1996**, *52*, 11–20. [CrossRef]
32. Hallberg, B.M.; Leitner, C.; Haltrich, D.; Divne, C. Crystallization and preliminary X-ray diffraction analysis of pyranose 2-oxidase from the white-rot fungus *Trametes multicolor*. *Acta Crystallogr. Sect. D Biol. Crystallogr.* **2004**, *60*, 197–199. [CrossRef]
33. Hamed, M.B.; Vrancken, K.; Bilyk, B.; Koepff, J.; Novakova, R.; van Mellaert, L.; Oldiges, M.; Luzhetskyy, A.; Kormanec, J.; Anné, J.; et al. Monitoring Protein Secretion in Streptomyces Using Fluorescent Proteins. *Front. Microbiol.* **2018**, *9*, 3019. [CrossRef]
34. Ward, J.M.; Janssen, G.R.; Kieser, T.; Bibb, M.J.; Buttner, J.M.; Bibb, M.J. Construction and characterisation of a series of multi-copy promoter-probe plasmid vectors for *Streptomyces* using the aminoglycoside phototransferase gene from Tn5 as indicator. *Mol. Gen. Genet.* **1986**, *203*, 468–478. [CrossRef]
35. Vrancken, K.; Van Mellaert, L.; Anné, J. Cloning and Expression Vectors for a Gram-Positive Host, *Streptomyces lividans*. *Methods Mol. Biol.* **2010**, *668*, 97–107. [CrossRef]
36. Sambrook, J.; Russell, D.W. Plasmids and Their Usefulness in Molecular Cloning. In *Molecular Cloning: A Laboratory Manual*, 3rd ed.; Argentine, J., Irwin, N., Eds.; Cold Spring Harbor Laboratory Press: New York, NY, USA, 2001; Volume 1, pp. 116–118.

6.5. Curriculum Vitae

Education

2018 - Present	PhD Student – Biomolecular Technology of Proteins 'BioToP' – BOKU University of Natural Resources and Life Sciences, Vienna Supervised by: Assoc. Prof. Dr. Clemens Peterbauer
2012 - 2014	Master of Science in Biotechnology - Atma Jaya Catholic University of Indonesia
2005 - 2009	Bachelor of Science in Biotechnology - Atma Jaya Catholic University of Indonesia

Publications

- Localization of Pyranose 2-Oxidase from *Kitasatospora aureofaciens*: A step closer to elucidate a biological role. **Int. J. of. Mol. Sci**. 2023. 24(3): 1975. https://doi.org/10.3390/ijms24031975
- Analysis and reconstitution of the menaquinone biosynthesis pathway in *Lactiplantibacillus plantarum* and *Lentilactibacillus bucheri*. **Microorganisms.** 2021. 9(7): 1476. doi:10.3390/microorganisms9071476.
- Prospecting of mannan degrading bacteria on treating palm kernel meal. **International Journal of Oil Palm.** 2018. volume I, number1.p18-27. ISSN:2614-2376
- The effect of corn substitution with palm kernel meal treated by enzyme on production performance and carcass quality of broiler. **Bulletin of Animal Science**. 2018. ISSN-0126-4400/E-ISSN-2407-876X
- Enhancement of lytic polysaccharide monooxygenase activity derived from *Neurospora sp*. in solid substrate
  fermentation of oil palm empty fruit bunch**. IOP Conf. Series: Earth and Environmental Science 209 (2018)**
  012010. IOP Publishing doi:10.1088/1755-1315/209/1/012010
- A consensus linkage map of oil palm and a major QTL for stem height. **Scientific Reports** 5:8232. 2015. DOI:10.1038/srep08232

Awards

Ernst Mach Grant – ASEA UNINET 2018 – 2021

Biomolecular Technology of Proteins (BioToP) 2019 – 2022

Marietta Blau Grant 2021 – 2022

Conferences

Lignobiotech 2022, Vancouver – Flash Oral Presentation

Oxizyme 2022, Siena – Oral Presentation, BioToP Session

European Federation of Biotechnology 2021 – Flash Oral Presentation

Biocatalyst open day 2020 – Flash Oral Presentation

ÖGMBT 2019, Salzburg – Poster

Research abroad

Nov 2021 – Jun 2022: University of Toronto, Department of chemical engineering and applied chemistry (BioZone)

2013 – 2014: National centre for genetic engineering and biotechnology (BIOTEC, Thailand)

Feb – May 2009: National centre for genetic engineering and biotechnology (BIOTEC, Thailand)

Organization skill

Student speaker of BioToP Doctroal Program (2019 – 2021)

Secretary of Indonesischer Studentinnen Verein in Österreich (2019-2020)

Coordinator for international communication and meeting organizer (2011 – 2018)

Secretary of Student Council (2001-2002, 2003-2004, 2007-2008)

Working experience

2009 - 2018	Research and Development Department, as Group Leader - **PT. Wilmar Benih Indonesia**
2017 - 2018	Enhancing novel lipase activity to fit the economic feasibility study for industry
2016 - 2017	Screening of potential fungi producing Lytic Polysaccharide Monooxygenase

	Biodiversity exploration for enzyme discovery through metagenomic approach
2011 - 2016	Mannanase research for chicken feed
2009 - 2011	Assessment of genetic diversity using SSR and QTL analysis in *E. guineensis* **(In collaboration with Temasek Lifescience Laboratory, Singapore)**
May - Aug 2015	Optimization and Pilot Scale Production of Recombinant Enzyme **Wilmar (Shanghai) Biotechnology R&D Center Co., Ltd**
2013 - 2014	Heterologous expression and characterization of alkaliphilic xylanase from metagenome of termite gut inhabiting bacteria in *Pichia pastoris.* **National Center for Genetic Engineering and Biotechnology (BIOTEC, Thailand)**
Feb - May 2009	Construction of New Plasmid Vector from Native Plasmid of *Pediococcus pentosaceus* BT520. **National Center for Genetic Engineering and Biotechnology (BIOTEC, Thailand)**
Aug 2008 - Feb 2009	SNPs detection in *pfmdr*1 gene in *Plasmodium falciparum* through real-time PCR. **United State Naval Medical Research Institute No. 2 (US-NAMRU 2)**
Jul - Aug 2008	Working on malaria detection through microscopic and molecular technique. **United State Naval Medical Research Institute No. 2 (US-NAMRU 2)**